Chapter 6
Methanol Utilisation Technologies

Martin Bertau, Hans Jürgen Wernicke and Friedrich Schmidt

6.1 Introduction

Martin Bertau, Hans Jürgen Wernicke and Friedrich Schmidt

Oil and gas are raw materials the availability of which is prognosticated to run short in the near future [1]. The peak oil discussion is an example generally perceived as proof of this development to come [2]. Other reports appear to calm these fears, stating that oil and gas production will even increase until 2050 [3–6]. Whether or not these forecasts hold true, shale gas exploitation will bring relief in supplying the chemical industry with fossil carbon.

Nevertheless, crude oil qualities will still be constantly declining. Crude oil compositions will move towards higher fractions of heavy hydrocarbons, while the fraction of lower-boiling hydrocarbon decreases, rendering low qualities more expensive [7]. Together with a growing demand for oil and gas in emerging economies (Brazil, Russia, India, Indonesia, China and South Africa), a severe shortage in oil and gas supply at economically reasonable prices will expectedly affect the chemical industry in the short to medium term.

It is therefore critical to have synthetic products on hand that can easily substitute for classic petrochemicals. To achieve this without impairing national economies, a substitute is required that can be used in lieu of oil and gas without the need for further investments in both national infrastructure and petrochemical plants. This central

M. Bertau (✉)
Institute of Chemical Technology, Freiberg University of Mining and Technology,
Leipziger Straße 29, 09599 Freiberg, Germany
e-mail: martin.bertau@chemie.tu-freiberg.de

H. J. Wernicke
Kardinal–Wendel-Straße 75 a, 82515 Wolfratshausen, Germany
e-mail: h.j.wernicke@t-online.de

F. Schmidt
Angerbachstrasse 28, 83024 Rosenheim, Germany
e-mail: fs-ro@gmx.de

M. Bertau et al. (eds.), *Methanol: The Basic Chemical and Energy Feedstock of the Future*, 327
DOI: 10.1007/978-3-642-39709-7_6,

requirement, the strict fulfilment of which is the only way to escape from problems with the supply and quality of fossil raw materials, is solely met by methanol. Any such approach will primarily run on synthesis gas, the main product of which is methanol.

Methanol use as an energy raw material has been extensively reviewed in this book so far; in this chapter, methanol's potential as chemistry raw material is explored. A series of technical processes to several intermediates that are accessible from methanol will be described, with the purpose of illustrating how important petrochemical products can be substituted by C_1-based chemistry. However, other approaches to the described compounds are beyond the scope of this book, so the reader is kindly referred to elsewhere to learn more about C_{2+}-based approaches.

Figure 6.1 gives examples of common processing methods of synthesis gas and methanol and how they can easily be interconverted. Table 6.1 shows the weight percent of synthesis gas that is eventually included in the final product.

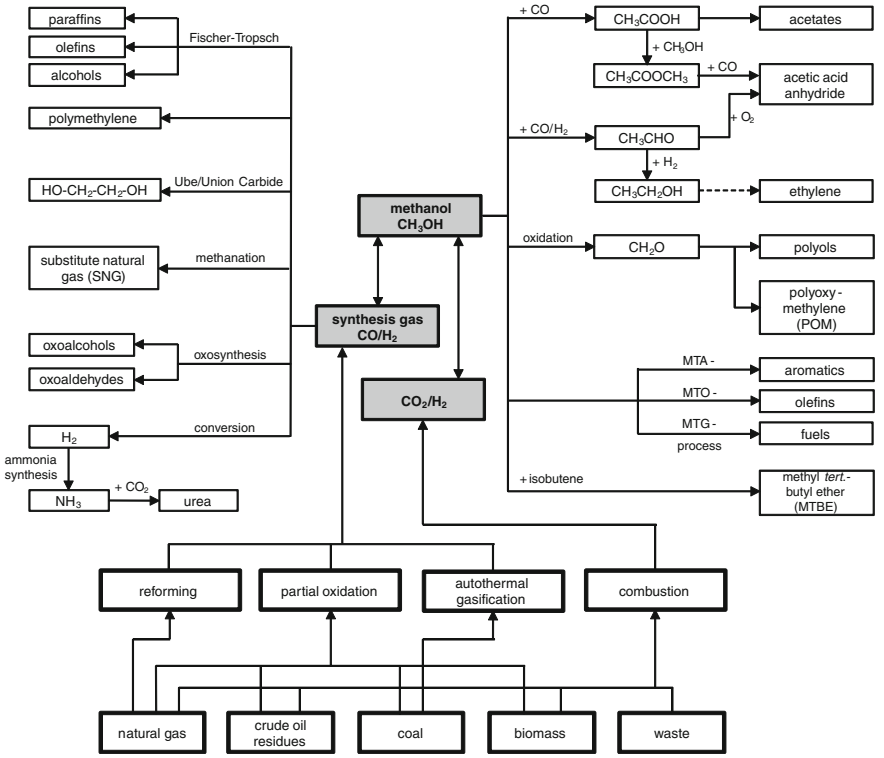

Fig. 6.1 Common processing and interconversion of synthesis gas and methanol. MTBE, methyl tert-butyl ether; MTG, methanol-to-gasoline

In Sects. 6.3 and 6.4, it becomes apparent how difficult it can be to draw a clear line between methanol use as a chemistry raw material or as an energy raw material when the latter application is as a fueling agent. As described extensively

Table 6.1 Consumption of synthesis gas for different products of C_1-chemistry

Synthesis gas product	Ratio CO:H_2	Wt% of synthesis gas in the product
Methanol	1:2	100
Acetic acid	1:1 (1:2 + 1 CO for carbonylation)	100
Ethylene glycol (direct synthesis)	1:1.5	100
Acetic acid anhydride (via methyl acetate)	1:1	85
Vinyl acetate (via methyl acetate)	1:1.25	71
Ethanol (Homologation)	1:2	72
Acetaldehyde	1:1.5	71
Ethylene and higher olefins (Mobil process)	1:2	44
Aromatics (Mobil process)	1:1.5	42
Gasoline (MTG, Mobil process)	1:2	44

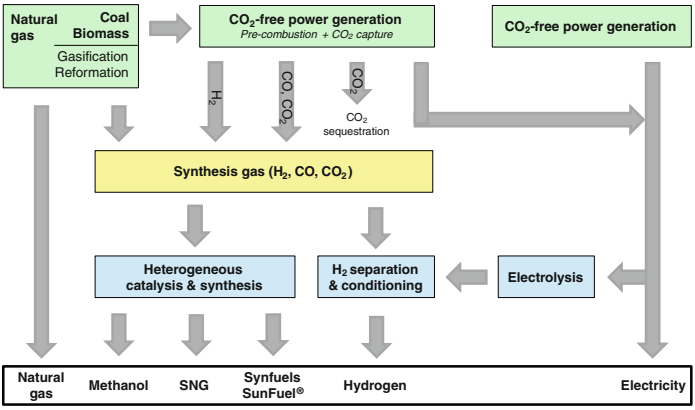

Fig. 6.2 Schematic pathways for syngas-based alternative fuels from fossil and renewable sources. SNG, synthetic natural gas. (Adapted from [8])

reviews by Höhlein et al. [8] and Olah et al. [9] and as schematically illustrated in Fig. 6.2, methanol is expected to play an increasingly important role as a substitute transport fuel or blending stock to conventional fuels. Also, derivatives of methanol such as dimethyl ether (DME) or fatty acid methyl esters (FAME) serve as alternatives to conventional crude oil-based fuels, which are readily available from fossil raw materials, as well as from biomass and organic waste.

Methanol-containing fuels for transportation have been investigated for many decades, with the purpose of using the alcohol both in ignition and in diesel engines [10, 11 and Sect. 6.3.1]. Methanol itself is mostly used as a blending stock, such as M15 (15 % methanol in gasoline), M85 (85 % methanol, 15 % gasoline) or even M100. It can be mixed in any ratio with gasoline and ethanol, has a high

octane number (RON 160) and is biodegradable. An addition of 15 vol% methanol to a 90-octane RON gasoline increases the octane number by 6–7 points [12]. The disadvantage (of any added oxygenate) is the lower heating value of methanol and a somewhat increased emission of formaldehyde in the exhaust gas.

In general, methanol fuel is toxic. In relation to conventional gasoline fuels, it is less toxic and not classified to be carcinogenic or chronically toxic. The short-term exposure limit of methanol is 250 ppm by inhalation. Small amounts of methanol taken up orally can be fatal. Symptoms are systemic acidosis, optic nerve damage, and central nervous system damage (see Sect. 5.2).

For geopolitical reasons, China is presently the most advanced country in the general use of (mostly coal-based) methanol in transportation fuels. The blending of methanol is presently exercised in 26 of 31 provinces. China's coal industry hub, the Shanxi province, is taking the lead, with more than 1,200 fuel stations offering methanol blends. All grades (M5–M100) are sold, depending on province or town. Most common in China is the use of M15, but large-fleet tests with taxis and other light duty vehicles have increasingly targeted the use of M85 and M100 fuel. In China, the estimated methanol consumption for fuel varies between 4.5 and 7.0 million tonnes (2010), representing about 5 % of China's fuel pool or a third of China's total methanol consumption of approximately 22 million tonnes in 2010 [13]. Outside China, the only major fleet test with a M85 fuel blend was started in Israel in 2012 with the purpose of investigating effects on cars and fuel pumps as well as to prepare broader introduction in the forthcoming years.

Cars with high compression engines (e.g. race cars) are often run with pure methanol for performance reasons, as well as for safety reasons because methanol fires are extinguishable with water [14]. Because of the low cetane number of methanol, there is no self-ignition in diesel engines—an issue which eventually has been overcome by adding incandescent devices or using pilot injections of conventional diesel fuel.

Increasing environmental concern about maritime transport emissions has led to new concepts for ship fuel used in special emission control areas (SECAs). In Europe, a SECA extends over the total area of the Baltic Sea, North Sea and the British Channel, restricting use of marine fuels to sulphur contents not exceeding 1 wt%—an amount that has to be reduced to 0.1 wt% sulphur by 2015. For marine diesel fuels, the limit is already 0.1 wt%. EU regulations require vessels to use 0.1 wt% sulphur fuel if remaining in port for more than 2 h. One option to meet those regulations is using the concept of alcohol/spirits and ethers as marine fuel (SPIRETH), which (temporarily) uses on-board methanol as a clean fuel. A pilot project started on a Swedish vessel in 2012 feeds a methanol/dimethyl ether (DME) mixture to an auxiliary diesel engine. DME is produced on-board by dehydration of methanol in the on-board alcohol-to-ether process (OBATE) [15].

Methyl tert-butyl ether (MTBE) produced from isobutylene and methanol is widely used as an octane enhancer to replace formerly used environmentally problematic metal-organic additives, such as tetraethyl lead. Before the broad introduction and usage of MTBE as a blending stock and octane enhancer for gasoline, processes and catalysts had been developed with the purpose of converting synthesis gas into a mix of methanol with higher alcohols through homologation reactions (Eqs. 6.1 and 6.2).

$$CH_3OH + CO + 2H_2 \rightarrow CH_3CH_2OH + H_2O \quad (6.1)$$

$$C_nH_{(2n+1)}OH + CO + 2H_2 \rightarrow CH_3(CH_2)_nOH + H_2O \quad (6.2)$$

Besides octane enhancement and replacement of lead-containing antiknock additives, the application of mixed alcohols improves methanol solubility in gasoline, increases water tolerance of the blend, and reduces Reid vapour pressure. Catalysts such as those used in Lurgi's Octamix process are copper-zinc based and contain promoters displaying certain Fischer–Tropsch activity, which enables them to generate higher carbon chain lengths in the alcohol product. Other catalysts are based on promoted MoS_2. A detailed review is given in Ref. [16].

DME made from methanol dehydration is the simplest ether molecule, with properties similar to liquid petroleum gas (LPG, Eq. 6.3).

$$2CH_3OH \rightarrow CH_3OCH_3 + H_2O \quad (6.3)$$

Apart from being used as a propellant, DME can be used in diesel engines with the advantage of high efficiency, a high cetane number, and low exhaust emissions (no particulates, no sulphur, and low NO_x). A first demonstration unit to produce bio-DME was started in 2010 in Piteå, Sweden, in which black liquor from a paper mill is gasified and converted into DME. The product is used to fuel a truck fleet [17]. DME blends with propane can also be used in gasoline engines adapted to be run with LPG.

Synthetic hydrocarbon mixtures suitable as gasoline or even diesel fuel and lubricants are accessible through methanol conversion over shape-selective (zeolite) catalysts, such as the methanol-to-gasoline (MTG) process (Eq. 6.4).

$$2n\ CH_3OH \rightarrow n\ CH_3OCH_3 + n\ H_2O \rightarrow \text{“}(CH_2)_n\text{”} + n\ H_2O \quad (6.4)$$

This process and other uses of methanol as precursor of petrochemicals are described in detail in Sect. 6.4.

Biodiesel is produced by transesterification of fats and oils. The triacyl glycerides are transformed into FAME, with glycerine as a byproduct (Sect. 6.2.20). Rape seed or palm oil, for example, can serve as feedstock, as can waste fats. The transesterification reaction to the methyl esters is run in the presence of approximately 10 vol% of methanol and an alkaline catalyst such as caustic soda or sodium methylate.

Usually, biodiesel is blended into conventional diesel in the amount of several volume percent; in Germany, this is 7 vol% (B7) [18]. In 2011, global biodiesel production amounted to approximately 18.7 million tonnes, with Europe representing 39 % of world output. The United States and Germany are the world's largest producers (3.2 million tonnes/year), followed by Argentina (2.8 million tonnes/year) and Brazil (2.7 million tonnes/year) [19].

Methanol properties for use as transportation fuel in cars and various related engine concepts are discussed in Sects. 6.3 and 6.3.2 addresses production and use of the most important fuel additive MTBE (and the corresponding amyl ether, TAME) in methanol-to-gasoline technology (MTG).

Synthesis gas is the key platform for the production of non-oil-based chemicals. Fuels, gasoline, jet fuel and middle distillates can be produced by Fischer–Tropsch synthesis or by methanol based processes such as MTG. Hydrogen, ammonia, and methanol are the most important chemicals that are also produced from synthesis gas. The paramount importance of methanol is that it can be converted into a plurality of other major bulk chemicals, as well as into fuel and fuel additives.

The supreme advantage of the methanol route versus the Fischer–Tropsch route is the flexibility of the methanol path with respect to the market. Depending on the market demand, methanol can either be sold as such or in form of its primary or secondary derivatives.

Most of the processes to convert methanol to hydrocarbons are based on zeolites of the pentasil type. These catalysts and the chemistry of the corresponding methanol conversion are discussed in Sect. 6.4. Sections 6.4.1 and 6.4.2 are devoted to the methanol-to-gasoline process and the methanol-to-olefin process, respectively. Special attention is given in Sect. 6.4.3 to the methanol-to-propylene process due to the paramount importance of polypropylene. Finally, a short review of the production of other methanol derivatives is given in Sect. 6.4.4.

In particular, when methanol conversion to gasoline and olefins is discussed, it becomes clear that the boundary between both uses is slim. The message of both sections, however, is obvious: Oil substitution by methanol is technically feasible and can be realised in an economically viable manner while maintaining our living standards (see also Chap. 7).

Parallel to the efforts deployed for the substitution of oil and gas as chemistry raw materials, new technologies were developed with the purpose of not only substituting oil but also the combustion engine itself. This development culminated in the development of fuel cells using a variety of concepts. Sect. 6.5 would not be complete without discussing the green hydrogen issue. Hydrogen generation from methanol as a clean hydrogen source in lieu of natural gas and applications of methanol in biotechnology are described, from which the enormous potential of methanol becomes intriguingly evident.

6.2 Methanol-Derived Chemicals: Methanol as a C_1-Base

Martin Bertau[1], Konstantin Räuchle[1], Nicola Ballarini[2] and Matthias S. Wiehn[3]

[1]*Institute of Chemical Technology, Freiberg University of Mining and Technology, Leipziger Straße 29, 09599 Freiberg, Germany*

[2]*Clariant Catalysis Italia, Via G. Fauser, 36/B, 28100 Novara, Italy*

[3]*Evonik Industries AG Luelsdorf, Feldmühlestraße 3, 53859 Niederkassel-Luelsdorf, Germany*

Methanol is of particular interest for the chemical industry because it can easily be interconverted as a chemistry or energy raw material. A series of chemical syntheses can be operated on the basis of methanol instead of classic petrochemicals. As can be seen in this chapter, attempts to switch to the use of methanol as a raw

material in classic refinery processes have to be regarded with the same restraint as for every facile change in complex matters. The reader will see that some processes, such as acetic acid synthesis, have always been methanol based, whereas others are new processes in industrial chemistry. Indeed, the great majority of established petrochemical products are achievable using both crude oil and methanol as a raw material base.

6.2.1 Acetic Acid Anhydride

Acetic anhydride mostly serves as an acetylation reagent, such as in the production of acetyl cellulose, pharmaceuticals (e.g. acetyl salicylic acid), acetanilide and other intermediates.

6.2.1.1 Acetic Acid Anhydride Through Carbonylation of Methyl Acetate

Acetanhydride was the first large-scale product based on synthesis gas produced using the process by Halcon SD and Tennessee Eastman (a division of Eastman Kodak), who combined their technical knowledge, through catalytic carbonylation of methyl acetate according to the following reaction:

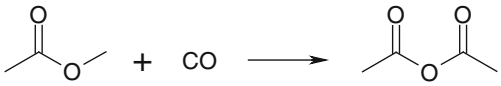

Converting 2 mol of methyl acetate with 2 mol of CO gives 2 mol of acetic anhydride. Of these 1 mol is removed as the final product, while the other 1 mol is converted with methanol to give 2 mol of methyl acetate, which are re-used for the reaction. Proceeding this way, acetic anhydride synthesis requires nothing else but methanol and CO. The latter is recovered from synthesis gas; hydrogen is used for the synthesis of methanol. When acetic anhydride is used for the production of cellulose acetate, the acetic acid being released from the acetylation reaction can be recovered and used for the esterification of methanol, which increases the amount of acetanhydride produced in a plant. The first large-scale plant based on coal with a capacity of about 230,000 t/a of anhydride was put into operation in Kingsport, Tennessee in 1983. Since then, its capacity has been increased to 300,000 t/a [20, 21]. In theory, only synthesis gas is needed as a starting material: once converted into methanol, once used for CO supply. To start up the system, however, methyl acetate is required.

The most developed route to acetanhydride on a technical scale is the carbonylation of methyl acetate, which preferably is realised at 150–200 °C and 25–75 bar in the presence of rhodium catalysts, such as $[RhI_2(CO)_2]$ (Monsanto catalyst; see Sect. 6.2.8), methyl iodide and an inorganic iodide or hexacarbonylchromium/picoline, for instance, as promoters.

To start the reaction, methyl acetate is required, which is produced from acid catalysed esterification of acetic acid with methanol. In Fig. 6.3, the rhodium-catalysed reaction (a) corresponds to acetic acid synthesis according to the Monsanto process. Without addition of inorganic iodide, the reaction proceeds according to the acid cycle (Fig. 6.3, left), where CH_3I is generated from a reaction of methyl formate and HI (b). Acetyl iodide and acetic acid react in an equilibrium reaction to give acetic acid anhydride and HI (c).

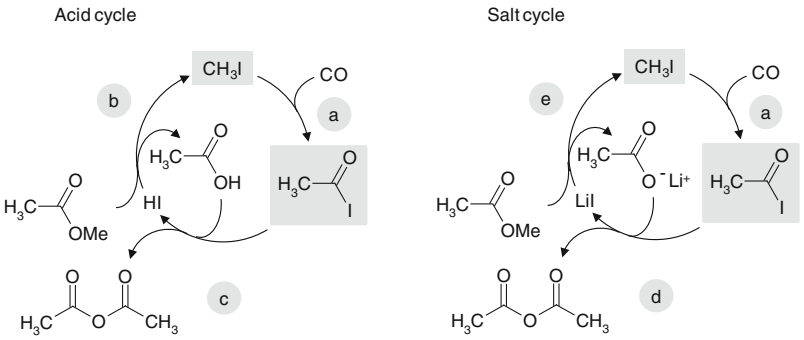

Fig. 6.3 Iodide cycles in acetic anhydride production without promoter (acid cycle, left) and with LiI as promoter (salt cycle, right). Starting material and product of the rhodium-catalysed cycles are marked in grey. (After [22])

In contrast to the Monsanto process, the reaction system is free of water, what leads to a long induction period; furthermore, the reaction proceeds rather slowly. It was therefore necessary to optimise the process. The induction period is due to the fact that there is no suitable reducing agent for the catalyst formation ($Rh^{III} \rightarrow Rh^{I}$). The addition of H_2 does not only shorten the induction phase, inactive Rh^{III} complexes that have been formed in the course of the reaction are subject to reduction, too.

Upon addition of inorganic iodides (LiI, $(NR_4)I$ or $(PR_4)I$) as promoters, the reaction proceeds according to the salt cycle (Fig. 6.3, right). Here, it is the inorganic iodide instead of HI from which CH_3I is regenerated from the reaction with methyl acetate (e). The resulting lithium acetate reacts with acetyl iodide to give acetic acid anhydride (d), with the advantage of the equilibrium of this reaction (in contrast to the analogous reaction (c) in the salt cycle) being far on the right side.

The individual steps can be summarised as follows:

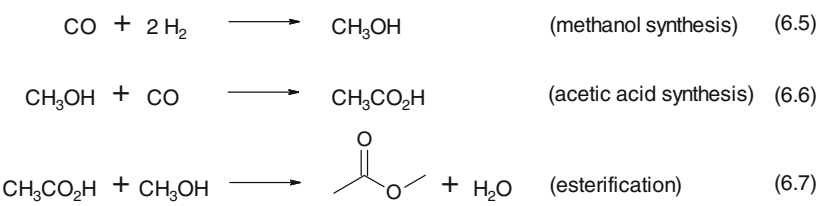

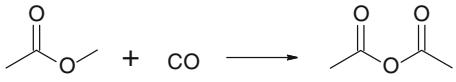

Besides methanol synthesis (6.5), reactions (6.6) and (6.7) are continuously operated reactions. Reaction (6.8) and (6.9) need to be conducted only once. The net gas reaction is

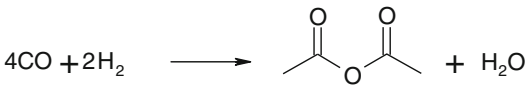

The methyl acetate process is the dominant synthetic route to acetanhydride in the United States. In Europe, approximately 50 % is produced via the addition of ketene to acetic acid (see Sect. 6.2.1.2); in Japan, this is the sole industrially realised process.

Follow-up approaches by Halcon and Hoechst pursue the homogeneously catalysed carbonylation of dimethyl ether (DME) and methyl acetate [23, 24]. Other approaches work with glacial acetic acid as the solvent. The reaction proceeds via intermediary formed methyl acetate. With nickel acting as a catalyst, the reaction furnishes methyl acetate only [23, 25, 26].

6.2.1.2 Wacker Process

The Wacker process uses acetic acid that is dehydrated to give ketene in the presence of triethyl phosphate at reduced pressure and 700–750 °C. The H_3PO_4 that is formed in the course of the reaction is neutralised with NH_3 or pyridine and the fission gas is cooled down rapidly in order to freeze the reaction. After purification, ketene is funnelled in glacial acetic acid, where it reacts at 0.05–0.2 bar to acetic acid anhydride.

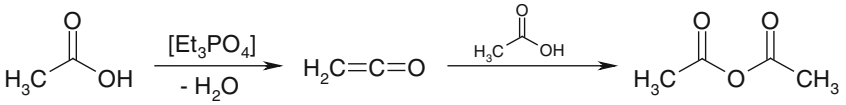

The Wacker process benefits from the availability of ketene, which can be isolated as reactive intermediate. Starting from acetic acid is economically favourable because the starting material can be produced cost-effectively by methanol carbonylation (see Sect. 6.2.8). Moreover, acetic acid recovered from acetylation reactions can be reintegrated into the process, thus creating a cheap raw material base.

6.2.1.3 Other Processes

Alternatively, acetic acid anhydride can be obtained from dimethyl carbonate carbonylation, where CO inserts in the O–CH_3 bond:

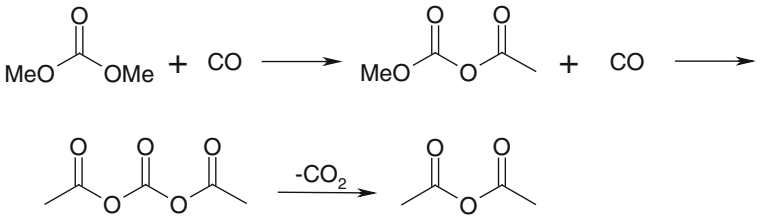

Also, DME has been used, where methyl acetate is formed as an intermediate:

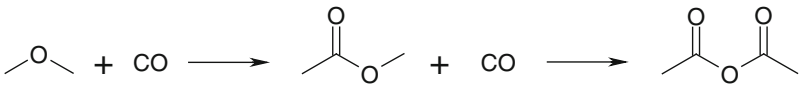

Whatever process is chosen, industrial acetic acid anhydride production can be realised exclusively on the basis of synthesis gas or on coal or gas (i.e., a cost-effective C-base).

6.2.2 Production of Vinyl Acetate Monomer on the Basis of Synthesis Gas

In 2005, vinyl acetate production capacity amounted to approximately 5.5 million tonnes. Its synthetic use consists solely of its reactive vinyl group, which has been used for homo- and co-polymer production, with polyvinyl acetate (PVA) as its most important product. The world's largest manufacturer of vinyl acetate monomer (VAM) is Celanese (22 %) with a capacity of $\sim$1.2 million t/a.

For VAM production, there exist four major routes:

1. Addition of acetic acid to acetylene
2. Conversion of acetaldehyde with acetanhydride via ethylidene diacetate
3. Hydrocarbonylation of methyl acetate via ethylidene diacetate
4. Acetoxylation of ethylene

Among these, routes 1–3 are generally economically unfeasible. The predominant process delivers VAM through acetoxylation of ethylene. All processes can be realised on the basis of synthesis gas with acetic acid as starting material on the one hand and methanol-derived ethylene and its derivatives acetaldehyde and acetylene on the other.

6.2.2.1 VAM Through Acetoxylation of Ethylene

Modern catalytic production processes for VAM from acetic acid and ethylene are based on an observation by Moiseev and co-workers (1960) who found that ethylene oxypalladation (using the Wacker process to acetaldehyde) can be extended to nonaqueous solvents. These act themselves as nucleophiles instead of water, what is the reason why they are found in the final product. Conversion in acetic acid/sodium acetate delivers VAM via intermediary-formed acetoxyethyl palladate(II). It was this discovery that allowed for a rapid access to VAM starting from ethylene and acetic acid (Fig. 6.4).

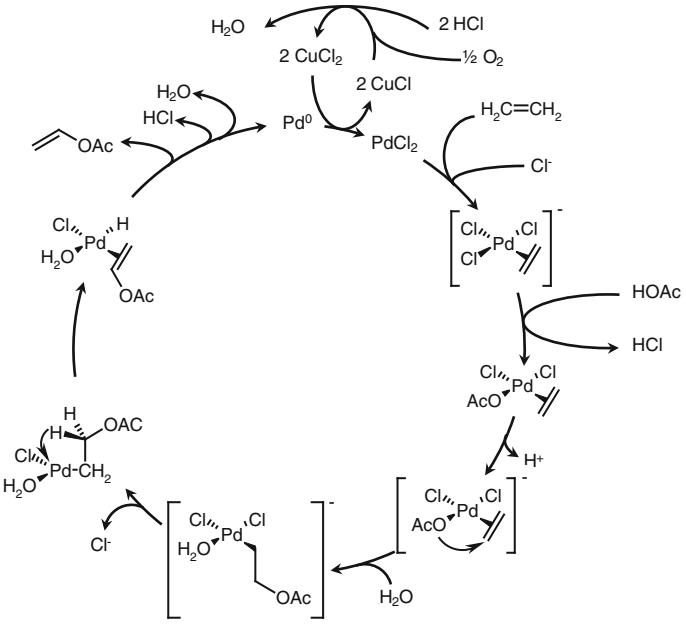

Fig. 6.4 Palladium catalysed acetoxylation of ethylene. (Modified from [21, 27])

The process is similar to classic ethylene oxidation to acetaldehyde. However, because an acidic hydrogen is missing in the vinyl acetate ligand, there is no reductive elimination leading to the vinyl compound. It is the hydrido complex that decomposes to release VAM.

Although it was the elucidation of a homogeneously catalysed reaction that led to a commercial process, on a technical scale the reaction is conducted as heterogeneous process:

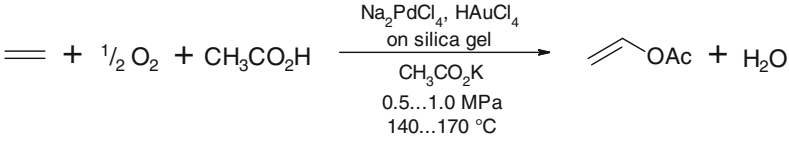

6.2.2.2 VAM Through Hydrocarbonylation of Methyl Acetate via Ethylidene Diacetate

The hydrocarbonylation route was developed by Tennessee-Eastman with the purpose of directly integrating coal as a carbon source into the production of VAM. The required synthesis gas is provided by coal gasification according to a modified Texaco/Ruhrchemie/Ruhrkohle gasification process. An integrated gasification/VAM plant has a production capacity of 220,000 t/a from 1.8 million tonnes of lignite.

As shown above (Sect. 6.2.1.1), carbonylation of methyl acetate yields acetic anhydride. If, however, the reaction is conducted with the same or similar catalysts, such as $RhCl_3$ + CH_3I + picoline or triphenylphosphine, but with synthesis gas instead of pure CO at 150 °C and 40–70 bar, acetic acid and ethylidene diacetate are formed as summarised in Fig. 6.5:

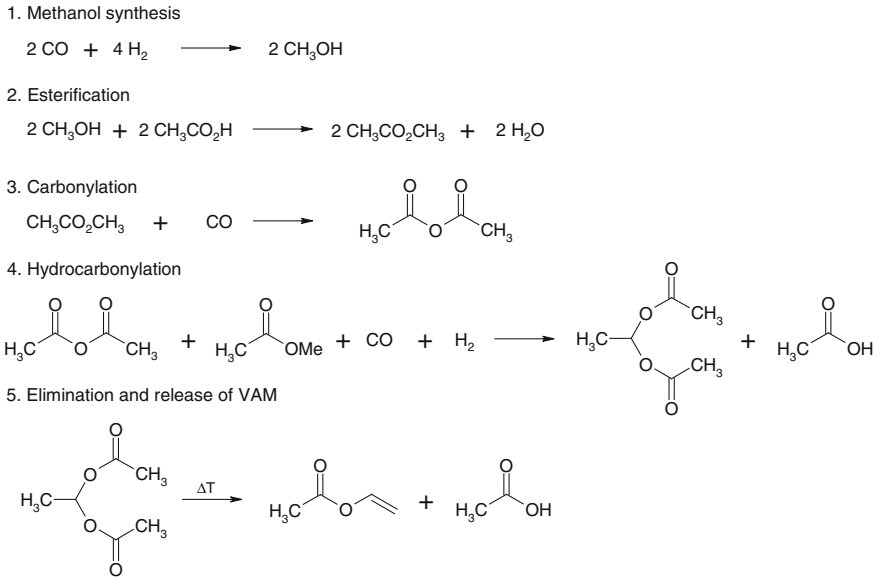

Fig. 6.5 Vinyl acetate monomer formation from synthesis gas via methyl acetate and ethylidene diacetate

At 170 °C, in the presence of benzene sulphonic acid in the liquid phase, accompanied by elimination of acetic acid, ethylidene diacetate can be converted into vinyl acetate (Fig. 6.5). The central process in this reaction sequence is the concerted conversion of acetic anhydride and methyl acetate with carbon monoxide and hydrogen—the hydrocarbonylation step—in the course of which acetic

acid and ethylidene diacetate are being formed (reaction 6.8). In the presence of CO alone, the reaction does not proceed further than the formation of acetic anhydride. Only in the presence of hydrogen (from the synthesis gas) are consecutive reactions initiated. This reaction does not proceed in the absence of halogen sources. Instead of methyl iodide, acetyl chloride and other methyl halogenide come into use.

Both processes are characterised by extraordinarily corrosive reaction conditions, which require the devices to be made from tantalum, titanium, zirconium, or Hastelloy steels. In addition, chlorinated byproducts are formed, thus necessitating sumptuous removal processes.

6.2.3 Ethylene Glycol

6.2.3.1 Ethylene Glycol on Basis of Synthesis Gas

Currently, the production of ethylene glycol is based on ethylene oxide. In fact, it is the largest derived product from ethylene oxide, and the majority of glycol processes are based on ethylene. However, with C_1-chemistry gaining increasing importance in industrial chemistry, the use of synthesis gas as a starting material is of growing interest [20].

There are two major fields of application for ethylene glycol: antifreezing agents (in which glycol is contained in up to 95 %) and diol for polyester synthesis. Polyethylene terephthalate (PET), which is the most important product, is used for the production of fibres, one-way beverage containments, foils, and resins. Further applications exist in surfactant synthesis. Polyethylene glycol is used as brake and hydraulic fluid, as plasticiser and an antifriction agent (Fig. 6.6).

By the end of the 1940s, DuPont demonstrated the suitability of synthesis gas for ethylene glycol production by hydrogenating CO in aqueous cobalt salt solution. In the 1970s, Union Carbide investigated synthesis gas conversion in homogeneous rhodium carbonate systems using various different promoters and Lewis acids containing nitrogen. In a high-pressure reaction at 1,400–3,400 bar and 125–350 °C, a mixture of ethylene glycol, 1,2-propanediol and glycerine is obtained with a selectivity sum of $\leq$70 %. It is apparent that these extreme reaction conditions coupled with the insufficient catalytic effectivity stand against realisation on a technical scale. This is in line with a series of investigations undertaken by other companies, mostly focusing on rhodium, palladium, copper and ruthenium, for which no significant progress was made either. Figure 6.7 provides an overview of ethylene glycol synthesis starting from synthesis gas.

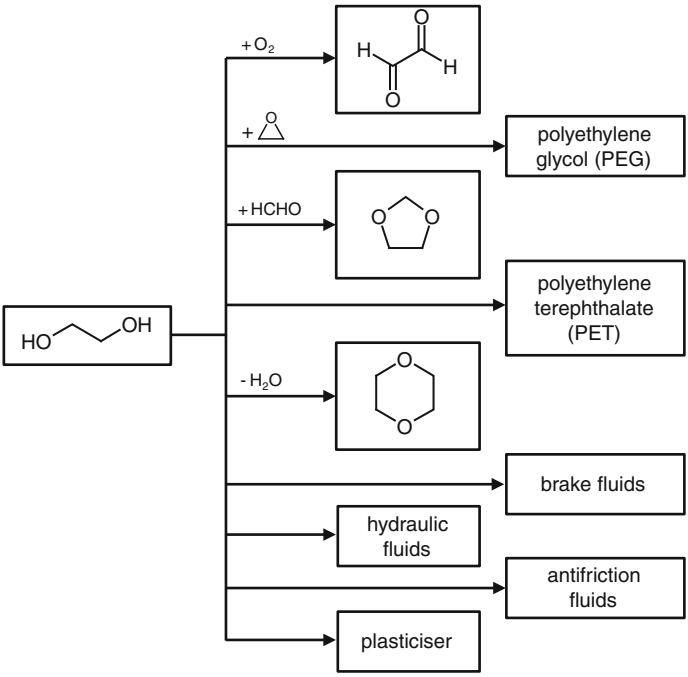

Fig. 6.6 Utilisation of ethylene glycol

1. Methanol synthesis

$$CO + H_2 \longrightarrow CH_3OH$$

2. Dehydrogenation to formaldehyde

$$CH_3OH \longrightarrow H_2C{=}O + H_2$$

3. Glycolic acid synthesis

$$H_2C{=}O + CO + H_2O \xrightarrow{H_2SO_4} HO{-}CH_2{-}COOH$$

4. Esterification

$$HO{-}CH_2{-}COOH + CH_3OH \longrightarrow HO{-}CH_2{-}COOMe + H_2O$$

5. Hydrogenation of glycolic acid methyl ester and release of ethylene glycol

$$HO{-}CH_2{-}COOMe + H_2 \xrightarrow{\Delta T} HO{-}CH_2{-}CH_2{-}OH + CH_3OH$$

Fig. 6.7 Ethylene glycol synthesis on the basis of synthesis gas. [28]

For these reasons, the direct conversion of synthesis gas was not further pursued in favour of indirect routes starting from the synthesis gas products methanol or formaldehyde instead. Here, the strategy is to subject the latter to hydroformylation, oxidative carbonylation, or carbonylation to intermediates (the hydrogenation of which delivers ethylene glycol). In this context, the Ube process (1978) has attracted the most economic interest, in particular through further developments in the second process step by Union Carbide (UCC), who is currently undertaking test runs. On this basis, among the synthesis gas routes to ethylene glycol, the Ube/UCC process has the best chance of being commercially realised. The Ube/UCC approach consists of an oxidative carbonylation of methanol to dimethyl oxalate followed by hydrogenolysis to ethylene glycol and methanol:

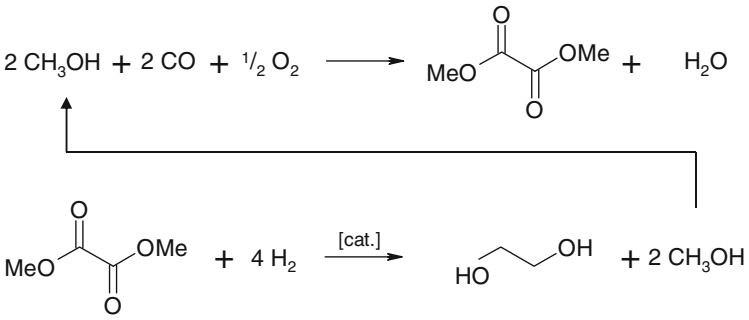

The first process step is conducted at 90 bar and 110 °C with 97 % yield in the presence of a palladium catalyst in 70 % HNO_3. Nitric acid is needed to convert methanol into methyl nitrite as a reactive intermediate. The second hydrogenation step proceeds with ruthenium oxide, for instance, in ~90 % yield under reformation of methanol. Instead of methanol, other alcohols such as *n*-butanol can be used. In fact, through the use of methanol as a synthesis gas-derived substrate and both CO and H_2, it is synthesis gas on which this process is based [29].

DuPont developed a three-step synthesis starting with formaldehyde from a hydrating carbonylation with sulphuric acid as catalyst at 500–700 bar and 200–250 °C, which is followed by esterification of intermediary glycolic acid with methanol (Fig. 6.8).

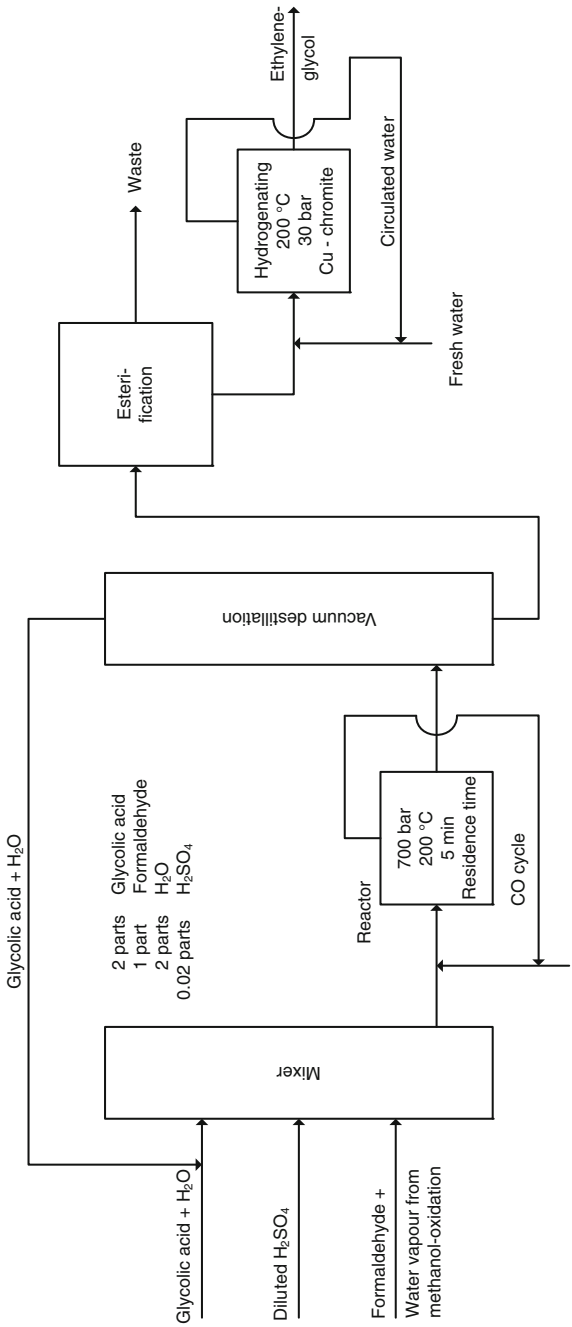

Fig. 6.8 DuPont's ethylene glycol process. (Adapted from [20])

Finally, the methyl ester is hydrogenated to give ethylene glycol:

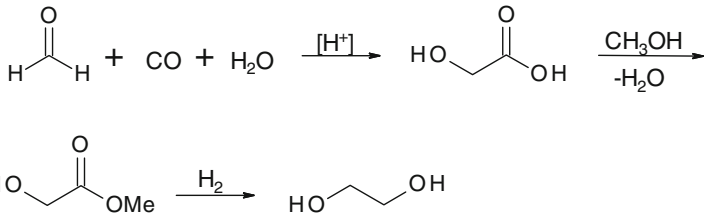

Glycol production using this process ceased by end of the 1960s, but plants were kept in operation for glycolic acid production (≤60,000 t/a). With growing interest in C_1-chemistry, several companies have developed alternative approaches, although none of which have yet come to realisation on a technical scale.

Glycolic acid serves as cleaning agent for boiler plants and conduits or as chelating agent for Ca and Fe ions in boiler feed water. It is used in textile, leather, and paper processing and the esters serve as solvents for varnishes.

6.2.3.2 Ethylene Glycol from Transesterification of Dimethyl Carbonate

See Sect. 6.2.10.2.

6.2.4 Methyl Formate and its Role as Synthetic Building Block in C_1-Chemistry

Methyl formate is produced from CO and methanol. As such, it is a useful synthetic C_1 building block. The compound can be used as chemical storage for both CO and CH_3OH, from which the latter can be released in the course of a reaction. Because of this property, methyl formate has attracted increased interest for synthetics in recent decades [20].

6.2.4.1 Methyl Formate Production Through Methanol Carbonylation

As early as in 1925, methyl formate was manufactured by BASF by reacting carbon monoxide with methanol. The reaction proceeds exothermically under pressure in the presence of sodium methylate (see Sect. 6.2.20) as a catalyst with approximately 29.3 kJ/mol (Fig. 6.9).

The methanol carbonylation to methyl formate resembles the process leading to acetic acid. Which product is formed depends on the catalyst used and the locus of CO insertion. If it is the carbinolic O–H bond (Fig. 6.9a), methyl formate is produced; if CO is inserted into the C–O bond (Fig. 6.9b), acetic acid is formed.

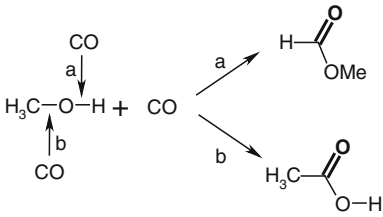

Fig. 6.9 Methanol carbonylation products methyl formate and acetic acid are produced according to regioselectivity of the catalytic reaction. **a** Insertion into the O–H bond furnishes methyl formate. **b** Insertion into the C–O bond furnishes acetic acid

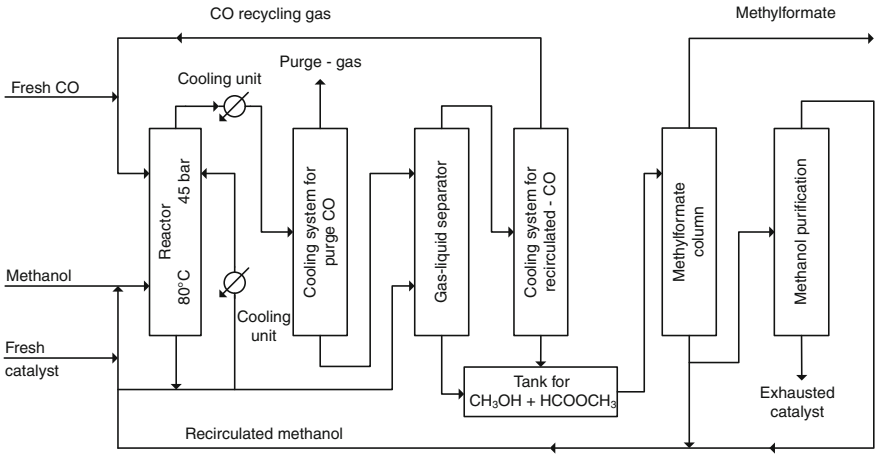

Fig. 6.10 The carbon monoxide from the top of the reactor is passed through a cooler in a cooling system in order to remove entrained product and methanol, which are fed into a gas–liquid separator. Impure CO (purge gas)is utilised as fuel gas. At the reactor bottom, the mixture of methanol and methyl formate is removed. One portion of the mixture is recycled via a cooler as a cycle product for reactor temperature maintenance. Together with the methanol/methyl formate mixture from the cooling system (purge gas separation), the remainder is separated from cycled CO in a gas–liquid separator. In a second cooling system, the cycle-CO is liberated from entrained liquids before it is fed to the reactor together with fresh CO. The product streams are combined and introduced into the methyl formate column. Pure methyl formate is taken overhead. Methanol still contains some catalyst, for which reason it is cycled back to the reactor from the bottom of the column, thereby adding some fresh catalyst. In another column, a portion of backcycled methanol is liberated from heavy fractions and spent catalyst. The purified methanol is funnelled into the back-methanol stream. (Adapted from [30])

Figure 6.10 shows the principle of a methyl formate production plant. In backward-feed operation, methanol and carbon monoxide are brought into reaction in a continuously operated reactor at 45 bar and about 80 °C in the presence of 2 % sodium methylate in methanol. All reagents and devices must be completely

free of water; otherwise, sodium formate will be formed, which precipitates and can clog the pipes. CO_2, H_2S and O_2 must be removed, too, but methane and hydrogen do not interfere. One can use for these purposes highly CO-enriched gases from second-generation coal gasification plants, which can contain up to 75 % CO and allow for less complex conversion into pure CO. CO conversion is 95 %, whereas methanol conversion is 30 %. The yield in terms of CO and methanol conversion is 99 %. Per hour and litre of reaction space, 800 g of methyl formate (b.p. = 31.8 °C) are formed.

6.2.4.2 Methyl Formate Production Through Methanol Dehydrogenation

A more recent approach to methyl formate was developed by Mitsubishi. Under yet unpublished copper-catalysed reaction conditions, methanol is dehydrogenated in the gas phase:

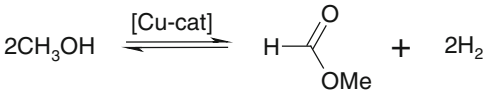

As a byproduct, formic acid is formed, mostly in undesirable nonselective oxidative degradation reactions. The amounts are rather small and in most cases do not sum up to economically viable concentrations. However, the formic acid impurities account for the greater process effort because the corrosive byproduct requires titanium columns for distillative separation. Yet, HCO_2H-formation was reported to reach up to 18 % in the product. Under these conditions, the additional process effort is overcompensated by formic acid separation, and the bycomponent even contributes to overall process economy.

The Mitsubishi process has roots in early activities by Industrial Alcohol Co. in the 1920s, who were the first to report on the dehydrogenative variant to methyl formate [31, 32]. As catalyst copper was used, however, conversions and yields were unsatisfactory. In the late 1970s, Japanese companies regained interest in this approach. Particularly with Cu-Zr-Zn- and Cu-Zr-Zn-Al catalysts, $\leq$50 % conversion with methyl formate selectivity (up to 90 %) were obtained [33–36]. Based on these catalysts, Mitsubishi Gas Chemical erected a plant on the semi-technical scale in 1979. The catalysts displayed long run times, and space-time yields up to 3,000 kg m^{-3} h^{-1}were obtained. Figure 6.11 provides a simplified scheme of a methanol dehydrogenation plant [30].

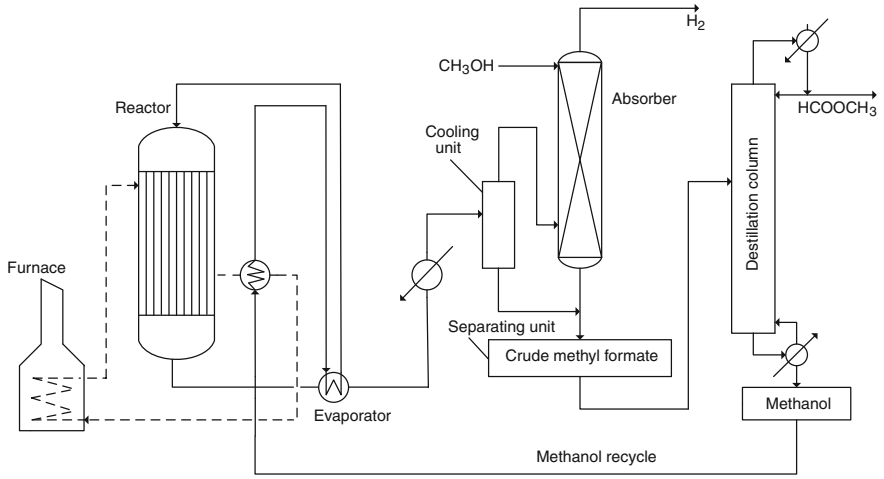

Fig. 6.11 Methyl formate production by dehydrogenation of methanol. (Adapted from [37])

Although current dehydrogenation catalysts consist of copper, several compositions have been tested since, particularly those containing Ti, Zr or rare earth metals. However, none provided the productivity of copper [38].

6.2.4.3 Methyl Formate Production catalysed by Potassium Methylate

Novel approaches pursue methyl formate production through nucleophilic attack of methoxide at CO under H_2 atmosphere with $Mo(CO)_6$ as a co-catalyst [39]:

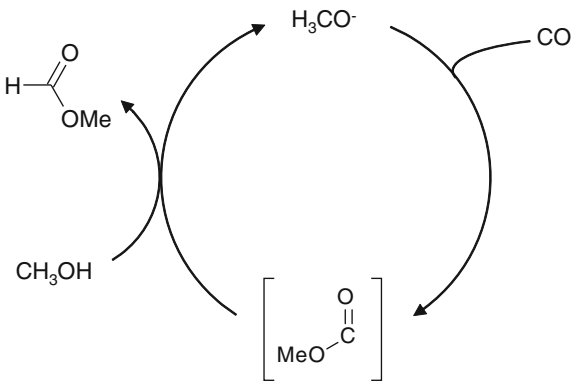

6.2.4.4 Methyl Formate as a Synthetic Building Block

Because its production is based exclusively on synthesis gas, as well as the fact that it is a versatile starting material for a series of chemical processes, methyl formate has great synthetic potential in industrial C_1-chemistry [20, 40].

Hydrolysis to Formic Acid

See Sect. 6.2.5.2.

Glycolic Acid Methyl Ester and Ethylene Glycol

Reacting methyl formate with formaldehyde in presence of Brønsted (e.g. H_2SO_4 or organic sulphonic acids) or Lewis acids at ambient pressure and 70–200 °C leads rapidly to glycolic acid methyl ester, which can be converted to ethylene glycol by copper-catalysed hydrogenation:

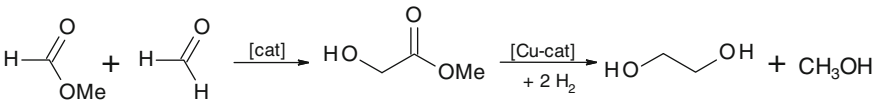

Alternatively to formaldehyde, paraformaldehyde or trioxane can be used. This reaction resembles hydrating carbonylation of formaldehyde, which along similar reaction parameters yields ethylene glycol as well (see Sect. 6.2.3), thus constituting an alternative to the DuPont process to glycolic acid, with the difference of methyl glycolate being produced directly. Solid Lewis acids are also suitable but require higher reaction temperatures (6 bar and 110 °C).

The follow-up chemistry of methyl glycolate is manifold. Reaction with CO delivers malonate ester, an important intermediate in fine chemistry, such as in the production of pharmaceuticals or pesticides:

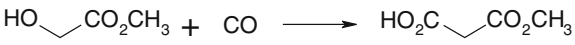

When reacted with ammonia, glycine, the simplest amino acid is formed:

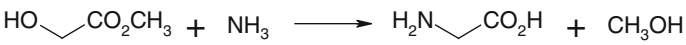

Hydrolysis to glycolic acid and methanol allows the former to undergo self-condensation to polyglycolate, which is of particular interest as a surgical suture because it is easily hydrolysed in vivo:

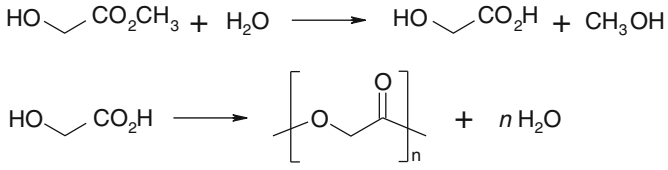

Methyl Propionate

In polar solvents in the presence of Ru or Ir complexes, methyl formate and ethylene react at 190–200 °C to give methyl propionate:

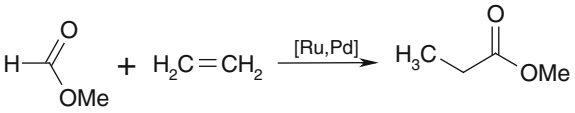

When the reaction takes place in the presence of iodide at 80 bar and 180 °C in N-methyl pyrrolidone (NMP), methyl ethyl ketone (MEK) is the major product, with up to 50 % selectivity [41]:

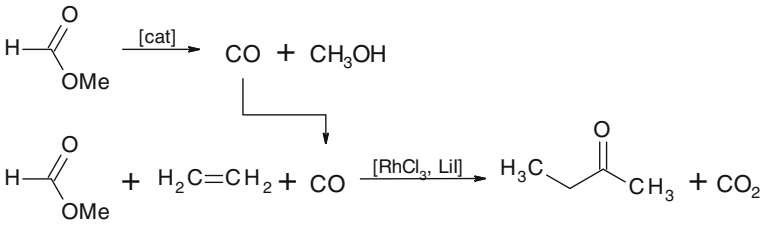

However, if the reaction is conducted with LiBr present, methyl formate has been observed to be subject to a disproportionation reaction. As the outcome of this reaction, gaseous CH_4 and CO_2 are formed as the sole products [41]:

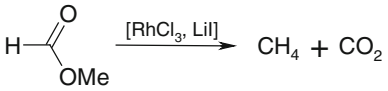

Isomerisation to Acetic Acid

Upon heating at 300 bar with CO in the presence of iodine and metal salts such as cobalt, iron, nickel or mercury, acetic acid is formed at 220 °C from methyl formate within one hour in 94 % yield [42]. The reaction proceeds particularly smoothly with rhodium methyl iodide and CO. Acetic acid is formed with 98 % yield at 100 °C, with the reaction being very much like methanol carbonylation according to the Monsanto process.

Mechanistically, methyl formate isomerisation to acetic acid can be regarded as a sequence of backward reaction to methanol and CO followed by methanol carbonylation:

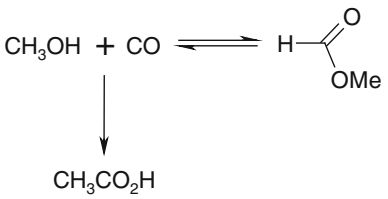

Formally, methyl formate can be regarded as a reservoir for methanol and CO, from which the final product acetic acid is produced. In terms of process economy, a reaction sequence via two differently catalysed single steps will hardly be able to compete with a direct route. Indeed, because of the superiority of the Monsanto and Cativa processes, this reaction has no technical relevance.

Hydroisomerisation over Ir or Rh Catalysts to Acetaldehyde

Comparable to acetic acid formation from methyl formate either a reductive carbonylation of methyl formate into acetaldehyde or its homologation into methyl acetate takes place under CO pressure in an Rh/RhI_2 catalysed reaction. Acetaldehyde formation occurs selectively only in dipolar aprotic solvents, such as NMP (or related solvents) with high Rh/I^- ratio, low methyl formate concentration, and high CO pressure. Methyl acetate is formed at a lower Rh/I^- ratio, higher methyl formate concentration, and under lower CO pressure [43, 44].

Oxidative Conversion with Methanol at Se Catalysts to Dimethyl Carbonate

The conversion of methyl formate and methanol over Se catalysts produces dimethyl carbonate (DMC; see Sect. 6.2.10) in the presence of oxygen [45]:

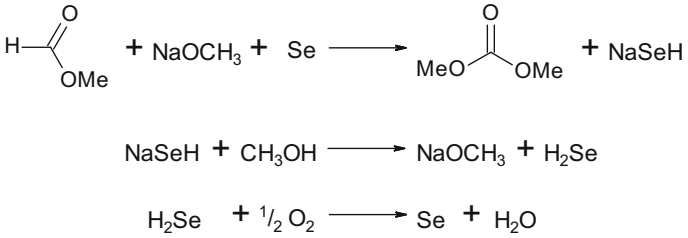

The reaction suffers from methyl formate decarbonylation to methanol as a competing reaction. In addition, selenium displays poor catalytic selectivity.

Synthesis of Formamide and its *N*-methyl Derivatives

Formamide and its *N*-methyl derivatives are technically versatile compounds. For their polar properties, they are highly useful selective solvents and extractants. Dimethyl formamide (DMF) is one of the few solvents that are suited for fibre production. DMF worldwide production is estimated to 220,000 t/a, with the largest manufacturer being BASF. Analogous to methyl formate ammonolysis to formic acid, both *N*-methyl and *N*,*N*-dimethyl formamide are obtained by reactions with methyl and dimethyl amine, respectively:

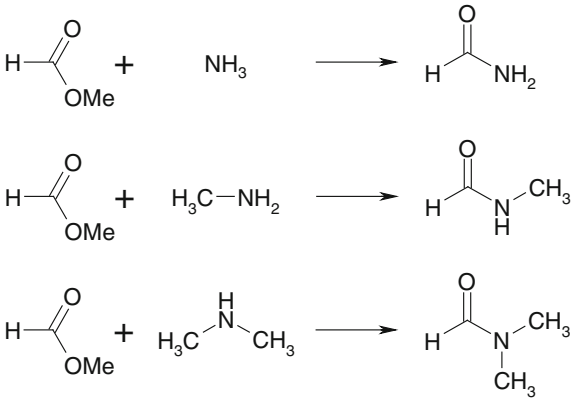

Alternatively, formamide as well as *N*-methyl and *N*,*N*-dimethyl formamide are accessible directly through reacting CO and NH_3 in methanol at 20–100 bar and 80–100 °C in the presence of sodium methanolate:

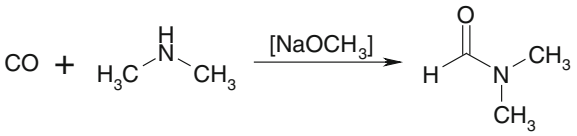

Here too, the synthetic basis for all reactants and solvents is synthesis gas. Using the latter approach, DMF yield can reach up to 95 %. On a technical scale, this process is operated in several plants, such as in the Leonard process.

Palladium Catalysed Oxidative Carbonylation of Olefins

Oxidative carbonylation of olefins makes use of the property of methyl formate to form an equilibrium with CO and CH_3OH in the presence of methylate anions; thus, it serves as a CO reservoir, avoiding direct use of CO.

Key steps of the process are methyl formate decarbonylation and formation of the methoxy-carbonyl complex, followed by insertion of the olefin and ß-elimination, furnishing the olefinic ester and Pd^0 (Fig. 6.12). Consequently, the reaction requires catalyst regeneration, which is best accomplished by $CuCl/CuCl_2$. Therefore, it very much resembles the Wacker process (see Sect. 6.2.1.2). Alternatively, $FeCl_2/FeCl_3$ are also suited, but to the detriment of selectivity favouring benzaldehyde byproduct formation [46]. Further improvements can be achieved by conducting the reaction in the presence of one aliquot of triethyl amine, thus allowing for very mild reaction conditions (1.0 bar, 30 °C) [47].

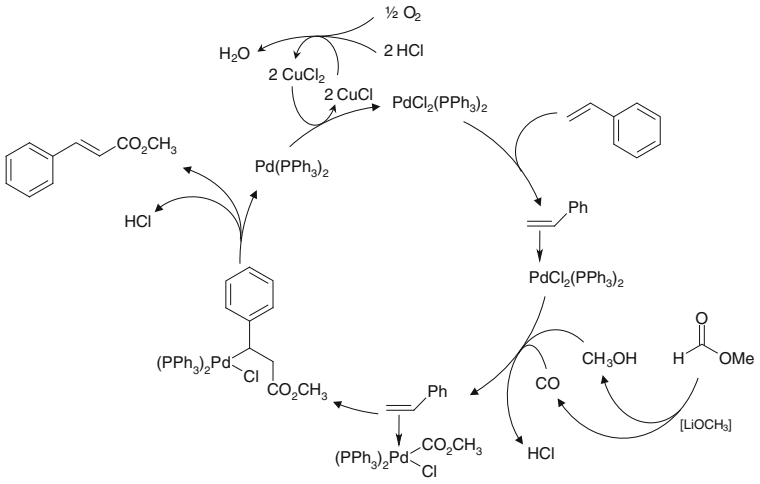

Fig. 6.12 Palladium catalysed oxidative carbonylation of styrene to methyl cinnamate. (Adapted from [46])

The oxidative carbonylation is suited for olefins other than styrene, too. It has to be taken into account that mild reaction conditions favour this reaction; however, with harsher conditions, aldehyde and polymerisation occur in disfavour of carbonylation.

Methanol Synthesis

As an alternative to classic methanol production, synthesis gas conversion to the C_1-carbinol can be carried out in the liquid phase, too. The two-step process consists of an alkali metal alkoxide (typically sodium methoxide)–catalysed carbonylation of methanol to methyl formate, which here acts as an intermediate rather than starting point for follow-up synthetic procedures. Hydrogenolysis over a copper-chromite type catalyst then delivers 2 mol of methanol per mole of methyl formate. However, because one mole of methanol is required for subsequent carbonylation in order to keep the cycle upright, the net output is 1 mol of methanol (Fig. 6.13). The process can be run also with higher alcohols.

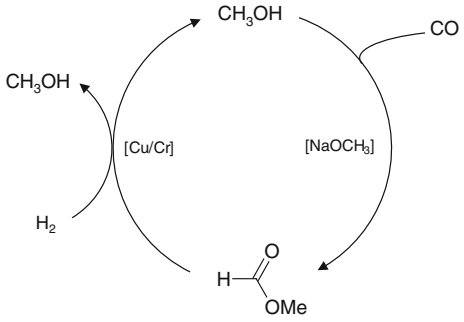

Fig. 6.13 Methanol synthesis through intermediate formation of methyl formate. (Adapted from [40])

The mild reaction conditions and the favourable thermodynamic equilibrium for product formation make this route interesting. However, the process is highly sensitive towards the presence of CO_2, for which reason a rigorous removal of CO_2 has to be ensured. The reaction is conducted at 1.0 bar and 140 °C with a selectivity >90 % and methyl formate conversion of 70–80 %. Higher H_2 pressures are in favour of this process [40].

Halogenation

Monochlorination and complete chlorination of methyl formate deliver methyl chloroformate and trichloromethyl chloroformate, respectively:

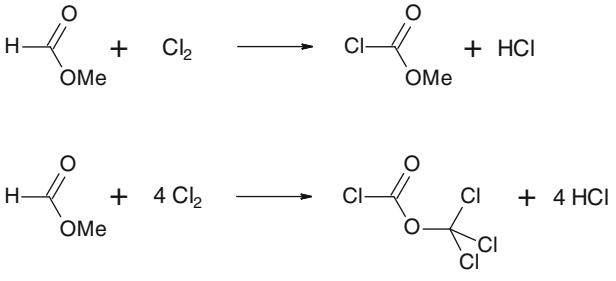

Methyl chloroformate is used for the synthesis of methoxy carbonyl compounds. Trichloromethyl chloroformate is also known as *diphosgene*. It is more convenient to transport and handle than phosgene and serves as a synthetic reagent in fine chemical synthesis where substitution of the latter is required. It is produced under ultraviolet irradiation in the presence of PCl_3 as a catalyst. Diphosgene is converted into phosgene when brought into contact with activated carbon or iron oxide [40].

An overview of the synthetic spectrum of methyl formate is given in Fig. 6.14.

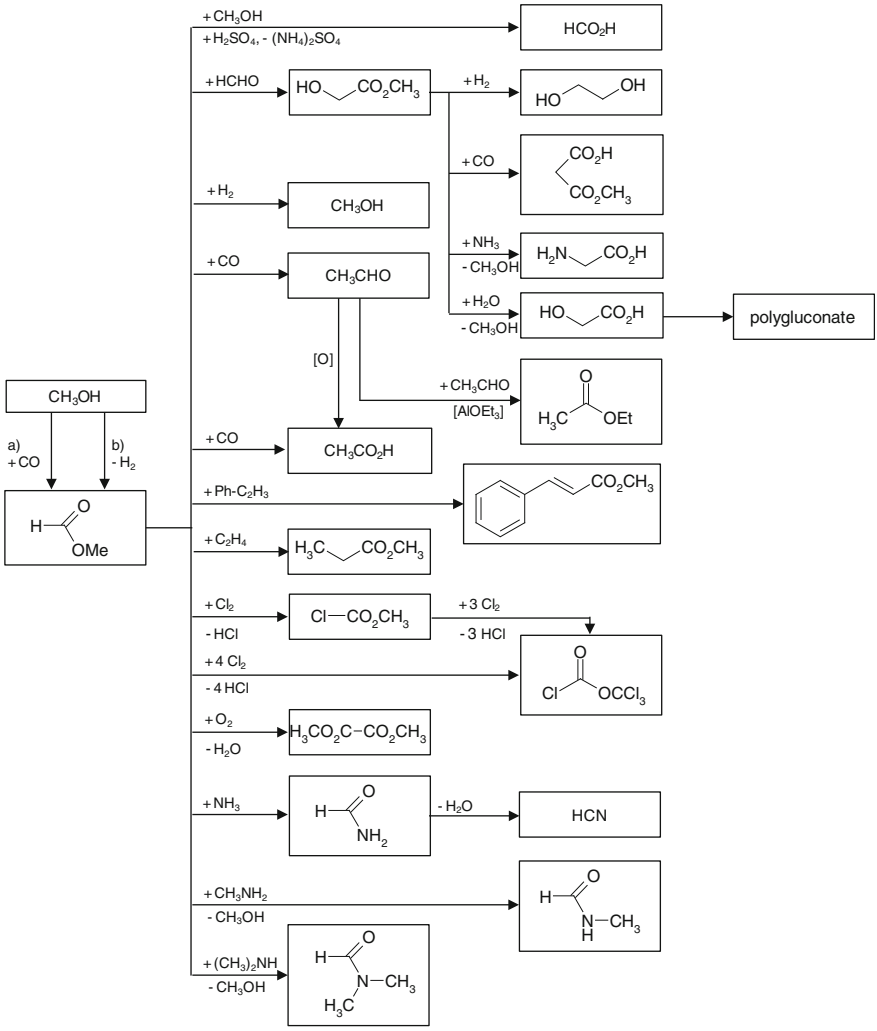

Fig. 6.14 Products derivable from methyl formate as a C_1-building block

Others

Because of its empirical formula, $C_2O_2H_4$, methyl formate can be understood in terms of $(CO)_2H_4$—that is, a condensed phase storage for oxo gas ($CO/H_2 = 1:1$), which can be obtained from methyl formate pyrolysis:

The same reaction, but under mild conditions (1.0 bar and 30 °C), can be carried out with alkali metal alkoxides, where an equilibrium between methyl formate, CO and H_2 is established. Removal of synthesis gas forces the equilibrium to furnish the latter until methyl formate is consumed completely [40, 48].

Synthesis Gas Production Through Methanol Dehydrogenation to Methyl Formate and its Pyrolysis

As outlined previously, methyl formate can be regarded as a storage for CO and methanol. It can also serve as storage for synthesis gas, thus constituting an alternative to methanol reforming to CO and H_2. Figure 6.15 illustrates a process for producing methyl formate from methanol through dehydrogenation. The hydrogen formed in the course of this reaction is drawn off and methyl formate is subjected to pyrolysis over activated carbon, zeolites, or alkaline earth oxides, yielding CO in 98 % purity and methanol, which can be recycled in the process.

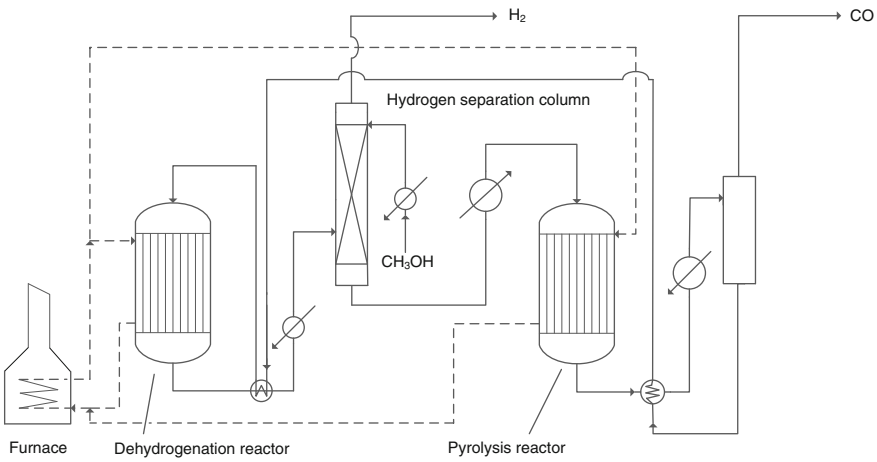

Fig. 6.15 Process for methanol dehydrogenation to H_2 and methylformat and the subsequent pyrolysis to methanol and CO. (Adapted from [30])

6.2.5 Formic Acid

Formic acid is the simplest organic acid. Its technical meaning is based upon its properties as carbonic acid and, because it is formally conceivable as hydroxyl formaldehyde, also as a reducing agent. Production capacity in 2009 was 720,000 tonnes, with BASF, Feicheng Acid Chemicals and Kemira as world's largest producers. It is commercially available in solutions of various concentrations between 85 and 99 w/w% at prices ranging from 650 EUR/tonne in Western Europe to 915 EUR/tonne (1,250 USD/tonne) in the United States.

A major use of formic acid is as a preservative and antibacterial agent in livestock feed. In Europe, it is applied on silage (including fresh hay) to promote the fermentation of lactic acid and to suppress the formation of butyric acid. Formic acid arrests certain decay processes and causes feeding stuff to retain its nutritive value longer, so it is widely used to preserve winter feed for cattle. In the poultry industry, it is sometimes added to feeding stuff to kill *E. coli* bacteria. Use as a preservative for silage and animal feed constituted 30 % of the global consumption in 2009. Formic acid is also significantly used in the production of leather (23 %) and in the dying and finishing of textiles (9 %). Use as a coagulant in the production of rubber constituted 6 % of the global consumption in 2009. Formic acid is also used in place of mineral acids for various cleaning products, such as limescale remover and toilet bowl cleaner. Some formate esters are ingredients of artificial flavourings or perfumes. Beekeepers use formic acid as a miticide against the tracheal mite (*Acarapis woodi*) and the *Varroa* mite. Before the (direct) methanol fuel cell, formic acid was discussed as hydrogen source for fuel cells [49, 50]. Formic acid is stable for years, such as methanol; however, upon contact with a platinum-group metal (PGM), such as platinum or rhodium, it decays readily at room temperature to CO_2 and H_2:

$$HCO_2H \xrightarrow{[PGM]} CO_2 + H_2$$

Because only a very simple device is needed for hydrogen mobilisation, formic acid appears to be an ideal hydrogen storage. A disadvantage, however, is that 1 kg of formic acid provide only about 500 L of H_2 gas, whereas both methanol ($CH_3OH + H_2O \rightarrow CO_2 + 3H_2$) and ammonia ($2NH_3 \rightarrow N_2 + 3H_2$) yield about 2,100 L of H_2 per kg.

Methanol requires reforming at elevated temperatures in the presence of a catalyst; likewise, liquid ammonia is transferred at higher temperatures in ammonia splitting gas. The technical effort is therefore greater, while e.g. 1 % palladium on activated carbon formic acid catalyses immediate hydrogen supply at ambient temperature.

Formic acid is a raw material for silage and is used in the textile industry (dying, finishing, carpet dying, leather tanning, rubber industry, chemical synthesis, etc.). It is also an important reducing agent for the reduction of enamines

and inorganic compounds. In addition, it replaces zinc in dithionite production from sulphite and allows for reducing nitrate to nitrite [51]. The free acid is also used for pickling of steel.

Because each mole of formic acid contains 38.5 kJ (9.2 kcal) more energy than the fission gases $CO_2 + H_2$, one would expect spontaneous decomposition to occur. In fact, this takes place only in the presence of a catalyst, such as 1 % Pd on activated carbon. Because in the oxidation to water 1 mol H_2 yields 238 kJ, as much as 86 % of the energy content of formic acid can be recovered.

Historically, formic acid was obtained by the reaction of sulphuric acid with sodium formate in concentrations ≤85 %. Sulphuric acid concentration and temperature must not be too high; otherwise, carbon dioxide is produced [52]. Alternatively, formic acid can be obtained from formal formic acid nitrile, i.e. hydrogen cyanide (HCN), or by hydrolysis of orthoformic acid trichloride, chloroform ($CHCl_3$) with KOH.

Commercially, the acid can be derived from targeted production or is obtained as a byproduct, such as in methyl formate production through methanol dehydrogenation (see Sect. 6.2.4.2) [20].

In general, two approaches exist:

1. Direct synthesis: reaction of CO with water.
2. Indirect synthesis: reaction of CO with an alcohol followed by hydrolysis:

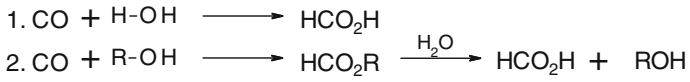

6.2.5.1 Direct Synthesis

CO can be conceived as a chemically inactive acid anhydride of formic acid—the hydration of which leads to the latter. The reaction benefits from bases present, such as NaOH or $Ca(OH)_2$, as well as pressure. Typical process conditions are 8–30 bar and 115–150 °C. Instead of pure CO, synthesis gas may be used. The free acid is obtained through acidification and extraction, such as with diisopropyl ether or by distillation. The direct synthesis is operated in a 40,000 t/a plant in Russia.

6.2.5.2 Formic Acid Through Methyl Formate Hydrolysis

Conversion of CO with alcohols, preferably with methanol, is the first step of the most important production process for formic acid. Formally a CO insertion into the O–H bond of methanol, this reaction is different from methanol carbonylation to acetic acid (Fig. 6.9). The process is conducted with catalytic amounts of sodium methylate at 2–200 bar and 70 °C. With an excess of methanol, CO conversion reaches ≤95 %.

Current methyl formate hydrolysis processes with technical significance have been developed by BASF, Halcon SD and Leonard. They are very similar in their carbonylation conditions and mainly differ in the process engineering concepts for the autocatalytic hydrolysis to formic acid at 3–18 bar and 80–140 °C, where cycle methanol needs to be prevented from competing re-esterification. The molar HCO_2CH_3/water ratio typically ranges between 2:1 and 4:1. Alternatively, excess water is used, which requires instant distillative methanol removal (i.e., minimal contact time between formic acid and methanol).

For this reason, an indirect route via formamide formation with NH_3 at 4–6 bar and 80–100 °C and follow-up hydrolysis is often favoured. Formamide saponification proceeds continuously above 85 °C with 70 % H_2SO_4 to formic acid and ammonia sulphate:

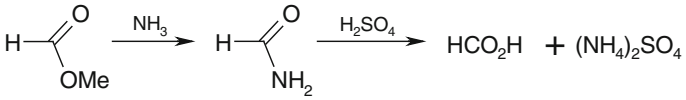

Workup of the reaction product is realised in a rotary kiln. The obtained acid is purified in a column made from V4A or polypropylene with a cooler made from silver or graphite. A technical process of this kind had been developed by BASF and was in operation until 1982, when it was substituted by direct hydrolysis.

Figure 6.16 illustrates the Leonard process to formic acid in a simplified flow scheme [53]. Methanol is being converted at a CO pressure of 42 bar in the presence of a catalyst. The resulting mixture of methanol and methyl formate is funnelled into a degassing column where it is freed from residual CO gas. From there,

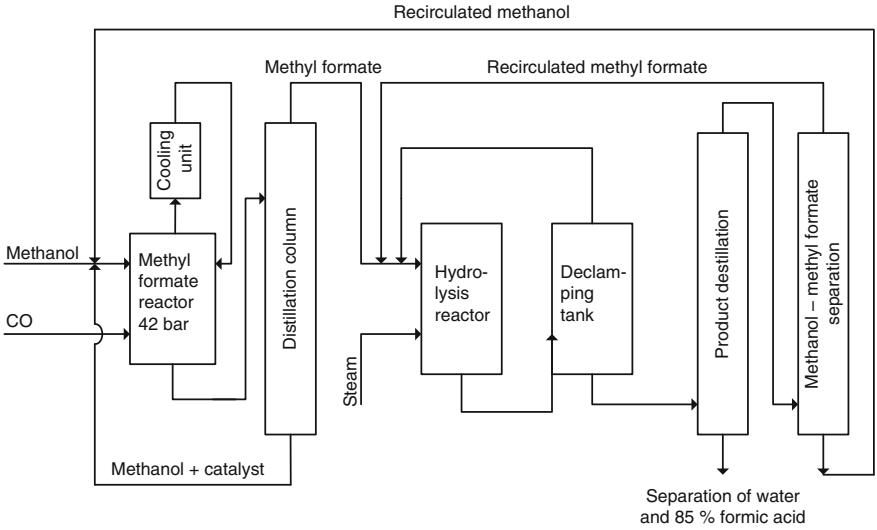

Fig. 6.16 Leonard process for the indirect synthesis of formic acid via methyl formate. (Adapted from [53])

the mixture is fed into the hydrolysis column without prior separation of methyl formate from methanol. The hydrolysate, which has been obtained at mild temperatures in the presence of water vapour, is continuously fed into a distillation column, where methyl formate and unreacted methanol are removed overhead and then separated by distillation. Methyl formate is recycled to hydrolysis, with methanol in the reactor. Eventually, formic acid is separated from water by distillation and the product is obtained as a maximum-boiling azeotrope with a content of 85 %. Alternatively, methyl formate separation from unreacted methanol can be realised prior to the hydrolysis step, thereby entering pure ester into hydrolysis.

6.2.5.3 Formic Acid from Carbon Monoxide

Alternatively, formic acid preparation can be accomplished according to the Marcellin Berthelot method from 1855, which is a two-step synthesis starting with the reaction of NaOH with CO at 6–8 bar and 130 °C. The resulting sodium formate can be marketed directly or is reacted with sulphuric acid to formic acid and sodium sulphate:

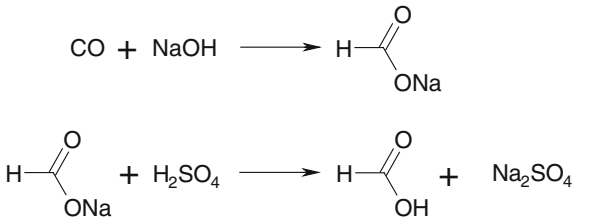

6.2.6 Carbon Monoxide for Organic Syntheses

Because methanol can easily be reformed to synthesis gas, the alcohol not only stores hydrogen but also CO. The latter is separated from synthesis gas (directly or obtained by reforming methanol) by low-temperature separation or absorption in aqueous copper salt solutions.

6.2.6.1 Carbon Monoxide from Low-Temperature Separation of Synthesis Gas

Prior to low-temperature separation of synthesis gas (e.g. according to the Linde process or the Air Liquide process), the crude gas is freed from CO_2 by ethanol amine wash until the content does not exceed 50 ppm. In molecular sieve adsorbers, water and residual CO_2 are removed. Both components would cause clogging through freeze-out. In addition the synthesis gas must be free from N_2

since for vapour pressures being too similar N_2-separation would cause uneconomically high process effort.

The actual low-temperature separation is realised as a two-step process, starting with partial condensation of CO at 40 bar and −180 °C. When synthesis gas has been produced from sources other than methanol in a subsequent step, an expansion into a CO/CH_4 separation column follows. CO is removed overhead with less than 0.1 vol% CH_4. The process is characterised by a highly effective gas recirculation, allowing for recovery of most of the cold energy.

6.2.6.2 Carbon Monoxide Separation from Synthesis Gas by Absorption in Aqueous Copper Salt Solutions

CO absorption in hydrochloric CuCl solution, ammoniacal Cu_2CO_3, or Cu formate solution is conducted under pressure up to 300 bar. CO desorption is realised under reduced pressure at 40–50 °C. The Uhde process binds CO in the form of $[Cu(CO)]^+$ with copper salts in NH_3–H_2O [54]. Process parameters may differ greatly depending on whether CO is to be recovered from gas mixtures or whether gas mixtures are to be freed from CO traces.

The Cosorb process by Tenneco Chemicals uses a solution of CuCl and anhydrous $AlCl_3$ in toluene. It makes use of the temperature dependence of CO-forming complexes with $Cu[AlCl_4]$. The Cu(I)-CO complex is formed at ≤20 bar and about 25 °C and releases CO at 1–4 bar and 100–110 °C. Water (hydrolysis of $AlCl_3$) and acetylene (acetylide formation) must be removed prior to CO separation. The Cosorb process has been in use worldwide after its introduction in 1976.

6.2.6.3 CO Separation Using Membrane Technology

Novel approaches enrich CO from gas mixtures using semipermeable membranes.

6.2.6.4 CO use in Synthetic Organic Chemistry

CO is a starting material for a multitude of reactions. Pure CO is used rather rarely, however. Typically, the pure gas is used for metal carbonyl or phosgene synthesis from the reaction of CO with Cl_2 (starting material for isocyanates; e.g. toluylene diisocyanate for polyurethane production). Other processes comprise methanol carbonylation reactions to methyl formate (Sect. 6.2.4) or acetic acid.

On a technical scale, CO use in combination with H_2 is of much greater significance. Apart from classical synthesis, gas chemistry to methanol, and Fischer–Tropsch synthesis, hydroformylation reactions (oxo aldehydes, oxo alcohols) are commercially important. In combination with a nucleophilic partner such as water

or alcohols, the Reppe carbonylation reaction to acrylic acid (acetylene), propionic acid (ethylene), and their esters is of technical importance, as well as the Koch reaction to branched carbonic acids (Fig. 6.17).

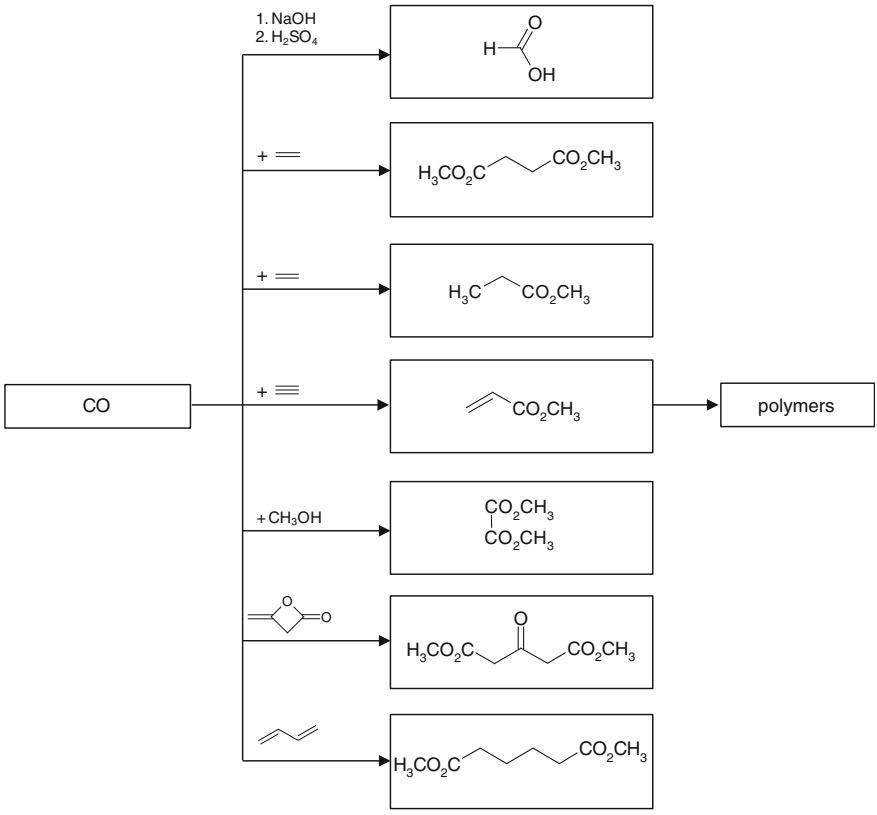

Fig. 6.17 Use of carbon monoxide in synthetic chemistry

6.2.7 Methanol Homologation to Ethanol

The direct coupling of classic petrochemical ethanol production to ethylene prices makes alternative routes to ethanol economically more interesting. Novel developments therefore preferably focus on synthesis gas. One possible route is the so-called methanol homologation to ethanol, which was discovered by BASF in 1941. In this reaction, methanol is converted in the gas or fluid phase with CO/H_2 in the presence of Rh- or Co-containing multicomponent catalysts:

$$CH_3OH + CO + 2H_2 \rightarrow C_2H_5OH + H_2O$$

Depending on reaction conditions, this reaction can be used to produce either ethanol or acetaldehyde from methanol.

In the original experiment at 200 bar and 160–170 °C, $CO/H_2 = 1{:}1$ was reacted with methanol in the presence of cobalt carbonyl, leading to a complex mixture containing ethanol, acetaldehyde, acetic acid and other compounds [55]. With CO alone instead of synthesis gas, acetic acid methyl ester is obtained [56, 57]. Because of the potential of this reaction, it is clear why it was investigated in detail in Europe and the United States. It can be used for the synthesis of ethanol, acetaldehyde, acetaldehyde dimethyl acetal and acetic acid methyl ester:

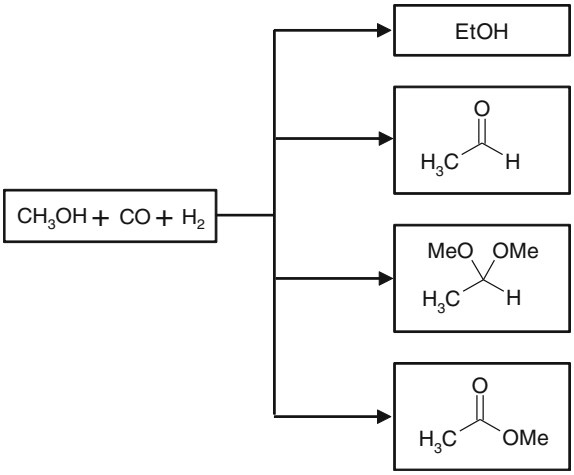

Although the process has been elucidated and understood in detail with catalysts having been optimised, no technical application currently exists.

6.2.8 Acetic Acid

Acetic acid is among the most important aliphatic intermediates. It is also the carbonic acid that has been in use for the longest time. Worldwide production capacity was 11.5 million tonnes in 2012. Consequently there are a number of processes for generating acetic acid through oxidative fermentation of ethanol. Alternatively, there are processes for its production from wood coking (pyroligneous acid) or from sugar cane molasses.

For decades, acetic acid was chiefly produced from acetaldehyde. At the beginning of the 20th century, Hoechst, Wacker and Shawinigan operated oxidation processes on a technical scale. Consequently, acetic acid production was closely linked to acetaldehyde availability. At the same time, the raw material base for acetic acid changed from acetylene to ethylene. For reasons of process economy, the necessity to use light paraffins caused oxidation routes to be developed in

the United States, Germany and England by Celanese, British Distillers, Hüls and Union Carbide. Bayer and Hüls were also active in using C_4 olefins.

In the 1920s, methanol carbonylation came into play. First introduced by BASF on a technical scale (Co-catalysis), this process was replaced by the Rh-catalysed Monsanto process, which in turn was surpassed by the Cativa process that uses an Ir-catalyst. Consequently, acetaldehyde oxidation lost its dominating role in favour of more economical methanol carbonylation. In 1979, approximately 62 % of acetic acid production was based on acetaldehyde; it was less than 28 % in 1995 and has continued to decrease since [20]. Figure 6.18 provides an overview on the intermediates and products that are derived from acetic acid in industrial chemistry.

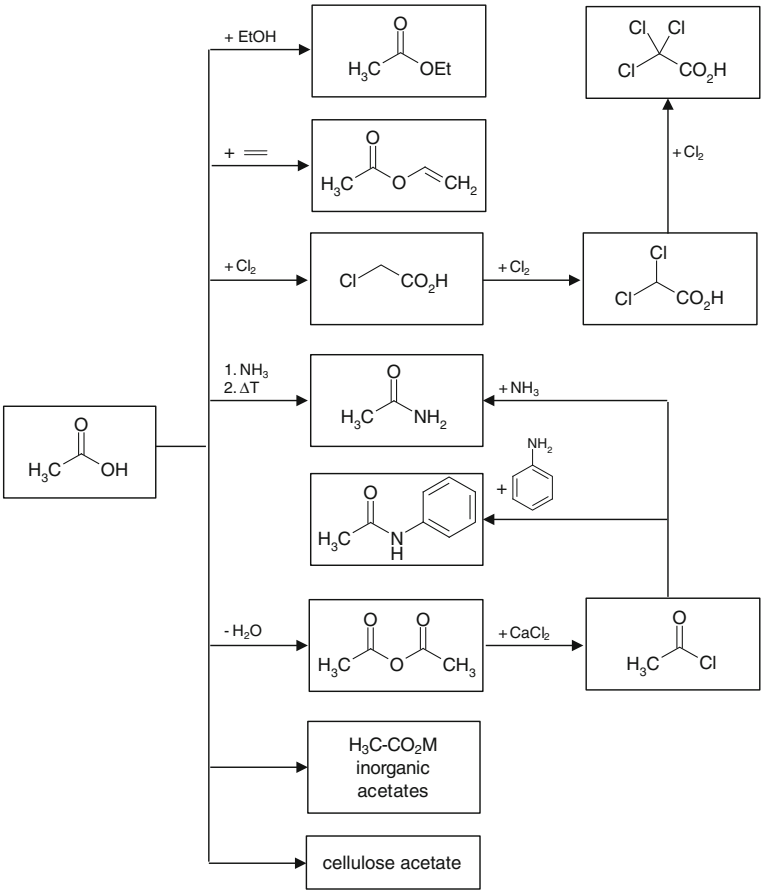

Fig. 6.18 Products derived from acetic acid

6.2.8.1 Acetic Acid Through Acetaldehyde Oxidation

For the sake of completeness and in order to understand the quantum leap methanol carbonylation entailed, acetaldehyde oxidation is discussed here briefly. The reaction proceeds as a radical reaction with air or oxygen via peracetic acid as an intermediate:

1. Acetyl radical formation is initiated by the action of a transition metal, such as Mn^{3+}

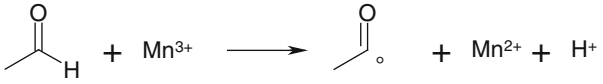

2. Oxidation

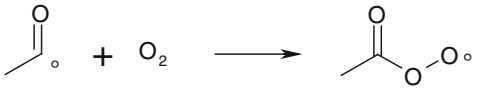

3. Peracetic acid formation and chain propagation

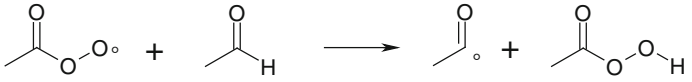

4. Acetic acid formation via hydroxyethyl peracetate

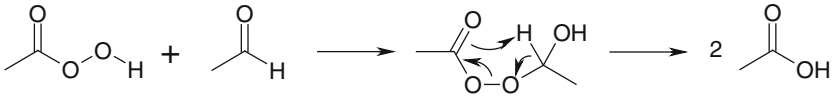

This process is still technically important because it allows peracetic acid to be easily derived as major product under mild conditions. The reaction is conducted without the need of a catalyst in ethyl acetate at 25–40 bar and −15 to +40 °C with air. Commercial plants in which this process is run are operated by British Celanese, Daicel and UCC.

6.2.8.2 Acetic Acid Through Methanol Carbonylation

The discovery that methanol is susceptible for carbonylation to acetic acid by BASF dates back to 1913. The reaction had little importance until the early 1920s, when methanol became available in considerable amounts on a technical scale at reasonable prices. This was the impetus for other companies, such as British Celanese, to adapt the process in 1925. From the very beginning, the process suffered from corrosion, what was overcome in the 1960s when a smaller plant was put into operation by BASF using Hastelloy as a reactor material.

BASF Process

Methanol alone or as a mixture with DME and little water is converted with CO in the presence of CoI_2 in the liquid phase at 680 bar and 250 °C. The process makes use of CoI_2 for in situ generation of $[Co_2(CO)_8]$ and HI:

$$2CoI_2 + 2H_2O + 10CO \rightarrow [Co_2(CO)_8] + 4HI + 2CO_2$$

Under these reaction conditions, $[Co_2(CO)_8]$ reacts in terms of a CO conversion:

$$CO + H_2O \rightarrow CO_2 + H_2$$

As a result, cobalt tetracarbonyl hydrogen, $[CoH(CO)_4]$, is produced in the hydrogenous atmosphere:

$$[Co_2(CO)_8] + H_2O + CO \rightarrow 2[CoH(CO)_4] + CO_2$$

After deprotonation, the cobalt complex is catalytically active. At the same time, methanol reacts with HI to methyl iodide:

$$CH_3OH + HI \rightarrow CH_3I + H_2O$$

Cobalt tetracarbonyl hydrogen and methyl iodide form methyl cobalt tetracarbonyl, which after CO insertion is hydrolysed to acetic acid, with cobalt tetracarbonyl hydrogen being regenerated:

1. $CH_3I + [CoH(CO)_4] \rightarrow CH_3Co(CO)_4 + HI$
2. $CH_3Co(CO)_4 + CO \rightarrow CH_3COCo(CO)_4$
3. $CH_3COCo(CO)_4 + H_2O \rightarrow CH_3CO_2H + [CoH(CO)_4]$

On a technical scale, Co and I_2 can be fully recovered. The selectivity for acetic acid is 90 % (CH_3OH) and 70 % (CO). Per tonne of product, ~40 kg of byproduct are formed, consisting of a complex mixture of different chemical entities. After distillation, the product is obtained in 98.3 % purity.

Monsanto Process

In 1968, Monsanto Co. (St. Louis, Missouri, USA) used a rhodium-catalysed process after it had been discovered that Rh in combination with I_2 constitutes a more active catalytic system than CoI_2. It works at considerably milder reaction conditions at 30–60 bar and 150–200 °C. In addition, it exhibits a far higher selectivity of ~99 % (CH_3OH) and 90 % (CO). From then on, the BASF process was no longer competitive, and today it is of historical interest only. In 1970, in Texas City, Texas, USA, the first technical plant was put into operation with a capacity of 150,000 t/a.

Mechanistically the Rh-catalysed reaction is completely different from the CoI_2 process, even though rhodium is directly placed under cobalt in the periodic chart. In the Monsanto process, the catalytic system consists of RhI_3 and an iodine containing co-catalyst, such as HI/H_2O. Under reaction conditions, a precatalyst is

formed, which is a tetragonal-planar diiodo dicarbonyl rhodate(I) complex and, secondly, methyl iodide from the reaction of methanol with HI:

1. $RhI_3 + 3CO + H_2O \rightarrow [RhI_2(CO)_2]^- + I^- + 2H^+ + CO_2$
2. $MeOH + HI \rightarrow CH_3I + H_2O$

From a mechanistic point of view, two cycles have to be differentiated:

- The rhodium cycle, which is the actual metal complex catalysed reaction.
- The iodide cycle, at the basis of which there are no metal catalysed reactions.

The active species is $[CH_3\text{-}Rh(CO)_2I_3]^-$. After insertion of CO into the CH_3–Rh bond, an acetyl rhodium complex is formed, which decomposes under formation of acetic acid and regeneration of $[Rh(CO)_2I_2]^-$ (Fig. 6.19).

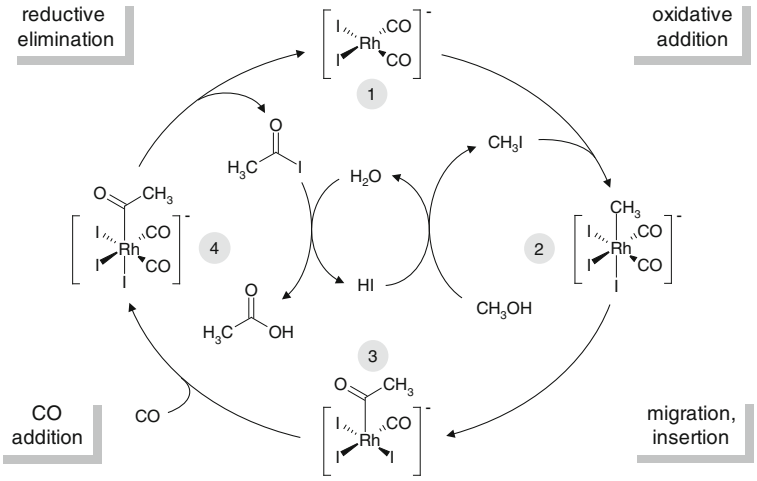

Fig. 6.19 The Monsanto process. (Modified from [22, 27])

The reaction profile obtained from kinetic data of oxidative addition of CH_3I (1 → 2) and subsequent migratory CO insertion (2 → 3) shows that the oxidative addition is the rate-determining step. The methyl rhodate(III) complex is instable with regard to reductive elimination (2 → 1) and migratory CO insertion (2 → 3). As a consequence, equilibrium concentrations of (2) are very low. Nevertheless, (2) was identified by infrared and nuclear magnetic resonance spectroscopy in reaction mixtures of $[RhI_2(CO)_2]^-$ and CH_3I.

Like the BASF process, the Monsanto process is conducted in polar solvents (acetic acid/water). Owing to the highly corrosive action of the acidic iodine-containing reaction media, there are high demands on the reactor material.

One drawback of the process is the capability of rhodium complexes to catalyse CO conversion as well:

$$CO + H_2O \rightleftharpoons H_2 + CO_2$$

$[RhI_2(CO)_2]^-$ (1) which is the active complex in methanol carbonylation catalyses establishing of the water gas equilibrium, too, thus causing a decreased CO-selectivity. There are two complex reactions on which CO conversion is based (Fig. 6.20):

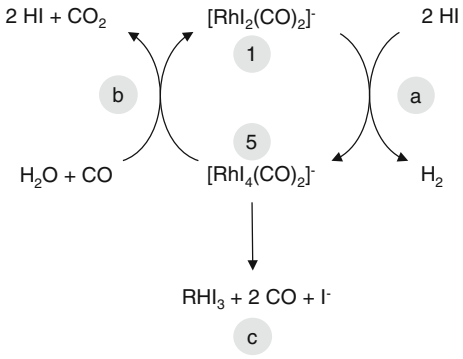

Fig. 6.20 Mechanism of CO conversion as catalysed by $[RhI_2(CO)_2]^-$ (1). Thus, the same complex that catalyses methanol carbonylation in the Monsanto process is the species by which competing CO conversion is catalysed. This latter process is responsible for reduced CO selectivity. The higher nucleophilicity of the respective Ir catalyst (see Fig. 6.21) causes shorter lifetimes of the $[MI_2(CO)_2]^-$ (M = Rh, Ir) complex, which finds its expression in higher CO selectivity. (Adapted from [22])

(a) Reduction of $H^+ \rightarrow H_2$ and formation of a dicarbonyl tetraiodorhodate(III) (5).
(b) Oxidation of $CO \rightarrow CO_2$, upon which (1) is regenerated.
(c) In addition, the Rh^{III} complex $[RhI_4(CO)_2]^-$ (5) tends to decompose under deposition of RhI_3.

As a result, H_2 and CO_2 are produced as major byproducts from CO conversion. Fully automated process control and full catalyst recovery are crucial for process economy.

In a novel process that is in use by BP in a plant based in England, methanol and methyl acetate are used as starting materials, allowing for the generation of acetic acid/acetic acid anhydride mixtures in a ratio of 40:60–60:40 (for acetic acid anhydride production from methyl acetate, see Sect. 6.2.1 and the Hoechst-Celanese process in this section).

Cativa Process

A significant optimisation of the Monsanto process is the Cativa process, which was introduced in 1995–1996 by BP Chemicals (Hull, England). The process uses an iridium complex (Fig. 6.21).

The fundamental steps of the rhodium- and iridium-catalysed reactions are similar but differ in their relative rates. This has significant consequences for the whole catalytic process with the oxidative addition of CH_3I at $[MI_2(CO)_2]^-$ (M = Rh, Ir) playing a key role. Kinetic investigations and quantum chemical calculations have shown that this reaction step proceeds under formation of methyl

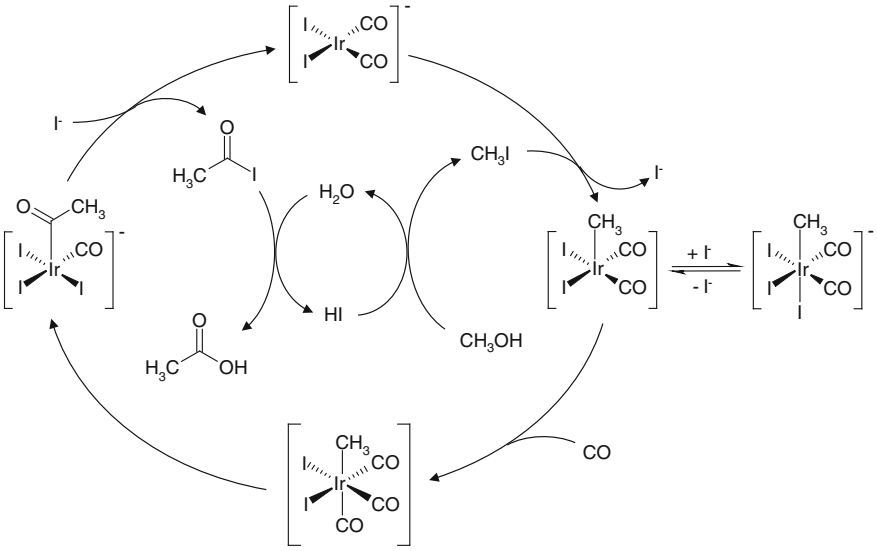

Fig. 6.21 The Cativa process. The iodide cycle is identical to that in Fig. 6.19 and is therefore not shown. (Adapted from [22])

metal(III) complex according to the S_N2 mechanism (Fig. 6.22). As the nucleophilic agent, the tetragonal-planar complex $[MI_2(CO)_2]^-$ (1) was identified in which the doubly occupied dz^2 orbital is the centre of nucleophilicity.

In the transition state (2), the M-C bond has been formed while the C–I bond has been broken. Thus, the energy required for C–I bond fission is partially compensated by M–C bond formation. For the binding energies of the complexes, Ir–C was found to exceed that of Rh–C. Hence, the activation barrier of the Ir complex is lower than for the Rh complex. For the same reason, rhodium complex formation is endergonic whereas iridium complex formation is exergonic (Fig. 6.22).

In fact, CH_3I is added to the iridium complex $[IrI_2(CO)_2]^-$ approximately 150 times faster than to the analogous rhodium complex. For this reason, the oxidative addition of CH_3I is no longer rate-determining in iridium-catalysed methanol carbonylation. However, for complexes that are constitutionally the same, migratory CO insertion (3 → 4) is several orders of magnitude slower in aprotic solvents for M = Ir than for M = Rh.

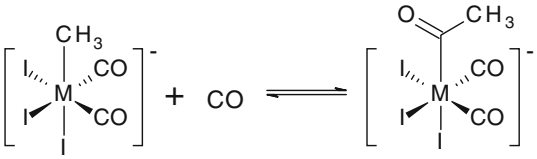

Therefore, a reaction is observed to be accelerated in protic solvents such as methanol, in which a dissociative substitution of I^- by CO (1 → A → B) is

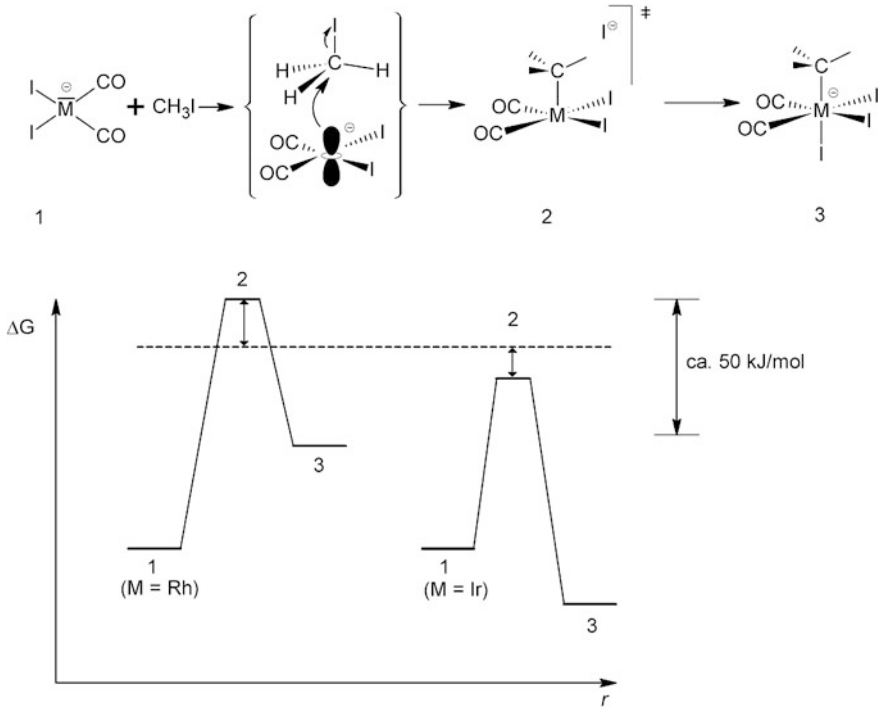

Fig. 6.22 Disparities in nucleophilic addition behaviour favour octahedral oxidative addition to octahedral complex 3 for iridium complexes, while the same is disfavoured for rhodium species. (Adapted from [22])

considerably faster. Complex B is subject to a substantially faster CO insertion than complex 1.

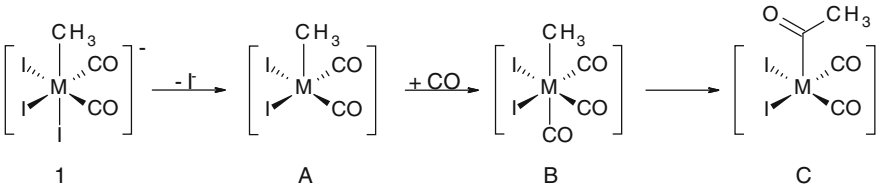

Table 6.2 summarises similarities and differences between the three processes. It is obvious how a higher CO selectivity reduces byproduct formation.

Hoechst-Celanese Process

A reduction of water content of the reaction mixture considerably affects the iodide cycle of the Monsanto process. As a consequence of a higher methanol ratio, acetyl iodide is preferably converted with methanol instead of water. This reaction furnishes methyl acetate, which can be saponified with HI to give CH_3I

Table 6.2 Comparison of technical methanol carbonylation processes. (Adapted from [22])

	Co	Rh	Ir
Technical introduction	1960 BASF	1970 Monsanto	1995 BP Chemicals
Process	BASF	Monsanto	Cativa
Temperature (in °C)	250	150-200	180
Pressure (in bar)	600-700	30-60	30-40
Selectivity			
MeOH (%)	90	99	99.5
CO (%)	70	90	>94
Major by-products	CH_4, CO_2, EtOH, CH_3CHO, EtCOOH	CH_4, CO_2, H_2, EtCOOH	Very few

and acetic acid. Acetic acid anhydride formation from methyl acetate was described in Sect. 6.2.1. In addition, methyl acetate is formed through an acidic catalysed reaction of methanol with acetic acid.

At high methyl acetate concentration, HI concentration is low, what decreases the hydrogen formation rate within the competing CO conversion (Fig. 6.20, reaction a). This results in lower CO release from (5) and consequently in a considerably higher CO selectivity. The lower HI concentration, however, would favour precipitation of insoluble RhI_3, which is avoided by adding soluble iodides such as LiI, $(NR_4)I$, or $(PR_4)I$.

Figure 6.23 shows the different iodine cycles of the Monsanto and the Hoechst-Celanese processes.

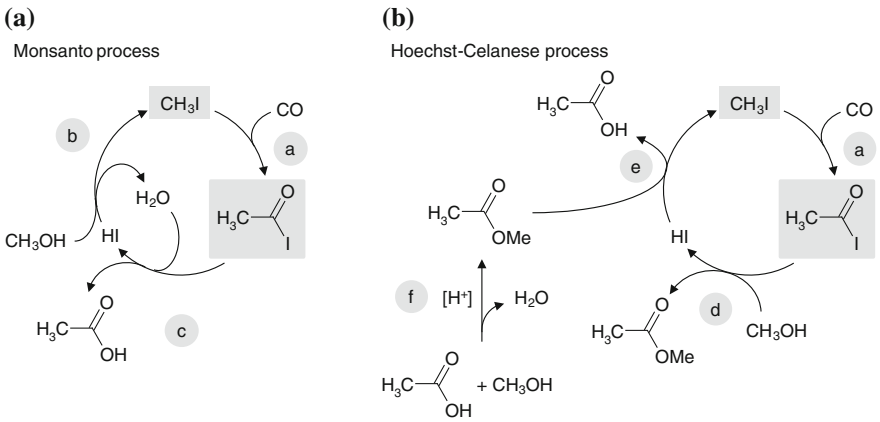

Fig. 6.23 Iodide cycles of the Monsanto (a) and Hoechst-Celanese process (b). Starting material and product of the rhodium-catalysed cycles are marked in grey. (Adapted from [22])

The centrepiece of the Monsanto process is a rhodium-catalysed formation of acetyl iodide from CO and CH_3I (a). The latter is formed from CH_3OH and HI (b), which in turn is regenerated from acetyl iodide hydrolysis (c). If sufficient water is present in the reaction mixture, methyl acetate formation from acetyl iodide and

CH_3OH (d), as well as methyl acetate conversion with HI to CH_3I and acetic acid (e), play only a minor role.

By understanding the reasons behind methyl acetate formation, it becomes evident how propionic acid (Table 6.2) emerges from methanol carbonylation. At the same time, it is obvious that acetaldehyde is formed through rhodium-catalysed acetic acid reduction with H_2 formed from CO conversion (vide supra). Follow-up reduction of acetaldehyde delivers ethanol [20, 22].

Other Processes

The isomerisation of methyl formate is one additional route to acetic acid (see Sect. 6.2.4.4). Acetic acid can also be produced from DME by hydrating carbonylation technology according to the Monsanto-process [58]:

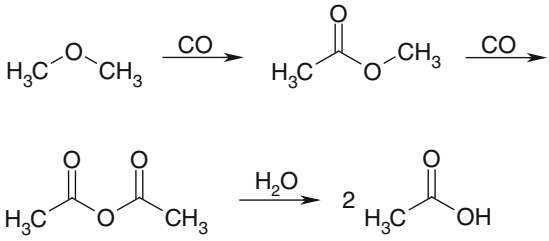

6.2.9 Formaldehyde

Formaldehyde (CH_2O) is an important molecule for global chemical economy; due to its reactivity, it is used in a whole range of industry: construction, textiles, carpeting, wood processing and chemical. At ambient temperature, formaldehyde is a colourless gas that tends to polymerise rapidly in the presence of small amounts of impurities. For this reason, three commercial forms have been established [20]:

1. Aqueous 35...55 % solution, with 37 % being the most widely used grade which may also contain 0–15 % methanol and a polymerisation inhibitor. In solution formaldehyde is present as hydrate or as a mixture of oligooxymethylene glycols.

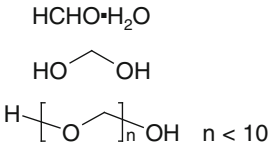

2. Trioxane, the cyclic, trimeric form that is obtained by acid-catalysed conversion of formaldehyde.

3. Paraformaldehyde, the polymeric form of formaldehyde which is produced upon boiling-down of aqueous formaldehyde solutions. The latter can be regenerated through heating or addition of acid.

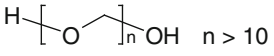

Since the first commercial production of formaldehyde in Germany in 1888 through methanol dehydrogenation, its synthesis has changed from radical oxidation of propane and butane or DME oxidation, respectively, to the two main routes starting from methanol that are in use today: (1) oxidation-dehydrogenation over a silver catalyst and (2) direct oxidation of methanol to formaldehyde using metal oxide catalysts (Formox process). Up to 50 % of methanol production is consumed for formaldehyde synthesis. In 2012, worldwide formaldehyde production amounted to 40.9 million tonnes, what is an increase of 77 % compared to 23 million tonnes in 2003. Globally leading manufacturers are Borden and BASF [59].

Formaldehyde is usually produced close to the point of consumption because it is fairly easy to make but cannot be shipped easily over long distances. It can develop stability-associated problems during transport. As a result, world trade in formaldehyde is minimal. Consumption of formaldehyde depends mainly on the construction, automotive and furniture markets. The main downstream demand for formaldehyde around the world is in the production of thermosetting resins. The largest group is the amino resins produced by condensing either urea or melamine with formaldehyde (Table 6.3) [60].

6.2.9.1 Formaldehyde Production from Methanol

Formaldehyde is produced industrially from methanol by the following three processes based on two different catalytic technologies, as described here.

1. Oxidative dehydrogenation

In this method, formaldehyde is formed by dehydrogenation of methanol. Vapourised methanol and air are passed over a thin bed of silver-crystal catalyst at 600–720 °C:

$$CH_3OH \rightarrow HCHO + H_2$$

Because of the high decomposition rate of formaldehyde, residence time must be kept below 0.01 s, which is accomplished through high-flow velocity and rapid cooling after passing the catalyst bed. The heat required for the endothermic reaction is obtained by burning the off-gas (N_2, H_2, H_2O, CO, CO_2, CH_3OH, HCHO) produced from the dehydrogenation reaction. Formaldehyde is isolated from the reaction gases by absorption in water and is obtained as a 37–44 % solution (formalin).

In the chemical industry, there are two different modes of operation:

(1a) *Single pass*

Using partial oxidation and dehydrogenation, the feed is composed of methanol, air and steam in the presence of silver crystals at 680–720 °C with an excess of methanol being used. In the BASF process, methanol conversion is 97–98 %.

Table 6.3 Commercial use of formaldehyde [60]

Product	Use	Remarks
Formaldehyde	• Disinfectant • Conservation • Chemicals	Commercial forms: • Formaldehyde hydrate • Trioxane • Paraformaldehyde
Urea formaldehyde resins	• Binders in nonstructural wood-based panels for particle board and medium-density fibreboard	Largest sector
Melamine formaldehyde resins	• Adhesives • Binders • Clear coats for automobile industry • Paper-impregnating resins • Surfacing of panels	
Phenolic formaldehyde resins	• Composites • Durable binders and adhesives in structural wood panels • Binders in mineral wool insulation • Insulation foams • Brake linings • Foundry binders • Oil well productivity enhancers in oil industry	Water resistant, high thermal stability
Polyoxymethylene	• Tough engineering thermoplastics replacing metals in electrical, electronic, automotive and consumer applications	Second largest use for formaldehyde
Methyl di-*p*-phenylene isocyanate	• Polyurethane foam • Polyurethane elastomers • Adhesives • Binders • Sealants	Fastest growing of the formaldehyde derivative markets
Butanediol	• Polyester thermoplastic resins used in textile fibres	
Pentaerythritol	• Alkyd resins • Lubricants • Tall oil esters	Produced from alkaline condensation of formaldehyde with acetaldehyde; demand for pentaerythritol is falling around the world
Trimethylol propane	• Textile and leather impregnation	

(1b) *With recycle*

Partial oxidation and dehydrogenation with air and steam in the presence of crystalline silver (or silver gauze) at 600–650 °C with an excess of methanol yields a primary conversion of methanol between 77 and 87 %. The conversion is completed by distilling the product and recycling the unreacted methanol in the main feed.

2. Methanol oxidation

The second technology involves pressureless methanol oxidation by an excess of atmospheric oxygen over a catalyst of molybdenum and iron oxide with $Fe_2(MoO_4)$ as the actual active component at approximately 350 °C. With a modified iron-molybdenum-vanadium oxide catalyst, the process is run at 250–400 °C. The reaction is conducted in catalyst-packed reactor tubes where the metal oxides act as an oxygen carrier on to hydrogen to be cleaved off the methanol. The reduced catalyst is simultaneously reoxidised by atmospheric oxygen:

$$CH_3OH + {}^1/_2O_2 \rightarrow HCHO + H_2O$$

The reaction is highly exothermic, for which reason it is realised in a multitube fixed-bed reactor and generates heat to provide steam for turbines and process heating. Methanol conversion is 98–99 %.

Crude aqueous methanol obtained by high-, medium-, or low-pressure synthesis contains low concentrations of inorganic impurities and limited amounts of other organic compounds (byproducts). The methanol for this process must first be subjected to purification processes and preliminary distillation to remove undesired contaminants (as low-boiling components) because most of the byproducts act as catalyst poisons or they favour side reactions over the catalyst in the process, thus resulting in less pure formaldehyde.

Yields from the oxidation process are around 90–92 %. The oxidation route has a lower reaction temperature and the metal catalyst is more cost-effective than silver. Nevertheless, the oxidative dehydrogenation route is still the most prevalent.

In the following sections, both approaches—oxidative dehydrogenation and methanol oxidation—are described in detail.

Oxidative Dehydrogenation

General aspects

This route is the classical method for the industrial production of formaldehyde. The two main reactions governed by this process are dehydrogenation and partial oxidation. The silver catalyst processes are generally carried out at atmospheric pressure and 600–720 °C using a feed with an excess of methanol. The reaction temperature depends on the excess of methanol present in the methanol/air mixture. The composition of the mixture must be outside the explosive limits. The amount of air in the feed is determined by the catalytic quality of the silver surface. The main reactions occurring during methanol conversion to formaldehyde are the following:

1. $CH_3OH \rightleftarrows CH_2O + H_2$ $\Delta H = +84\,kJ/mol$
2. $H_2 + {}^1/_2O_2 \rightarrow H_2O$ $\Delta H = -243\,kJ/mol$
3. $CH_3OH + {}^1/_2O_2 \rightarrow CH_2O + H_2O$ $\Delta H = -159\,kJ/mol$

Process parameters determine the extent to which each of these three reactions occur. Byproducts result from secondary reactions:

4. $CH_2O \rightarrow CO + H_2$ $\Delta H = +12.5\,kJ/mol$
5. $CH_3OH + {}^3/_2O_2 \rightarrow CO_2 + 2H_2O$ $\Delta H = -674\,kJ/mol$
6. $CH_2O + O_2 \rightarrow CO_2 + H_2O$ $\Delta H = -519\,kJ/mol$

Other important byproducts are methyl formate, methane and formic acid, with all of them not only being formed in the reactor but also in the absorption column.

The endothermic dehydrogenation reaction (1) is highly temperature-dependent. Conversion increases from 50 % at 400 °C to 90 % at 500 °C and to 99 % at 700 °C. Kinetic studies with supported silver show that reaction (1) is a first-order reaction [61]. Therefore, the rate of formaldehyde formation is a function of the available oxygen partial pressure (concentration) and the oxygen residence time on the catalyst surface. However, for the reaction of methanol to formaldehyde over a silver catalyst surface, no complete reaction mechanism has been proposed so far. Some authors postulate a change in mechanism occurring at approximately 650 °C [62]. New insight into the reaction mechanism is available from recent spectroscopic investigations that demonstrate the influence of different atomic oxygen species on reaction pathway and selectivity [63–65]. Formaldehyde synthesis over a silver catalyst is carried out under strictly adiabatic conditions. The reaction is very fast and only few millimetres lie in between sites with high methanol concentration and sites with high formaldehyde concentration.

The oxygen in the process is shared between the exothermic reactions, which is primarily reaction (2) and, to a lesser extent depending on the process used, the secondary reactions (5) and (6). Thus, oxygen concentration in the feed determines the desired reaction temperature as well as the extent of conversion of the endothermic reactions (1) and (4). Another important factor affecting the yield of formaldehyde and the conversion of methanol, apart from catalyst temperature, is the addition of inert material to the reactants. Water is added to reactor feed and nitrogen is added to air feed, as well as air/off-gas mixtures that are recycled to dilute the CH_3OH/O_2 reaction mixture. The throughput per unit of catalyst area provides another way of improving the yield and affecting side reactions. [66, 67].

Silver Catalyst Process with Complete Methanol Conversion (BASF Process)

The BASF process for the complete conversion of methanol to formaldehyde is illustrated in Fig. 6.24.

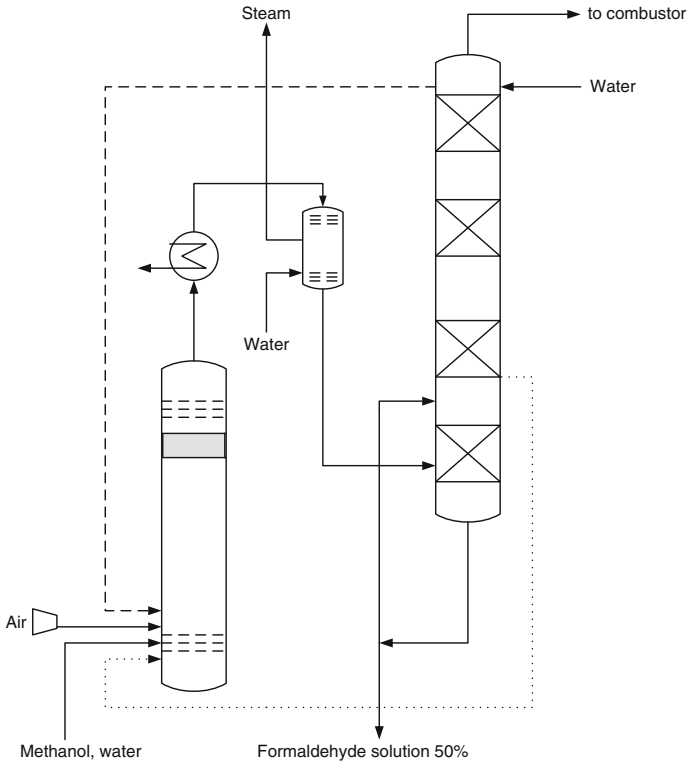

Fig. 6.24 BASF process for formaldehyde production from methanol. (Redrawn from [59])

In this process, a mixture of methanol and water is fed into the evaporating column. Fresh air and, if necessary, recycled off-gas from the last stage of the absorption column enter the column separately [68]. A gaseous mixture of methanol and oxygen is thus formed, in which an inert gas content (N_2, H_2O or CO_2) is fed in order to prevent the upper explosive limit from being reached.

Methanol and gas are mixed in a molar ratio of 60 parts of methanol to 40 parts of water, with or without inert gases. The packed evaporator constitutes part of the stripping cycle. The heat required to evaporate the methanol and water is provided by a heat exchanger, which is linked to the first absorption stage of the absorption column [69]. After passing through a demister, the gaseous mixture is superheated with steam and fed to the reactor, where it flows through a 25–30 mm thick bed of silver crystals. The crystals have a defined range of particle sizes, from 0.4 mm in the first layer to 2 mm in the last [70]. They rest on a perforated tray covered with a fine corrugated gauze, thus permitting optimum reaction at the surface.

The bed is positioned immediately above a water boiler (cooler), which produces superheated steam and simultaneously cools the hot reaction gases to a temperature of 150 °C corresponding to that of the pressurised steam (5 bar). The

almost dry gas from the gas cooler passes to the first stage of a four-stage packed absorption column, where the gas is cooled and condensed. Formaldehyde is eluted countercurrent to water or to the circulating formaldehyde solutions, the concentrations of which increase from stage to stage.

The product circulating in the first stage may contain 50 wt% formaldehyde if the temperature of the gas leaving this stage is kept at approximately 75 °C; this temperature provides sufficient evaporation energy for the feed stream in the heat exchanger. The final product contains 40–55 wt% formaldehyde, as desired, with an average of 1.3 wt% methanol and 0.01 wt% formic acid. Formaldehyde yield of the process is 89.5–90.5 mol %.

Some of the off-gas is removed at the end of the fourth stage of the column [63] and is recycled (Fig. 6.24, route indicated by dashed lines). The residual off-gas has a net calorific value of 1,970 kJ/m^3 and is fed to a steam generator, where it is combusted [71]. Prior to combustion the gas contains approximately 4.8 vol% CO_2, 0.3 vol% CO and 18.0 vol% H_2 as well as nitrogen, water, methanol and formaldehyde. The combusted off-gas contains no environmentally harmful substances. The total steam equivalent of the process is 3 tonnes per tonne of 100 wt% formaldehyde.

In an alternative procedure to the off-gas recycling process (Fig. 6.24, dotted line), the formaldehyde solution from the third or fourth stage of the absorption tower is recycled to the evaporator, and a certain amount of steam is used in the evaporation cycle. The resulting vapour is combined with the feed stream to the reactor for the purpose of obtaining an optimal methanol/water ratio. [72] In this case, the temperature of the second stage of the absorption column is approximately 65 °C. The yields of the two processes are similar and depend on the formaldehyde content of the recycled streams.

Catalyst lifetime depends strongly on reaction temperatures, throughput rates, and impurities. Upon exposure to excessively high reaction temperatures and high throughput rates, the silver crystals get matted, thus causing increased pressure across the catalyst bed. This effect is irreversible and requires the catalyst bed to be changed after 3–4 months. The catalyst is regenerated via electrolytic processes. Impurities such as inorganic salts in the air and methanol feed may lead to catalyst inactivation. Some impurities cause poisoning effects that are reversible within few days, yet with catalytic properties that are not fully restorable compared to the initial situation. Because formaldehyde solutions corrode carbon steel, all parts of the manufacturing equipment exposed to formaldehyde solutions must be made of a corrosion-resistant alloy, such as certain types of stainless steel.

If throughput and reaction temperature have been optimised, the capacity of a formaldehyde plant increases in proportion to the diameter of the reactor. One of largest known reactor appears to be that of BASF in Germany, which has an overall diameter of 3.2 m and a production capacity of 72,000 t/a (calculated as 100 wt% formaldehyde).

Incomplete Conversion and Distillative Recovery of Methanol

Another approach to industrial formaldehyde production is that of partial oxidation and distillative recovery of methanol. This process is used by numerous companies (e.g. ICI, Borden and Degussa) and is based on recent developments (Fig. 6.25) [73–78].

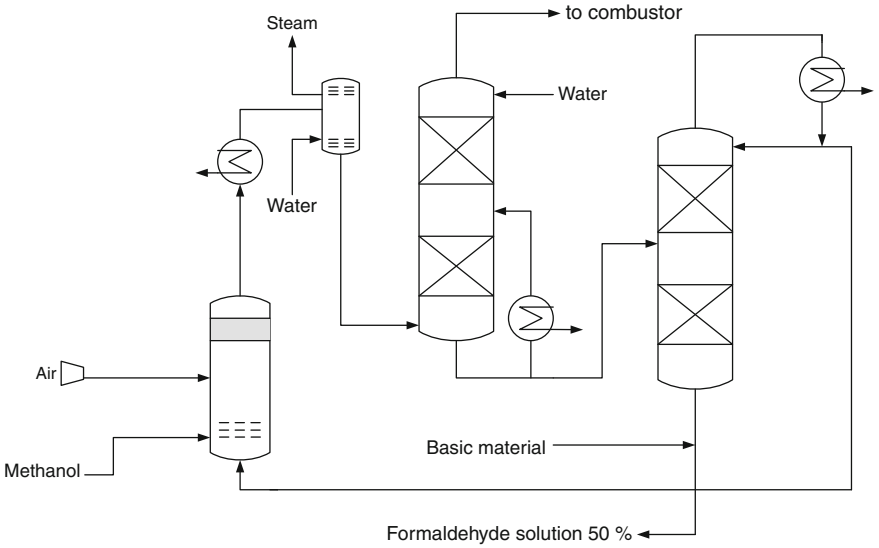

Fig. 6.25 Formaldehyde production through incomplete conversion and distillative recovery of methanol

A feed mixture of pure methanol vapour and freshly blown-in air is generated in an evaporator. The resulting vapour is mixed with steam and then fed into the reactor. The reaction mixture contains excess methanol and steam and is very similar to that used in the BASF process.

The vapour passes through a shallow catalyst bed made from silver crystals or layers of silver gauze. Conversion is incomplete and the reaction takes place at temperatures between 590–650 °C. A low temperature compared to the BASF process minimises undesirable secondary reactions. For these purposes, reaction gases are cooled indirectly with water immediately after leaving the catalyst bed, thereby generating steam. The remaining heat of reaction is then removed from the gas in a cooler and is fed to the bottom of a formaldehyde absorption column. At the top of the column, all condensable portions of the remaining formaldehyde and methanol are washed out from the tail gas by countercurrent contact with process water.

A 42 wt% formaldehyde solution from the bottom of the absorption column is fed to a second column for distillation, which is equipped with a steam-based heat exchanger and a reflux condenser. Methanol is recovered at the top of the column and is recycled to the bottom of the evaporator. From the bottom of the distillation

column, a solution containing up to 55 wt% formaldehyde and less than 1 wt% formic acid is taken, which is funnelled into an anion-exchange unit to remove formic acid to the specified level of typically <50 mg/kg.

Formaldehyde concentration in the final solution is adjusted by process conditions and in particular distillation conditions:

- 50–55 wt% formaldehyde with ≤1.5 wt% formic acid is obtained if steam addition is restricted and a larger excess of methanol is employed. The ratio of distilled recycled methanol to fresh methanol ranges between 0.25 and 0.5.
- 40–44 wt% formaldehyde is produced by applying an energy-intensive distillation protocol for methanol removal, saving steam and electrical power as well as capital costs. In this case, the off-gas from the absorption column has a similar composition to that described for the BASF process.

The off-gas is combusted to generate steam, thus avoiding environmental problems caused by residual formaldehyde. Alternatively, the tail gas from the top of the absorber can be recycled to the reactor. This inert gas is introduced with additional steam in the feed, thus reducing excess methanol in the reactor feed, with the consequence of providing a more concentrated product with less expenditure on distillation. The yield of the process is 91–92 mol %.

A process variation to increase yields of the incomplete conversion of methanol process employs two-stage oxidation systems [79–82]. First, methanol is partially converted into formaldehyde using a silver catalyst at a comparably low reaction temperature of 600 °C, for instance. The reaction gases are subsequently cooled and excess air is added in order to convert remaining methanol in a second stage, employing either a metal oxide (Formox Process) or another silver bed as a catalyst.

Formox Process

In the Formox process, a metal oxide (e.g. iron, molybdenum, vanadium oxide) is used as a catalyst for the conversion of methanol to formaldehyde (Fig. 6.26). Many such processes have been patented since 1921 [83–86]. The oxide mixture usually has an Mo:Fe atomic ratio between 1.5 and 2.5, and small amounts of V_2O_5, CuO, Cr_2O_3, CoO and P_2O_5 serve as promoters [87–90].

The Formox process has been described as a two-step oxidation reaction in the gaseous state, which involves an oxidised (Cat_{ox}) and a reduced (Cat_{red}) catalyst site [91–94]:

1. $CH_3OH(g) + Cat_{ox} \rightarrow CH_2O(g) + H_2O(g) + Cat_{red}$
2. $Cat_{red} + {}^1/_2O_2(g) \rightarrow Cat_{ox} \qquad \Delta H = -159\ \text{kJ/mol}$

Formaldehyde production works fine in the temperature range of 270–400 °C. Conversion at atmospheric pressure is virtually complete as a function of residence time. However, conversion is temperature dependent, too. At a temperature >470 °C, the formaldehyde oxidation side reaction increases considerably:

3. $CH_2O + {}^1/_2O_2 \rightarrow CO + H_2O \qquad \Delta H = -215\ \text{kJ/mol}$

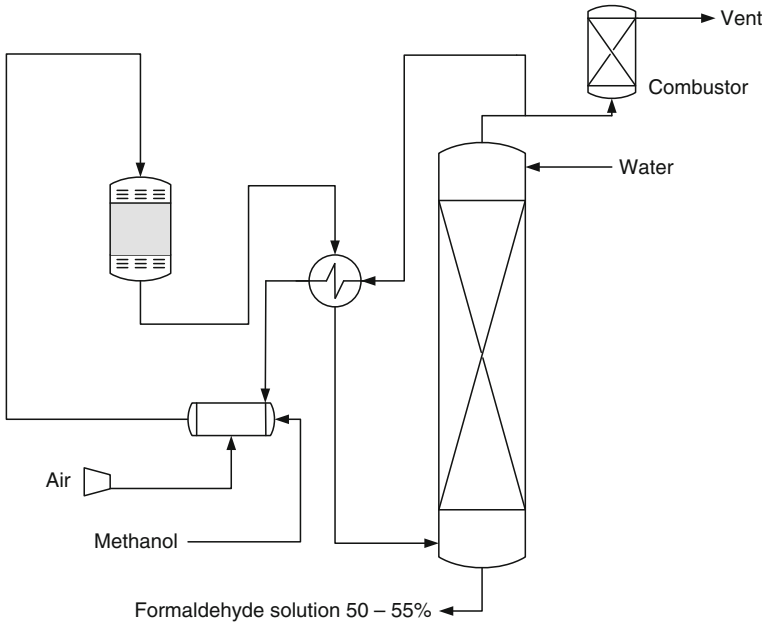

Fig. 6.26 Formox process

Methanol oxidation is inhibited by steam and very pure methanol is required to obtain high conversion. Kinetic studies on the reaction rate of formaldehyde formation indicated that the rate is independent of the formaldehyde partial pressure.

As shown in Fig. 6.26, methanol feed is passed to a steam-heated evaporator. Fresh air blown in and recycled off-gas from the absorption column are mixed and, if necessary, preheated through the product stream in a heat exchanger before being fed into the evaporator. The gaseous feed passes through catalyst-filled tubes in a heat-exchanging reactor. A typical reactor for this process has a shell with a diameter of approximately 2.5 m, which contains between 10,000 and 18,000 tubes that are 1.0–1.5 m in length. A high-boiling heat-transfer oil (or molten salt mixture) circulates outside the tubes and removes the heat of reaction generated from the catalytic reaction inside the tubes.

The process employs excess air and temperature is controlled isothermally to a value of approximately 300–340 °C. Steam is simultaneously generated in a boiler and is used to generate electric power. The air/methanol feed is a flammable mixture. To prevent it from spontaneous combustion, the oxygen content is reduced to approximately 10 mol % by mixing introduced air with tail gas from the absorption tower, whereas the methanol content in the feed can be increased without generating an explosive mixture [95, 96].

After leaving the reactor, the gases are cooled to 110–125 °C in a heat-exchange unit and are passed to the bottom of an absorber column. The formaldehyde concentration is regulated by controlling the amount of process water

added at the top of the column and the temperature in the top of column. The product is removed from the water-cooled circulation system at the bottom of the absorption column and, if necessary, is fed through an anion-exchange unit to reduce the formic acid content.

The final product contains up to 55 wt% formaldehyde and 0.5–1.5 wt% methanol, the resulting conversion of which ranges from 95 to 99 mol %. Formaldehyde yield depends on selectivity, activity and spot temperature of the catalyst, with the latter being effected by the heat transfer rate and the throughput rate. The overall plant yield is generally 90–93 mol %.

Well-known processes using the Formox method have been developed by Perstorp/Reichhold (Sweden, United States, Great Britain) [97, 98], Lummus (United States) [99, 100], Montecatini (Italy) [101], Hiag/Lurgi (Austria) [102], and DB Western (United States).

6.2.9.2 Polyoxymethylene

Polyoxymethylene (POM; also known as acetal, polyacetal and polyformaldehyde) is a semicrystalline engineering thermoplastic formed by polymerisation of formaldehyde. It mainly consists of unbranched oxymethylene units, $–[OCH_2]_n–$ [103]. Based on basic research of Hermann Staudinger in the 1920s, the first homopolymer polyoxymethylene was developed and marketed by DuPont in 1959. In 1962, the first copolymer polyoxymethylene was introduced onto the market by Celanese, who raised their market share to >75 % of all produced polyoxymethylenes today. POM shows a high mechanical resistance and stability against common solvents, for which reason it is a favoured engineering plastic to form metal-free technical precision parts [105–111].

POM is characterised by low water uptake, high stiffness and a high elastic recovery. The long-term heat resistance temperature is 110 °C for glass fibre–reinforced POM. These excellent properties are the outcome of the high crystallinity of POM, which is approximately 75 % for homopolymers and 65 % for a copolymer with 3 % co-monomers. The notched impact is low. Disadvantageous characteristics of POM are its flammability and inconsistency against acids. The main differences between homopolymeric and copolymeric POM lies in lower stiffness and toughness of the homopolymer compared to the copolymer. On the other hand, the copolymer exhibits higher thermal and chemical stability (Table 6.4).

POM is mainly used without further modifications. For special applications, several modified variants of POM have been developed and are still under development. Impact-modified products can be realised by blending of POM with thermoplastic polyurethane. Improved stiffness and structural strength is the result of a modification with glass fibres. Those mineral-reinforced products are destined to build low-distortion components. The high abrasion and wear resistance of POM can further be improved by additives such as polytetrafluoroethylene, MoS_2, silicon oil, or graphite. Main application branches for POM products are the

Table 6.4 Properties of polyoxymethylene homopolymer and copolymers. [104]

	Homopolymer Delrin 500 (Du Pont)	Copolymer ultraform N2320 (BASF/ Degussa)	Copolymer celcon M90 (Celanese-Ticona)
Melting point (°C)	177	165	165
Glass temperature (°C)	-60	-60	
Water uptake (°C) (23 °C/50 % relative humidity)	0.2	0.3	0.2
Elastic modulus (N/mm^2)	3,200	2,800	2,760
Yield strength (N/mm^2)	72	65	66
Yield strain (%)	8	8	10
Notched impact (N/mm^2)	9	7	6
Long-term heat resistance (°C)	110[a]	110[a]	101

[a] With 25 % glass fibre

automotive and electronics industries, in which polymer resistance against fuels and high dimensional stability are of particular interest. The good sliding friction behaviour of POM often leads to applications in ball bearing or transport chain construction.

Homopolymeric Polyoxymethylene

Evaporating aqueous formaldehyde solutions lead to the formation of oligomeric polyoxymethylenediols, also known as paraformaldehydes. However, the resulting gelatinous material with polymerisation grades up to 100 does not show high thermal stability. Due to its hemiacetal end groups, these low-molecular polymers depolymerise at the chain ends in a zip-type reaction:

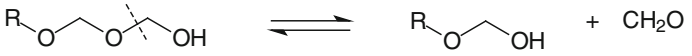

This depolymerisation reaction can be avoided by transforming the terminal hemiacetal moieties into thermally stable ones by acetylation with acetic anhydride:

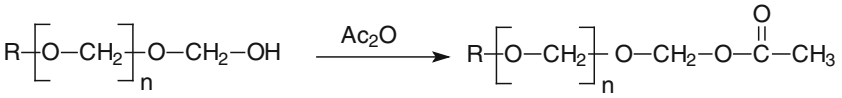

In addition to this preferred method, alternative transformations into ester, ether and urethane end groups have been developed.

There exist further decomposition mechanisms of polyoxymethylenes. Autoxidative cracking processes take place below the melting point of about 160 °C, even in those cases where end groups had been transformed. The presence of acids accelerates degradation processes. In this respect, formaldehyde released as a fission product can be oxidised by air to formic acid, thus causing an auto-catalytic decomposition process.

High-Molecular Polyoxymethylene

The synthesis of high-molecular POM can be performed by cationic or anionic polymerisation of purified formaldehyde at low temperatures (−80 °C) using boron triflouride or trimethyl amine as a catalyst. Even though the absence of water leads to high-molecular products, traces of water as well as acids and bases catalyse polymerisation, too. Without further end group modification, the resulting polyoxymethylene is thermostable until approximately 150 °C.

Polymerisation of Trioxane

The cationic polymerisation of molten trioxane, the cyclic trimer of formaldehyde, is easier to handle than the conversion of gaseous formaldehyde, which is owed to a lower polymerisation rate compared to formaldehyde. Trioxane can easily be obtained by trimerisation of formaldehyde in the presence of strong acids. The polymerisation process has thoroughly been investigated for the system trioxane/methylene chloride/boron triflouride. After a ring-opening step induced by Lewis-acidic BF_3, the resulting cationic species is starting point for further trioxane insertions:

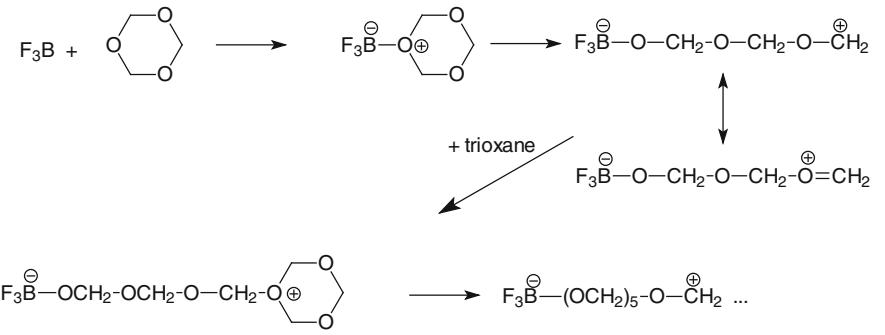

Technological Implementation of Polyoxymethylene Synthesis

Highly pure formaldehyde is the basis for high-molecular polyoxymethylene synthesis. A process for the manufacture of high-purity formaldehyde is the thermal decomposition of semiformals [112, 113]. Undesired byproducts are extracted from the reaction mixture. The resulting formaldehyde, with a residual water content <0.1 wt%, is being polymerised in suspension in the presence of an inert organic solvent [114]. Mass polymerisation cannot be handled due to the high reaction rate and generated heat. In general, two alternative methods are being used for that reason:

(a) Dry gaseous formaldehyde is added together with nitrogen at 30 °C to an inert solvent containing a starter reagent.
(b) The starter reagent is being added to a water-free solution of formaldehyde at −60 °C.

In both cases, a high-grade polymer is being realised by fast polymerisation rates under continuous stirring. Typical solvents are *n*-heptane, cyclohexane, benzene, toluene, xylene, decaline and ether, but also chlorinated hydrocarbons such as methylene chloride. Though formaldehyde starts polymerisation at −80 °C and an addition of a starter reagent is not mandatory, its presence improves the handling of the polymerisation process (Table 6.5).

The mechanical properties of the resulting polymers are a direct outcome of their molar masses. POM polymers with masses in the area of 30,000–50,000 u are well suited for injection molding applications and show improved mechanical stability. Molecular mass distribution can be controlled by selectively using additives such as water, methanol, formic acid, acetic acid anhydride, or ethyl acetate during the polymerisation process with the aim to interrupt chain propagation. As already mentioned, a transformation of thermally unstable hemi-acetal end groups into stable ones is mandatory. Commercially, this is done by acetylation [116].

The lower reactivity of trioxane, compared to its monomer formaldehyde, brings about the option for trioxane mass polymerisation under adiabatic conditions [117]. Though progressing conversion rates increase reaction mass temperature up to 130–140 °C, thereby exceeding the trioxane boiling point of 115 °C, polymerisation can be controlled well because the majority of the trioxane remains polymerised and the evaporated trioxane can be recovered adsorptively in a scrubbing column. Nevertheless, reaction and crystallisation heat removal is a major challenge in synthesising polyoxymethylene under continuous conditions.

Typically, the polymerisation process is carried out below the melting point of POM. As a result, the reaction mass changes fast from the liquid to the solid state at higher conversion rates. To deal with this problem, the reaction is performed in specially designed reactors. Hoechst and Celanese developed a polymerisation process using a kneading stirrer. Degussa developed a band-polymerisation process where the monomer and starter is filled into a PE tube [118]. The welded tube is rolled to flat band of about 2 cm thickness, which is dragged through a bath of water at 70–80 °C to initiate polymerisation and to remove generated reaction heat.

Thermally Stable Polyoxymethylene by Copolymerisation of Trioxane

Another strategy to obtain thermally stable polyoxymethylene is the copolymerisation of trioxane with small amounts of suitable co-monomers, in particular oxocyclic compounds such as 1,3-dioxane, 1,3-dioxolane, or ethylene oxide [119–121]:

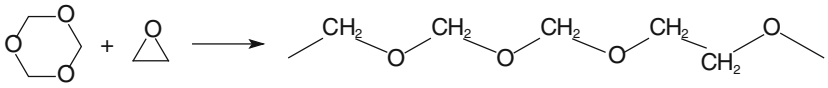

Primarily, the resulting trioxane copolymers are thermally unstable. Chain degradation starts as already mentioned at the terminal hemi-acetal moieties, but it will be interrupted by C–C bonding in the chain that origins from co-polymer integration. By optimising the minimum necessary amount of co-monomers, POMs can be obtained. They show initial thermal degradation of approximately

Table 6.5 Typical classes of starters for the polymerisation of formaldehyde to polyoxymethylene. [115]

Class of starters	Typical amount based on formaldehyde [wt%]	Typical starters	Remarks
Tertiary amines	~0.2	Tris-*n*-butylamine, octadecyl dimethylamine, diphenylamine, morpholine, or hydrazine	Building of high-molecular products
Phosphine, arsine, stibnine	~0.05	Triphenylphosphine, tributylphosphine, trinaphthylarsine, triethylstibnine	Triphenylphosphine shows a higher reactivity than triphenylamine or other amines
Metal carbonyls	~0.005	Carbonyls of Fe, Co, Ni	–
Organometallics R_nM with M = main group or transition metals and R = alkyl, aryl, alkoxyl, acyl	~0.05	Phenyllithium, sodium decanolate, methyl magnesiumiodide, calcium hydride, aluminium triisopropylate, dimethylcadmium, triphenylbismuth, diphenylmercury, diphenyltin	Diphenyltin leads to the highest molar weights

1–2 wt%, after which they are thermally stable, comparable with acetylated homopolymeric polyoxymethylenes.

A summary of the two discussed synthesis routes to get thermally stable polyoxymethylene is given in Fig. 6.27.

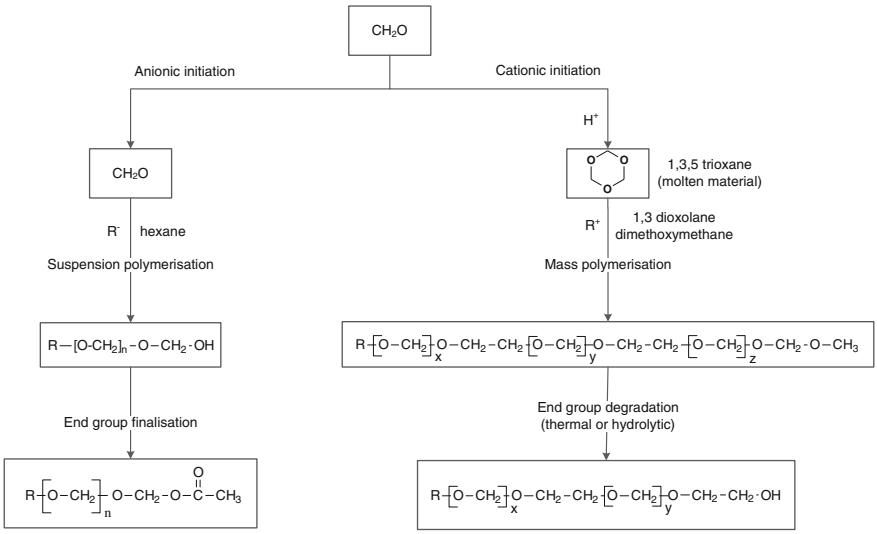

Fig. 6.27 Synthesis routes of thermally stable polyoxymethylene by postfinalisation of homopolymeric POM or copolymerisation of trioxane. (Adapted from [104])

6.2.10 Dimethyl Carbonate

Carbonic acid dimethyl ester, dimethyl carbonate (DMC), is a chemical that is being produced in rapidly increasing amounts. In 1990 global production amounted to 45,000 t/a, in 1997 it was 62,000 t/a and in 2009 overall production totalled approx. 370,000 t/a with China as the world's largest producer, but based on transesterification processes only. Enichem, who developed the methanol oxycarbonylation process (Fig. 6.29), produced 70,000 t/a in 2001 [122, 123].

About half of DMC production is used for the production of coatings and adhesives, where it is mainly used to replace solvents such as toluene, ethyl acetate, butyl acetate, acetone, or methyl ethyl ketone. Another large amount goes to pesticide and pharmaceuticals production, where it is mostly used as a methylation agent to replace dimethyl sulphate.

Phosgene, $COCl_2$, is a highly reactive and highly toxic carbonylation reagent for the synthesis of isocyanates, diisocyanates, polycarbonates and others. However, phosgene is a hazardous chemical, compared to which DMC is about 1,000

times less toxic and, in addition, considered to be environmentally benign. It is highly reactive towards nucleophiles, making it a valuable reactant for carbonylation reactions. In methylation reactions, DMC can replace dimethyl sulphate (see Sect. 6.2.15.4) and methyl halides (see Sect. 6.2.14), which themselves through their strong methylation potential are highly toxic as well [124].

6.2.10.1 Dimethyl Carbonate Production Through Phosgenation

Until the 1980s, like alkyl carbonates in general, DMC was produced by reacting methanol with phosgene. This manufacturing process was chiefly pursued by Bayer (Germany) and the Societé Nationale des Poudres et Explosifs (France). The base-catalysed two-step process involves methyl chloroformate as an intermediate:

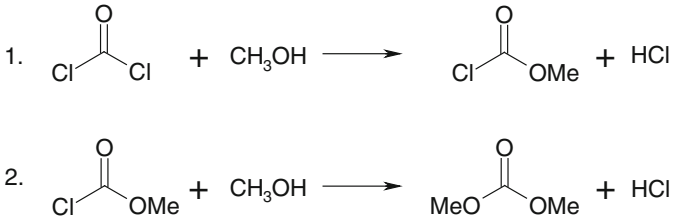

This process benefits from high yields of 82–85 %, yet it suffers from the need to neutralise large amounts of the base used (pyridine or NaOH) and to dispose of the salts [125–128].

6.2.10.2 Dimethyl Carbonate Production Through Transesterification

The vast majority of global DMC production is obtained from transesterification of ethylene or propylene carbonate with methanol. Although it is most important in industrial chemistry, transesterification processes as industrialised by Texaco, Shell and Shenghua Chemical Group (China) suffer from ethylene and propylene carbonate being expensive raw materials. The reaction is conducted in batch operations at 80 bar and 100–150 °C over a tetravalent Lewis acidic catalyst such as $ZrCl_4$, or $Ti(acac)_2$, with 98 % selectivity for methanol [129].

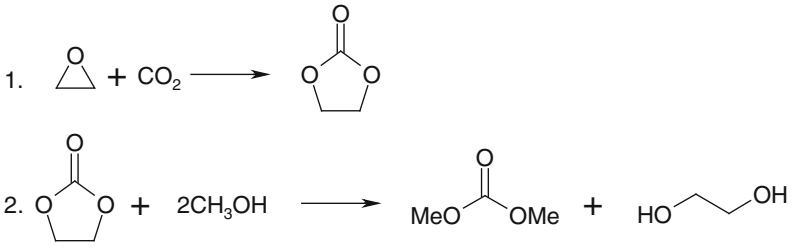

Formally, the process can be realised as a pure C_1 route if oxirane is obtained from methanol derived ethylene. However, DMC production suffers from the reaction equilibrium being in strong favour of the reactants, which leads to separation problems for the product/reactant mixture because DMC and methanol form an azeotrope.

In fact product separation and purification accounts for about 25 % of the total production costs of DMC. Additionally, the cost-effectiveness of DMC production processes via the transesterification route is ruled by the marketability of ethylene (propylene) glycol co-product, a situation that is aggravated by the market, demanding pharmaceutical-grade glycol qualities preferably. With biological routes to propylene glycol (PG) emerging, thus causing PG prices to drop and rendering co-product marketing economically less attractive, processes have been switched to ethylene glycol (EG) as a raw material.

As an alternative, ethylene carbonate can by regenerated from ethylene (propylene) glycol by conversion with urea:

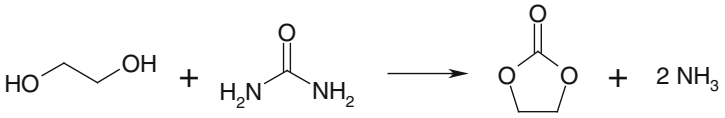

Urea can directly be used as carbonyl source for DMC production, too. The process again suffers from the equilibrium lying far on the left; however, it avoids separation problems because no azeotropic mixture is formed with DMC. The first step yielding methyl carbamate is done at approximately 100 °C over Al(*i*Bu)$_2$H as a Lewis acidic catalyst. Full conversion to DMC is achieved upon heating up to 180–190 °C over a Lewis base such as PPh_3.

There are two other commercial processes in operation: Enichem's oxycarbonylation of methanol and Ube's methyl nitrite process, for which a first plant for selective gas phase carbonylation of methanol has been put into operation. Daicel and Sekka pursued the same reaction in the liquid phase [130].

6.2.10.3 Dimethyl Carbonate from Methanol Oxycarbonylation

The oxidative carbonylation of methanol is a catalytic route to produce DMC from CH_3OH, CO and O_2. Oxygen is required in order to oxidise the carbonyl carbon from oxidation state II to oxidation state IV (carbonic acid).

In 1983, Enichem (Italy) industrialised this process, which makes use of the catalytic properties of copper, i.e. the ability to switch between Cu^I and Cu^{II} [131, 132]. The oxidative carbonylation of methanol is conducted in the liquid phase in a slurry reactor, which is continuously fed with CO, O_2 and CH_3OH (Fig. 6.28).

The reaction is strongly exothermic, thus furnishing gaseous products that can easily be removed from the slurry together with excess unreacted reactants. Like the transesterification variants, a methanol/DMC azeotrope is obtained, from which DMC is separated and CH_3OH is funnelled back into the reactor. The sole byproducts are CO_2 and water. Although CO_2 can be recycled to produce CO, water

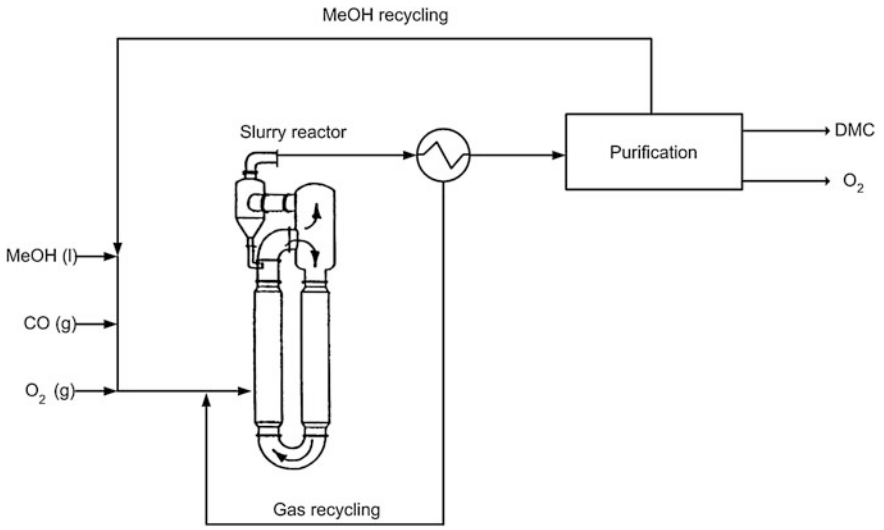

Fig. 6.28 Conceptual scheme of Enichem's dimethyl carbonate (DMC) process. (Adapted from [124])

formation is critical. The reason is competing formation of $CuCl_x(OH)_y \cdot n\ H_2O$-like phases, which are less reactive for DMC production [45]. Secondly, water allows CuCl be reduced to metallic copper in the presence of CO, causing catalyst inactivation and formation of HCl. Last but not least, the latter either reacts with methanol to give $CHCl_3$ or DME formation is catalysed. For that reason, water content was found to be optimal at 3 wt%, with the overall reaction taking place in excess methanol.

Typical reaction conditions are 20–40 bar and 120–140 °C. In any case, oxygen remains the limiting reaction in order to avoid explosive risks, which occur upon oxygen contents exceeding 4 mol % in zones where CO is the main component [45, 125, 133].

Figure 6.29 shows the current model of methanol oxycarbonylation. Although it remains contradictory in some respects, it is the generally accepted mechanism for this process.

The ENI plant was originally designed for 5,000 t/a and was expanded in 1993 to 12,000 t/a [134].

6.2.10.4 Dimethyl Carbonate from Methyl Nitrite Carbonylation

Another approach to DMC is Ube's methyl nitrite process, which is a two-step synthesis. It starts with methyl nitrite formation (I) from CH_3OH, NO and O_2 in reactor I:

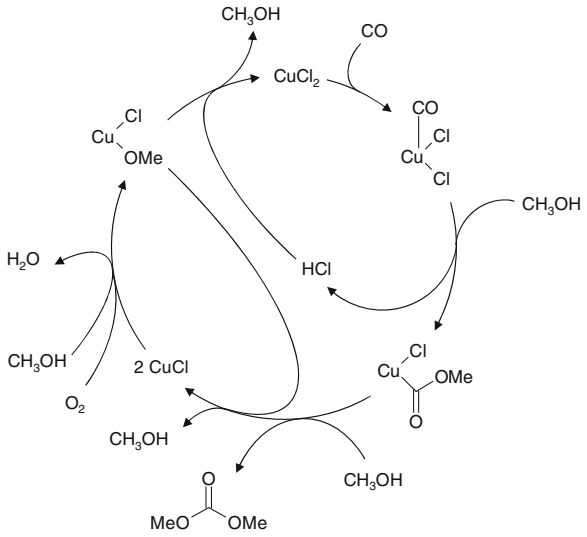

Fig. 6.29 Catalytic cycle of copper-catalysed methanol oxycarbonylation to dimethyl carbonate. (Modified from [131])

$$1.\ 2\,NO + {}^{1}/_{2}\,O_2 \longrightarrow N_2O_3$$

$$2.\ 2\,CH_3OH + N_2O_3 \longrightarrow 2\,H_3C{-}ONO + H_2O$$

$$2\,CH_3OH + 2\,NO + {}^{1}/_{2}\,O_2 \longrightarrow 2\,H_3C{-}ONO + H_2O$$

This reaction is performed in the liquid phase at 60 °C with a residence time of 0.5–2 s and does not require a catalyst. Product water must be removed in order to maintain catalyst activity in the second step.

Methyl nitrite is brought to reaction with CO in the gas phase (both reactants are approximately 5–30 vol%) in reactor II over an activated charcoal-supported $PdCl_2$ catalyst in a fixed-bed reactor with small amounts of chloride compounds diluted in an inert gas present. The catalytic reaction takes place with a contact time of approximately 0.5–5 s at 5–10 bar and 100–120 °C:

$$2H_3C{-}ONO + CO \xrightarrow{[PdCl_2]} \underset{MeO}{\overset{O}{\underset{}{}}}\!\!\overset{}{\underset{}{}}\!\!\underset{OMe}{} + 2NO$$

The outlet stream of reactor II contains DMC and unreacted reactants. As co-products, dimethyl oxalate, methyl formate and dimethoxymethane (methylal) are obtained. Over an adsorption column, CO, NO and methyl nitrite are separated from the product mixture with the purpose of reinjecting them in reactor I. This procedure avoids contact between water, DMC and methanol, thus circumventing the separation problems caused by azeotrope formation between these compounds. Figure 6.30 shows methyl nitrite formation (I) and the catalytic cycle (II) of Ube's methyl nitrite process.

Among the above mentioned byproducts dimethyl oxalate is the only significant one obtained by the Ube process. It is formed as a result of the decomposition of

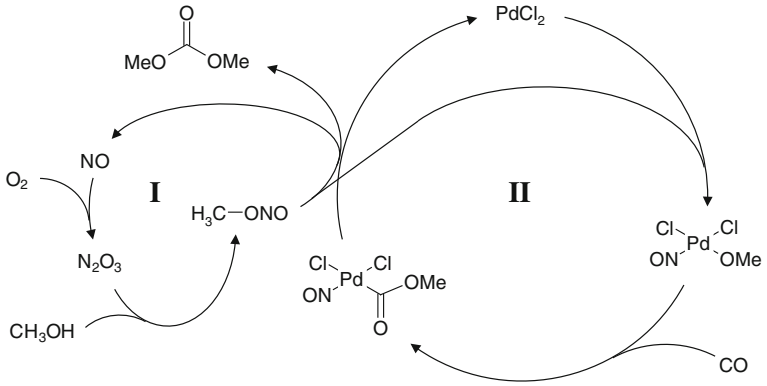

Fig. 6.30 Catalytic cycle of methyl nitrite carbonylation to DMC. With NO being regenerated, CH_3OH, CO and O_2 are the actual raw materials of the process. Oxygen is required to formally oxidise CO to C^{IV}. (Modified from [130])

the intermediate $[Pd(CO_2CH_3)(NO)Cl_2]$ complex into methyl chloroformate, NO and metallic palladium. The latter reacts with methyl chloroformate under regeneration of $PdCl_2$, thereby producing dimethyl oxalate:

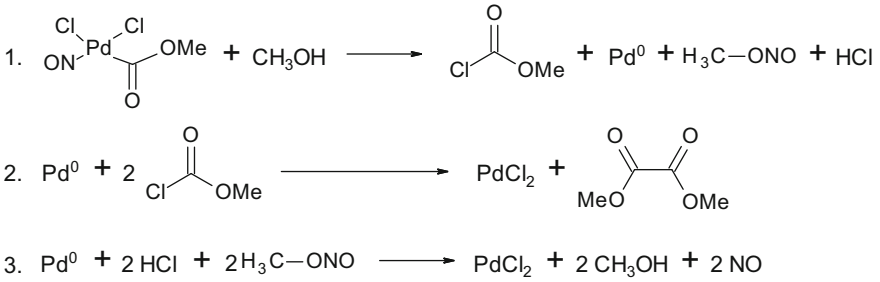

Hence, methyl nitrite plays a double role in the Ube process. It acts as a reactant for the synthesis of DMC and also as an oxidising agent for keeping palladium in the $PdCl_2$ form (i.e. regenerating the catalyst).

6.2.10.5 Dimethyl Carbonate from Methyl Formate

See Sect. 6.2.4.4.

6.2.10.6 Direct Synthesis from CO_2

Direct DMC synthesis starting from CO_2 appears compelling because it is a true C_1 route.

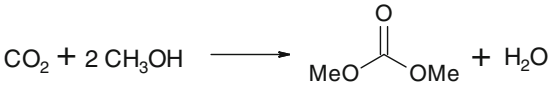

In fact, a multitude of approaches have been tested, although with no noticeable commercial significance so far. Comparable to transesterification variants, direct synthesis requires catalysts and suffers from unfavourable positions of equilibrium as well as the need for continuous product removal from azeotrope mixtures. Typical yields range between 1 and 4 % [125]. Details of the numerous approaches are beyond the scope of this chapter, though.

Like with classical catalysts, DMC is accessible by enzymatic methods. However, conversions <4 % do not surpass classical approaches and necessitate recirculation processes with continuous product removal. Enzymatic DMC synthesis is done in water using hydrolases as a biocatalyst. It is inspired by the high productivity of carbonic anhydrase, which catalyses the reaction:

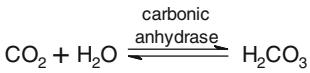

The enzymatic conversion was found to succeed with methanol instead of water as a nucleophile [135]:

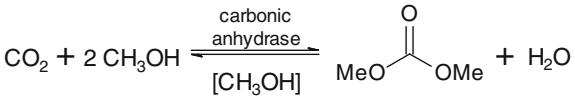

6.2.11 Hydrogen Cyanide

Hydrogen cyanide is an important synthetic building block (Fig. 6.31) for which two synthetic routes exist:

1. Dehydration of formamide.
2. Ammonoxidation of Methane
3. Ammondehydrogenation

In addition, HCN is formed as a byproduct in acrylonitrile production through ammoxidation of propylene.

Being the formal C_1-approach starting from methanol, formamide dehydration (see Sect. 6.2.4.3) is conducted under reduced pressure at 480–530 °C in iron made tube reactors filled with $FePO_4$ or $AlPO_4$ using Mg, Ca, Zn, or Mn as promoters with an HCN selectivity of 92–95 %:

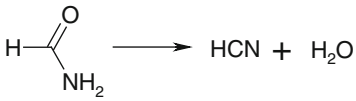

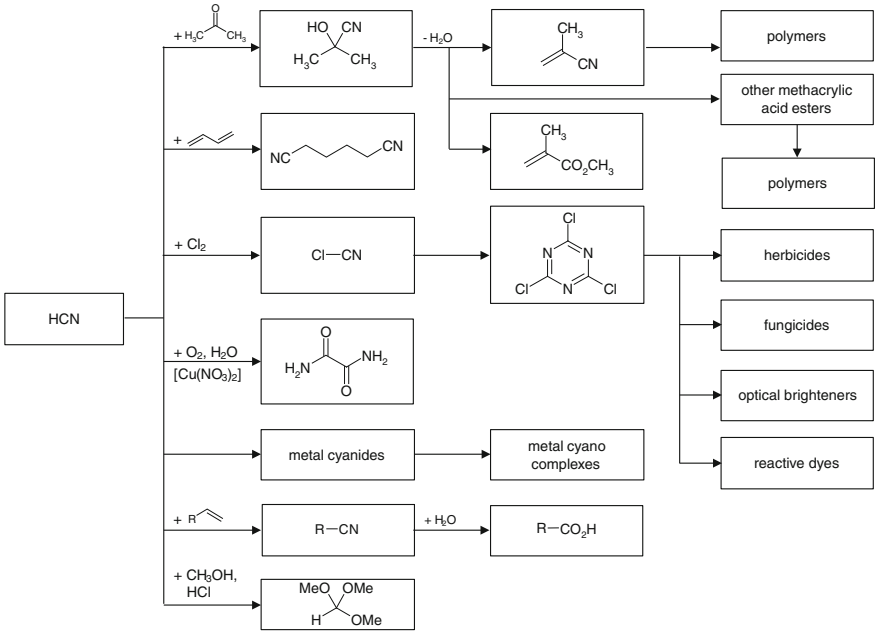

Fig. 6.31 Products derived from hydrogen cyanide

The product gas is rich in HCN (60–70 %), for which reason it is suitable for direct liquefaction. The process (developed by BASF, Degussa and Knapsack) is no longer economically significant, however. It has been replaced by oxidative or dehydrogenating conversions of hydrocarbons with ammonia, where preferably methane is used according to the Andrussow or BMA process, respectively.

6.2.12 Methyl Methacrylate

Methyl methacrylate (MMA) is starting material for the production of Polymethyl methacrylate (PMMA), which is commonly known as Plexiglas®, a highly transparent and bright polymer. In addition MMA finds application in the production of oil additives (e.g. Viscoflex®), film coatings of pharmaceutical preparations Pharma (Eudragite®) and dental products. Further, MMA is used as wettener as well as thickener for emulsion paints. MMA production has experienced steady growth over the last years. In 2007, 3.15 million tonnes were produced on a global scale. In 2009, Evonik installed another MMA plant in Shanghai, China with approximately another 100,000 tonnes of production capacity, which equals an increase of 33 % in global MMA production within only 6 years [136, 137].

There are 9 different processes industrialised for MMA production among which the direct oxidation process and the direct oxidation esterification process deserve more detailed description within the scope of this book. Till present however saponification of acetone cyanhydrine (ACH) through concentrated H_2SO_4 with subsequent acid recycling is the dominating process. Recent improvements have been achieved by introducing Evonik's Aveneer® catalyst.

6.2.12.1 Direct Oxidation Process

The isobutylene direct oxidation process has been in operation for more than 25 years now. As pointed out in Sect. 6.2.16, this process profits from methyl tert-butyl ether (MTBE) and tert-butyl alcohol (TBA) being cheap and easily transportable vehicles for isobutylene. In particular, MTBE has an economic advantage because MMA production consumes both isobutylene and methanol recovered from catalytic MTBE decomposition.

MMA production commences with either using isobutylene as a starting material (Sumitomo Chemical, Nippon Shokubai), TBA (Mitsubishi Rayon, Kururai, Mitsui Chemicals) or MTBE (Evonik). TBA and MTBE are used as starting materials because they are easily decomposed to give isobutylene and water or methanol, respectively. For TBA, the endothermic reaction is carried out at an elevated temperature over inexpensive alumina as decomposition catalyst. For MTBE, silica impregnated with metal sulphate or an aqueous heteropolyacid solution is used (Fig. 6.32).

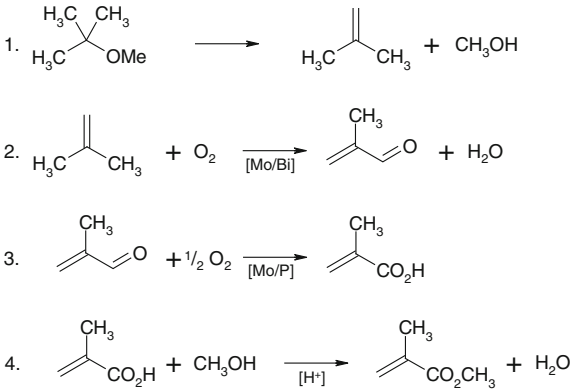

Fig. 6.32 Methylmethacrylate production according to the direct oxidation process starting from methyl tert-butyl ether

Isobutylene oxidation is divided into two steps, with the first delivering methacroleine and the second only furnishing methacrylic acid. The first oxidation step is conducted over a Mo-Bi–Fe-Co/Ni-A (A: alkali metal, alkaline earth, Tl) composite oxide catalyst in the gas phase. Although the catalyst is similar to that used for propylene oxidation, the catalyst for the latter purpose would be far too active, always bearing the risk of total oxidation. In the second step, a catalyst of

molybdophosphoric acid, $H_3PMo_{12}O_{40}$, is used. The acid catalyst must be anhydrous and present in the Keggin structure, under which conditions uniform Brønstedt acidic properties are provided due to protons sharing oxygen centres. The hydrated species is not quite as active and exerts detrimental effects on the reaction for being thermally not sufficiently stable. Another benefit of using molybdophosphoric acid results from its molybdenum centres, which promote the reaction through their ability of switching between oxidation states. Nevertheless, second-step catalyst performance is not yet satisfactory, for which reason catalyst optimisation is a major issue in MMA industry.

Esterification of methacrylic acid—the final product obtained from isobutylene oxidation—is carried out with methanol under acidic conditions. Production routes starting from MTBE benefit from using the methanol obtained from MTBE decomposition. [136, 137]

6.2.12.2 Direct Oxidation Esterification Process

As depicted in Fig. 6.33, a modification of the direct oxidation process was developed by Asahi. It shortens the process to three reaction steps by realising the second oxidation step in methanolic solution over a Pd-Pb catalyst. Under these conditions, once methacrylic acid is formed, it is instantly converted into its methyl ester.

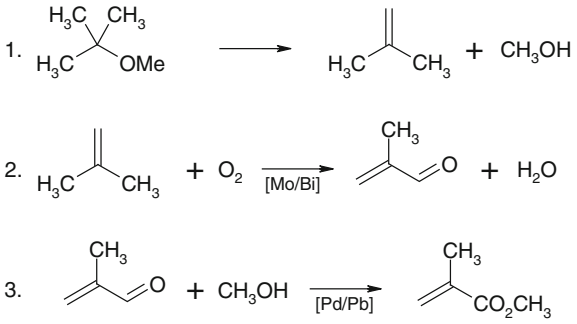

Fig. 6.33 Methylmethacrylate production according to the direct oxidation esterification process

The reaction proceeds with maximum 95 % selectivity. Although the economic attractiveness is obvious, there are still problems to be solved, such as heat flux reintegration. Nevertheless, this method has great potential for replacing the four-step route. [136]

6.2.13 Methyl Amines

All three methyl amines are important intermediates in the synthesis of solvents, insecticides, herbicides, pharmaceuticals and detergents. The demand for each

species is rather different, with dimethyl amines being the most important product as they are required for the synthesis of *N*,*N*-dimethyl formamide (DMF) (see Sect. 6.2.4.4). Monomethyl amine, which is used for the production of methyl urea, NMP and methyl taurine (used in CO_2 scrubbing or as washing agent ingredient) is also important. Trimethyl amine has less importance but is used in choline chloride synthesis (Fig. 6.34).

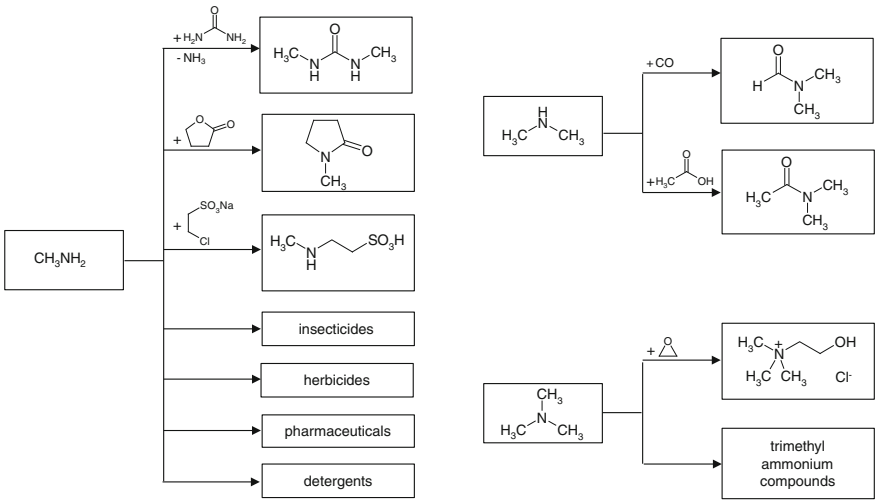

Fig. 6.34 Products derived from methyl amines

Regarding methanol consumption, methyl amines are in the fifth position among the methanol derivatives with approximately 3–5 % methanol consumption, after formaldehyde, acetic acid, methyl halogenides and MTBE. Large-scale producers are BASF, Montedison, DuPont and Air Products.

For commercial production, CH_3OH and NH_3 are converted at 15–30 bar and 350–500 °C in the presence of aluminium oxide, silicate, or phosphate:

$$CH_3OH + NH_3 \xrightarrow{[cat]} CH_3NH_2 + H_2O$$

Because pressure exerts a rather insignificant effect on the course of reaction, amine synthesis is done mostly at 20 bar. The alkylation does not stop at the stage of monomethyl amine; the reaction simultaneously furnishes all three possible amines. Excess NH_3 and addition of H_2O favour mono- and dimethyl amine formation. At 500 °C and with a NH_3/CH_3OH-ratio of 2.4:1, 54 % monomethyl amine, 26 % dimethyl amine and 20 % trimethyl amine are obtained. Byproducts are CO, CO_2, CH_4, H_2 and N_2. The overall selectivity for methyl amines is approximately 94 %. For the reason of azeotropes being formed, the reaction products are separated by a set of pressure distillations and extractive distillation.

Alternatively to aluminium salts, acidic zeolite catalysts can be used, which shift the product composition. The Nitto process furnishes ≤86 % dimethyl amine and 7 % monomethyl amine and trimethyl amine. This variant is of importance when dimethyl amine is the most desired product, such as for DMF synthesis [20].

6.2.14 Methyl Halogenide Production from Methanol

Chloromethanes are typically produced through chlorination of methane at 440 °C:

$$CH_4 + Cl_2 \longrightarrow \underset{37}{CH_3Cl} + \underset{41}{CH_2Cl_2} + \underset{19}{CHCl_3} + \underset{3}{CCl_4}$$

6.2.14.1 Chloromethane (Methyl Chloride)

Methyl chloride also can be obtained by reacting CH_3OH with HCl in the liquid phase at 100–150 °C at elevated pressure. The reaction can be accomplished without a catalyst or in the presence of a Lewis acid, such as $ZnCl_2$ or $FeCl_3$. CH_3Cl production succeeds in the gas phase as well, at 3–6 bar and 300–380 °C over $ZnCl_2$ or $CuCl_2$. Alternatively, H_3PO_4 on SiO_2 can be used:

$$CH_3OH + HCl \rightarrow CH_3Cl + H_2O$$

The conversion is highly selective (98 % for CH_3OH). Only small amounts of DME are formed as a byproduct (see Sect. 6.2.19). Today, this methanol hydrochlorination process is the preferred access to CH_3Cl. This approach has growing importance, with increasing methanol availability at reasonable prices.

Further contributions resulted from development of the Tokuyama Soda process, according to which higher chloromethanes are produced by follow-up chlorination of CH_3Cl at 100 °C. The off-product, "chlorination hydrochloric acid" finds re-use in esterification processes for methanol. In this way, methanol is the raw material base for all chloromethanes, too [20].

6.2.14.2 Methanol-Based Methyl Chloride Recovery in the Müller-Rochow Direct Process

Prior to polydimethylsiloxane (silicone) production, silicon was required to be converted into dimethyldichlorosilane according to the Müller-Rochow process by converting Si with CH_3Cl. In classic silicone synthesis, dimethyldichlorosilane is hydrolysed whereupon HCl is produced, which in turn serves to regenerate CH_3Cl from methanol:

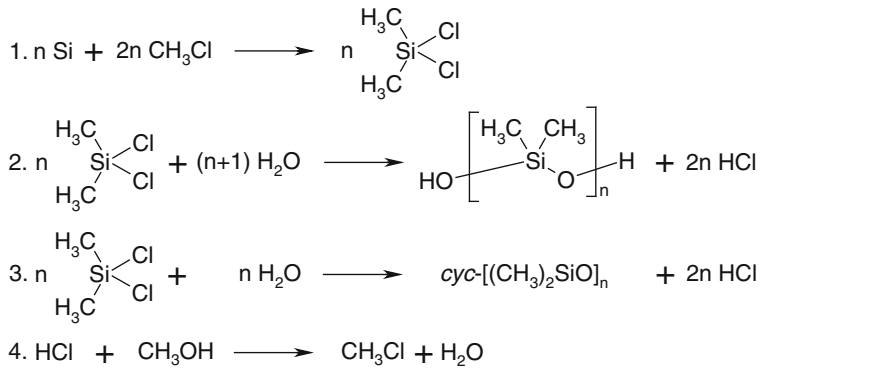

CH_3Cl regeneration is conducted both in the liquid and the gas phase.

Contemporary approaches shortcut CH_3Cl regeneration by using methanol as an OH source instead (direct process). Again chloromethane is recycled from the process, yet from methanolysis in lieu of two-step hydrolysis/HCl conversion:

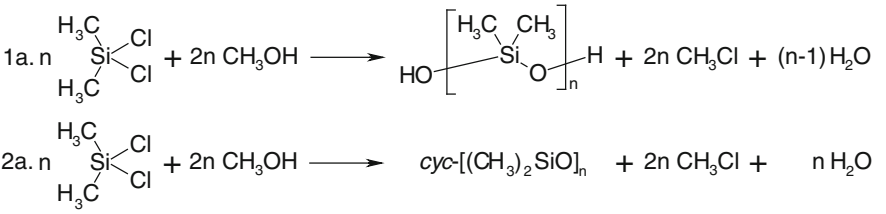

Continuous methanolysis is performed in the gas phase. Depending on the reaction conditions, cyclic or linear siloxanes are retrievable in line with the classical approach. Linear siloxanes are preferably obtained if cyclic siloxanes, which can be distilled, are funnelled back into the process. DME (see Sect. 6.2.19) is a possible byproduct [138–141].

6.2.15 Sulphur Compounds Derived from Methanol

6.2.15.1 Methanethiol

Methanethiol (methyl mercaptane) has a persistent unpleasant odour. For this reason, it is added as an odouriser to natural gas or propane in order to draw attention to leaks. Synthetically, it is chiefly used to produce methionine, an animal feedstuff additive in poultry and animal feed. Methanethiol is also used as a precursor in the manufacture of pharmaceuticals, pesticides and other agricultural chemicals (Fig. 6.35) [142–145]. Evonik produced approximately 200,000 tonnes in 2012 with about 190,000 tonnes for methionine production compared to

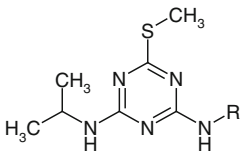

R	Commercial product
-*i*-Pr	Semeron
-$(CH_2)_3$-O-CH_3	Gesaran
-Et	Ingran

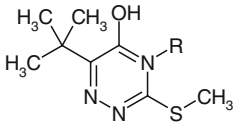

R	Commercial product
-NH_2	Sencor
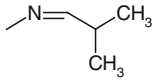	Tantizon

Fig. 6.35 Examples of herbicides derived from methanethiol. (From [149])

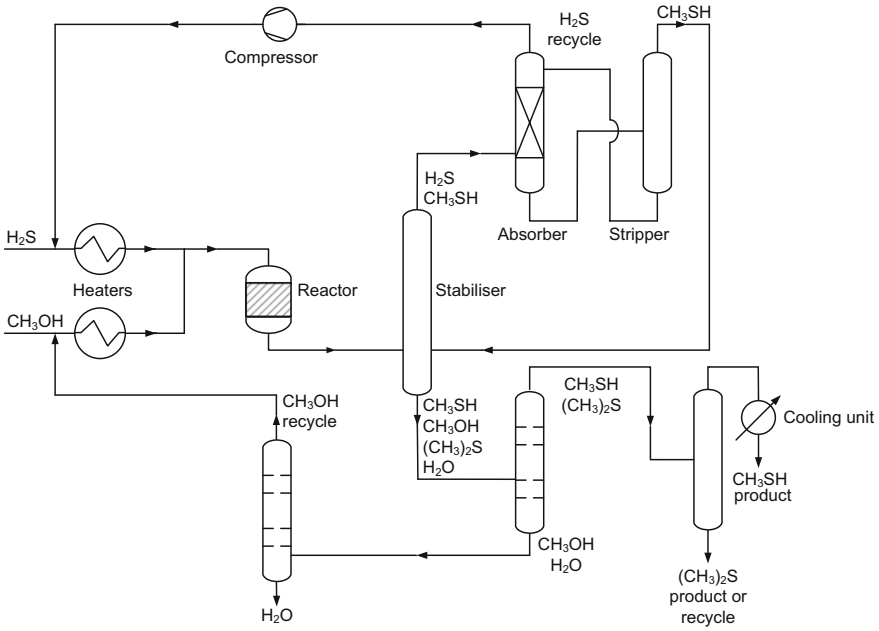

Fig. 6.36 Methyl mercaptane production process. (From [150])

~50,000 tonnes in 2003 [146]. In addition, methanethiol is released as a byproduct of wood pulping [147–149].

Methyl mercaptane is produced in a gas phase reaction from methanol and hydrogen sulphide over basic Al_2O_3 as the dehydration catalyst at ≥300 °C:

$$CH_3OH + H_2S \rightarrow CH_3SH + H_2O$$

Figure 6.36 illustrates a methyl mercaptane production process. As can be seen there, dimethyl sulphide (see Sect. 6.2.15.2) is also obtained as a byproduct, which can be understood in terms of the similar reaction conditions for the synthesis of each species.

Alternatively, methyl mercaptane can be obtained from the reaction of methyl iodide with thiourea [147].

6.2.15.2 Dimethyl Sulphide

Commercially, dimethyl sulphide (DMS) is used in petroleum refining and petrochemical production processes to control formation of coke and CO. Another use is dust control in steel rolling mills. DMS serves as a reagent in a variety of organic syntheses. In the food industry, DMS is employed as a flavouring component. Oxidation furnishes dimethyl sulphoxide (DMSO), which is an important industrial solvent.

DMS is obtained from reacting methanol in an acidic medium [150]:

$$2CH_3OH + H_2S \rightarrow (CH_3)_2S + H_2O$$

6.2.15.3 Dimethyl Sulphoxide

In technical applications, DMSO is mainly used as a solvent. Therapeutically, it has antiphlogistic and analgetic properties, for which reason it is applied percutaneously for the local treatment of pain, and it serves as percutaneous absorption promoter. DMSO itself has a low toxicity, yet concentrated DMSO is reported to be neurotoxic at levels >0.3 mL/kg. [151–153]

DMSO is commercially produced by oxidation of dimethyl sulphide with O_2 and/or N_2O:

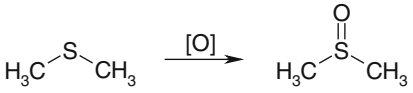

6.2.15.4 Dimethyl Sulphate

As a strong methylating agent, dimethyl sulphate is used for the production of methyl esters, ethers and quaternary amines in the synthesis of dyestuffs, pharmaceuticals, perfumes, pesticides, or phenol derivatives. It is highly toxic and carcinogenic.

Dimethyl sulphate is produced from converting DME with liquid SO_3 which is continuously funnelled under cooling into a reactor made from stainless steel or aluminium filled with dimethyl sulphate as the reaction medium:

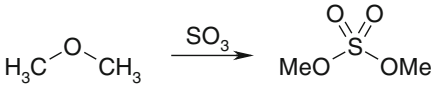

6.2.16 Methyl Tert-Butyl Ether and Tert-Butanol from Isobutylene

Isobutylene constitutes the major component of raffinate I (44–49 %) in the workup of the C_4 fraction. In steam cracker gases, it is removed from the gas mixture by acid-catalysed conversion with methanol to give MTBE. The addition of water leads to tert-butanol.

These processes make use of isobutylene being the most reactive component, meaning a tert-butyl carbenium ion is easily formed under acid catalysis. Similarly, in the backward reaction, isobutylene is released from either of these species. The benefit of these operations is the rapid and easy separation of isobutylene from gas mixtures. In addition, MTBE and tert-butanol serve as transport vehicles for isobutylene. Being liquids, there is no further effort required to compress and safely store and transport gaseous isobutylene. Using MTBE is doubly beneficial because two chemicals are available in one process: methanol and isobutylene.

6.2.16.1 Tert-Butyl Alcohol

Tert-Butanol (tert-butyl alcohol, TBA) is used as a solvent and as an intermediate in the synthesis of methyl tert-butyl ether (MTBE) and/or ethyl tert-butyl ether (ETBE), where these two latter are not obtained directly from gaseous resources. Together with H_2O_2, tert-butyl hydroperoxide is obtained. In fuel chemistry, it serves as an octane booster for gasoline, i.e. as an oxygenate gasoline additive. In final product formulations, it is found in paint removers, flavours and perfumes.

In the presence of diluted mineral acid or an acidic ion exchanger, isobutylene is converted to tert-butanol in a reversible reaction. Most companies use 50–60 % H_2SO_4. HCl is in use by Nippon Oil, and the Hüls process works with ion exchanger.

Isobutylene is extracted in a countercurrent flow from C_4-raffinate I at 10–20 °C. After dilution with water, tert-butanol is isolated by distillation. In the Nippon Oil process, which uses HCl, a mixture of tert-butanol and tert-butyl chloride is obtained, from which isobutylene and HCl are regenerated:

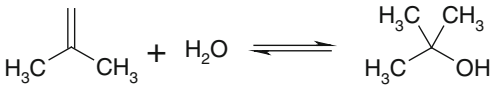

The reverse reaction, tert-butanol fission to isobutylene, is accomplished according to a process by Arco. Isobutylene regeneration is in as much favourable, as tert-butanol is obtained as a co-product; for instance from the oxirane process in propylene oxide production, it can be recovered and used as an isobutylene raw material.

The fission process is realised in the gas phase at 14 bar and 260–370 °C over a high-surface alumina catalyst. tert-Butanol conversion is $\leq$98 % with high selectivity for isobutylene. Other processes work in the liquid phase below 150 °C in the presence of heterogeneous catalysts [20].

6.2.16.2 Methyl Tert-Butyl Ether

Apart from its use as a component in fuel for gasoline engines (see Sect. 6.3.1), MTBE is used as solvent. Its use as a vehicle for isobutylene has been discussed above. For its use as a solvent, MTBE possesses one distinct advantage over most ethers: it does not form dangerous hydroperoxides for a methylene group in α-position to the ether oxygen is missing (Fig. 6.37):

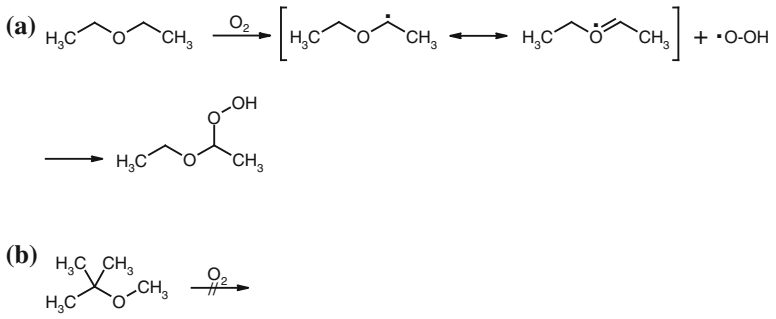

Fig. 6.37 Hydroperoxide formation in ethers. a) When a secondary carbon is present adjacent to ether oxygen, hydroperoxide formation is considerably facilitated through resonance stabilisation of the intermediary radical. Recombination of the ether radical and hydroperoxide radical furnishes ether peroxides highly liable for detonative decomposition. b) With a primary and a tertiary carbon neighbouring oxygen, hydroperoxide formation is substantially disfavoured

MTBE is raising environmental concerns because it can render large quantities of groundwater nonpotable. One source of MTBE release into water-supply aquifers are leaking underground storage tanks (UST) at gasoline stations or gasoline containing MTBE that is spilled onto the ground. The higher water solubility and persistence of MTBE cause it to travel faster and farther than many other components of gasoline when released into an aquifer. A further discussion of this issue is beyond the scope of this book. For reasons of objectification, however, it has to be emphasised that any chemical entity, including table salt, has to be kept off water-supply aquifers. It is no distinctive property of MTBE to spoil drinking water. When discussing the banning of a chemical compound, advantages and disadvantages need to be evaluated carefully in terms of a holistic view. The actual reason why MTBE has been recommended phasing out as an additive to gasoline by the US Environmental Protection Agency (EPA) were reports on probable occurrence of cancerous tumours in laboratory rats which had been injected with it [154].

Production of MTBE from isobutylene and methanol proceeds at slight overpressure and 30–100 °C in the liquid phase over acidic ion exchangers. The process is realised either in one or two reactors or in a two-stage tower-reactor in order to achieve complete isobutylene conversion (>99 %).

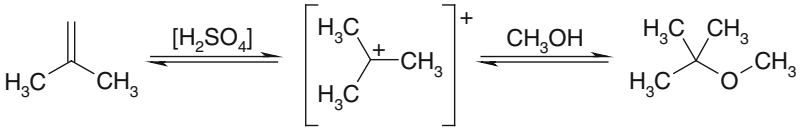

The pressure-dependent azeotrope formation between methanol and MTBE necessitates a multistage pressure distillation. Alternatively, methanol can be removed by adsorption to adsorber resins (Bayer and Erdölchemie). Contemporary approaches pursue methanol removal by means of hydrophilic pervaporation, such as over polyvinyl alcohol membranes [20].

6.2.17 Tert Amyl Methyl Ether

Tert Amyl Methyl Ether (TAME) is chiefly used as an oxygenate to gasoline (cf. Sect. 6.3.1) in order to increase octane enhancement and to raise the oxygen content in gasoline. TAME in fuel reduces exhaust emissions of volatile organic compounds (VOC).

Conversion of methanol with isopentene from C_5 fractions is accomplished similarly to MTBE production (see Sect. 6.2.16.2) over an acidic ion exchanger. The reaction profits doubly from an intermediary isoamyl cation being formed. In this way, not only is methanol addition facilitated, but carbenium ion formation also allows for unifying 2-methyl-1-butene and 2-methyl-2-butene into one common product, TAME:

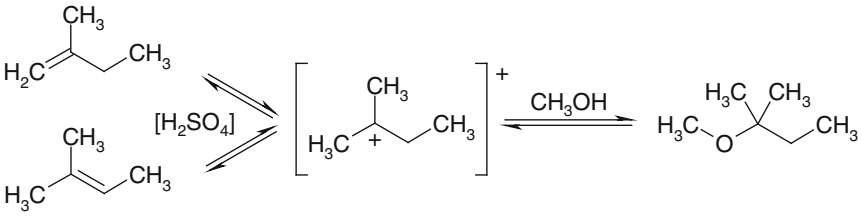

Novel developments by Erdölchemie allow for the reaction to be realised over bifunctional catalysts. The first TAME plant was established in the United Kingdom in 1987. TAME production was 1.26 million tonnes in 1999 compared to 12.25 million tonnes of MTBE [20].

6.2.18 Dimethyl Terephthalic Acid

Predominant use of dimethyl terephthalate (DMT) is polymer synthesis with polyethylene terephthalate as the most important plastic material. DMT is produced according to a series of different liquid-phase oxidation processes starting from *p*-xylene. The process developed by Chemische Werke Willen consists of

p-xylene oxidation at 6 bar and 150–170 °C in liquid medium in the presence of Co and Mn salts as a first step, which takes place in an oxidation reactor and furnishes *p*-toluic acid. The latter is reacted with methanol in a second reactor, the esterification reactor. The reaction is conducted at 20 bar and 250–260 °C and requires no further catalyst addition.

Upon distillation of the reaction mixture, *p*-toluic acid is recovered overhead and refunnelled into the oxidation reactor, where it is subjected to another oxidation step at the unreacted methyl group. This reaction takes place parallel to *p*-xylene oxidation in the same reaction medium. Likewise, the second esterification step is conducted parallel to *p*-toluic methyl ester synthesis, yet with the difference of DMT being poorly volatile and as such accumulating in the bottom product, from where it is recovered through recrystallisation from methanol. Further purification may be achieved by distillation (Fig. 6.38) [155].

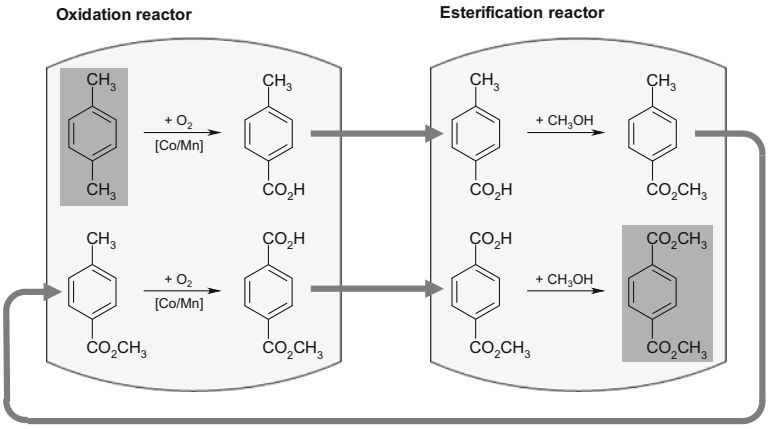

Fig. 6.38 Dimethyl terephthalate (DMT) synthesis starts with the Co/Mn-catalysed oxidation of *p*-xylene to *p*-toluic acid, which in the esterification reactor is transformed into the respective methyl ester. The latter is refunnelled into the oxidation reactor, where the second methyl group is oxidised. Terephthalic acid monoester is once again transferred into the esterification reactor, where the final esterification step to the diester DMT takes place. Thus, both the oxidation and the esterification reaction steps are passed through two times each. For reasons of process economy, *p*-xylene together with *p*-toluic acid methyl ester and *p*-toluic acid together with *p*-toluic acid monoester, respectively, are converted in one reaction step. (Modified from [155])

Figure 6.39 illustrates a DMT production unit.

Other variants accomplish *p*-xylene oxidation and methyl ester formation at 10 bar and 150 °C in the presence of Co salts in the same reaction medium.

6.2.19 Dimethyl Ether

Technical-quality DME is an alternative to liquefied petroleum gas (LPG). It has excellent combustion characteristics due to a low autoignition temperature.

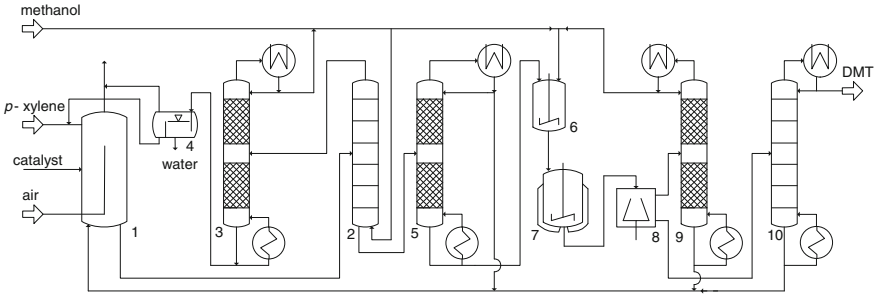

Fig. 6.39 Dimethyl terephthalate production through *p*-xylene oxidation. 1 – oxidation reactor; 2 – esterification reactor; 3 – methanol column; 4 – separation vessel; 5 – ester column; 6 – solvent container; 7 – crystallsation; 8 – centrifuge; 9 – centrifugate distillation; 10 – DMT column. (Adapted from [155])

As oxygenated fuel additive it promotes establishing a favourable fuel/air-mixture and consequently prevents soot formation and reduces NO_x production.

Ultrapure DME is commonly applied as an aerosol propellant. Another large fraction of DME production (15,000 t/a) in Western Europe is converted with SO_3 to dimethyl sulphate, $(CH_3O)_2SO_2$ (see Sect. 6.2.15.4). World total production volume was 11.3 million tonnes in 2012. DME carbonylation gives acetic acid (see Sect. 6.2.8) or acetic acid anhydride (see Sect. 6.2.1) via methyl acetate. It is also an intermediate in the synthesis of olefins, such as ethylene or propylene from methanol (methanol-to-olefins (MTO); see Sects. 6.4.2 and 6.4.3, Fig. 6.40). Refrigerant R723 is an azeotropic mixture of DME and NH_3 [156].

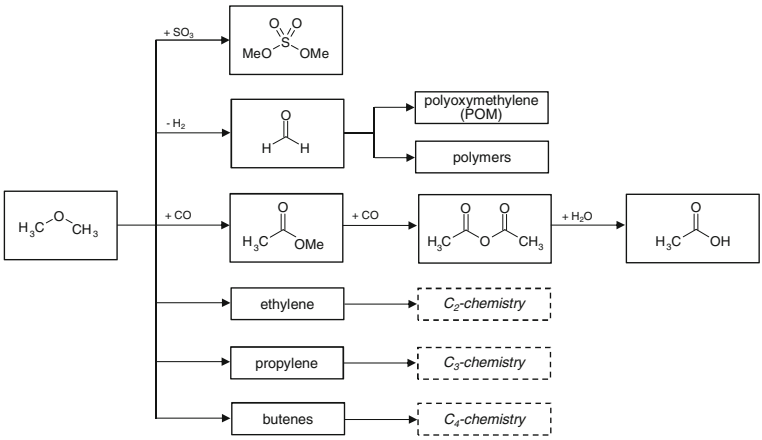

Fig. 6.40 Dimethyl ether use in synthetic chemistry

With a cetane number of 55–60, DME can be used as a substitute for diesel fuel in a diesel engine. Only slight modifications to the engine are needed. DME in

diesel engines burns clean without soot (see Sect. 6.3.1). According to the biofuels directive 2003-30-EC, DME counts as biofuel if it is "produced from biomass and intended for use as a biofuel". In the long term, DME is intended to replace LPG [157]. As a raw material for the production of synthesis gas, black liquor from the paper and pulp industry is envisaged [158].

DME was obtained as a byproduct in the high-pressure synthesis of methanol until about 1975. In this process, 3–5 wt% were contained in the product mixture, from which it was obtained by distillation. The low-pressure methanol processes developed by and ICI mostly avoided DME byproduct formation and replaced almost all high-pressure plants by 1980 (see Sect. 4.4). For that reason, catalytic processes for the synthesis of DME had to be developed.

DME synthesis is a two-stage process. In the first step, methanol production is catalysed over $CuO/ZnO/Al_2O_3$ at 50–100 bar and 270 °C. In a second step, CH_3OH is dehydrated in the presence of a Brønstedt or Lewis acidic catalyst, such as Al_2O_3, ZSM-5 or else (see Sect. 6.4) [58, 159, 160]:

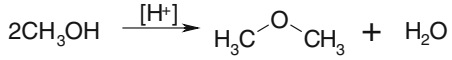

As raw-material base for DME the synthesis of which intermediarily typically involves synthesis gas, in particular coal and natural gas are used. Also biogas and biomass are of interest. DME is directly accessible from synthesis gas, too [161]. Figure 6.41 illustrates Lurgi's MegaDME® production process.

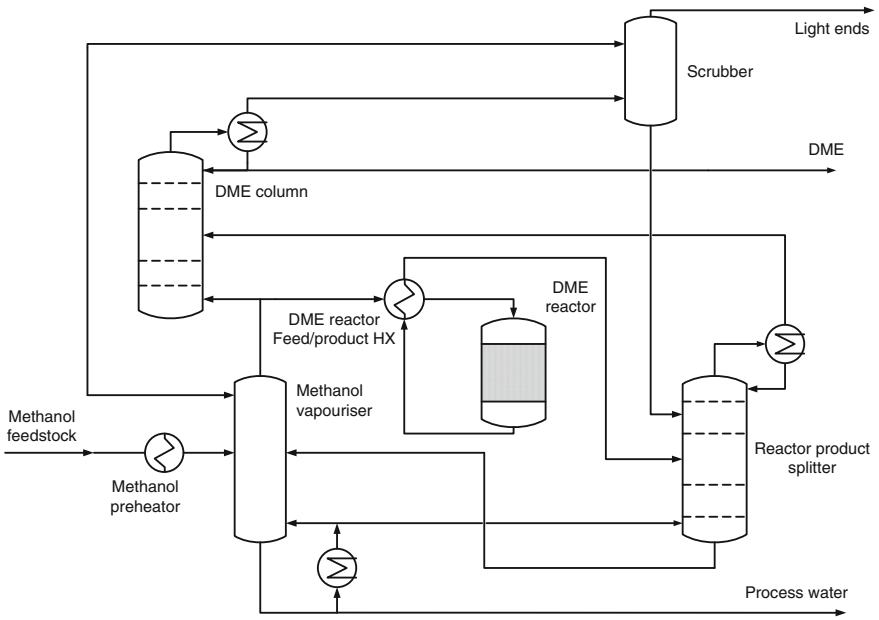

Fig. 6.41 Lurgi's MegaDME process. (Adapted from [159])

6.2.20 Sodium Methylate

Sodium methylate (also sodium methanolate or sodium methoxide) is a colourless, combustible and caustic solid. It self-ignites at 70 °C when exposed to air. There is no defined melting point and decomposition of the substance begins at 280 °C. It is used either in powder form or as methanolic solution. Like all alcoholates of highly electropositive metals, it is a very basic compound of ionic nature. The hygroscopic solid reacts heavily with water to give sodium hydroxide and methanol. Contact of both powder and methanolic solution with air must be avoided as carbon dioxide is absorbed and soda, Na_2CO_3, is formed through CO_2 uptake. Sodium methanolate is soluble in alcohols such as methanol and ethanol but insoluble in hydrocarbons [162]. The maximum solubility in methanol is 32 % at 20 °C.

$NaOCH_3$ is a standard reagent in organic chemistry. It is widely used in a series of pharmaceutical and agrochemical processes, e.g. vitamin A synthesis. It serves as a strong base (the pKa of methanol is 15.5) in various alkylation/elimination reactions, such as dehydrohalogenations, or condensation reactions, like the Aldol, Claisen and Knoevenagel types. Due to the high nucleophilicity of the methanolate ion, it is also used in substitution reactions like Williamson ether synthesis or nucleophilic aromatic substitution. Moreover, the methyl esters of inorganic acids like boronic, silicic, sulphuric and phosphoric acid are produced from sodium methanolate and the corresponding chlorides [163, 164].

Based on the total volume, one of the biggest sales markets for sodium methanolate is the biodiesel industry. Biodiesel consists of fatty acid methyl esters (FAME). In 2010, approximately 17 million tonnes of biodiesel [165] have been produced from vegetable oils, in which sodium methanolate is involved as a catalyst in the majority of the processes. The main feedstock for biodiesel production is rapeseed, soybean and palm oil as well as animal fats. The catalyst is used for triglyceride transesterification with methanol to give the corresponding fatty acid methyl esters (FAME) (Fig. 6.42).

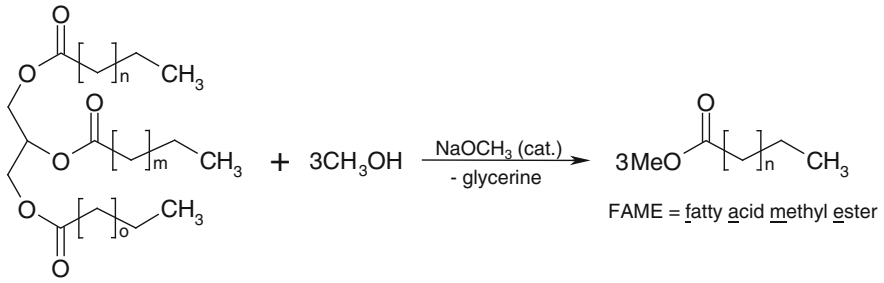

Fig. 6.42 Transesterification of vegetable oils or animal fats to give biodiesel (fatty acid methyl ester, FAME) using NaOMe as catalyst

Depending on the process, 0.5–0.6 % of the catalyst related to the amount of oil is used. Compared to the corresponding hydroxide catalysts, which in principle can

also be used for transesterification, $NaOCH_3$ and its potassium analogue do not show undesired saponification as a side reaction. With the reaction completed, the catalyst is hydrolysed to give sodium hydroxide and methanol.

Another industrial application of sodium methylate is its use as an initiator for anionic polymerisation reactions. Nucleophilic attack of methanolate at formaldehyde produces POM, for instance (see Sect. 6.2.9.2), and its reaction with ethylene oxide produces polyethylene glycol, also known as polyethylene oxide:

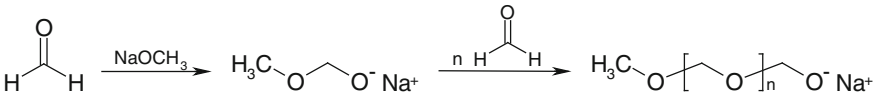

Sodium methylate is industrially produced via three different routes:

1. Reaction of methanol with sodium metal:

$$2Na + 2CH_3OH \rightarrow 2NaOCH_3 + H_2$$

The reaction is very exothermic. Molten sodium is slowly added at a metred rate to an excess of methanol in a stirred vessel or the molten sodium, as well as methanol, is added to a solution of $NaOCH_3$ in methanol. Temperature is maintained at 80–86 °C. The reaction can be carried out batchwise or in a continuous process [166, 167].

2. Reaction of methanol with sodium amalgam:

$$2NaHg_x + 2CH_3OH \rightarrow 2NaOCH_3 + H_2 + 2x\ Hg$$

Figure 6.43 illustrates the amalgam process, which is initiated by the production of sodium amalgam, $NaHg_x$, at the cathode of a sodium chloride electrolysis (a). The amalgam is then transferred into a separate reactor, the decomposer (b), where it reacts with methanol over a catalyst like activated carbon or iron catalysts to give $NaOCH_3$ solution and hydrogen [168–170]. Alternatively, lumpy anthracite covered with nickel and molybdenum oxide is used as a catalyst [171]. The alcoholate solution is purified and concentrated to give the methanolic solution or (after complete drying) $NaOCH_3$ powder. The sodium-depleted mercury, $NaHg_y$, is fully converted with water in a second decomposer (c) and then recycled into the electrolysis process.

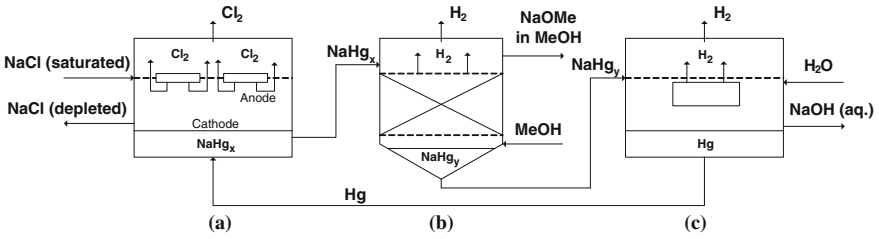

Fig. 6.43 Sodium methylate amalgam process: a) electrolyser, b) decomposer I, c) decomposer II. (Courtesy of Evonik Industries AG)

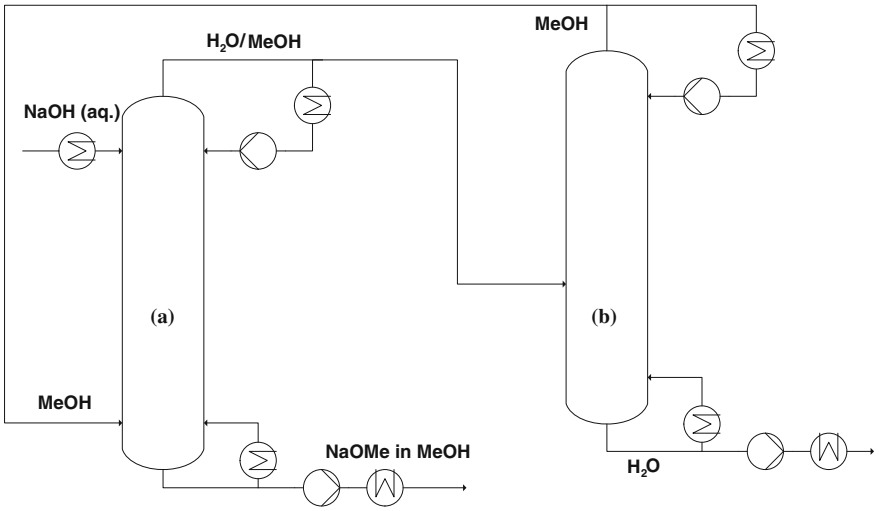

Fig. 6.44 Evonik's sodium methylate reactive distillation process: a) reaction column, b) H_2O/CH_3OH separation column. (Adapted from [172])

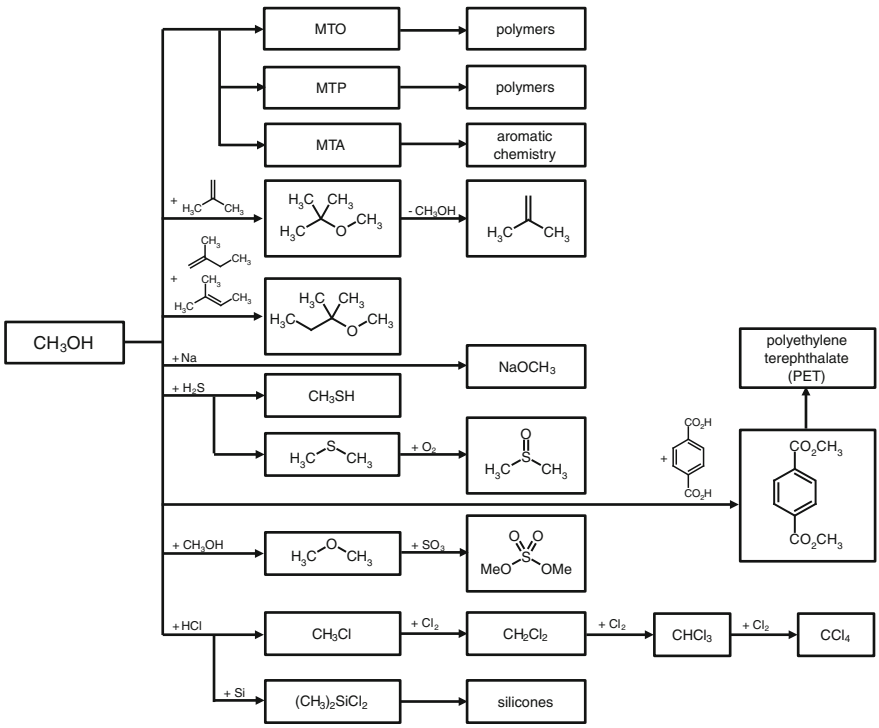

Fig. 6.45 Methanol-derived products

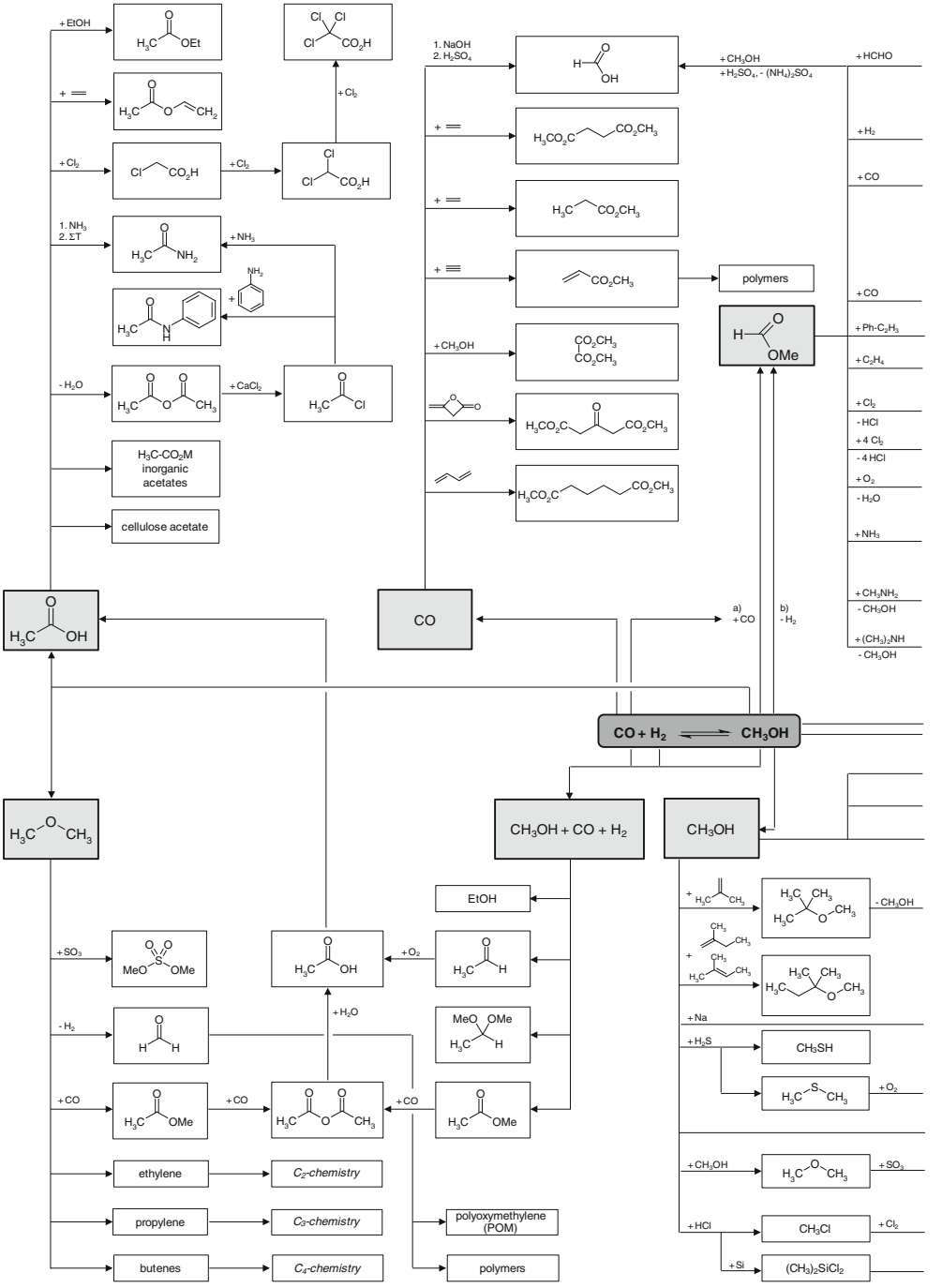

Fig. 6.46 General overview of methanol chemistry

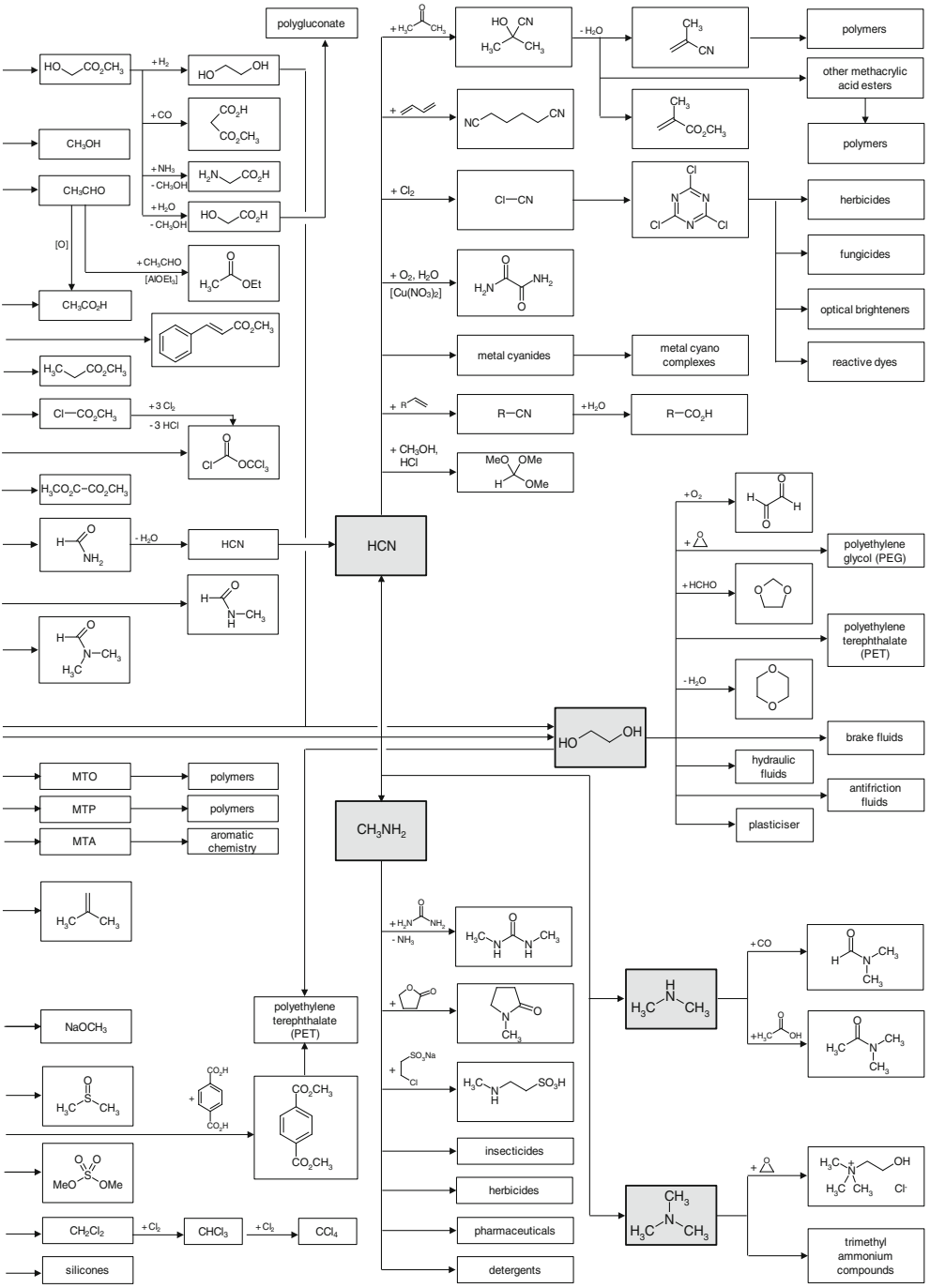

Fig. 6.46 continued

3. Reactive distillation of methanol with aqueous sodium hydroxide:

$$NaOH + CH_3OH \rightleftarrows NaOCH_3 + H_2O$$

In a continuous process, sodium hydroxide solution is fed in the top and methanol is fed in the bottom of the countercurrent reaction column (Fig. 6.44a). The reaction equilibrium is shifted to the product by removing water with the distillate using an excess of methanol. The water/methanol distillate is then transferred to a second column (b), where the organic solvent is separated from the water and recycled to the reaction column. $NaOCH_3$ in methanol is continuously taken as product stream from the sump. Afterwards, it is either directly filled as methanolic solution or separated from the solvent and dried to give sodium methanolate powder.

6.2.21 Miscellaneous

The different products resulting from methanol (the synthetic routes to which have been discussed in Sects. 6.2.14–6.2.20) are graphically summarised in Fig. 6.45.

A general overview of all products derivable from methanol is given in Fig. 6.46. As can be seen there, a large number of established petrochemicals are accessible via methanol. It is also obvious that from C_1-chemistry there is a link to C_2-chemistry, as well as to C_3- and C_4-chemistry. Via the established protocols of MTO, MTP and MTA (see Sects. 6.4–6.4.3) higher C-numbers as well as aromatics can be obtained from this alternative chemical feedstock. Whether or not substitution of classical petrochemical routes by methanol chemistry is economically viable is beyond the scope of this chapter. Additional information on this issue is given in Chap. 7.

It has to be emphasised that a large quantity of chemical entities are already produced starting from methanol as feedstock. Likewise, synthetic protocols that appear to be secondary choices now may become more economically attractive as a result of straightforward research and development efforts. However, no one expects the chemical industry to switch immediately to C_1-chemistry simply for the reason of its existence as a powerful alternative. The raw material markets will decide on the feedstock. Be it oil or methanol, the road ahead is clear.

6.3 Methanol as Fuel

6.3.1 Methanol Fuel in Combustion Engines

Ulrich-Dieter Standt and Frank Seyfried

Volkswagen Group Research, Volkswagen AG, Berliner Ring 2, 38436 Wolfsburg, Germany

Since the early 1970s, many studies have attempted to find alternative fuels that are not derived from fossil sources. Because of their relatively simple production

pathways, alcohols such as methanol and ethanol have been considered as substitutes for conventional fuels. Because alcohols are quite miscible with gasoline, gasoline-alcohol-fuel blends were the focus of early investigations. Later, an increasing shortage of diesel fuel induced considerable efforts to establish diesel-alcohol-fuel blends [173] (Fig. 6.47).

Fig. 6.47 Methanol structure

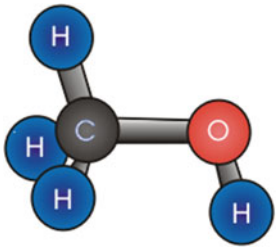

Development Results in the Literature

Basic work on methanol-fueled engines has been performed by Menrad et al. [174], who pointed out the advantages of a passenger car powered by a spark-ignition engine with a carburetor:

- Lower energy consumption.
- Better thermodynamic efficiency at an increased compression ratio.

Because the engine in this study was equipped with an outdated fuel preparation system, their engine modifications for methanol are not as applicable for today's engines, which are designed with respect to emission regulations.

A project group of the former German Federal Department for Research and Technology (BMFT; now the Federal Department for Education and Research) has stated the conditions for methanol fuel introduction:

- Up to 3 vol% methanol content: no materials have to be changed.
- More than 3 vol% methanol content: the materials that have contact with the fuel have to be altered; phase separation has to be avoided; drive and cold-start ability and engine knock have to be regarded.
- More than 89 vol%: a hydrocarbon component such as isopentane has to be added to improve starting and warm-up ability; the compression ratio can be adjusted to higher values in order to improve the level of thermodynamic efficiency [175].

Low blending rates of methanol (up to 2.5 vol%) have shown no adverse effects, such as material wear. The acceptable limit of methanol content in gasoline, however, could not be exactly stated. A 15 vol% methanol blend (M15) has been shown to cause material problems in unmodified cars [176].

Volkswagen (VW) performed a fleet test with methanol- and ethanol–diesel fuel mixtures in diesel passenger cars of the German Post Company. For this, the

standard VW 1.6 L (40 kW) diesel-engine with a swirl chamber and a compression ratio of 23 was used in the VW Golf. The methanol fuel consisted of 15 vol% methanol, 15 vol% solubiliser, 1 vol% cetane improver and 69 vol% diesel fuel. This mixture exhibited a density of 0.820 g/mL (lower limit of the DIN/EN 590 standard: 0.815) and a kinematic viscosity of 3.5 mm^2/s. The cetane number of the mixture was 37 without the cetane improver and 45 with the cetane improver. The fuel did not unmix at prolonged storage tests.

The following engine parts had to be modified for the methanol-fuel mixture: the distributor fuel injection pump, the injector mounting, the fuel filter, the glow plugs and the glow plug control. The cars have been driven between 3,000 and 21,000 km. During the test period, a slight wear of the distributor fuel injection pumps was found. The injectors did not exhibit wear, however. The test cycle emissions of NO_x and particulate matter were reduced, whereas emissions of hydrocarbons and carbon monoxide were increased. With respect to nonregulated emissions, polycyclic aromatic hydrocarbons were reduced and aldehydes increased. During the summer, some hot start problems (vapour bubble formation) were reported [177, 178].

Volkswagen performed a methanol fleet test with eight Santana models in China in 1987 and 1988. The fuel was methanol with 10 vol% of a low boiling gasoline fraction or 15 vol% of ordinary gasoline, respectively [179]. The vehicles were equipped with a carburetor engine; the carburetor was a special design for methanol use from Pierburg. The displacement of the engine was 1.8 L and the rated power output was 66 kW. As the engine lube oil, special oil from Shell (LA 1060) was used. Mileage was between 34,000 and 83,000 km per car, with a total mileage of 449,000 km for the whole fleet. Emission reductions were found for hydrocarbons, carbon monoxide and NO_x; an emission increase was found for formaldehyde. In cold periods, a slightly worse acceleration was reported. The reliability of the methanol vehicles was comparable to that of the conventional gasoline type. The fleet test was supported by the German BMFT and the State Science and Technology Commission of China [180, 181].

A heavy-duty compression-ignition (CI) engine constructed for methanol was designed by Hino Motors. The resulting low exhaust-gas temperatures had to be compensated for by an electric heater for the catalyst in order to accelerate the start of its conversion [182].

Volkswagen developed a port-injection spark-ignition (PISI) methanol flex-fuel engine with a compression ratio of 10 for passenger cars. Full flexibility of the methanol content was given using an alcohol sensor, based on the dielectric constant, conductivity and temperature of the fuel. The sensor signal was processed by the engine control unit (ECU), which at that time was a Volkswagen in-house development called Digifant. The ECUI adapted the injection timing and fuel mass to the alcohol content of the fuel. The cars took part in a demonstration fleet programme in California from 1990 to 1992. All materials used in the fuel system were modified for the methanol operation, as well as for ethanol operation.

Special multigrade engine oil, altered with respect to its viscosity index improvers, was used. The regulated emissions (HC, CO and NO_x) were lower than of corresponding gasoline usage. For some of the nonlimited emissions, such as reactive hydrocarbon components as precursors for ozone, distinctly lower values were found. Only formaldehyde was found to be significantly higher than for gasoline fuel [183]. This flexible fuel sensor was originally invented by FEV Motorentechnik and was supplied and further developed for broader applications by Siemens Automotive [184–186] (Fig. 6.48).

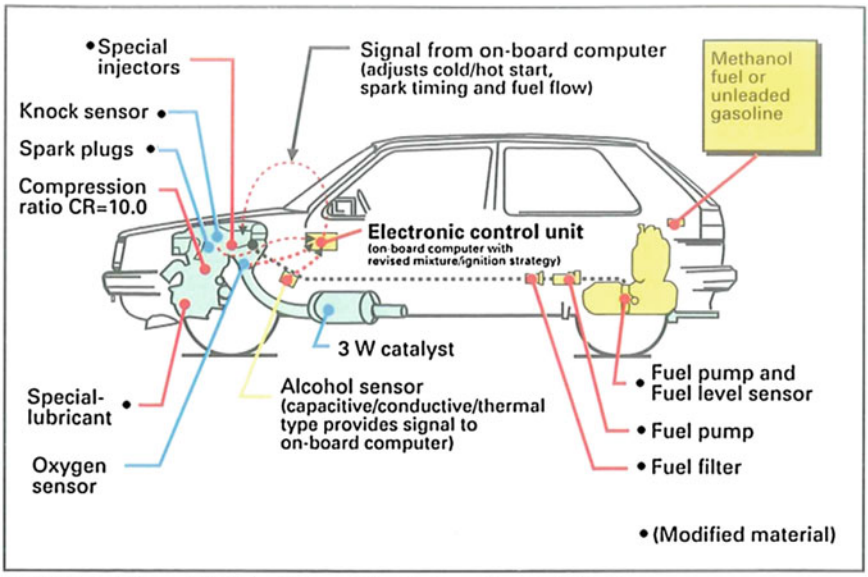

Fig. 6.48 Multifuel concept car

TNO developed a similar flexible fuel engine for methanol-gasoline mixtures in co-operation with Volvo Car Corporation and Robert Bosch GmbH. The compression ratio was altered to 12.5. The ECU was a Bosch Motronic M2.1. For the fuel sensor, an optical device (NTK TFF 8510) was used. Practical field usage up to some 80,000 km was reported. Due to the higher compression ratio, better fuel consumption for methanol was found. The baseline engine for gasoline use had a compression ratio of 9.8 [187].

At the same time, Mercedes-Benz reported that technical solutions for flexible methanol-gasoline engines should include the following:

- Use methanol-resistant electromagnetic fuel injection valves, tanks and fuel pumps.
- Apply a suitable fuel sensor for detecting the methanol content in gasoline-methanol-mixtures.

- Reduce the exhaust emissions, especially formaldehyde.
- Take into consideration driving at low temperatures, cold start and exhaust cloud formation.
- Apply a special engine lube oil without viscosity-index improvers.

As a fuel sensor, Mercedes-Benz tested an optical sensor and a capacitive sensor measuring the dielectric constant. Because the optical sensor exhibited a deviation, when coloured gasoline-methanol mixtures were used, the capacitive sensor was determined to be the better solution [188].

Hyundai reported that methanol use caused severe corrosion of engine parts such as crankshafts, camshafts and cylinder liners in their durability tests. They stated that acid formation at lower temperatures caused wear. The oil viscosity is higher when methanol is used as a fuel. Gasoline mixes with the lube oil, whereas methanol forms emulsions with it, causing a higher viscosity. Furthermore, preignition of methanol is described, which can be avoided by special spark plugs [189].

Honda reported that their methanol engines exhibited substantial wear of valve trains, cylinder liners and piston rings at low-temperature operation. The valve seats and valve guides of the fuel injector wore more rapidly with methanol due to a lack of lubricity of methanol. Deposits of polymer components from the lube oil were detected at those parts. An additional fuel additive for methanol fuels had to be added to avoid these deposits. Honda has formulated special lube oil for methanol as a fuel, which exhibited better results in the camshaft wear test. An optical sensor exhibited a cross-sensitivity to aromatics; therefore, they have decided to select a capacitor-type sensor. Methanol fuel caused increased fuel tank pressures; in order to avoid damages, fuel lines, fuel vapour lines and the fuel vapour canister had to be enlarged [190].

Toyota identified cold starting ability as a problem using pure methanol (M100), so they adopted a dual fuel system using gasoline assistance at low temperatures to enable the engine start. Further technical problems included injector clogging, fuel pump malfunction, poor driving ability at elevated temperatures, wear and corrosion of engine moving parts. In tests with M85 fuel, Toyota used an altered fuel injector with a ball-type valve to prevent injector clogging, an in-tank fuel pump with a brushless drive and special lube oil with a higher calcium ash content in order to neutralise formic acid. Because of the higher octane number of methanol-gasoline mixtures, it was possible to raise the compression ratio from 9.5 to 11.

For methanol CI engines, Toyota developed a dual fuel system to obtain stable ignition and combustion of methanol under various operating conditions. A small quantity of diesel fuel is predelivered at the nozzle tip by the fuel loader, before the injection pump supplies methanol to the injector. Methanol and diesel are injected in an unmixed state, and methanol penetrates the diesel fuel plume. The

compression ratio is 21. Increased formaldehyde formation has been reported as a problem of the CI and the PISI engines [191].

Mitsubishi established that some changes in materials have to be made due to the corrosive nature of methanol and its combustion products. Several materials in the fuel supply system and the powertrain components have to be modified or subjected to surface treatment in order to avoid excessive wear:

- The tank has to be constructed using stainless steel.
- The fuel tubes have to be plated with nickel.
- A brushless in-tank fuel pump was adopted.
- All elastomers which have contact to the fuel have been replaced by fluorocarbon elastomers (FKM).

In addition, specially formulated engine oil has to be used and an optical fuel sensor was applied. For the cold and hot starting abilities, additional measures have been taken [192]. Automotive suppliers have pointed out that methanol-gasoline mixtures are the worst case for many materials in the engine. Even ordinary FKM O-rings swelled significantly. They proposed a special-grade FKM for methanol engines [193].

Research Work

Pre-ignition and engine knock may be undesirable effects when alcohol-containing fuel blends are used. Methanol-gasoline blends have been investigated with respect to its knock properties and pre-ignition at higher loads. It has been described that pre-ignition of methanol blends often do not correspond to standard knock measures, such as RON or MON, at higher speed. Methanol has been described to be the fuel that is most susceptible to self-ignition. The admixture of isopentane or other suitable fuel additives reduce pre-ignition tendencies. Air–fuel ratios in the range of 5–10 vol% rich, compared to the stoichiometric air-to-fuel ratio, favour pre-ignition [194].

The pre-ignition properties of various alcohol-gasoline blends, including methanol, have been investigated with various gasoline engines of the MPI and DI type. It has been shown that the type of fuel mixture preparation, the evaporation behaviour, and the combustion process have shown occasionally opposite effects on their full load potential. Methanol-gasoline mixtures containing 10, 25 and 50 vol% have been evaluated as splash blends. The methanol blends showed the lowest air efficiencies of all alcohol-gasoline fuels, relative to conventional gasoline. The methanol blend M50 showed the highest increase of torque, measured at equal centres of combustion in a turbocharged direct-injection engine [195].

Pischinger et al. investigated methanol-diesel fuel mixtures with a single-cylinder test engine with a compression ratio of 23 using the Volkswagen swirl-chamber combustion system. Mixtures of 65 or 20 vol% methanol, respectively,

and 15 vol% solubiliser were used; in a second test series, a mixture of pure methanol and an ignition improver (c-hexyl nitrate, 12 vol%) was investigated. An alcohol-resistant fuel pump was used. The partial fuel substitution enables a reduction of particulate matter combined with an increase of NO_x emissions at a reasonable level of fuel consumption. The mixture of pure methanol with the ignition improver enables a higher diesel fuel substitution degree at higher loads and no particulate matter emissions but high NO_x emissions. The higher burning rate and shorter burning period with methanol fuel causes higher NO_x and lower particulate matter emissions [196].

In an early attempt to construct a DI methanol engine with compression ignition, Volkswagen developed a turbocharged and intercooled prototype engine for methanol as a fuel, demonstrating the favourable efficiency of a state-of-the-art diesel engine with very low NO_x and particulate emissions, using an oxidation catalyst for conversion of HC and aldehyde emissions. The concept engine combined a high compression ratio with a turbocharger, an electronically controlled EGR and electronically controlled glow plugs [182].

A direct-injection methanol engine has been constructed by FEV Motorentechnik (Pischinger et al.). The 1.9 L engine has been described with 66 kW power at a declared engine speed of 4,000 rpm and a maximum torque of 186 Nm (at 2,500 rpm). It had a turbocharger and a charge air cooler. The ignition of the methanol was assisted by a glow plug. The potential to minimise the relatively high NO_x emissions is given by variation of injection timings and exhaust gas recirculation. The engine does not produce particulate matter emissions. The exhaust gas has been treated by an oxidation catalyst [197, 198].

Nakamura et al. [199] pointed out that methanol causes a significantly higher formation of calcium sulphate in the engine oil. They have given evidence that it is formed by the reaction between intermediately formed calcium formate, $Ca(HCOO)_2$ (from basic calcium compounds such as $CaCO_3$), and zincdithiophosphate, which is degraded.

Wang et al. [200] investigated methanol for dual-fuel applications, based on a diesel engine with a compression ratio of 18. With respect to methanol, the engine has a port injection; the diesel fuel, however, is directly injected for pilot use. The high methanol content reduces smoke and NO_x emission. At lower loads, the heat release is bimodal; at higher loads, the heat release changes to an unimodal type, indicating a better fuel economy.

A problem encountered in methanol-gasoline mixtures is the separation of phases at higher methanol contents and at higher water contents. Phase separation can be avoided by the addition of ethanol to increase the possible methanol content. Care has to be taken to prevent swelling of the elastomers [201]. The compatibility of elastomers was the subject of a development by Freudenberg. The company reports of an elastomer that is fit for use in engines driven with alternative fuels, such as FAME, triglycerides and methanol [202].

A Chinese working group has reported that China favours methanol as the most promising alternative fuel when it is blended to gasoline. Measurements with two cars fulfilling the Euro III and Euro IV emission limits are presented. To avoid phase separation of the blends, mixtures were made just before the experiments were carried out, additionally using automatic and manual blenders. Methanol contents were set from 10 to 30 vol%. Experimental data of the conversion of the catalyst have been presented only up to 15 vol% methanol. For the higher methanol contents, which are expected to cause deviations of the air/fuel sensor, no conversion efficiency data have been reported. The Euro IV limits were fulfilled [203].

Volkswagen investigated a series of gasoline alcohol blends at an engine dynamometer using a single cylinder engine of 0.35 L displacement. The engine was constructed with respect to optimal reproducibility of the thermodynamic properties. As the reference fuel, European standard fuel for EU IV legislation was used because this fuel did not contain alcohols, below fuel labelled with M0. At the time, the European standard DIN/EN 228 limited the methanol content of gasoline to 3 vol%; therefore, a mixture of gasoline with 3 vol% methanol is used as the second fuel. The upper limit for the ethanol content is limited to 10 vol%, corresponding to a mixture of gasoline with about 7 vol% methanol containing the same oxygen content; therefore, these two blends were chosen as additional fuels. The third fuel containing 7 vol% methanol does not match the limits of the DIN/EN 228 standard (see Table 6.6).

Table 6.6 Methanol fuel blend matrix

Feature	M0	M0 + 3 vol% Methanol	M0 + 7 vol% Methanol	M0 + 10 vol% Ethanol
RON	101	101	101	101
Antiknock index	95	95	95	95
Density at 15 °C (kg/m^3)	753	755	756	757
Energy density (MJ/L)	32.21	31.54	30.97	30.89
Air/fuel ratio	14.55	14.34	14.05	13.97
Content C/H/O (% m/m)	86.9/13.1/< 0.1	84.7/14.0/1.3	82.8/13.7/3.5	82.7/13.8/3.5

The blends differ from each other mainly in their boiling properties (see Fig. 6.49). Adding methanol-to-gasoline does not affect the initial and the final boiling point, but it affects the distillation centre. The changes in volumetric fuel consumption of the methanol/ethanol blends, relative to M0, are in good accordance with their volumetric energy content.

Methanol and ethanol exhibit lower knock sensitivities than gasoline. An earlier centre of combustion, however, was not detected for the observed blends (see Fig. 6.50). The observed changes in combustion differ in the range of about 1 %, which is the limit of detection for this type of measurement. If the base fuel, which

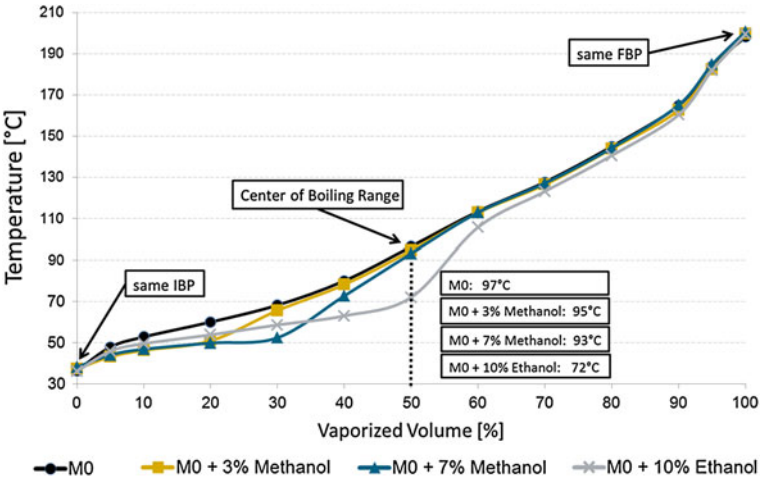

Fig. 6.49 Boiling properties of methanol/ethanol blends

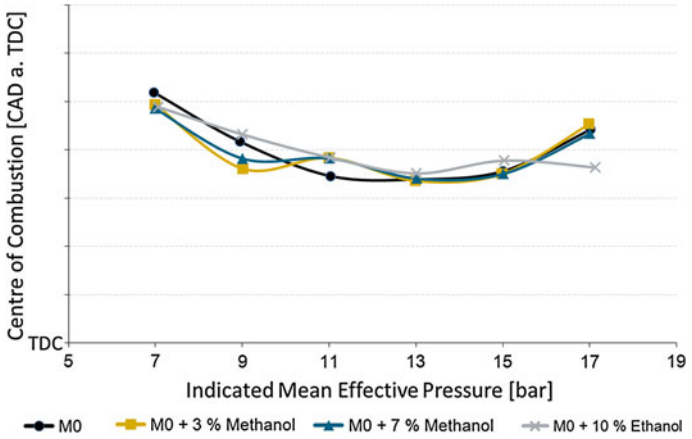

Fig. 6.50 Centre of combustion at 2,000 rpm

has been used for blending, had been of lower quality (i.e. lower RON), differences in RON and knock sensitivities should have been found between M0 and the methanol or ethanol blends, respectively.

Conclusions

The following conclusions can be made regarding the use of methanol fuel in combustion engines:

- Gasoline blends up to 3 vol% methanol fulfil the limits of the standard DIN/EN 228 and may be used without further technical changes. For higher methanol-containing blends, special care has to be taken.
- When using higher contents of methanol in gasoline, one has to prevent adverse effects such as corrosion of engine parts and swelling of elastomers, and the engine lube oil has to be adopted to methanol. Care must be taken for enabling cold starting ability; hot starting may cause vapour bubbles at certain mixture ratios with minimum boiling point.
- Phase separation has to be avoided using solubilisers.
- Methanol blends with diesel fuel are a technically more ambitious task: a solubiliser has to be used, care has to be taken to prevent oxidation and swelling of elastomers, and a special lube oil has to be used. For higher methanol contents, starting ability and cold driving ability have to be enabled using a cetane improver. Higher methanol contents can be applied using a dual fuel system.
- Further work has to be done to evaluate the degradation mechanism of viscosity improvers by methanol fuel mixtures and to the adaption of direct injection gasoline engines to methanol blends (Fig. 6.51).

Fig. 6.51 Volkswagen Golf I fleet test vehicle running an extended period with methanol

6.3.2 *Methanol-based Fuel Additives*

Stefan Buchholz[1], Gereon Busch[2] and Markus Winterberg[2]

[1]*Evonik Industries AG, Creavis Technologies and Innovation, Paul-Baumann-Straße 1, 45772 Marl, Germany*

[2]*Evonik Industries AG Luelsdorf, Feldmühlestraße 3, 53859 Niederkassel-Luelsdorf Germany*

Methyl tert-Butyl Ether

Methyl tert-butyl ether (MTBE) is produced by the reaction of methanol and isobutene on acidic ion exchange resins at mild temperatures.

$$(CH_3)_2C=CH_2 + CH_3OH \rightarrow (CH_3)_3COCH_3 \qquad \Delta_r H = 36.8\ \text{kJ/mol} \qquad (6.10)$$

MTBE is mainly used as blending component for gasoline fuels due to its high octane number. Therefore, the availability of MTBE enabled the phase-out of metal-containing anti-knock additives, such as tetraethyl lead or methylcyclopentadienyl manganese tricarbonyl; thus, it has been a prerequisite for the introduction of catalytic converters in passenger cars. Besides the application in fuels, MTBE is also used for the production of high-purity polymer-grade isobutene by catalytic cleavage into its starting materials.

MTBE is a colourless liquid with low viscosity and a characteristic terpene-like odour. Stoichiometrically, 360 kg methanol and 640 kg isobutene are required to make 1 tonne of MTBE. Table 6.7 summarises the most important physical and fuel-related properties of MTBE. MTBE has unlimited miscibility with all ordinary organic solvents and all hydrocarbons. At 20 °C, the solubility of MTBE in water is approximately 4 vol%, whereas water solubility in MTBE is 1.3 vol%. MTBE is stable under alkaline, neutral and weakly acidic conditions. In the presence of strong acids, MTBE is cleaved to methanol and isobutene.

Table 6.7 Selected properties of MTBE

Molecular weight	88.16 g/mol
Melting point	−108.6 °C
Boiling point	55.3 °C
Density (20 °C)	740.4 kg/m^3
Viscosity (20 °C)	0.36 mPa·s
Heat of vapourisation (at boiling point)	337 kJ/kg
Heat of combustion	−34.88 MJ/kg
Flash point (Abel-Pensky)	−28 °C
Ignition temperature	460 °C
Explosion limits in air	1.65–8.4 vol%
Research octane number	117
Motor octance number	101
Reid vapour pressure	550 hPa

At present, most of the isobutene used for MTBE production comes from C_4 containing streams in refineries or petrochemical production complexes. Raffinate 1 and fluid catalytic cracking units (FCC) C_4 (from refinery catalytic crackers) are the most important sources for the production of MTBE and provide isobutene for more than 50 % of world's total MTBE production [204]. Table 6.8 shows the composition of these C_4 streams.

These feedstocks can be used directly in MTBE synthesis. Other sources of isobutene are based on dedicated isobutene production processes, such as isobutane dehydrogenation, which is used to produce the feedstock for approximately 35 % of the MTBE production, and the dehydration of tert-butanol, which is a co-product of propylene oxide from the Halcon/Arco process, which is expected to decline in the future and is of minor importance already today. Production of

Table 6.8 Typical composition of raw material streams for MTBE production

Component	Raffinate 1 (wt%)	Fluid catalytic cracking (wt%)
Isobutene	44–49	10–25
Isobutane	2–3	20–35
1-Butene	24–28	10–20
2-Butene	19–21	20–35
n-Butane	6–8	5–15

MTBE is closely related to the availability of isobutene; consequently, the amounts produced depend on isobutene supply.

All MTBE processes have in common the reaction of isobutene with a certain molar excess of methanol on a macroporous acidic ion exchanger operating at 50–90 °C. In most industrial plants, isobutene conversion of 95–97 % is sufficient. Residual butenes are mainly used for the manufacture of alkylate gasoline or they are recycled to the cracker. If they are to be used for other chemical purposes, such as the production of polymer-grade 1-butene, the degree of isobutene conversion must be significantly increased. This high conversion can be obtained by using highly sulphonated acidic resins in the reaction section followed by an additional catalytic distillation column in the refining section.

Catalytic distillation (CD) or reactive distillation refers to a process, in which both catalytic reaction and distillation are carried out simultaneously in the debutaniser column. From the viewpoint of reaction engineering, this column acts as a two-phase countercurrent-flow, fixed-bed catalytic reactor. The most important advantage of using CD for MTBE synthesis lies in the elimination of equilibrium limitation of isobutene conversion as a result of continuous removal of the reaction product MTBE from the reaction mixture. The partly reacted mixture from the reaction section, which is usually in chemical equilibrium, enters the CD column below the catalyst packing zone to ensure the separation of the high-boiling component MTBE from the feed stream. The catalyst packing is installed in the upper mid-portion of the column with normal distillation sections above and below [205]. An example for this approach is the Evonik CD process, which has been developed by UOP and Hüls in 1992 and is commercialised as the Ethermax process (see Fig. 6.52).

Changes in legislation and complete or partial replacement of MTBE with ethanol or ethyl tert-butyl ether in gasoline blending in the European Union, North America and Japan have lowered the global MTBE demand. Therefore, the corresponding global production of more than 21 million tonnes in the early years of the 2000 decade declined to 14.4 million tonnes in 2009 [207]. In 2009, approximately 12 % of global methanol production were used to make MTBE [207, 208]. MTBE production in Europe amounted 1.8 million tonnes in 2009 [207]. By now, the transition away from MTBE in developed countries is nearing completion. The main underlying drivers for the future MTBE demand growth include a growing population and a higher standard of living in major emerging markets, along with the resulting increasing consumption of gasoline. In addition, demand for higher

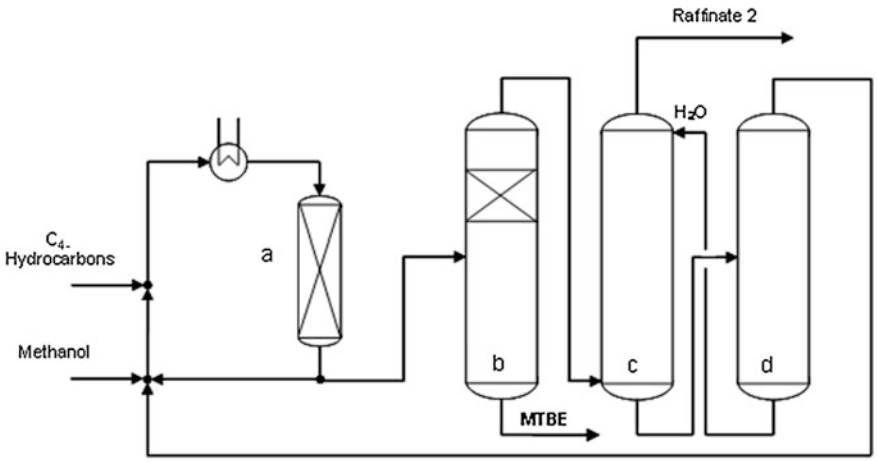

Fig. 6.52 Evonik catalytic distillation methyl tert-butyl ether (MTBE) process: a) Reactor, b) Catalytic distillation column, c) Methanol extraction, d) Methanol column [206]

octane and cleaner-burning gasoline in many developing countries is also supporting MTBE consumption.

Tertiary Amyl Methyl Ether

In addition to MTBE, tertiary amyl methyl ether (TAME) is made from methanol and an olefin—in this case, isoamylenes (C_5s). TAME can be made by etherification of the isoamylenes in a process analogous to the MTBE process. The primary feedstock comes from FCC and cokers and is thus readily available within refineries. Steam crackers are another source of C_5s. At present, most isoamylenes are blended directly into gasoline. Their etherification removes some of the highest vapour pressure olefins from gasoline [209]. The C_5s from an FCC are usually combined with the light naphtha as the bottom product from a debutaniser. The overhead stream from the debutaniser contains the isobutylene used to synthesise MTBE. The isoamylene component can be separated from the light naphtha by either adding a debutaniser or by revamping the debutaniser to act also as a debutaniser. In the former case, the isoamylenes can be converted in a separate TAME unit; in the latter case, a mixed C_4/C_5 stream can be used to manufacture a combination of MTBE and TAME.

Unlike a typical MTBE feedstream, the feed to a TAME unit must usually undergo a more complex pretreatment, involving selective hydrogenation, isomerisation, Merox treatment, or a combination of these processes. Selective hydrogenation is required for FCC C_5 in order to eliminate the diolefins, whereas the Merox treatment is used to remove sulphur-containing impurities. The TAME reaction occurs in the liquid phase and is exothermic. High temperatures, although favouring the reaction kinetics, decrease equilibrium to TAME. Compared to MTBE synthesis, the conversion of isoamylene to TAME is lower because of less

favourable reactivity and equilibrium. Similar to MTBE processes, two stages of etherification are commonly used, including catalytic distillation technology, which can boost the TAME yield to more than 90 %. TAME production is small compared to MTBE production and TAME is usually produced as a coproduct of MTBE. The estimated TAME production in Europe was approximately 170,000–250,000 tonnes in 2008 [210].

6.4 Catalysis of Methanol Conversion to Hydrocarbons

Friedrich Schmidt[1], Lydia Reichelt[2] and Carsten Pätzold[2]

[1]*Angerbachstrasse 28, 83024 Rosenheim, Germany*
[2]*Institute of Chemical Technology, Freiberg University of Mining and Technology, Leipziger Straße 29, 09599 Freiberg, Germany*

Introduction

The formation of hydrocarbons from methanol is catalysed by zeolites and was discovered by accident by the scientists at Mobil Oil in the 1970s. Many new process routes were developed after this discovery, including the methanol-to-gasoline (MTG), the methanol-to-olefins (MTO) and the methanol-to-aromatics (MTA) processes. This high product selectivity is caused by the catalyst used and by the reaction conditions.

Zeolites and Zeotype Materials

Zeolites are crystalline aluminosilicates whose special catalytic properties are determined by their structure of well-defined pore openings and channels. Due to these special structural properties, zeolites can also be used as molecular sieves. In addition to the zeolites (which are characterised by tetrahedral coordinated Si and Al atoms), molecular sieve materials include a variety of other microporous and mesoporous materials, for example carbon sieves, MCM-41, zeotypes, for example aluminophosphates (AlPO; with tetrahedral coordinated Al and P atoms) and silicon aluminium phosphates (SAPO; with tetrahedral coordinated Si, Al and P atoms), as well as metalloaluminates, silicates and metal silicates [211].

Structure and Related Properties

Zeolites and zeotype materials are distinguished by a three-letter code that is assigned to the different structure types (topologies), with a specific connectivity to characteristic topological properties. For example, the zeolite Zeolite Socony Mobil 5 (ZSM-5) belongs to the MFI structure type (having MFI topology), whereas the zeolite SSZ-13 and the zeotype SAPO-34 are members of the

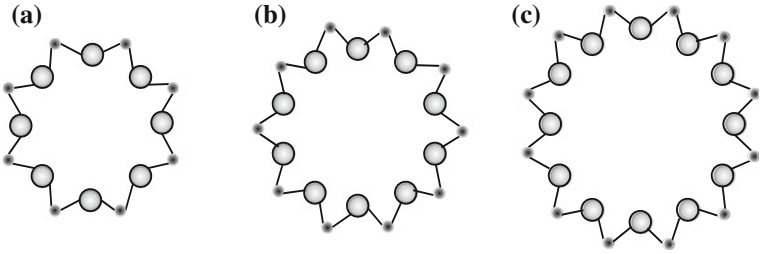

Fig. 6.53 Schematic channel profile of small pore (a), medium pore (b) and large pore (c) zeolites and zeotypes, with oxygen atoms (big) and silicon, aluminium, or equivalent atoms (small)

chabazite (CHA) structure type. Additional information about the various structures can be found in the *Atlas of Zeolite Framework Types* [212].

The zeolite framework consists of repeating structural units, the so-called secondary building units (SBUs) [213, 214], which leads to a uniform, highly ordered structure with channels and cavities of molecular dimension [215]. These channels form monolithic structures or three-dimensional intersecting networks that are permeable in one, two, or three dimensions of the crystal, depending on the type of zeolite. They are usually occupied by water molecules and exchangeable cations. The channels in the dehydrated zeolites are large enough to allow diffusion and adsorption of molecules. The dehydration can be achieved almost completely at temperatures around 400 °C and is almost completely reversible.

Regarding the channel diameters, zeolites and zeotype materials can be divided into three groups (see Fig. 6.53): those formed of eight corner-linked tetrahedra (small pores, for example SAPO-34), those with 10-membered rings (medium pores, such as ZSM-5), and those with large pores of 12 oxygen atoms. The pore diameter varies from 0.2 to 1.3 nm [211, 216, 217].

The differences in size of the pore openings as well as the channel diameters and structures result in a high shape selectivity of the diffusing molecules concerning molecular weight and structure. Additionally, the catalytically active sites are situated inside the crystal channels [218, 219]. Therefore, these structural constraints have a major influence on the formation of hydrocarbons in terms of the following: [215, 218, 220]

- *Reactant selectivity:* Only reactants that are small enough to fit into the channels can reach the catalytically active sites.
- *Transition state selectivity:* During the formation of hydrocarbons, only transition states that fit into the structure can occur.
- *Product selectivity:* Only products that are small enough to pass the channels can move to the surface of the catalyst and may leave it.

Bulkier hydrocarbons need to undergo cracking reactions before being able to leave the catalyst [221]. Therefore, focusing on the formation of hydrocarbons in the

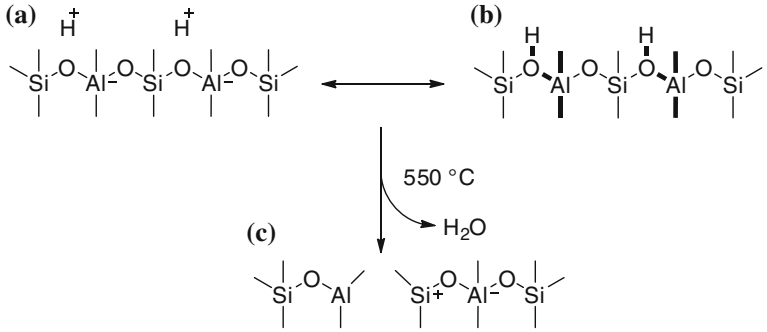

Fig. 6.54 Brønsted acidic sites (a, b) and their transformation into Lewis acidic sites (c) [220]

gasoline boiling range, only medium-pore zeolites such as ZSM-5 [215, 221, 222] and ZSM-11 [215] with channels of 10 oxygen atoms are suitable [215].

The crystal lattice is negatively charged due to the tetrahedral coordinated cations (usually aluminium and silicon atoms; see Fig. 6.54) within the specific network of corner-linked oxygen tetrahedra [215, 218, 220, 223].

In a mere silicate structure, all silicon atoms are topologically equivalent. The same applies for the pure aluminium phosphate structure, where all phosphorous atoms and all the aluminium atoms are topologically equivalent. It has been observed that there are no two adjacent aluminate tetrahedra in either natural or synthetic zeolites (Loewenstein rule), because the resulting electrostatic repulsion would destabilise the zeolite framework [224]. A small fraction of the aluminium atoms is situated on the outer surface of the zeolite or inside on nonlattice sites. The latter increases with progressing deactivation of the catalyst [218].

Tetrahedra corners that are not shared with adjacent tetrahedra may be saturated by (OH, F) groups [225, 226]. The crystal becomes neutral through exchangeable cations. Therefore, zeolites can be described by the following formula [215]:

$$M_{x/n}\left[(AlO_2)_x(SiO_2)_y\right] \cdot z\ H_2O$$

in which n stands for the charge of the cation, which is usually an alkali metal ion, an ammonium or alkylammonium ion, or, as in those materials that are important for catalysis, a proton. The proton forms a hydroxyl group with the lattice oxygen of Si-O-Al bonds of the bridged tetrahedra and builds up a strong Brønsted acidic site, like it is shown in Fig. 6.54a and b [215, 220, 227]. These sites are essential for the catalytic activity of the zeolite, whereupon the acidic site density and strength (in an aqueous system equivalent to the pK_a value) are crucial for the properties of each material. Therefore, with regard to the shape selectivity and catalytic applications, it is important whether catalytically active sites are situated on the outer surface of the crystals or inside the pores [228]. The number and thus the density of Brønsted acidic sites can be determined by proton nuclear magnetic resonance (^{1}H-NMR) spectroscopy and infrared spectroscopy. For pure H-zeolites,

it can be determined in a good approximation simply by back-titration with sodium or silver ions.

All such acidic sites exhibit a uniform acidic strength due to the high degree of crystalline order [229]. The Si/Al-ratio is generally ≥ 1 [215] and is indirectly proportional to the density of the acidic sites and directly proportional to the pH value because an ideal zeolite possesses only one cationic deficiency per aluminium atom, which in turn can form an acidic site [229–231]. A ZSM-5 catalyst with a Si/Al-ratio lower than approximately 80 is very active, but the high density of acidic sites causes a rapid further reaction of lower olefins to undesired byproducts if applied in the MTO process; a low Brønsted acidity favours the formation of olefins, especially if the conversion is not complete [231]. Even in the MTG reaction, a very high activity is not favoured because the aromatic fraction and coking increases [223]. Despite their relatively high octane number, aromatics have only limited desirability because of legal restrictions on the aromatic content in gasoline and the disproportionate increase in durene, which causes drivability problems at higher ratios.

With increasing Si/Al-ratios, the acid strength of the individual centre increases. Therefore, the Si/Al-ratio can be constrained to $5 < \mathrm{Si/Al} \leq \infty$ for the application of ZSM-5 and ZSM-11 in the MTG process [215], although aluminium atoms need to be present in order to maintain catalytic activity [221]. There is a correlation between the aluminium content of the zeolite and the catalytic activity, in the range of 10 to 10,000 ppm of aluminium [223].

An ideal zeolite does not have any Lewis acidic sites. They emerge from imperfections in the structure of the crystal, such as from coordinative unsaturated aluminium-containing species. Those structural defects occur after dealumination by steam contact or ion exchange (see Fig. 6.54c) [223, 229, 232]. Under certain circumstances, Lewis acidic sites can increase the strength of the neighbouring Brønsted centres (pK_a value), causing an indirect effect on the catalytic activity [217]. The distribution of the acidic site strength in zeolites is determined by using a temperature-programmed desorption of bases.

The acidity of the SAPOs depends on the (Al + P)/Si-ratio. With decreasing silicon content, and thus with increasing (Al + P)/Si-ratios, the acidic strength of the individual centre increases but the number of centres decreases, whereby the pH value increases. For zeolites and zeotype materials, the superposition of the two opposite effects, pK_a on the one side and pH on the other, leads to the formation of a maximum of total acidity.

Material with MFI Topology: ZSM-5

A reasonable conversion of methanol into gasoline with a commercially acceptable cycle length (controlled by the catalyst) was first discovered on ZSM-5 catalysts. ZSM-5 is a medium-pore synthetic aluminosilicate zeolite from the pentasil family of MFI structure type. It was first synthesised by Argauer and Landolt in 1972 [233]. Currently, it is the most commonly used zeolite for the commercial production of hydrocarbons from methanol.

ZSM-5 exhibits the common formula [215, 223, 229]

$$Na_zAl_zSi_{96-z}O_{192} \cdot H_2O \quad \text{with } z < 27 \text{ and typically } z \approx 3.$$

For application in methanol-to-hydrocarbon (MTHC) processes, sodium ions are substituted by protons whereby a solid acid arises, which is often called H-ZSM-5.

The crystal lattice of ZSM-5 is characterised by a channel structure (see Fig. 6.55) of straight channels running parallel to the [010] direction with an elliptical shape and appropriate free dimensions of 0.51 × 0.54 nm and sinusoidal channels running parallel to [100] direction with a nearly circular cross-section area of 0.54 × 0.56 nm [215, 221, 223]. At the crossings of the channels, an opening of 0.89 nm is formed [233, 234], which is ideal for the MTG process because there is enough space for cyclisation reactions and intermolecular hydride transfers [235] but not enough free volume for the formation or release of higher aromatics. As a result, using ZSM-5 a hydrocarbon product for MTG processes with a maximum chain length of C_{10} and mainly methyl substituted aromatics is accessible. Durene (1,2,4,5-tetramethylbenzene) is the bulkiest molecule built [215]. It is a very undesirable product, because it has a melting point of 79 °C and therefore leads to drivability problems if its content in gasoline exceeds 2–3 vol%.

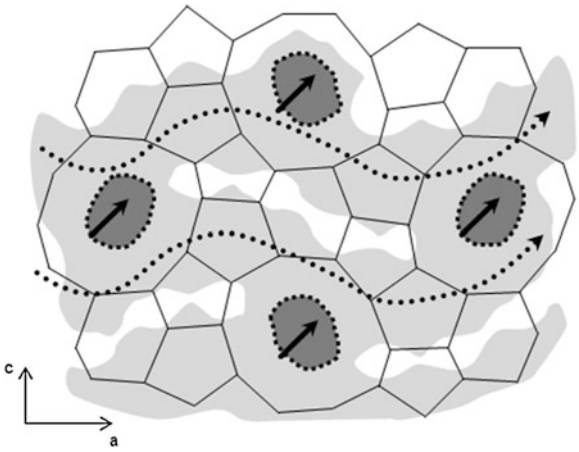

Fig. 6.55 Crystalline structure scheme of ZSM-5 with straight channels (into the plane, marked with bold arrows) and sinusoidal channels (marked with dotted arrows). Adapted from Ref. [211]

The highly branched channel network promotes the diffusion of reagents and causes a large inner surface. Additionally, the availability of two different channel types with intersections results in a higher transportation rate because reactants can use one system on their way to the catalytic active sites and the products are able to diffuse through the other channels out of the catalyst [223].

Materials with CHA Topology: SAPO-34 and SSZ-13

Materials with CHA topology are characterised by a cage structure, wherein relatively large pores are connected through small windows with a width of 0.38 nm (see Fig. 6.56) [235–239]. They possess the general formula

$$(Si_xAl_yP_z)O_z \quad \text{with } 0.01 \leq x \leq 0.98,\ 0.01 \leq y \leq 0.6,\ 0.01 \leq z \leq 0.52$$

The most commonly used zeotype material for MTHC reactions is SAPO-34, which has a channel system of cages. The cages can include a sphere of 0.737 nm [211] and are accessible through six 8-rings [211]. Because of this, the maximum diameter of a sphere that can diffuse along *a*, *b*, or *c* is 0.372 nm [211].

Because the catalytic active sites are situated inside the pores and channels, chemical reactions are limited to molecules that are small enough to enter and leave these positions. Also, large molecules cannot diffuse in or out of the crystal. This implies that large molecules, which may have been formed in the cages during the reaction, are encapsulated inside. As a consequence, SAPO-34 is in particular highly selective for the production of the desired linear olefins ethylene and propylene.

As H-SAPO-34 and H-SSZ-13 have the same topology, the only difference lies in the composition. H-SSZ-13 is a zeolite with an Si/Al-ratio of 11, corresponding to one aluminium ion per cage and its associated proton. For the comparable H-SAPO-34 with an (Al + P)/Si-ratio of 11, this proton is adjacent to a silicon ion. This leads to different acidities; thus the density of Brønsted acidic sites (in the aqueous system equivalent to the pH value) of H-SSZ-13 is the same as in SAPO-34, but the acidity value (equivalent to the pK_a value) of H-SAPO-34 is less than that of H-SSZ-13 [240].

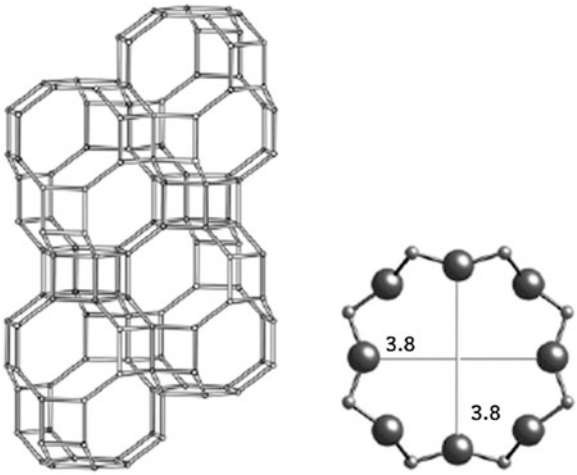

Fig. 6.56 Structure of SAPO-34 [211] and pore cross-section with central atoms (small) and oxygen atoms (big)

In a chabazite aluminosilicate, the substitution of a silicon atom with an aluminium atom results in four topologically distinct Brønsted acidic centres. Three centres belong to protons (or other cations), which are connected to oxygen ions in 8-rings and hence belong to two cages. The fourth acidic centre is adjacent to an oxygen ion in a 6-ring and thus lies only in one cage. Analogously in an aluminophosphate, a Brønsted acidic centre is created by replacing a phosphorous ion by a silicon ion.

Catalyst Synthesis

Zeolites are formed by a multilevel self-assembly process of dissolved silicate and aluminosilicate anions, in which the solvent and structure-directing agents (e.g. organic cations) interact with the silicate and aluminosilicate anions to build organic–inorganic composites. These composites assemble into ordered arrays. Subsequent condensation processes result in nucleation and finally in the growth of three-dimensional covalent crystalline networks [241].

The preparation of zeolite-based catalysts, such as ZSM-5 catalysts for MTHC reactions, includes the following steps: [242, 243]

- Contacting a silicon source with aluminium species, alkali and optionally a template in aqueous suspension to get a gel.
- Converting the gel into a crystallised aluminosilicate at elevated temperature and normal or elevated pressure.
- Separating the crystalline product from the suspension.
- Drying and calcination of the solid to remove the template.
- Substitution of the enclosed alkali ions by protons or proton-providing substances in aqueous medium.
- Drying and calcination.
- Milling the aluminosilicate to get small particles, which are mixed with a binder, such as finely divided hydrated alumina, alumina, silica or $AlPO_4$.
- Shaping the mixture and final calcination, for example at a relatively low temperature in the range of 470–650 °C for 5 h.

There are a lot of parameters that influence the production of a special catalyst, such as the sources of silicon, aluminium, and alkali. The used template has a major influence on the topology of the formed zeolite as well. Furthermore, there may be an influence of the sequence of the addition of the chemicals, the stirrer type and the stirring speed. The heating rate in the commercial synthesis and the synthesis time influence the catalyst properties as well as the synthesis temperature. During the calcination steps, the heating rate and temperature also play an important role, as does the type of furnace. Finally, during the shaping of the catalyst, the desired porosity is created, which is not only determined by the source of binder precursor but also by its physical properties, such as the grain size distribution, the alkali content, the kinetic of the solubility and the type of shaping aids.

The various parameters influence each for itself, as well as in combination with one another, the constitution of the catalyst and its catalytic properties, such as the

distribution of the aluminium ions in terms of a depletion of aluminium in the core or on the outer surface of the individual zeolite crystals [244]. Therefore, H-ZSM-5 crystals without any substantial concentration gradient can be obtained by crystallisation from inorganic gels, whereas all types of gradients can be created when organic templates are used [245].

Catalyst Modification

In addition to the targeted production of gradients of the acidic sites, the acidity of zeolites can be modified by treating the material with steam, which causes dealumination and thus an irreversible deactivation along with an increase of catalytic activity. Exposure of pure and binder-free zeolites with relatively low Si/Al-ratio to mild steaming causes the formation of aluminium pairs, with one aluminium ion of the pair being proposed as to be not tetrahedrally coordinated. This ion acts as a strong electron-pulling centre for the adjacent tetrahedral aluminium ion, creating a stronger Brønsted acidic centre [217]. This behaviour cannot be transferred straightforwardly to the technically interesting zeolites with relatively high Si/Al-ratios.

Leached aluminium atoms can also interact with bridging hydroxyl groups, which results in the formation of Lewis acidic centres [223]. These centres are also accessible by heating the material up to 550 °C, so that water gets lost (see Fig. 6.54) [220]. Moreover, dealumination processes occur during catalyst usage and regeneration. Another possibility of introducing Lewis acidity into zeolites is to contact the material with alkalines. Thus silicon atoms are removed by desilylation and free Al–OH groups are formed [232].

Dealumination methods can also be used in order to change the Si/Al-ratio in zeolites after synthesis. This is accompanied by a reduction of the number of acidic sites. Alternatively, all zeolites can be dealuminated by acid treatment, which means that aluminium ions are dissolved from the zeolite lattice and then remain inside the cavities as so-called extra-framework aluminium (EFAL) [246, 247]. On the other hand, aluminium can be incorporated into the zeolites by treatment with aluminium halides. Furthermore, to a limited extent, aluminium can be incorporated into the zeolite lattice by solid state reaction at high temperatures when aluminium oxide is used as a binder [246, 248–251].

For a ZSM-5 zeolite, specifically, the Si/Al-ratio in the product can be varied within a wide range by adjusting the Si/Al-ratio in the synthesis batch. A low-cost ZSM-5 with a low Si/Al-ratio can be prepared without expensive organic templates. Starting from such a strongly acidic material, the desired acidity can be adjusted by means of an on-purpose dealumination through steam treatment. However, for ZSM-5-based catalysts for MTHC processes, this method has drawbacks in practice. In addition to the change of acidity profile, selectivity and Si/Al-ratio, the leaching of aluminium from the lattice of ZSM-5 causes the hydrothermal stability of the zeolite to be promoted. Therefore, the on-purpose steam treatment is also used as a method to stabilise the catalyst prior to use.

The selectivity of SAPO catalysts for olefin formation can be enhanced by a reduction of acidity, higher Si/Al-ratios, or exchange of silicon atoms with

magnesium, zinc, iron, cobalt, nickel, manganese, or chromium [252–255]. For SAPO-34, a pretreatment, especially with ammonia, is discussed to increase the hydrothermal stability. As with ZSM-5, in SAPO-34 the selectivity to olefins is improved when the catalyst is exposed to a mild steam treatment. By an acidic treatment of SAPO-34, the selectivity to olefins, particularly to ethylene, is also improved.

Additionally, CHA framework components, which are grown together with an AFI type substance such as SAPO-5 or AlPO-5, possess a high selectivity for propylene production [256]. However, with nickel-containing SAPO-34, the ethylene selectivity can be raised up to 86 % at nearly complete methanol conversion and medium reaction temperatures of around 425 °C without significant deactivation [257].

Parameters for the Optimisation of Technical MTHC Catalysts

Mainly in the laboratories of Mobil Oil, Union Carbide and Exxon, favourite catalysts and reaction conditions for MTHC reactions have been developed on the basis of extensive laboratory experiments in the 1970s and 1980s. As a result of the attained insights, a model based on correlations of empirically determined parameters was evolved. The investigated factors influencing activity and selectivity of the MTHC reaction concern the most important process parameters of pressure, temperature and space velocity, as well as the main catalyst properties. The latter can be particularly easy shown by the example of ZSM-5.

The profile of the different acidic sites and the spatial distribution of acidic sites in the crystal are adjusted through the used synthesis conditions and latter modifications of the catalyst stated above. Besides the zeolite or zeotype material, the binder also plays a role. In the case of MTHC reactions, the binder is preferably made of an alumina precursor, which after calcination has acidic properties and thus also catalyses dehydration reactions, essentially the dehydration of methanol to DME (dimethyl ether). Ideally, about one-third of the total heat released in the dehydration of methanol is produced at the alumina contact (pre-reactor and binder).

The disadvantages in product composition caused by low Si/Al-ratios can be compensated within certain limits by an increased space velocity. However, the space velocity cannot be arbitrarily increased because it is important that the product distribution at the reactor outlet has closely reached equilibrium, which cannot be achieved at very high space velocities. Also, the application of small primary crystallites of less than 0.1 μm as precursor for the catalyst has an analog influence on product selectivity as the raised space velocity. However, primary crystallites of less than 0.1 μm also have distinct disadvantages. So, the gaps between the primary crystallites have a diameter of the same dimension as the pores and thus represent a certain diffusion barrier, which encourages undesirable secondary reactions. Additionally, such small crystallites are expensive to produce. A remedy can be found in either using a wide or a bimodal distribution of crystallites, in which small crystallites grow together into larger agglomerates or by adopting the so-called zeolite bound zeolite technique, where the zeolite in the binder is converted in a secondary synthesis into a microcrystalline ZSM-5.

Whereas the morphology of the entire catalyst, if it has a three-dimensional pore system, is of some importance for the selectivity, the morphology of the primary crystallites plays only a minor role.

Deactivation

Zeolites and zeotype materials deactivate in two ways: reversible deactivation due to coking and irreversible deactivation, which is mainly caused by dealumination and results in structural defects.

Reversible Deactivation

Reversible deactivation takes place when coke is formed. This happens during a reaction along the catalytic active zone, which migrates down the catalyst bed if a fixed-bed reactor is used [215, 221, 258–262]. Coking starts at the catalytic active sites inside the channels [227, 259, 263], with the formation of methyl substituted aromatics within the hydrocarbon pool mechanism [227, 264, 265] or on the active sites of adsorbed oxygenates [259]. These precursors are very mobile and able to migrate through the channels onto the surface, [223] although this process is still controversial [227]. Hence, coke can deposit on the surface, especially at strong coking, [227] as well as block the channels [227, 259, 263]. Additionally, external coke can be formed on the outside [263].

The rate of coking depends on the structure of the zeolite because it is a shape-selective reaction [215, 223, 260, 266–268]. Therefore, 8-membered-ring [215] and 12-membered-ring zeolites [215, 259] coke much faster than 10-membered-ring materials such as ZSM-5 [215, 223, 259] and ZSM-11 [259]. Additionally, three-dimensional channel systems coke slower than two-dimensional ones because blocked channels can be bypassed and the activity decreases only slowly. Therefore, H-ZSM-5 possesses special advantages in comparison to other zeolites, resulting in a much longer lifetime [259, 260]. Generally, zeolites with a high rate of methane formation deactivate very fast [221, 269].

Coking depends on the reaction temperature as well, with high temperatures supporting the formation of coke through higher rates of crack reactions. A minimum in coking can be observed at a reaction temperature of 400–450 °C [260, 270]. Below the temperature range of 270–300 °C, coke consists mainly of ethyltrimethylbenzenes, isopropyldimethylbenzenes and unsaturated compounds, which can be dealkylated at 475 °C to reactivate the catalyst. At higher temperatures, other coke molecules are formed slowly and can only be removed by burning. With elevated temperatures and particular pressures, more and more aromatics are formed and the C/H-ratio of the formed coke increases [260].

Longer contact times increase coking [259, 266–268]. Also the degree of conversion, the occurrence of special molecules and the actual activity of the zeolite have an impact on coking [263, 266–268]. Finally, the Si/Al-ratio also influences the kind of coke formed, [266–268, 271] with silicon-rich materials (e.g. H-ZSM-5) causing a hydrogen-rich coke, which can be burnt easily [259].

As coking progresses, the spectra of products formed changes because acidic sites become blocked. This change is very similar to a shortening of contact time or the decrease of active sites. Therefore, the rate of C_3 and C_4 paraffins decreases; formation of isoparaffins, naphthenes, olefins and nonaromatic C_{5+} compounds increases; and the amount of aromatics declines or stays unaffected [215, 221, 258, 260, 261, 272]. These changes can be modelled quite easily [263]. The formation of methane increases significantly. It is formed as a consequence of catalytic dehydrogenation of methanol getting in contact with external coke [260]. The highest yield of gasoline components is reached before methanol breakthrough, marking the total deactivation of the catalyst. Over the catalyst's lifetime, the octane number stays nearly constant [215, 221, 258, 261].

The catalyst can be reactivated by burning the coke. The achievable activity after reactivation depends on the activity in deactivated state and the length of reactivation [271]. Usually, reactivation is carried out with air or oxygen containing gases at 500–600 °C [259, 263, 271]. In this temperature range, permanent deactivation processes can occur. Therefore, normally it is not possible to reactivate a catalyst completely [263, 271].

Irreversible Deactivation

Dealumination causes irreversible deactivation. This process is supported by higher temperatures [221, 227, 258, 259, 263, 273] and pressure [274]. It takes place in the course of the catalytic cycle over several hundred hours if steam is present, [221, 227, 258, 259, 263, 273] especially during regeneration [227, 263, 271]. Hence, the reduction of steam production during hydrocarbon synthesis by the application of a dehydrogenated ether feedstock leads to an extended catalyst life due to a higher stability of the catalyst [255].

By losing crystalline-bound aluminium atoms, structural defects [263, 271] and aluminium atoms situated on nonlattice sites of the zeolite or zeotype material are generated. This causes a modification of the acidity profile resulting in a changed selectivity of the catalysts in hydrocarbon synthesis [218]. Therefore, crucial for the determination of a reliable correlation of the acidity profile and the selectivity is that both the acidity profile and selectivity remain constant for a significant period of several days—that is, a steady state has been reached.

In a process based on several reactor trains as well as a fluidised bed process with continuous regeneration, these fluctuations of the selectivity are compensated to a certain degree. However, in the MTG process with a fixed-bed arrangement, the gasoline yield after regeneration increases with each cycle, although the yield at the end of the cycle remains unchanged. In addition, the catalyst productivity increases, whereas at the same time changes in product distribution during each cycle decrease. This is due to permanent deactivation [258, 261, 275]. Also along the fixed bed, a permanent gradient of activity evolves as the different parts of the bed are subjected to varying partial pressures of steam and different temperatures. This permanent gradient is reflected in the broad product spectra observed in different

cycles [258, 261]. ZSM-5 exhibits a very low tendency for permanent deactivation with significant influences observed above 500–550 °C [259, 263, 273].

Reaction Mechanism

The formation of hydrocarbons is a process that is difficult to explore while all reactions take place inside the channels of the catalyst. In addition, primary products are hardly detectable because their formation is controlled by diffusion and secondary reactions have a higher reaction rate [230]. In general, it is assumed that methanol dehydrates first to form DME. This reaction reaches equilibrium, [218, 220, 221, 223, 235, 261, 276, 277] although during the reaction the equilibrium is moved towards the starting material methanol because water is formed as a byproduct in hydrocarbon synthesis [276]. This can be explained by DME having a higher reaction rate than methanol. DME reacts to C_2 to C_5 olefins, which form paraffins, aromatics and higher olefins in further reaction steps [215, 218, 223, 258, 261, 276, 278]. This general concept was the basis for several approaches to describe the overall reaction kinetics, as discussed by Keil [261].

The primary olefins that are built and the further reactions that take place depend on many parameters. Influencing parameters are the properties of the catalyst, especially:

- Acid strength.
- Density of acidic sites (decreasing density favouring heavier primary products)[230].
- Si/Al-ratio (silicon-rich materials support propene and butenes, whereas silicon-poor materials favour ethane [230]).
- The ratio of Brønsted and Lewis acidic sites (Lewis acidic sites are held responsible for catalysing reactions, leading to the formation of heavier products [232]).
- Catalyst topology [264].
- Crystallinity [264].

Furthermore, reaction conditions such as temperature, pressure and space velocity also affect the catalytic reactions [215, 218, 230, 235, 276]. At last, the present partial pressure of steam affects the product distribution and modifies the acidic strength of the catalytic active sites [221, 222].

Because of the above-mentioned difficulties in detecting primary products, there are a lot of experimental and theoretical approaches to describe the catalytic processes [215, 276, 279]. Initially, methanol reacts on the Brønsted acidic sites to DME [222, 230, 278, 279]. Using NMR technology, it is possible to follow the different reaction steps, initiated by methanol interacting with a bridging hydroxyl group, as shown in Fig. 6.57. As a function of methanol concentration, neutral complexes with hydrogen bonds or partly protonated clusters are formed, which dehydrate with elevated temperature to form methoxy groups. DME is generated along two reaction paths. The first path includes the reaction of a methoxy group with a methanol molecule followed by regeneration of the active site. The second

path describes the reaction of two adsorbed methanol molecules, which are bond side-on or end-on onto the surface [276] (Fig. 6.57).

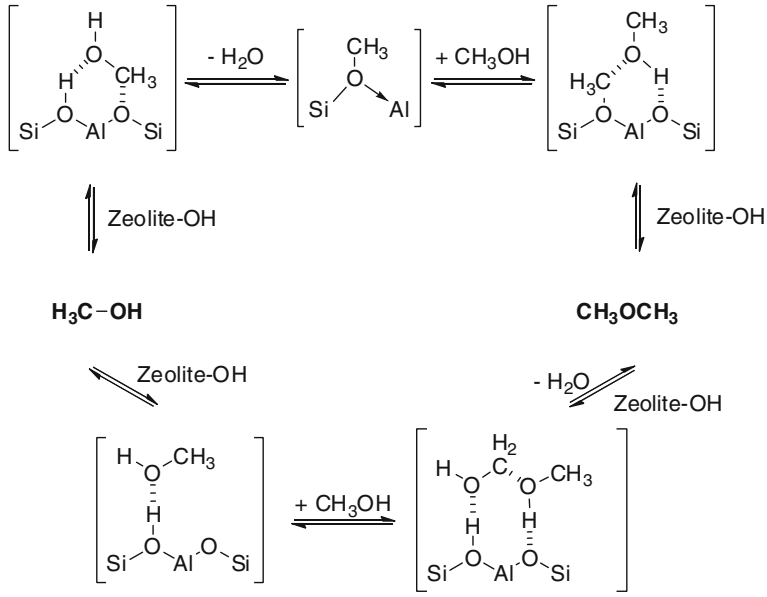

Fig. 6.57 Formation of dimethyl ether from methanol [276]

For the following reactions, regarding the formation of the first C-C-bond, more than 20 different mechanisms have been postulated, mostly excluding the induction period. These mechanisms can be categorised as oxonium ylide mechanisms, carbene mechanisms, carbocationic mechanisms, mechanisms with radicals and combinations of the different types [221, 277, 279]. Because of the insufficient acidity of the zeolites, the formation of carbenium ions can be excluded [276].

Today, the dual-cycle concept is used for the description of hydrocarbon production [264]. The first cycle is called the hydrocarbon pool mechanism and was first postulated during the 1990s [280–282]. It is based on the formation of aromatics on the acidic sites by hydrogen transfer [272]. The reaction is catalysed by aromatics (e.g. benzene, toluene, or *p*-xylene) [218, 283, 284] and proceeds autocatalytically [218, 276]. An increase in reaction temperature changes the product distribution, favouring smaller over larger olefins [218]. The catalytic active species consist of an organic–inorganic hybrid compound of the zeolite and active organic intermediates, which are situated inside the channels and intersections [235, 264, 265]. These intermediates are cyclic carbenium ions, such as 1,3-cyclopentenylcarbenium ions, which are in equilibrium with their neutral dienes, as well as methylbenzenes and polymethylnaphthalenes, which are not able to leave the catalyst because of their volume [221, 229, 235, 264, 265, 276, 285]. Cyclopentenylcarbenium ions are able to form methylbenzenes, which in turn

react with methanol to give polymethylbenzenium ions [276]. The occurrence of particular molecules depends on the zeolite type and the reaction conditions.

As the reaction proceeds, the organic intermediates react with methanol [264, 280–282] or DME [235, 264] and eliminate olefins, especially ethene and propene [221, 264, 265, 276]. Elimination is postulated to proceed through side-chain alkylation, which is characterised by the existence of an exocyclic double bond that adds methanol molecules [265, 283, 284]. A possible reaction scheme for the side-chain alkylation is shown in Fig. 6.58. Alternatively, the pairing mechanism occurs with growing alkyl side chains in consequence of ring-contraction and ring-expansion reactions (see Fig. 6.59) [229, 265]. Experimental results show that the side-chain alkylation dominates, although the pairing mechanism proceeds at least under certain circumstances [276].

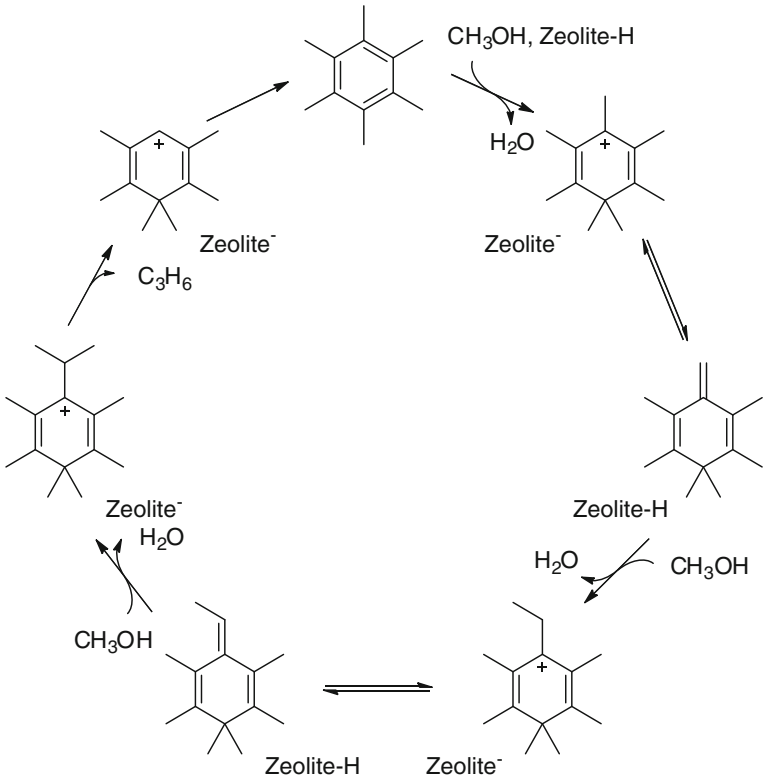

Fig. 6.58 Formation of propene using the side-chain mechanism [235]

The catalytic active species have to be formed as a first step; therefore, no hydrocarbons are released during the induction period [229, 269, 276]. These reactions proceed in the presence of radicals [221]. The induction period can

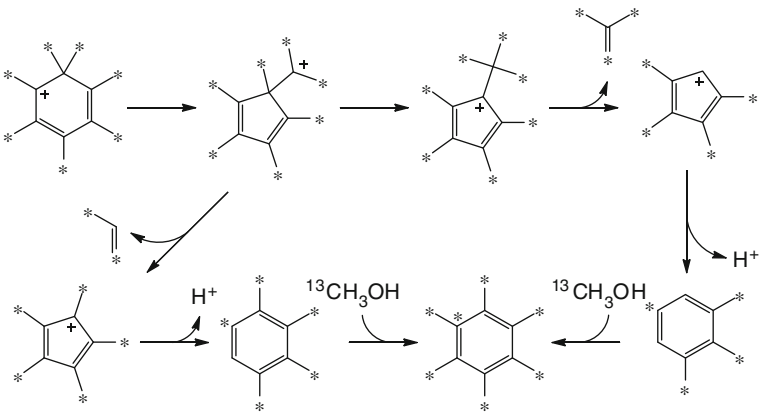

Fig. 6.59 Scheme of the pairing mechanism. Adapted from Ref. [286] (* denotes ^{13}C atoms)

be shortened by co-adsorption of water [287], co-injection of methylbenzenes [283, 284], propene or butene [269] and the application of contaminated reagents with organic substances [229, 285]. The induction period does not occur if cyclopentenylcarbenium ions are present.

In further steps of the hydrocarbon pool mechanism, it is necessary that aromatics are built through cyclisation reactions and hydride transfer of alkenes outside of this catalytic cycle [264].

This second cycle is called the Dessau mechanism, during which hydrocarbons are formed by methylation of alkenes with methanol molecules [218, 264]. Alkenes formed through this mechanism undergo cracking reactions, yielding products being able to oligomerise, become methylated by methanol, or desorb out of the catalyst. In this cycle, ethene is a secondary product in contrast to the higher alkenes, which are mainly formed therein [221, 264]. In contrast to the hydrocarbon pool mechanism, this cycle can proceed isolated, for instance in zeolites with two-dimensional channels as H-ZSM-22, which do not have enough free space for the formation of aromatics [264].

Commercial MTHC Catalysts

Often, hydrocarbon synthesis from methanol is done by a two-stage process. First, methanol is dehydrated to form DME, which is afterwards transformed into hydrocarbons. This procedure exhibits some advantages in terms of catalyst lifetime, process and heat control. As a result, catalysts that are important for MTHC processes include dehydration catalysts for DME synthesis, as well as zeolite and zeotype catalysts for hydrocarbon formation. Additionally, catalysts for olefin splitting are important for the refining of crude hydrocarbon products.

DME Catalysts for MTHC Processes

Methanol may be converted to gasoline in a two-stage operation. In the first step, methanol is partially dehydrated, whereupon an equilibrium mixture of DME, methanol and water is formed in a conventional dehydration reactor. The dehydration reactor has an equilibrium range of 75–80 %. Thus, a large portion of water is already created during this dehydration reaction, which can be optionally separated from the DME before hydrocarbon synthesis. The reaction is rapid, reversible and exothermic with liberation of approximately 30 % of the total reaction heat.

The dehydration of methanol to DME is catalysed by a number of solid acids, such as γ-Al_2O_3, H-ZSM-5, amorphous silica-alumina, or titanium-doped zirconium oxide. As early as 1928, Adkin published his research results on the dehydration of methanol over aluminium and zinc oxide [288]. For the MTP process, the commercially available catalysts DME-1 (Süd-Chemie) and its equivalent Girdler T126 catalyst [289] are used. Further suitable catalysts are Catapal carrier, T-4021 (Süd-Chemie) and DK-500 (Haldor Topsøe).

Catalysts for the Conversion of Methanol

Using methanol as raw material, a wide variety of hydrocarbon products are accessible. For the selective production of a special hydrocarbon fraction, the different catalyst providers developed special catalysts for the different products and processes. These processes are the MTG, MTO, MTA and MOGD processes by ExxonMobil, the TIGAS process, an advanced modification of the MTG process by Haldor Topsøe, as well as Lurgi's methanol-to-synfuel (MTS) process, with its major product being diesel fuel (Cetane Number $\sim$55) and approximately one-fifth being a gasoline boiling range product with a RON of 80 [290].

MTG Catalyst

The original MTG catalyst was developed based on the ZSM-5 zeolite, which was invented by Argauer and Landolt [233]. To date, no other material has proved to be as suitable for this application as ZSM-5. Clariant (formerly Süd-Chemie) produces the ZSM-5-based catalysts (the brand of this series of catalysts is CMG) for application in MTG processes. The preparation and some properties of this type of catalysts are discussed elsewhere [291]. In comparison to the MTP catalyst MTPROP-1, which is also a modified ZSM-5 catalyst offered by Clariant, they have a lower acidic site density; however, their acidity is higher than that of the COD-9 catalyst. As a result, the acidity of these catalysts in terms of acidic site density as well as with respect to the profile of acidic strength is designed for superior performance of the MTG process, which could be demonstrated on commercial plant scale.

MTO Catalysts

Argauer and Landolt [233] invented the original MTO catalyst, which was also based on ZSM-5 zeolite. Further research showed that the zeotype material SAPO-34 is more selective with respect to lower olefins compared to ZSM-5 for application in MTO processes. However, this occurs at the expense of converting approximately 10 mol% of the carbon in the methanol feed to coke, which is transferred to useless carbon dioxide upon regeneration [292].

SAPO-34

The UOP SAPO-34 based catalyst is especially designed to produce lower olefins [293]. This has been demonstrated on a pilot plant scale and will be applied in China by China's Wison (Nanjing) Clean Energy Company to convert methanol into building blocks for chemical products at an existing coal chemical complex [239].

ZSM-5

Clariant offers the ZSM-5 based MTO catalyst CMO-12 [291] with an acidic site density higher than that of the MTG catalyst CMG-1. On pilot plant scale, this catalyst has demonstrated exceptional performance for the Mt-Synfuel process. In general, the catalyst is ready for commercialisation. ZSM-5 or ZSM-11 catalysts are used by UOP in the UOP/Hydro MTO process using a raiser regenerator system for olefin synthesis. This process includes a downstream fixed-bed heavy olefin interconversion step (olefin cracking process) [294].

Catalysts for the Conversion of Olefins

The conversion of olefins to hydrocarbons is used in the MOGD process to get a gasoline boiling range product. Clariant offers for this and analog applications, like their COD process, the ZSM-5 based COD catalyst [291], with an acidic site density higher than that of the MTG catalyst CMG-1 [295]. The catalyst has been produced and used on a commercial scale for approximately 10 years [296].

Olefin-Splitting Catalysts

It is well known that the propylene yield of an MTP product stream could in principle be increased by a metathesis of ethene and 2-butene, if ethene and 2-butene would be present in the right ratio. Another possibility to increase the yield of propene is to re-equilibrate the C_{4+} or C_{5+} olefin fraction from the first MTP reactor in a succeeding second MTO unit, thus delivering additional propylene. This method is independent of the ethane-to-butene ratio after the first reactor.

The Clariant catalyst for this step recommended by Lurgi is a ZSM-5 based catalyst [291], with an acidic site density higher than the MTG catalyst. It is sensitive to dienes and similar potential oligomerisation precursors. The catalyst is

ready for commercialisation and has already demonstrated its exceptional performance for the MTP process on pilot plant scale.

Lyondell's Superflex process and Mobil's Olefin Interconversion (MOI) process are two new secondary olefin conversion technologies that crack C_4-C_8 olefins to predominately ethylene and propylene. Both technologies are based on a reactor/regenerator design similar to conventional fluid catalytic cracking. The catalyst applied in the Superflex process consists essentially of ZSM-5 [297], whereas the MOI process uses ZSM-5 or ZSM-11 as catalysts, which can be modified by metals such as gallium or phosphorus and have a high Si/Al-ratio [298]. The Superflex process is the only commercial olefin interconversion process; it was first applied at Sasol in the Republic of South Africa in 2006. It is used to convert a highly olefinic $C_{6/7}$ stream to propylene and ethylene, with a propylene production capacity of approximately 250 kt per year. JiHua is the second Superflex licensee, located in Jilin City, China.

6.4.1 Methanol-to-Gasoline Process

Lydia Reichelt[1] and Friedrich Schmidt[2]

[1]*Institute of Chemical Technology, Freiberg University of Mining and Technology, Leipziger Straße 29, 09599 Freiberg, Germany*

[2]*Angerbachstrasse 28, 83024 Rosenheim, Germany*

Introduction

In the early 1970s, researchers at Mobil Central Research discovered that methanol can be converted into higher hydrocarbons over Zeolithe Socony Mobil 5 (H-ZSM-5), a group of zeolites that was developed in the laboratories of Mobil Oil (*Socony* stands for "Standard Oil Company of New York") [299–301]. These hydrocarbons consist of a mixture of aromatic compounds, olefins and paraffins, with reaction conditions and the kind of catalyst determining the achieved predominant species. In contrast to the methanol-to-olefins (MTO) process and the methanol-to-aromatics (MTA) process, which aim for the production of olefins (MTO) and aromatics (MTA), the methanol-to-gasoline (MTG) process is capable of producing a high-quality gasoline.

The discovery of this MTG process was the biggest step in fuel synthesis since the development of the Fischer-Tropsch process in the 1920s; it led to intensive research, especially during the oil crises in the 1970s and 1980s. In consideration of the shrinking oil and gas resources as well as the ability to produce methanol from a wide variety of starting materials (e.g. coal, petroleum, natural gas, shale gas, pyrolysis oil from organic material, heavy fuel oil, biomass and organic waste), the so-found reactions are today of enormous societal significance again because they have the potential to secure and broaden the raw material base for mobility and the production of polymers, especially polyethylene and

polypropylene. The associated declining dependency on the availability of crude oil becomes increasingly attractive with each energy crisis.

Fuels from a MTHC technology completely satisfy the requirements for the usage as motor fuel in terms of octane number, cold-start behaviour, driveability, and emissions [302]. Compared to the application of pure methanol, they have the advantage of already existing worldwide safe distribution and storage networks as well as optimised engines for its usage. Furthermore, the development of alternative drive systems is presently taking place but has still not concluded. Therefore, the production and application of MTG-derived fuels can be seen as a transitory technology with a future in special areas in which alternative engines are inapplicable.

Therefore, MTHC processes, and especially processes for the production of fuels, receive high attention in scientific research and industrial applications. For instance, a new industrial facility using these technologies started up in 2009. This is remarkable because the first (and prior to that, unique) industrial plant for fuel synthesis from methanol—a fixed-bed MTG plant situated in Motunui, New Zealand—only operated from 1986 [302–307] until 1996 [308] due to too high methanol prices and low fuel prices.

The Catalytic Formation of Hydrocarbons

For the formation of hydrocarbons from methanol and related raw materials, a catalyst is generally required. The structure and properties of the catalytic active sites affect the obtainable products. The underlying chemical reactions are today mostly known. In contrast, the reactions during the induction period, until the catalyst reaches its complete activity and for the formation of the first C-C bond, are still part of the scientific discussion.

Catalysts and Raw Materials

Solid acids or immobilised mineral acids are known to be active for the catalysis of heteroatom elimination and the oligomerisation of olefins. If both processes are combined, hydrocarbons can be synthesised from compounds of type R_1-X-R_2, wherein R_1 is an alkyl, R_2 is an alkyl or a hydrogen atom, and X often is oxygen or sulphur, such as alcohols and ethers. For MTHC processes, methanol and DME are the most important raw materials; their conversion has been studied intensely during recent decades.

Zeolite H-ZSM-5 is the only known suitable catalyst for high-quality fuel synthesis from methanol. Zeolites are crystalline aluminosilicates with regularly ordered tetrahedral-coordinated Si and Al atoms. Thus, highly ordered structures with channels and cavities of molecular dimension [302] are formed, in which the catalytic active sites are situated. Because of this structure, strong constraints influence the catalytic reactions since the diameters of the channels and cavities determine the biggest molecules able to form and enter or leave the catalyst.

The H-ZSM-5 zeolite has MFI topology with a three-dimensional channel system with channel windows of 10, 6, 5 and 4 rings. In Fig. 6.60, the 10-ring is schematically shown. The maximum diameter of a sphere that can be included in

the channel crossing is 0.636 nm. The maximum diameter of a sphere that can diffuse along direction *a* is 0.470 nm and along *b* or *c* is 0.446 nm [309]. Further information on suitable catalysts for application in MTHC processes and their properties is given in Sect. 6.4 above.

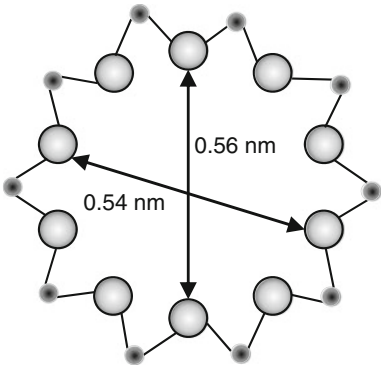

Fig. 6.60 Channel profile of ZSM-5 with Si or Al central atoms (small) and oxygen atoms (big)

Reaction Mechanism

The catalytic reactions of oxygenates to hydrocarbons take place inside the channels of the porous solid acid, especially zeolite H-ZSM-5. Using a fresh catalyst, until the induction period is passed, no hydrocarbons are set free. According to Mokrani et al., during this time methanol is completely converted in the presence of radicals [308] to give organic and aromatic substances. They add to the evolution of an inorganic–organic hybrid compound, which later acts as a catalyst for the formation of the hydrocarbon product. The question of which mechanism leads to the formation of the first C-C-bond is still not fully clarified, and thus it has led to numerous experimental and theoretical studies with more than 20 proposed mechanisms [310].

Generally, it is assumed that methanol dehydrates first to give an equilibrium mixture of DME and water [303, 308, 311–316]. DME is afterwards converted into C_2 to C_5 olefins, which form paraffins, aromatics and higher olefins: (Eq. 6.11) [302, 311, 312, 315–318].

$$CH_3OH \xrightarrow{-H_2O} CH_3OCH_3 \xrightarrow{-H_2O} C_2 \ldots C_5 \text{ olefins} \rightarrow \begin{matrix} \text{paraffins} \\ \text{aromatics} \\ \text{higher olefins} \end{matrix} \qquad (6.11)$$

The formation of hydrocarbons through hydrogen transfer, alkylation, elimination and polycondensation is shown in detail in Sect. 6.4 above. For 100 mass units of methanol, stoichiometric yields of approximately 44 wt% hydrocarbons and 56 wt% water are obtained [317]. The product spectrum comprises paraffins, olefins and mainly methyl-substituted aromatics with a maximum chain length of C_{10}. Durene (1,2,4,5-tetramethylbenzene) is the bulkiest molecule built, which is very undesirable because of its high melting point of 79 °C [302].

The thermal energy release of this reaction is approximately 1.74 MJ/($kg_{methanol}$), with approximately 15–30 % of this heat being set free during DME formation from methanol.

Deactivation

Zeolites can be reversible or irreversible deactivated. Reversible deactivation takes place when coke is formed. The rate of coke formation depends on the structure of the zeolite [302, 312, 319–322], the Si/Al-ratio [320–323], the reaction temperature, [319, 324] and the contact time [320–322, 325]. As reversible deactivation progresses, the spectra of the products formed change because acidic sites become blocked. Therefore, as the rate of C_3 and C_4 paraffins decreases, the formation of isoparaffins, naphthenes, olefins and nonaromatic C_{5+} compounds increases while the amount of aromatics declines or stays unaffected [302, 308, 315, 317, 319, 326].

In a fixed-bed reactor, a catalytic active reaction zone occurs, which moves during usage to the reactor outlet and is called band aging. When this zone reaches the outlet and the methanol content in the product rises to a certain value, the catalyst has to be regenerated [317, 327]. This is done by burning the coke with air or oxygen containing gases at 500–600 °C [323, 325, 328].

Irreversible deactivation appears when desalumination occurs and structural defects are generated [323, 328]. This process occurs at rising temperatures [308, 317, 325, 328–330] and pressure [331] if steam is present [308, 317, 325, 328–330] and takes place especially during regeneration [323, 328, 329].

Using a fixed-bed process, a permanent activity gradient along the catalyst bed evolves because of varying permanent deactivation due to different steam pressures and the S-shaped temperature profile, which is typical for adiabatic reactors.

ZSM-5 exhibits a very low tendency for reversible [319, 325] as well as irreversible deactivation, with significant influences of structural defects observed only above 500–550 °C [325, 328, 330]. The rate of overall aging decreases with increasing numbers of cycles [315].

Reaction Conditions and General Dependencies

The product selectivity and the activity profile strongly depend on the specific process parameters (temperature, pressure and contact time [302, 323]) and particular catalyst properties, whereupon the main influences are known from experimental work since the early development of MTHC processes. These experimental results can only partially be reproduced or simulated because of continuous changes in catalyst properties as a consequence of reversible and irreversible deactivation [302]. A steady state is mostly reached after several days. Additionally, the selectivity is often related only to the products at the exit of the catalytic reactor system; instead, the total carbon balance should be considered (i.e., to take the remaining coke on the catalyst into account).

When operating the MTG process at temperatures less than 300 °C, the conversion is not 100 % and DME is the main product [302, 308, 332]. Above this temperature range, conversion increases [308, 330] and hydrocarbons are formed

according to chemical equilibrium [325, 330]. Beyond 450 °C, secondary cracking reactions occur and result in a larger amount of methane and light olefins [302, 308, 330] and less C_{5+} hydrocarbons (naphtha), until above 500 °C more and more hydrogen and carbon monoxide are observed as a consequence of decomposition of methanol [302, 308]. Normally, MTG processes are performed at 300–450 °C with lower reaction temperatures leading to higher volumes of raw gasoline. However, the octane numbers decrease and the concentration of durene grows, as can be seen in Table 6.9 for the fluid-bed MTG process [333–335].

Table 6.9 Effect of temperature at constant pressure on yield and quality of total gasoline (naphtha and alkylate) from the fluid-bed methanol-to-gasoline demonstration plant. (Actual data were not disclosed) [335]

Temperature	*Low temperature*	*High temperature*
Gasoline yield	88.5 %	85.5 %
Research octane number	94.6	97.5
Motor octane number	85.3	87.4
Durene	6.5 %	3.0 %

Table 6.10 Effect of pressure at constant temperature on yield and quality of total gasoline (naphtha and alkylate) from the fluid-bed methanol-to-gasoline demonstration plant. (Corresponding temperature data were not disclosed) [335]

Pressure	1.7 *bar*	3.2 *bar*
Gasoline yield	87.5 %	89.5 %
Research octane number	96.3	95.6
Motor octane number	87.3	86.3
Durene	3.5 %	5.0 %

The operating pressure influences the relative rates of the formation of olefins and aromatics. Low pressure uncouples both processes, supporting the formation of olefins, as shown in Fig. 6.61, whereas a high pressure level results in an overlap with an increased selectivity for substituted aromatics (Fig. 6.62) [302, 308, 336]. With increasing pressure, the volume of raw gasoline increases although the research octane number (RON) and motor octane number (MON) decrease, whereupon especially the content of durene increases quickly with growing pressure (see Table 6.10) [302]. For this reason, the MTG process in several studies is performed at pressures of approximately 100 kPa [325].

The exothermic character of the conversion reaction (1.74 $MJ/kg_{methanol}$) results in an adiabatic temperature increase of about 670 °C for pure methanol feed. Therefore, careful management of the methanol feedrate in relation to the catalyst loading (e.g. as weight hourly space velocity (WHSV) or liquid hourly space velocity (LHSV)) is required. In general, the MTG process is carried out at contact times ranging from 0.01 to 0.1 h [325]. Based on the catalytic reaction pathway, a short contact time supports the formation of olefins [308, 315, 323, 337], as shown in Fig. 6.63, whereas even shorter contact times lead to the formation of DME [302]. Conversion increases with contact time [302].

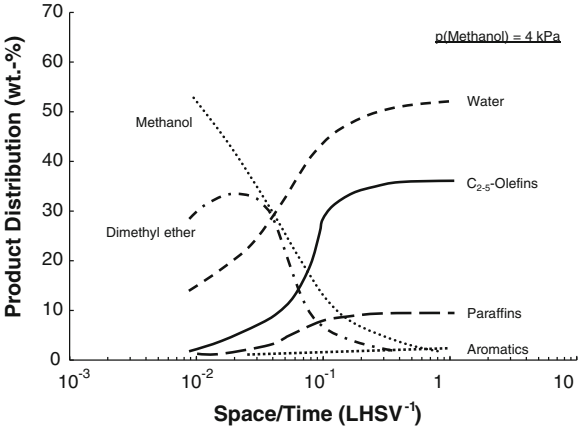

Fig. 6.61 Product distribution at low pressure [302]

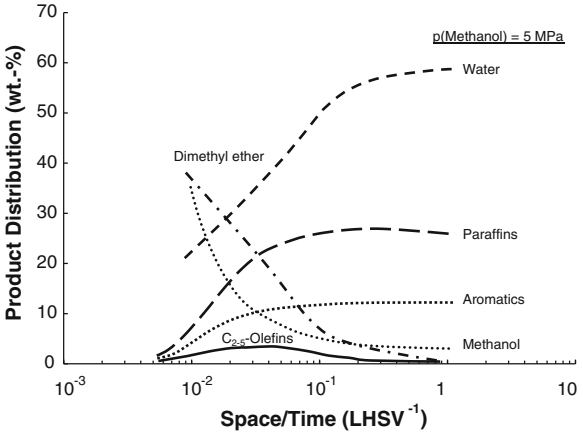

Fig. 6.62 Product distribution at high pressure [302]

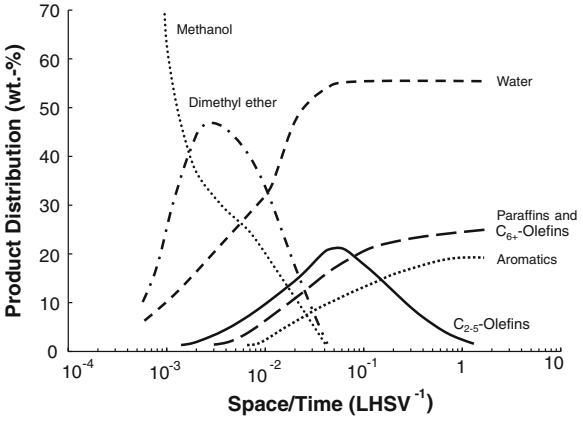

Fig. 6.63 Product distribution in dependency on contact time [302]

The production of gasoline boiling range hydrocarbons has an optimum at a certain space velocity. The maximum yield increases with increasing temperature and decreasing contact time [323]. MTHC processes are predominantly carried out at complete conversion of methanol. This way, the aqueous product can be used directly as process water and the disposal of excess water does not bear any problems regarding the toxicity of methanol. So, when methanol breaks through, the process cycle has to end and the catalyst needs to be regenerated.

Industrial Processes

Microporous crystalline solid acids have been widely used for several decades in the chemical and petrochemical industry as catalysts for the conversion of aromatics [338] and for the cracking of hydrocarbons [339, 340]. Their application in MTHC processes is mainly limited to the fixed- and fluid-bed processes by Mobil, although there are several other concepts of minor importance. Hence, today there are only a few industrial (MTG: Methanex, NZ [341, 342], dismantled in 2004; Jincheng Anthracite Mining Group, China [299–301, 343]; conversion of olefins to diesel, COD: RSA [344], similar to the second part of the MOGD process) and demonstration plants besides some projects (e.g. 15,000 barrel/day plant for DKRW's coal-to-liquids (CTL) project in Medicine Bow, Wyoming, USA, based on commercially proven ExxonMobil MTG [345]).

Fixed-bed MTG Process

The fixed-bed process was developed by Mobil Oil Corporation during the 1970s using a bench-scale reactor (4–8 L/d methanol) [317]. After successful tests in a pilot plant (640 L/d) and the discovery that upscaling has no negative but only positive effects [317, 346], the industrial plant at Motunui (New Zealand) was constructed [302, 304, 308, 315, 317, 346]. In 2009, JAMG started up yet another plant at Jincheng (China), using coal instead of natural gas as raw material for methanol synthesis.

Plant at Motunui

Due to the oil crises in 1973 and 1978, the government of New Zealand decided to become more independent from fuel imports in 1979 [303]. It aimed to use its own resources of natural gas to synthesise fuels. As a result of these considerations, it was planned to build an industrial MTG plant, with preference to the MTG process over the alternative Fischer-Tropsch process.

The construction of the plant at Motunui started in 1982. It was mechanically completed in 1985 and put into normal operation in 1986, [302–307] although the first synthetic fuel was synthesised in October 1985. The plant exhibited a capacity of 570,000 t/a gasoline [304, 305, 307, 308, 315, 317], which sufficed to satisfy one-third of New Zealand's demand for gasoline [303, 305, 306]. Until March 1987, about 739,000 t of gasoline had been produced [304, 305]. In 1996, [308]

the plant was shut down for economic reasons and sold to Methanex. Today, only the part producing methanol is still in operation [303, 308, 347]. The equipment for methanol conversion was dismantled in 2003–2004 [348].

Process

In general, the MTG plant consists of two parts. The first part is used to transform natural gas into methanol using the ICI low-pressure methanol process. In the second part, the MTG plant converts methanol to gasoline boiling range hydrocarbons, which is schematically shown in Fig. 6.64. Therefore, crude methanol, which includes about 17 wt% of water [304, 305, 315, 317], is heated up to 300–320 °C [302, 304, 305, 308, 315] and compressed to 2.6–2.7 MPa [305, 308, 315]. Then, it passes a first adiabatic fixed-bed reactor with an average space velocity of 1.6 h^{-1} (based on methanol) [302], where DME is formed on a catalyst consisting of γ-alumina. In this first step, approximately 15–30 % of the total heat of reaction (1.74 $MJ/kg_{methanol}$) is released, [302, 305, 308, 315, 317, 346] heating the reactor effluent up to 410–420 °C [302, 304, 305, 308, 315].

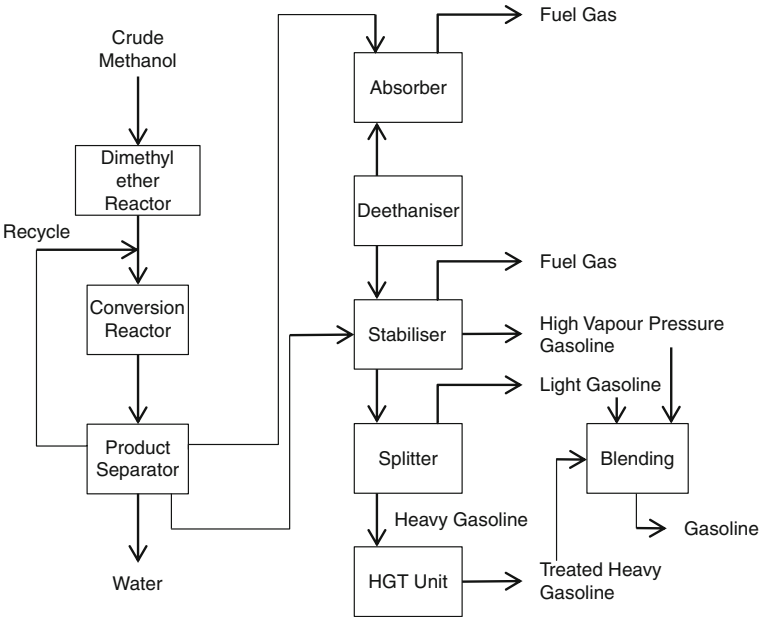

Fig. 6.64 Schematic flow diagram of the fixed-bed methanol-to-gasoline process. HGT, heavy gasoline treating

The product, in its chemical equilibrium, is mixed with a recycle gas, [304, 305, 308, 315, 346] which is needed to control temperature rise in the following adiabatic reactor from 350–370 °C [305, 308, 315] to 412–420 °C [302, 304, 308]. This reactor contains the ZSM-5 fixed bed and is used to form hydrocarbons at

1.9–2.3 MPa [305, 308, 315]. The hot product is used to preheat the recycle gas and crude methanol as well as to produce steam [304, 305, 315, 346]. Finally, the product can be separated into a recycle stream, water and hydrocarbons [304, 308, 315, 317] at 25–35 °C and 1.6 MPa [305, 315]. Afterwards, the hydrocarbon stream is split into a heavy gasoline, gasoline and liquid gas [304, 308, 315, 317].

C_3 and C_4 olefins are alkylated to increase the gasoline yield [302]. The heavy gasoline with a boiling point of ≥177 °C passes the heavy gasoline treating (HGT) unit, in which disproportionation, isomerisation, transalkylation, ring saturation, and dealkylation/cracking occur on a multifunctional catalyst at 220–270 °C and 3.1–4.1 MPa [305], resulting in reduction of the durene content from 5.5 to 2 wt% [304, 305, 308, 315, 317] without changing the octane number [305, 308, 317]. Product water is processed in a biological wastewater treatment unit to remove dissolved oxygenates (0.1–0.2 wt%) [305, 308, 315, 317].

In the continuos process at Motunui, the plant consisted of five parallel MTG reactors, with four reactors on stream and one in regeneration [305, 315, 323, 346]. This regeneration was necessary every 20–50 days [349, 350] (depending on the operating conditions and on the catalyst age [346, 351]) and the catalyst had to be changed after a certain number of cycles. The catalyst is reported to have a life of about 2 years [352]. From these data, an average cycle length of 35 days can be estimated. The average number of cycles can be expected to be approximately 20.

Products

In this process, methanol is converted to 43.4 % hydrocarbons, of which 85 % are hydrocarbons in the gasoline boiling range [302], 56 % is water and traces of carbon monoxide, carbon dioxide and coke (see Table 6.11) [302, 304]. The reaction is virtually complete and stoichiometric [302, 304, 305, 308, 315, 317, 346]. Only 5 % of the thermal energy of the methanol feed is liberated during reaction,

Table 6.11 Product distribution, based on wt% methanol charged, using the fixed-bed methanol-to-gasoline process [302]

Fixed-bed reactor		
Yields	Methanol + ether	0
	Hydrocarbons	43.4
	Water	56.0
	CO, CO_2	0.4
	Coke, other	0.2
Reactor effluent composition	Light gas	1.4
	Propane	5.5
	Propylene	0.2
	i-Butane	8.6
	n-Butane	3.3
	Butenes	1.1
	C_{5+} gasoline	79.9
Commercial hydrocarbon products	Gasoline	85
	Liquefied petroleum gas	13.6
	Fuel gas	1.4

but 95 % is preserved in the hydrocarbon product [342]. The resulting gasoline is fully compatible with conventional gasoline and has a RON of 92–95 [302, 304, 305, 308, 315, 317] and a MON of 82.6–83 [308, 315, 317].

The Mobil Shanxi Jincheng Anthracite Coal Mining Plant

In 2006, JAMG awarded a contract to Uhde for the engineering and supply of a coal-based MTG plant. It was planned to produce 100,000 t of gasoline annually starting in 2008 [353]. However, the plant was first put into service in 2009 [343]. The new MTG plant is part of a complex on a pilot-plant scale, which was constructed at Jincheng, Shanxi Province (approximately 600 km southwest of Beijing). This complex also includes a fluidised-bed hard-coal gasification plant and a methanol plant. From 1,000 t of methanol, the process produces 387 t of gasoline, 46 t of LPG, 7 t of fuel gas and 560 t of water, which is recycled as process water.

Fluid-bed MTG Process

Besides studies on the fixed-bed MTG process, Mobil developed an isothermal fluid-bed process. Therefore, at first a bench-scale reactor was used [315]. Afterwards, from 1982 to 1985, a demonstration plant was developed in Wesseling (Germany) with a capacity of 4,000 t/a [303, 306, 315], which was additionally used to carry out the MTO process. This plant had approximately 8,600 h on stream to investigate a variety of process conditions [308]. It was assembled and operated by Mobil Research and Engineering, Uhde GmbH and Union Rheinische Braunkohlen Kraftstoff AG in a joint project under sponsorship of the U.S. Department of Energy and the German BMFT. Thereafter, a commercial-scale study was carried out based on the results of that plant. However, no commercial fluid-bed MTG plants have yet been built.

Process

The fluid-bed MTG process operates at almost complete conversion and yields a high-quality gasoline in addition to LPG and fuel gas. Further information on yields and product composition are given in Table 6.12. The process uses distilled [307, 308] or crude methanol [308] as a starting material, which is vapourised and fed into the reactor. Within the reactor, immersed coils serve as a heat exchanger, which is advantageous for heat transfer through the fluid catalyst [307, 308, 315] and for producing a homogeneous temperature profile. Additionally, a part of the catalyst can be continuously externally or internally cooled in a heat exchanger [315].

Catalysis proceeds at 380–430 °C, 0.24–0.45 MPa, 500–1,050 kg/h methanol feed, 0.5–1.3 h^{-1} and 0.2–0.55 m/s gas superficial velocity [302, 307]. The catalyst is continuously withdrawn and regenerated by burning off the coke in a second reactor. The catalyst is separated from the gaseous product through cyclones. Afterwards, the product gas is cooled down and separated into a gas, liquid hydrocarbons and water using a three-phase separator. Additional separation steps are used to obtain product gasoline, C_3 and C_4 hydrocarbons, which are alkylated, and a recycle of light olefins (Fig. 6.65).

Table 6.12 Product distribution, based on wt% methanol charged, using the fluid-bed methanol-to-gasoline process [302]

Fluid-bed reactor		
Yields	Methanol + ether	0.2
	Hydrocarbons	43.5
	Water	56.0
	CO, CO_2	0.1
	Coke, other	0.2
Reactor effluent composition	Light gas	5.6
	Propane	5.9
	Propylene	5.0
	i-Butane	14.5
	n-Butane	1.7
	Butenes	7.3
	C_{5+} Gasoline	60.0
Hydrocarbon product composition	i-Paraffins	44.6
	n-Paraffins	9.2
	Olefins	16.5
	Naphthenes	5.0
	Aromatics	24.7
Commercial hydrocarbon products	Gasoline including alkylate	88.0
	Liquefied petroleum gas	6.4
	Fuel gas	5.6

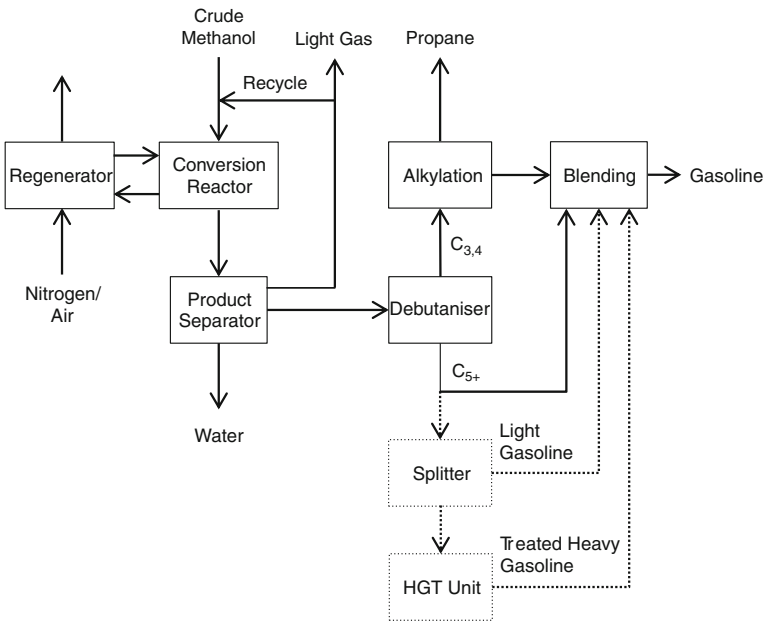

Fig. 6.65 Schematic flow diagram of the fluid-bed methanol-to-gasoline process

The alkylation of C_3 and C_4 hydrocarbons is very important to improve gasoline yield because the rate of alkylate petrol in total gasoline yield is approximately 25–30 %. However, the application of an HGT unit is not essentially needed, because the concentration of durene is less than in the fixed-bed process due to the lower pressure [307, 308, 315].

Products

The fluid-bed MTG process operates at almost complete conversion and yields a high-quality gasoline besides LPG and fuel gas. Further information on yields and product composition are given in Table 6.12.

Comparison with the fixed-bed process

The most important difference between the fluid-bed and the fixed-bed process is that the product distribution does not depend on time [308, 315]. The product contains an increased fraction of light olefins and fewer C_{5+} components, particularly less durene [302, 308], as can be seen in comparison of Tables 6.11 and 6.12.

By alkylating the light olefins with isobutene, the yield of gasoline can be improved, resulting in an about 7.5 % higher yield of gasoline than using the fixed-bed process [306, 307, 315]. Furthermore, the alkylated product gasoline possesses a similar RON of 95 but a higher MON of 85 [306, 307, 315].

In all, the fluid-bed MTG process proved to be more economical than the fixed-bed process because the heat of reaction is recovered as high-pressure steam, whereby this energy can be used more efficiently, causing a 10 % reduction in energy demand [308]. In addition, investment costs are lower, the specific throughput is higher and a liquid injection to tailor the steam balance is possible.

Other processes

Topsøe's Integrated Gasoline Synthesis

Topsøe's Integrated Gasoline Synthesis (TIGAS) process was the first process to use DME as an intermediate without isolation of methanol. The formation of DME instead of methanol has some advantages. The chemical equilibrium of methanol formation does not limit the yield of this first step and thus decreases the volume of the recycle stream and the pressure needed for synthesis. In addition, the permanent deactivation of the zeolite declines because less water is formed during hydrocarbon synthesis [331]. A fundamental benefit of the direct synthesis of DME is the possibility of using a synthesis gas with a H_2/CO-ratio of 1. This is very important for the production of synthesis gas from biomass or coal. The high vapour pressure of DME is crucial because separating DME from the product is expensive. However, in comparison to the MTG process, only two reactors are necessary, resulting in lower investment costs.

The TIGAS process was developed for application in remote areas, where natural gas is cheap but investment costs determine economic efficiency [306, 315, 331]. A pilot plant was tested from 1984 till 1987 in Houston, Texas, with a capacity of

1 t/d gasoline. Haldor Topsøe A/S developed the DME process (with a bifunctional catalyst) but used the knowledge gained from the MTG process for hydrocarbon synthesis [331]. The whole process is carried out in one train with only one recycle-stream from hydrocarbon separation back to the synthesis of DME [306, 315, 331]. A schematic flow diagram can be seen in Fig. 6.66. This necessitates the realisation of all reaction steps at one pressure level (2 MPa), which is not possible when methanol is isolated. Furthermore, the recycle stream passes the hydrogenation catalyst of the DME synthesis. The olefins included in that stream are hydrogenated, which results in a stable product with low olefin content but increases the consumption of hydrogen [306, 331]. However, unreacted hydrogen passes the zeolite, where durene formation and coking are decreased, thus regeneration is just required every 6 months [331]. Because of the slow formation of coke, the product distribution remains nearly unchanged over the cycle and the selectivity for the synthesis of C_{5+} hydrocarbons is approximately 80 % [331].

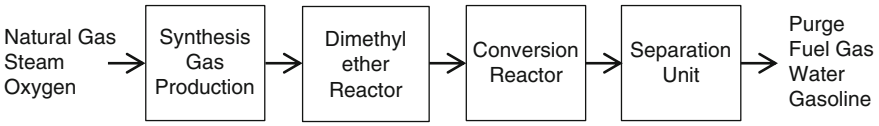

Fig. 6.66 Schematic flow diagram of the TIGAS process [331]

Although produced gasoline has a lower RON than the product from the MTG process [306, 331], its MON is nearly identical. This difference is caused by the decreased content of olefins and depends on the actual reaction conditions, especially the hydrogen content of the synthesis gas [331].

MtSynfuel and MOGD

Lurgi developed the MtSynfuel process as an alternative to the Mobil's olefin-to-gasoline and distillate (MOGD) process up to pilot plant scale [354]. The commercial MtSynfuel process would use a MegaMethanol plant for the production of methanol. The methanol is converted in a second step into DME and further into dominantly propene, using the MTP process [355] with a zeolite catalyst at temperatures between 300 and 550 °C and at pressures of 0.1–2 MPa. Afterwards, the olefins are oligomerised at 150–350 °C and 3.5–8.5 MPa using a zeolite as catalyst (COD) [356]. From the product, the C_{10+} fraction is separated by distillation and hydrogenated. Afterwards, the streams are blended to form a high-quality gasoline [357, 358] or diesel, which is even suitable for application in polar regions [359]. The overall efficiency of this process is according to Lurgi approximately the same as for the Fischer-Tropsch process, whereupon the MtSynfuel process yields a higher-quality gasoline but the Fischer-Tropsch process yields a higher cetane number of the distillate fraction.

The MOGD process [306] developed by Mobil is based on the MTO process, and it was tested in 1981 in a Mobil refinery. For the reaction, three reactors are operated in series with interstage cooling. The product consists mainly of C_5 to C_{20} i-olefins, with the C_{10} to C_{20}-fraction needing additional hydrogenation [315]. Additionally, MTO and MOGD processes can be combined to produce gasoline (RON $>$ 92) and diesel (cetane number $\approx$ 50), and an alkylation unit can be added to improve yield. This configuration results in high flexibility according to seasonal variations in fuel demand [360]. Because of the olefinic intermediates, both processes are explained in more detail in Sects. 6.4.2 and 6.4.3.

Others

The syngas-to-fuel (STF) process includes the formation of methanol and its further reaction to form a gasoline boiling range hydrocarbon product. It can be regarded as a successor of the MTG process and has been tested in a pilot plant in Freiberg, Germany. The STF process uses a new zeolite catalyst and a novel reactor concept, which abolishes the need for an HGT unit. First results are promising but final tests have yet to be carried out.

A demonstration plant for the so-called bioliq process was completed at the Karlsruher Institute for Technology. This process aims for gasification of biomass, especially using straw as feedstock for the synthesis gas production, which is converted into DME and finally into a hydrocarbon product.

The University of Akron and the Electric Power Research Institute developed the dimethyl ether-to-gasoline process. Synthesis gas reacts on a bifunctional catalyst of $Cu/ZnO/Al_2O_3$ and γ-alumina [315] at 250 °C [361] to DME. The synthesis of hydrocarbons occurs at 250–375 °C [361].

Summary

Synthetic fuels made of methanol have a high quality, whereupon methanol can be produced from a wide variety of feedstocks. These fuels are free of sulphur or nitrogen and match all legal restrictions. Using MTG technology, a high overall energy efficiency of 92–93 % (including processing energy) is possible, whereupon approximately 95 % of the thermal energy of the methanol feed is preserved in the hydrocarbon product [342]. Including the production of methanol from natural gas, the overall energy efficiency is within the range of 50–60 % [342], which is comparable to the production of diesel with the Fischer-Tropsch process (55–57 % [362]) without steam or energy export.

Although there are a lot of studies on MTG processes, only a few industrial MTG plants are at work or in the planning stage. In contrast, for the conversion of MTO or Fischer-Tropsch olefins to diesel, only few studies exist, but these technologies have already been industrially tested for approximately 20 years on zeolite catalysts, for example in South Africa.

6.4.2 Methanol-to-Olefins Processes

Friedrich Schmidt[1] and Carsten Pätzold[2]

[1]*Angerbachstrasse 28, 83024 Rosenheim, Germany*

[2]*Institute of Chemical Technology, Freiberg University of Mining and Technology, Leipziger Straße 29, 09599 Freiberg, Germany*

Introduction

The reactions of oxygenates, primary alcohols and more specifically methanol, to hydrocarbons have enormous societal significance because these reactions involve two of the most important areas of modern industrial society—namely, to secure and broaden the resource base (1) for mobility and (2) for the production of polymers (polyethylene and polypropylene for the production of consumer goods).

The worldwide outlook on light olefins seems to be positive for the years to come, with ethylene and propylene demand growing at 4–5 %, and 5–6 %, respectively, in 2009 [363]. The two primary propylene sources are steam crackers and refineries, as of 2003 represented 66 % and 32 % of the production share [364]. However, propylene production from steam crackers is expected to decline relative to ethylene production because of a growing share of ethane as cracker feedstock [365].

In the early 1970s, researchers at Mobil Central Research have discovered that methanol can be converted into higher hydrocarbons over the zeolite H-ZSM-5 [366–368]. More details about the catalyst are given in Sect. 6.4 above. The formed hydrocarbons consisted of a mixture of aromatic compounds, olefins and paraffins, delivering a gasoline of high quality. The process, named methanol-to-gasoline (MTG), is described in more detail in Sect. 6.4.1.

Efforts have been made to improve the selectivity of the MTG towards the production of dominantly lower olefins. MTO conversion is a very important process for the production of light olefins, such as ethene and propene, from alternative and abundant resources of natural gas or coal. Since this discovery, tremendous work has been devoted to the improvement of the catalyst and process performance [369, 370]. The first commercial MTO unit was the Mobil/Uhde fluid-bed MTO in Wesseling, Germany, which produced 100 barrels per day (BPD; corresponds to approximately 50 tonnes per year). Liu et al. reported on another commercial MTO unit with a production capacity of 600 tonnes of lower olefins per year, which proved to be completely successful in its first commissioning [371].

The MTO process provides an alternative route for increasing demand to light olefins, especially ethylene and propylene. These compounds are mainly manufactured by steam-cracking of naphtha. It is a thermal cracking process whereby the feedstocks (naphtha, but also lower paraffins) are mixed with steam (to reduce coke deposition) and then heated above 800 °C for pyrolysis [372]. Product

spectrum with C_2–C_5 compounds can only be changed in narrow margins; thus, additional routes (especially for propylene) are necessary [373].

Conversion of methanol to olefins has advantages compared to the steam-cracking of naphtha as well as to fluid catalytic cracking (FCC) and dehydrogenation of paraffins. Different raw materials as an alternative to oil can be used and processed to olefins with low energy consumption and CO_2 emissions. Moreover, olefins from a methanol-to-hydrocarbon route have the advantage compared to olefins from steam crackers, in that the olefins obtained via methanol are of polymer grade.

Some reviews have covered the MTHC topic from an academic viewpoint [374–376] and from a semitechnical viewpoint [367, 374]. A review by Stöcker covered the details of catalyst and reaction mechanisms of the MTHC processes, especially the MTG, MTO and Mobil's olefin-to-gasoline and distillate (MOGD) processes [377]. Keil presented a paper focusing on the technology of the MTG, MTO and MOGD processes but did not discuss those processes, which are presently operating commercially [367].

The Methanol-to-Hydrocarbon Reactions

The conversion of a number of organic compounds is catalysed by solid acids. An important group of such reactions is the elimination of heteroatoms, X, from compounds of type R_1–X–R_2 with the formation of hydrocarbons, wherein R_1 is an alkyl, R_2 is an alkyl or a hydrogen atom and X often is oxygen (rarely sulphur). Alcohols—predominantly methanol and ether, with DME in particular—are compounds of this type, whose conversion to hydrocarbons has been studied using solid acid catalysts. Another group of reactions that are catalysed by solid acids or immobilised mineral acids is the oligomerisation of light olefins to fuel. For several decades, both types of reactions on microporous crystalline solid acid catalysts have been the subject of intense scientific research. The work of the last three decades on MTHC concern, however, essentially only the MTO and MTG reactions, but not the conversion of MTO or Fischer–Tropsch olefins to diesel (COD), although the latter technology has already been industrially tested for about 20 years on zeolite catalysts. Reviews describe the state of scientific discussion until 1998 and by 2011, focusing primarily on the chemistry and mechanism of the MTO and MTG reaction, as well as to the appropriate catalysts for these reactions [377, 378]. The conversion of oxygenates was described in depth by Chang [379] and in U.S. Patents 3,931,349 to Kuo [380] and 4,404,414 to Penick et al. [381].

The reaction steps are given schematically as:

$$2CH_3OH \rightarrow CH_3OCH_3 + H_2O \rightarrow (CH_2)_2 + 2H_2O \tag{6.12}$$

In first step, methanol dehydrates to form DME. Further dehydration leads to olefins. Besides ethylene and propylene in high yields, small amounts of paraffins, higher olefins and aromatics are obtained.

Numerous studies on the MTO process have been carried out dealing with the effect of reaction conditions, influence of formed water, coke deposition, catalyst regeneration, or reactor design [382–389]. Kinetic models [390–397] were established and different catalysts such as silicoaluminophosphate SAPO-11 [385], SAPO-18 [398–401] or (H-)ZSM-X [402–405] (X stands here for various numbers, such as 5 or 22) instead of SAPO-34 were used for MTHC reactions. Objectives of these investigations were to find out advantageous conditions for methanol transformation into hydrocarbons with a high yield of desired olefins but also to derive the reaction mechanism. The temperature range was between 250 and 550 °C [390] in these studies.

The mechanism of the MTO reaction is still not clarified. More than 20 distinct mechanisms have been proposed concerning the first C–C bond formation for olefins starting from DME [377]. Union Carbide developed a process to convert methanol to olefins in 1986 using SAPO catalysts, which were invented by Union Carbide researchers [406]. The olefins yield exceeded 90 %, and they report that the process could be modified for high ethylene and propylene yield (about 60 %) [407–410].

Among the molecular sieves that have been investigated for use as oxygenate conversion catalysts, materials having the framework type of the zeolitic mineral chabazite (CHA) have shown particular promise. For example, SAPO-34 is a crystalline SAPO molecular sieve of the CHA framework type. It has been found to exhibit relatively high product selectivity to ethylene and propylene and low product selectivity to paraffins and olefins with four or more carbon atoms.

The preparation and characterisation of SAPO-34 have been reported in several publications [411–417]. In the early 1990s, UOP and Norsk Hydro carried out research activities for the MTO process. They used SAPO-34 as molecular sieve catalyst [418]. This catalyst showed an improvement in selectivity to carbon and light hydrocarbons up to 80 %, with dominantly light olefins at nearly complete methanol conversion compared to early Mobil pilot plant results on ZSM-5 catalyst.

The SAPO-34 catalyst is a microporous SAPO molecular sieve with CHA structure that has a pore size of only 3.8 Å [419–423]. Caused by the 8-membered ring of the SAPO-34, the chain length of the MTO product peaks at lower number compared to the 10-membered ring size of the ZSM-5 catalyst; however, along with this higher yield of lower olefins, a higher amount of C_1 as coke has to be accepted. Further information on the catalysts for MTO is found in Sect. 6.4 above.

Although microporous crystalline solid acids have been widely used for several decades in the chemical and petrochemical industry as catalysts for the conversion of aromatics [424] and the cracking of hydrocarbons [425], the industrial application of these types of catalysts for MTHC processes is still limited to few plants [426–431]. Due to the diversity of possible starting materials (e.g. coal, petroleum, natural gas, shale gas, pyrolysis oil from organic material, heavy fuel oil) and due to the relatively low dependence on the availability of crude oil, the method of synthesis gas to hydrocarbons via methanol becomes increasingly attractive with each energy crisis.

General Process Outline

General Process Description

In a review by Arné and Scheeline [432] on ethylene from synthesis gas, the economics of producing 1,000 million lb/yr of ethylene by direct Fischer–Tropsch synthesis from coal-derived synthesis gas was presented. The economics are compared with those of gas oil cracking and those of the conversion of methanol to olefins in all cases, a consistent set of feed and byproduct prices has been used. According to the authors, the economics for ethylene by direct synthesis are more favourable than that for the methanol route. These results must nonetheless be considered as speculative.

Process conditions and catalysts are selected accordingly so that the conversion of methanol or methanol equivalents to olefins is quantitatively accomplished. In addition to olefins and other hydrocarbons, water is a reaction byproduct.

It is expected that MTO processes will become the most important nonpetrochemical route for the production of light olefins from coal or natural gas—and in future, possibly from renewable carbon resources. A successful application of the MTO process requires a very high efficiency conversion of methanol to the desired products with very little by-product generation. The desired light olefins are dominantly propylene but also butylene and ethylene, all for the polymer industry. However, process variables must be carefully managed because the conversion of methanol to gasoline boiling components is a highly exothermic reaction.

The MTO reaction is strongly exothermic: Approximately 790 kJ (750 BTU) of heat per 450 g of methanol are released. This amount of heat release will result in an adiabatic temperature increase of about 649 °C (1,200 °F) for pure methanol feed. Therefore, two measures are taken to control the heat of reaction: (1) a two-step dehydration of methanol producing an equilibrium mix of methanol, DME, and water followed by a conversion of the mixture to olefins and (2) a suitable process concept, such as a multistage fixed-bed or fluidised-bed reactor.

In the first stage, methanol is catalytically converted to a mixture of methanol, DME and water to near-equilibrium. This mixture can then be processed, depending on catalyst and process conditions to either fuel (MTG) or olefins (MTO, methanol-to-propylene [MTP]), where $[CH_2]$ is the average composition of the hydrocarbon product, comprising olefins and aromatics plus paraffins according to Eq. 6.12. The light olefins react to paraffins, aromatics, naphthenes and higher olefins by hydrogen transfer, alkylation, and polycondensation. The above scheme is not a chemical reaction equation. It is still unclear whether the first product of all microporous solid acids is ethylene [433].

It is generally assumed that the first intermediate in the dehydration of methanol to DME (step 1 in Eq. 6.12) on solid acid catalysts is a protonated methoxy group on the surface. According to the previously cited review articles, a nucleophilic attack of methanol on the methoxy group is anticipated, but this assumption as well as the subsequent conversion to light olefins and further to paraffins, aromatics, naphthenes and higher olefins is not yet fully elucidated. For the first step (i.e., the

first C–C coupling), the following mechanisms are discussed: the oxonium ylide mechanism, the carbene mechanism, the mechanism of free radicals, the carbocation mechanism, the mechanism by consecutive addition of C_1-building blocks, and the so-called hydrocarbon pool mechanism.

With respect to the 8-membered ring molecular sieve catalysts for MTO, the ExxonMobil group of Xu and White were the first to determine the structure of the carbon pool that was active in the MTO reaction in 8-membered ring systems, such as H-SAPO-34, the first MTO catalyst system that was more precisely understood in view of the reaction mechanism. Their work, which began in 1998, resulted in the filing of two patents in early 2000, claiming for the first time that the hydrocarbon pool contains dominantly methyl-aromatic structures (e.g. toluene, xylenes, methylnaphthalenes) [434, 435].

The subsequent reactions of paraffins, aromatics, naphthenes and higher olefins are generally assumed to proceed in a known manner via a classical carbenium ion mechanism with simultaneous hydrogen transfer [436]. Although the mechanism of the first carbon–carbon bond formation has little relevance for the activity and selectivity of the dehydration of methanol or DME, there are numerous experimental and theoretical studies for the more than 20 proposed mechanisms [377]. None of these efforts, however, have so far led to a rational design for an improved catalyst and process. The reason is that the main influences on the dependence of the activity and selectivity on the process parameters are known from experimental work since the early development of MTHC processes, but the final products strongly depend on the specific process parameters and also depend on the particular catalyst properties. The detailed on-stream catalytic properties in the experiments of the various laboratories can only partially be reproduced or simulated.

As a consequence of the partially irreversible formation of byproducts such as coke and due to partially irreversible changes of the catalyst under reaction conditions (caused by the presence of steam at the high temperatures), the formation phase may take several days until a reasonably stable steady state is reached. When interpreting experimental results, it is therefore necessary to be sure that the results were obtained in a reasonable steady state. In addition, when experimental results are compared, it should be noted that the selectivity is often related only to the products at the exit of the catalytic reactor system; instead, consider the total carbon balance (i.e., take into account the remaining coke on the catalyst). For more details, see Sect. 6.4 above.

The exothermic character of the conversion reaction requires careful management of the methanol feed rate in terms of weight hourly space velocity (WHSV) based on catalyst loading. Methanol breakthrough—a term indicating the appearance of methanol in the aqueous product stream and, therefore, less than quantitative conversion—has generally been followed to signal the end of the process cycle and the need to regenerate catalyst. The number of methanol conversions at which the cycle limit is set depends on the particular design of the downstream workup equipment (i.e., the methanol and the DME recovery section). Usually, the cycle is finished if the conversion drops below 99 %.

How could the high level of MTHC technology be achieved? With respect to the catalysts, this is discussed in Sect. 6.4 above, taking the two most important representatives (i.e., ZSM-5 and SAPO-34) as examples.

The MTO Process

Today, two major designs for the MTO process are applied: the fixed-bed process and fluidised-bed process. The fixed-bed process operates on the basis of a protonated ZSM-5 catalyst. In the fluidised-bed process, H-ZSM-5 as well as H-SAPO-34 zeolite catalysts are applied.

Fluidised-Bed MTO

Mobil Pilot and Demonstration Plant

Mobil Oil developed a fluid bed process for methanol conversion initially for MTG (see Sect. 6.4.1) and later for MTO [437, 438]. For both processes, the Mobil ZSM-5 catalyst was used. The 100-BPD (approximately 11.56 m^3/day) fluid-bed MTG demonstration plant was constructed at the facilities of Union Rheinische Braunkohlen Kraftstoff AG in Wesseling, Germany [439]. The three industrial participants were Mobil Research and Development Corporation (MRDC), Uhde GmbH, and Union Rheinische Braunkohlen Kraftstoff AG.

The MTO process was developed by MRDC initially in laboratory scale and thereafter in a 4-BPD fluid-bed pilot plant. The latter was scaled-up to the existing 100-BPD MTG demonstration plant after converting the MTG mode to MTO by some modifications. This MTO programme included the following [437]:

- Pretests in MRDC's 4-BPD pilot plant to evaluate the preferred range of operating conditions set for the 100-BPD plant operation.
- Design and construction of plant modifications according to the new process conditions.
- Nine months of operation in the 100-BPD plant.

The simplified flow scheme is shown in Fig. 6.67. The reaction system contained two major vessels: the dense fluid-bed reactor (0.6 m internal diameter, 18 m in height), incorporating the cooling coils for reaction heat removal and the catalyst regenerator:

> The methanol was vaporised and fed to the reactor. The operating conditions were set so that a complete conversion is achieved. The catalyst was separated from the product gas and returned to the reactor. The product was cooled and separated downstream into gaseous hydrocarbons, C_{5+} hydrocarbons and water. The coke deposited on the catalyst in the reactor was burned off in the regenerator, with continuous catalyst circulation between the two vessels. [439]

The MTG process can be modified so that the hydrocarbon selectivity shifts towards olefin production MTO [440]. Gasoline and distillate can be co-produced

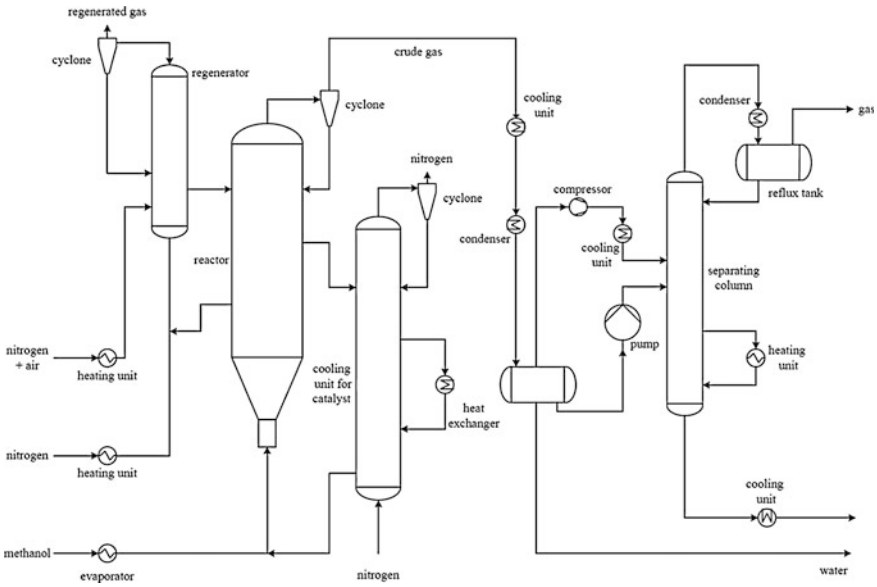

Fig. 6.67 Gasoline mode of the methanol-to-olefins gasoline plant at Wesseling, Germany (© Uhde, ExxonMobil)

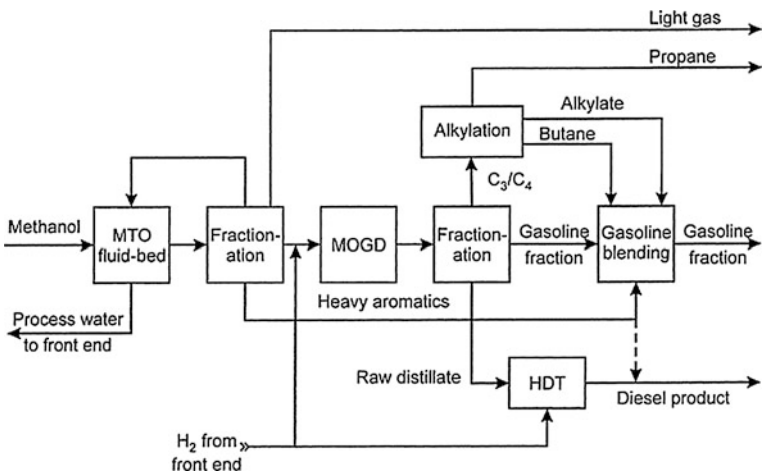

Fig. 6.68 The Mobil olefins-to-gasoline and distillate process (MOGD) flow scheme. MTO, methanol-to-olefins. (© Elsevier)

using an olefin oligomerisation step, such as MOGD [441, 442]. A scheme for the manufacture of gasoline and distillate from coal via Mobil processes is shown in Fig. 6.68.

Process Description

Pretest studies were conducted by MRDC in their 4-BPD fluid-bed unit to determine the effects of temperature, pressure and space velocity on MTO product selectivity. The results of these studies defined the preferred range of operating conditions for the 100-BPD unit. The 100-BPD MTO and MTG plant operating conditions are summarised in Table 6.13 [437].

Table 6.13 The 100-BPD methanol-to-olefins (MTO) and methanol-to-gasoline (MTG) process conditions

	MTG	MTO
Temperature, °C	380–430	470–515
Pressure, kPa	270–450	220–350
MeOH feed rate, kg/h	500–1,000	580–620
Hours on stream	8,600	3,600
On-stream factor, % Including scheduled shut-downs	65	57

The 100-BPD MTO plant was started up on February 22, 1985. According to Keim et al., "MTO operation started with a sensitivity study to determine the effect of reaction temperature on product selectivity (Fig. 6.69). This was followed by a pressure sensitivity study, and a steady state run was established in order to determine the fresh catalyst make-up requirements for continuous operation to compensate for chemical deactivation"[439] (Fig. 6.69).

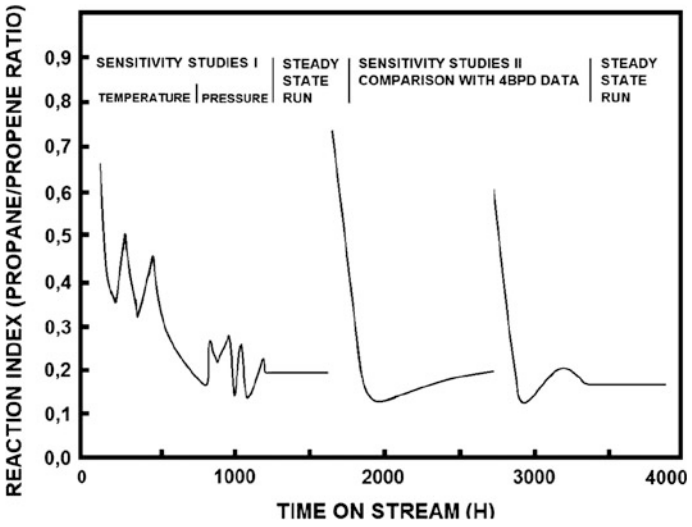

Fig. 6.69 Catalyst activity versus on stream hours [439]

A steady-state run at optimised MTO conditions, including ethene recycle simulation, could be demonstrated. The ethene recycle increases the process efficiency of the methanol-to-hydrocarbon reactions with respect to propylene because the product distribution of ethene conversion is very similar to that of methanol conversion.

The propane/propene ratio (also named reaction index, selectivity index, or R-factor) correlates with catalyst activity. With increasing cycle time, the R-factor decreases because the yield on olefins increases. The selectivity (particularly the yield) of light olefins increased by about 7 % when the reaction temperature was raised from 470 to 515 °C. Disadvantages of higher temperature are higher coke and light saturated hydrocarbons yields. Decreasing pressure allows the same conversion to be achieved at a lower reaction index, again increasing olefin yield.

The steady-state runs were performed at constant methanol conversion above 99.9 % and constant coke level on the catalyst. The catalyst makeup rate was lower than 0.5 wt% of catalyst inventory/day. This is equivalent to that observed at MTG conditions [437].

The MTO process allows remarkable shifts in olefin selectivity by adjustment of reaction conditions. This has a direct impact on the gasoline/distillate ratio in the combined MTO/MOGD processes.

The 100-BPD MTO plant had accumulated:

- 12,200 h of MTG/MTO operation, including 3,600 at MTO conditions.
- The actual MTO time on-stream factor was 57 %.
- 9,000 tonnes of methanol were processed, including 2,130 tonnes during MTO operation.

The scale-up of the fluid-bed MTO process has been successfully demonstrated in the 100-BPD plant. Results obtained in this unit are in close agreement with those obtained in the 4-BPD pilot plant under the same conditions: The total olefin yield for the 100-BPD demonstration plant was similar to that from the 4-BPD plant, and the methanol breakthrough occurred at approximately the same reaction index for both units. Lower pressure and higher temperatures were shown to increase olefin yields at constant methanol conversion [437].

UOP/Hydro Fluidised-Bed

The UOP/Hydro MTO process uses a fluidised-bed reactor system for both olefin synthesis and regeneration, like shown in Fig. 6.70. The raiser regenerator principle is known from the FCC process that is used in petroleum refining. Due to this catalyst management, a high stability and abrasion resistance of the catalyst is necessary, and resistance of the used catalyst towards frequent regeneration is essential.

The fluidised-bed system was chosen for two reasons: (1) due to the fact that MTO conversion is a strongly exothermic reaction, it is necessary to remove the high exothermic heat; and (2) the stronger coking tendency of the UOP catalyst compared to the Mobil ZSM-5 in the Mobil 100-BPD demonstration plant requires frequent regeneration of the catalyst.

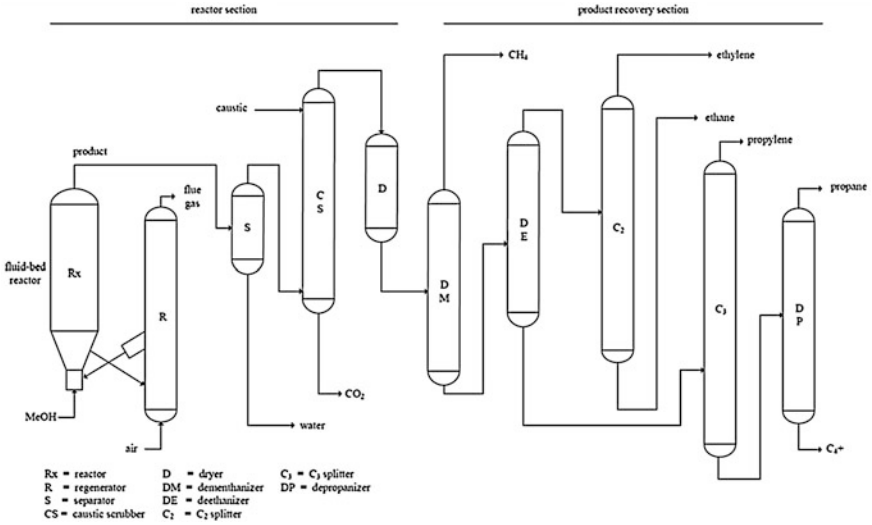

Fig. 6.70 UOP/Hydro methanol-to-olefins process [369]

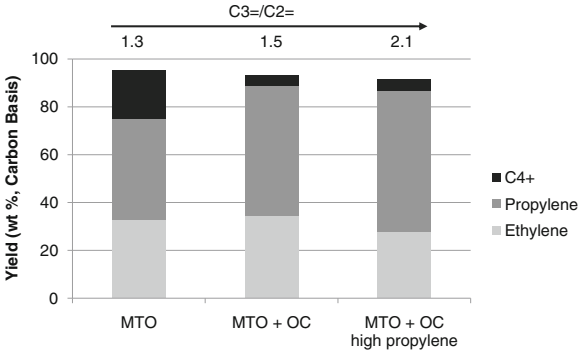

Fig. 6.71 Propylene/ethylene ratios: comparison of the methanol-to-olefins (MTO) and MTO/olefin cracking processes. OC, olefin cracking. (Adapted from [423])

Because the oxygenate impurities in the olefinic product are harmful for the downstream production of polyolefins, it is necessary to install additional equipment for removal of the major oxygenates from the product. A positive side effect of recycling these oxygenates back to the conversion reactor is the increase of the olefin yield.

The propylene/ethylene ratio can be adjusted in a wide range between 0.77 and 1.33, with a carbon-based total olefin yield of approximately 75–80 %. Process parameters are 350–600 °C and 1–6 bar [433]. At higher temperatures, more olefins are formed. However, because the SAPO-34 catalyst favours the

formation of light olefins, a higher yield of ethylene is perceived, which leads to an enhanced coke deposition and thereby in the end reduces the total olefin yield.

By an integration of the MTO process with the olefin cracking process developed by Total/UOP [423], a further boost of the propylene/ethylene ratio over 2.0 is possible. Thus, the selectivity to light olefins can be increased to about 85–90 % (Fig. 6.71).

The ExxonMobil Fluid-Bed MTO Process

In 1984, Mobil Oil filed a patent related to the conversion of alcohols and related oxygenates in a riser reactor and dense fluid catalyst bed comprising a ZSM-5-type catalyst circulated through a plurality of satellite stripping-cooling zones for temperature control [443]. Remarkably, they also claimed a partial regeneration to be advantageous for higher selectivity to olefins: their catalyst used 5–30 wt% coke for activity and selectivity control, promoting the formation of olefins and aromatics at temperatures below approximately 427 °C (Fig. 6.72).

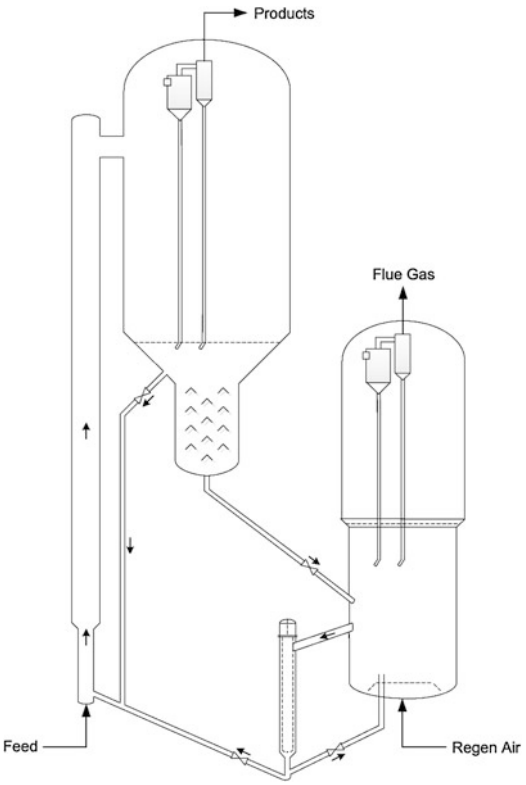

Fig. 6.72 ExxonMobil fluidised-bed methanol-to-olefins process. (Adapted from U.S. Patent 6,023,005 [444])

DMTO Technology

The DICP (Dalian Institute of Chemical Physics, Chinese Academy of Sciences) methanol-to-olefins (DMTO) technology converts methanol as the reactant to produce light olefins, such as ethylene and propylene for the further production of PE and PP. The first DMTO commercial unit in the world, with a production capacity of 600,000 tonnes of lower olefins per year, proved to be completely successful in its first commissioning operation in August 2011.

Chicago Bridge and Iron Company announced the process of converting syngas via DME to light olefins [445]. The syngas is produced by coal gasification. The gasification unit is one of the world's largest coal-to-olefins projects and started up successfully at the China Shenhua Coal to Liquid and Chemical Company's project in Baotou, Inner Mongolia (Shenhua Baotou Coal to Olefins project). The gasification unit uses advanced coal gasification technology provided by General Electric.

The plant combines the DMTO methanol-to-olefins technology of SYN Energy Technology with the Lummus Technology. Start-up was in Baotou, China. After the two commercial MTP plants in China (Shenhua Ningxia Coal Industry Group [446] in northwestern Ningxia province; see Sect. 6.4.3), this is the world's third MTO unit operating on a commercial scale. The plant is owned by China Shenhua Coal to Liquid and Chemical Company [447]. The technology enables licensees to produce olefins (ethylene and propylene) from methanol. The plant is designed to produce 600,000 tonnes per annum of olefins from methanol. On-spec ethylene and propylene product were achieved less than 72 h after methanol was introduced to the unit.

DICP developed the technology called DMTO consisting of coal gasification to obtain methanol, which is then converted to light olefins. The plant can convert 1.8 million tonnes of methanol per year into 600,000 tonnes per year of ethylene and propylene. This conversion takes place at a pressure slightly higher than the normal pressure, at a temperature between 400 and 550 °C. By variation of these operating conditions, the propylene/ethylene ratio changes between 0.8 and 1.2. A fluidised-bed catalytic reactor provides the ethylene and propylene, as well as butene, 1– 2 % coke and other light products and 55 % water [448].

Fixed-Bed MTO

The fixed-bed MTO is offered as a standalone process by Lurgi. Lurgi also offers the MTO technology as part of the Lurgi MtSynfuel process. Originally on behalf of the Central Energy Fund of South Africa in the late 1980s, Lurgi developed a fixed-bed MTO process aiming for 50 % olefins and 50 % gasoline. Using the economically highly attractive technologies of MegaMethanol and MTO, which compares to the MTP process with slightly different operating parameters, it was already proposed by Mobil [449] to combine the MTO technology with a conversion of olefins to diesel, with the latter being an industrially proven process. A gas-based synfuel plant using this process, then named COD, was developed and built by Lurgi for Mossgas (today PetroSA), RSA, in 1992 and has been performing well since its start-up in 1993. Remarkably, the industrial design was

based on a scale-up factor of 3,600 over the preceding demonstration plant. This basically was possible through the use of fixed-bed catalysis (on zeolite basis), which lends itself to easy scale-up. Other important process features are semi-continuous operation and a 98 % conversion of C_3- and C_4-olefins.

For the stand-alone fixed bed process, ethylene and propylene are the target products and gasoline is regarded as byproduct. In case of the MtSynfuel process, the ratio of olefin-based diesel to gasoline can be adjusted according to the market needs simply by adjusting the operating parameters. Compared to all other carbon valorisation, the MtSynfuel process has the highest flexibility. The Fischer–Tropsch technology is much less flexible. The MtSynfuel process allows the sale of DME, methanol, light olefins, gasoline, or diesel in optional ratios out of one single MegaMethanol plant. The plant has a capacity of more than 1 million metric tonnes per year, with the actual "standard" size being $1.7 \cdot 10^6$ t/a (equivalent to 5,000 t/d) (Fig. 6.73).

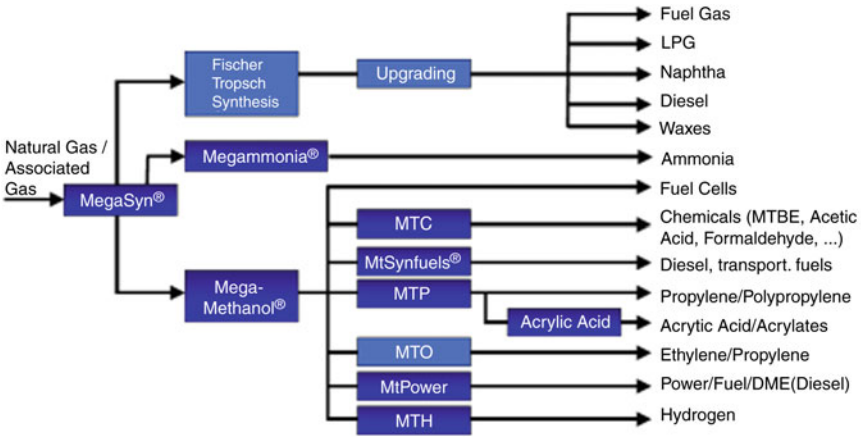

Fig. 6.73 Methanol to chemicals and fuels. DME, dimethyl ether; LPG, liquefied petroleum gas; MTO, methanol-to-olefins; MTP, methanol-to-propylene. (© Lurgi)

Boosting Olefin Yield: The Olefin Interconversion Processes

New propylene technologies, including propylene recovery from refineries, propane dehydrogenation (e.g. the Catofin or the Oleflex process), natural gas or coal conversion to light olefins via methanol (e.g. the Lurgi MTP process or the UOP/Hydro MTO process) and olefins to olefins conversion are gathering momentum. The latter includes ethylene-butene metathesis, as well as more recently developed olefins cracking technologies, such as the Lurgi Propylur process or the ATOFINA/UOP olefin cracking process (OCP) [450].

Olefin interconversion gets particular attention to boost the propylene yield from MTO or MTP plants by converting C_{3+} olefins to C_2–C_3 olefins. Olefin interconversion is offered for licensing by ExxonMobil/Washington (MOI),

Lyondell/Halliburton KBR (Superflex), ATOFINA/UOP olefin cracking process, and Lurgi/Linde (Propylur). These processes are based on thermodynamic equilibrium of olefins. Using a suitable catalyst, such as a modified ZSM-5 or other zeotype, higher olefins like C_4 and C_5 can be converted to lower olefins. Ethylene is not consumed. Propylene is the target product. Two types of technologies are offered on the market: fixed-bed and moving-bed technologies.

Fixed-Bed Process

Two fixed-bed processes are known: the Lurgi olefin conversion process [451] and the ATOFINA/UOP olefin cracking process.

The Lurgi Olefin Conversion Process

BP Köln (Cologne, Germany) demonstrated that for a C_4 cut, approximately 85 % of the C_4 olefins are converted. The Propylur plant was converting an olefin cut to propylene at yields of 60 %, with an additional 15 % yield of ethylene. A shape-selective heterogeneous ZSM-5 zeolite type catalyst, developed by Clariant (former Süd-Chemie), was used in a fixed-bed reactor operating at 500 °C and 1–2 bar. Steam was added to promote the selectivity of the reaction and reduce coking and polymer formation. The liquid C_4/C_5 feedstock is vapourised and mixed with the steam. However, dienes should be hydrogenated upstream of the unit to keep coking low.

The hydrocarbon/steam mixture is heated in a fired heater before entering the fixed-bed adiabatic reactor. By cooling the reactor effluent, the steam is condensed and separated, together with some gasoline byproducts. The remaining vapour is compressed to carry out the C_3/C_4 separation at reasonable temperatures. The C_4/C_5 stream from the depropaniser bottom is partially recycled to increase the overall propylene yield. A typical reactor product contains about 42 wt% propylene, 13 wt% ethylene and 31 wt% butenes. Due to the mild cracking conditions, the cycle length allowed the use of discontinuous in situ regeneration.

The ATOFINA/UOP Olefin Cracking Process

The Total Petrochemicals/UOP olefin cracking process converts C_4–C_8 olefins to propylene and ethylene at a high propylene/ethylene ratio. A demonstration unit was started up in 1998 at an industrial facility located at Antwerp, Belgium, which processes feed stocks from a commercial operating plant. The demonstration plant includes feed pretreatment, reactor section, catalyst regeneration facilities and internal recycle capabilities.

The ATOFINA/UOP olefin cracking process features fixed-bed technology, high space velocity, low reactor pressure (1–5 bar), 500–600 °C reactor temperature and a swing regeneration system. The process uses a proprietary zeolitic catalyst that yields 95 % propylene and ethylene in C_3 and C_2 fractions, while maintaining high olefin conversion. A key advantage of OCP is the absence of steam diluent, minimising the reactor size and saving on capital and utility costs. Unlike metathesis processes, the ATOFINA/UOP olefin cracking process does not consume valuable ethylene.

The chemistry of higher olefins cracking is more complex than it might appear at first glance. For example, butenes do not crack to $C_3 =$ or $C_2 =$ directly. Studies showed that butenes (and to some extent, higher olefins) oligomerise first; then, the oligomer species selectively crack to propylene and ethylene. The propylene/ethylene ratio is a function of the relative abundance of secondary and primary carbenium ions and therefore strongly depends on the temperature. C_5 and higher olefins can crack directly; therefore, higher ethylene yield is favoured if C_5-rich feed is used. Naphthene conversion under OCP conditions is negligible, whereas cyclo olefins tend to convert to aromatics. If C_6–C_8 aromatics are present in the feed, the toluene/benzene product ratio goes up, which can be important when the byproducts are blended into gasoline pools with limitations on benzene content.

An OCP unit can be integrated with an existing or grassroot plant that has olefinic products available, such as an FCC unit in a refinery, a steam cracker, or an MTO complex. An OCP unit has a very good potential for integration with an MTO unit. Because an MTO unit is designed primarily for stranded natural gas regions, the C_4–C_5 byproducts, which otherwise could be used, for example, as alkylation feed stocks, have very little value in such areas. Integration with an OCP unit increases overall light olefins production and can increase the propylene/ethylene weight ratio to as high as about 1.75:1. The improved utilisation in methanol for light olefin production can result in more than a 10 % reduction in methanol consumption for a fixed light olefin production [452].

Moving-Bed Process

An economical unit for processing large volumes of olefin-containing feedstocks to produce world-scale quantities of on-purpose propylene requires appropriate selection of a reaction system for the production, as well as downstream processing facilities for the recovery of the desired petrochemical products. A fluid solids reactor/regenerator configuration is well suited for such large-capacity units. Two moving bed processes are known: KBR Superflex and ExxonMobil MOI.

Superflex

In 2002, KBR (Houston, TX), the engineering and construction subsidiary of Halliburton, was building a 250,000 metric tonnes per year propylene and ethylene production facility for Sasol Technology's Synfuels Catalytic Cracker Project in Secunda, South Africa. KBR employed its Lyondell-licensed Superflex technology, which selectively converts light hydrocarbon streams to propylene and ethylene. JiHua is the second Superflex licensee, located in Jilin City, China. This unit, when commissioned, will have a design capacity of 200 kt/a of propylene production from C_4/C_5 feed.

The ExxonMobil PCCSM Process

ExxonMobil developed an on-purpose propylene technology based on catalytic naphtha cracking, called the ExxonMobil PCCSM Process. This process offers significant advantages over prior systems. The development of this technology was driven by the need for increased volumes of propylene to supplement supplies of

propylene currently produced as co-products in steam cracking and fluid catalytic cracking. The PCC process provides a possibility converting olefin molecules in naphtha streams to high value ethylene, propylene and (optionally) butylene. The process is also suitable to convert C_{4+} olefins from a MTP plant into C_2–C_3 olefins, thus boosting the yield of light olefins.

Advantages of a fluid-bed process include the following:

- No steam dilution (as in the case of Propylur)
- Continuous regeneration (i.e., no swing)

Disadvantages of a fluid-bed process include the following:

- High capital expenditure
- Operation has turned out to be not easy
- High scale-up efforts necessary

Summary

In Table 6.14 [453], a summary of natural gas-to-olefins routes is presented. All yields shown are maximum yields and are given as the mass weights of products divided by that of natural gas. Feedstock is natural gas to methanol via syngas.

Table 6.14 Summary

Technologies	UOP MTO[a]	ExxonMobil MTO[b]	Lurgi MTP[c]
	Via methanol and DME	Via methanol and DME	Via methanol and DME
Reactors	Fluidised-bed	Fixed-bed demonstration plant and fluidised-bed	Fixed-bed commercial plant
Catalysts	Silico-aluminophosphate (SAPO-34 or MTO-100)	MTO-100 ZSM-35, SAPO	ZSM-5
Temperature °C	350–525	350–500	450
WHSV			25
Ethylene yield	26 % with C_{4-5} upgrading	14 %	Negligible
Propylene yield	33 % with C_{4-5} upgrading	18 %	46 %
C_{4-5} yield	9 % (without upgrading)	Negligible	Negligible
Gasoline yield	Negligible	29 %	20
Fuel gas yield	2 %	0.1 %	6
Water yield	83 %	81 %	81 %
Total HVCs yield	62 %	45 % (61 % if gasoline is weighted 100 %)	57 % (65 % if gasoline weighted 100 %)

[a] UOP MTO data is based on Refs. [454, 455] Olefin upgrading data is based on Refs. [456, 457].
[b] ExxonMobil MTO data is based on Refs. [458, 459].
[c] MTP data is based on Refs. [460–462].
DME, dimethyl ether; MTO, methanol-to-olefins; MTP, methanol-to-propylene; WHSV, weight hourly space velocity.

Comparison of Fluidised-Bed (SAPO-34) and Fixed Bed (H-ZSM-5)

The striking differences in process design are simply a consequence of the different catalysts used. The SAPO-34 catalyst is more selective with respect to ethylene and propylene but suffers from severe coking, which requires very frequent regeneration. The ZSM-5 catalyst is less selective but much more stable due to a very low coking tendency.

The findings of Yingxu et al. [463] regarding an extensive and accurate investigation of the coke laydown in MTO reaction on CHA type zeolites are of utmost importance to underline the superiority of the MTP process compared to the UOP MTO process with respect to carbon efficiency. In case of the fluidised-bed process using SAPO-34 as catalyst, approximately 10 % of the carbon atoms in the methanol are burned to CO_2 upon regeneration. Moreover, apart from the environmental aspects, from a commercial point of view the fact that the Lurgi MTP process does not convert 10 mol% of the methanol feed to CO_2 upon regeneration translates into an economical advantage. Although the MTP process reveals also a small formation of carbon, there is still a clear benefit for the MTP process even if the loss caused by the lower value of the gasoline by product generated in the MTP process is compared to the higher propylene value in the case of the SAPO catalyst. It is assumed that the Dalian process uses the SAPO-34 catalyst. To date, there has been no confirmation of that assumption.

MTO/MTP Market

Details related to the global methanol market are discussed in Sect. 1.3. China has taken a leading role in the growth of the global methanol industry. The country already accounts for a little more than 40 % of demand, and its share is set to expand rapidly in the coming years. According to ICIS, China has become the main driver of global methanol markets. China has seen double-digit growth in methanol demand, with strong performances in the acetic acid sector, methanol blending in gasoline and the nontraditional sectors, which include MTO/MTP and DME. This production currently totals to about 10 million tonnes per year of methanol, which is about a third of China's total methanol consumption of about 30 million tonnes per year [464]. In the same source, it is reported that China will remain a driving force in the global methanol market.

Particularly in the area of feedstocks for the petrochemical industry, there has been considerable interest in MTO and MTP technologies, with pioneering projects in China because many producers are turning to coal-based methanol production. Coal-to-olefins project proponents in the country are looking for sites near coal mines where abundant coal can be sourced without having to incur transportation costs.

As for MTP economics, Lurgi estimated that the investment costs of starting up an MTP project in China would be much less than in the Arabian Gulf due to cheaper construction costs. However, because Chinese projects are mostly coal based, this would result in higher costs in the syngas production section. Hence, the overall investment and economics might be similar to that of a project in the Middle East.

Although Lurgi's technology is focused on propylene production, given the forecasts of a growing gap between supply and demand for this product, it can also deliver up to 8 % of ethylene, allowing the production of highly valuable high-impact polypropylene (see Sect. 6.4.3). The production of ethylene from MTO units will hardly be competitive to that from gas crackers in the Middle East. If necessary, an ethylene recycle increases the process efficiency of methanol-to-hydrocarbon reactions with respect to propylene, as was described here. However, the situation could be different in China, where ethylene production is mainly based on naphtha.

Ethylene will be produced cheaply from Middle East gas crackers; the MTO route based on natural gas or coal presently cannot beat this. For example, it will be more economical to import PE from the Middle East to China. As of 2005, it was expected that the production of propylene and PP from naphtha crackers and FCCs would be very competitive if only propylene (and PP + co-polymer) was produced [465]. The actual figures for 2013 are not yet available for various reasons (see Sect. 6.4.3). However, with China being the most important economy in Asia, it is pursuing MTO and MTP projects because of its huge reserves of coal, which in China is the most important raw material for methanol:

> Coal-produced methanol provides the country with a strong cost advantage over naphtha-based petrochemical production during times when oil prices are high. In China, sixteen MTO and methanol-to-propylene (MTP) projects spread across the country with a total capacity of around 10 million tonnes per year are due to come on stream from 2012 to 2015. By 2015, MTO/MTP is expected to account for more than 17 % of China's methanol demand, assuming all the other projects came on line as planned [466].

Four of the 16 MTO/MTP projects, with a combined capacity of 1.76 million tonnes/year, started production in 2012. Construction of the remaining 12 projects is expected to start soon.The existing MTO/MTP projects are listed in Table 6.15. MTO/MTP projects that are expected to be commissioned until 2015 are listed in Table 6.16.

Table 6.15 Existing methanol-to-olefins projects

Project	Location	Unit	Capacity	Status
Datang international power generation	Inner Mongolia	MTP	460,000 tonnes/year (1.68 million tonnes/year integrated methanol supply)	Operating
Shenhua group (Baotou)	Inner Mongolia	MTO	600,000 tonnes/year (integrated 1.8 million tonnes/year methanol unit)	Stable operation, unknown rates
Shenhua Ningxia coal industry group	Ningxia	MTP	500,000 tonnes/year (integrated 1.67 million tonnes/year methanol unit)	Operating
Sinopec Zhongyuan petrochemical	Henan	MTO	200,000 tonnes/year	80 %–90 %
Total			1,760,000	

MTO, methanol-to-olefins, MTP, methanol-to-propylene

Table 6.16 Upcoming approved methanol-to-olefins projects (planning projects excluded)

Project	Location	Unit	Capacity (tonnes/year)	Start date
Ningbo Heyuan (Skyford)	Zhejiang	MTP	600,000	November 2012
Zhejiang Xingxing new energy technology	Zhejiang	MTO	600,000	Pending; no exact startup date
Wison Nanjing Clean Energy	Jiangsu	MTO	300,000	2013
Zhengda (Changzhou) new material	Changzhou	MTO	1,000,000	2013
Shaanxi Pucheng clean energy chemical	Shaanxi	MTO	700,000 (300 kt/yr of ethylene, 400kt/yr of propylene; integrated methanol capacity 1.8 million tonnes/year)	2014
Ningxia coal industry	Ningxia	MTP	500,000	2014
Shanxi Coking	Shanxi	MTO	600,000 (existing methanol capacity 200,000)	End of 2014
Shenhua Shenmu chemical	Shaanxi	MTO	600,000	2014
Jiutai energy (Zhungeer)	Inner-Mongolia	MTO	600,000	2014
Sinochem (Zhonghua) YiYe	Shaanxi	MTO	800,000	2014
Shaaxi Yanchang (joint venture with Zhongmei)	Shaanxi	MTO	600,000	2014
Xinjiang Guanghui coal chemical industry	Xinjiang	MTO	1,000,000	2015
Total			7,900,000	

MTO, methanol-to-olefins, MTP, methanol-to-propylene

6.4.3 Methanol-to-Propylene Process

Sven Pohl[1], Ludolf Plass[2] and Friedrich Schmidt[3]

[1]*Air Liquide Global E&C Solutions, c/o Lurgi GmbH, Lurgiallee 5, 60439 Frankfurt, Germany*
[2]*Parkstraße 11, 61476 Kronberg, Germany*
[3]*Angerbachstrasse 28, 83024 Rosenheim, Germany*

Introduction

Methanol is currently one of the most important feedstocks for the chemical industry. Most of the nearly 60 million tonnes of methanol produced in 2012 are used for the production of a large variety of chemical products, such as

formaldehyde (approximately 30 %), acetic acid (approximately 9 %) and methyl tert-butyl ether/tert-amyl methyl ether (13 %). According to De Witt [467] approximately one-third of the production is consumed by the fuel sector.

In recent years, there has been a greatly growing interest in the conversion of coal-based synthesis gas or natural/associated gas via methanol to synthetic high-value petrochemical commodities and products that can be supplied to the consumer market. The driving forces to use coal-based or natural/associated gases include the following:

- Availability of abundant and competitive resources.
- Constant high crude prices.
- Advantageous spread between gas and crude oil pricing.
- Interest in diversifying the fuel supply.
- Minimised operating cost.

A strong growing demand comes from MTO and methanol-to-propylene (MTP) plants, which have recently started operation (approximately 4 million tonnes in 2012; see Sect. 6.4.2). Methanol-derived light olefins (ethylene and propylene) can replace such light olefins from cracker operation (in some applications), especially because of the growing price differences between oil and natural gas/coal (see Fig. 6.74).

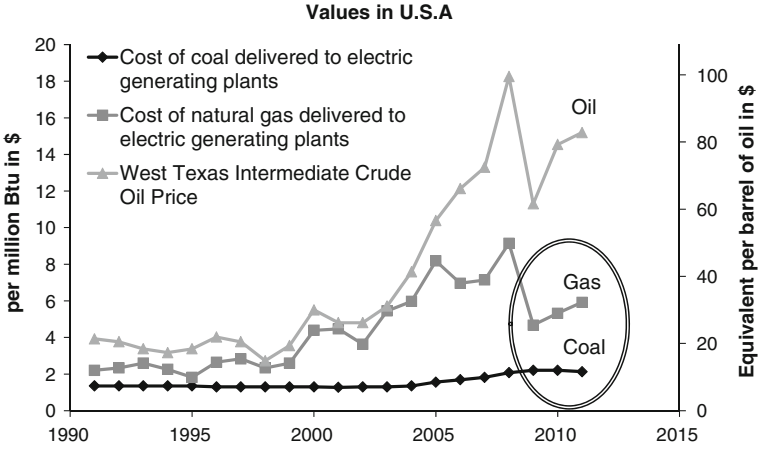

Fig. 6.74 Prices illustrate the growing advantage of using feedstocks derived from natural gas and coal[468]

Ethylene and propylene are by far the two largest volume chemicals produced by the chemical industry. Approximately 120 million tonnes of ethylene and 80 million tonnes of propylene were consumed worldwide in 2011 [467]. The demand for propylene is growing at a faster rate (approximately 4.5–5 % per year; in China 6 % per year) than that of ethylene (approximately 3–4 % per year). Because the majority of both chemicals is still produced by steam cracking and

fluid catalytic cracking, resulting in a given ratio of both chemicals, the increasing imbalance will need to be compensated by "on-purpose" production of propylene.

Technologies used for on-purpose production are mainly propane dehydrogenation (PDH), metathesis, olefin cracking and to a growing extent, MTO (see Sect. 6.4.2) and MTP. The common chemistry of MTO, MTP and MTG was described in Sect. 6.4. Figure 6.75 shows the projected strong increase of propylene from MTO/MTP plants through 2016 .

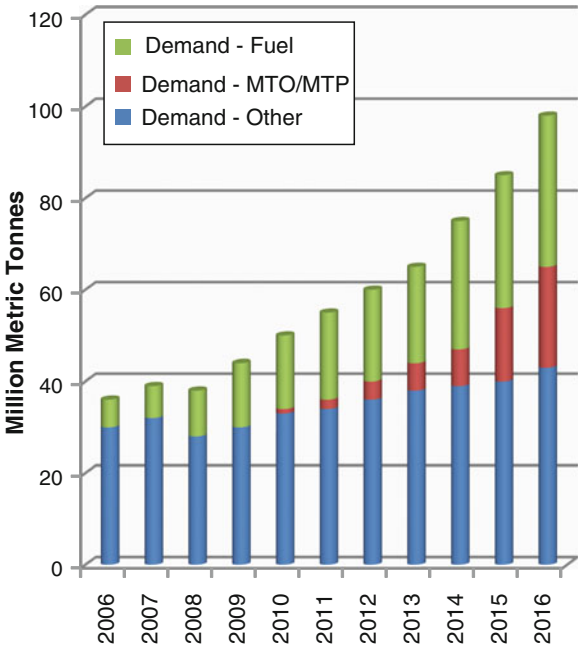

Fig. 6.75 Development of methanol-to-olefin (MTO) and methanol-to-propylene (MTP) demand through 2016 [469]. Fuel demand AAGR for 2006-2011: 9.2 %; MTO/MTP demand AAGR 2011–2016: 61.2 %; other demand AAGR 2011-2016: 4.6 %

The propylene demand is rising steadily, at an average of 6 % per year in the Chinese economy. Target production for propylene in China is an increase from approximately 13,500 kilotonnes (kt) per year in 2010 to 21,600 kt/year in 2015 [470]. To achieve this target, a large number (some sources mention up to 36) of coal-to-olefins projects are in the process of planning, erection, commissioning, and/or operation in China. Figure 6.76 shows a selected number of such projects in China, which are in operation or in the confirmed erection/planning phase.

Recent updates are given in Tables 6.17 and 6.18 below. The existing MTP projects with a combined capacity of 0.96 million tonnes per year have started production recently after a successful guaranty test with entire in-spec performance. However, according to ICIS [471], as of spring 2013 none of them could run at full capacity, partly due to poor petrochemical markets.

By 2015, MTO/MTP is expected to account for more than 17 % of China's methanol demand, assuming all the other projects come online as planned. Until 2015, about 1.8 million of the total 8.660 million tonnes per year of MTO/MTP is expected to be assigned to MTP technology [471].

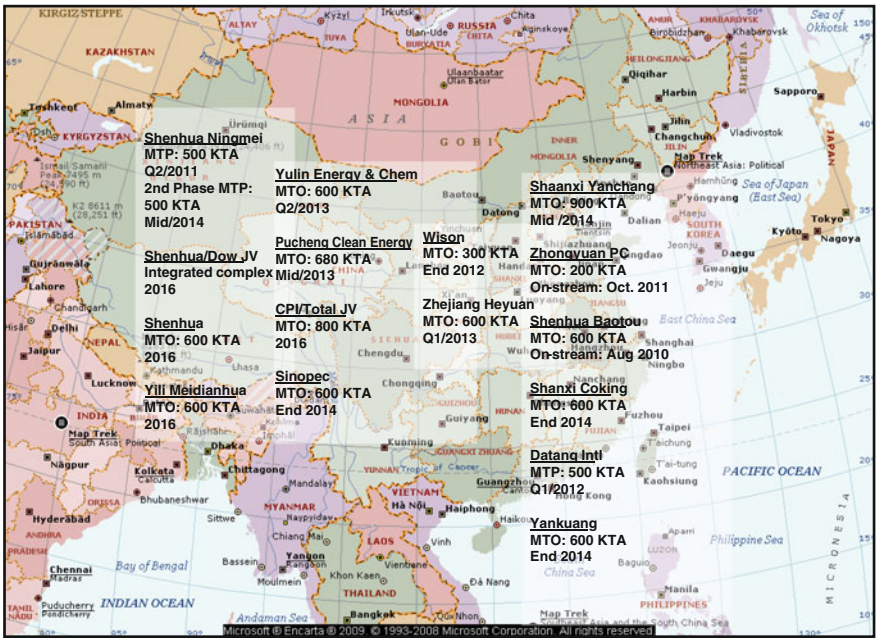

Fig. 6.76 Actual methanol-to-olefins (MTO) and methanol-to-propylene (MTP) projects in China

Table 6.17 China: Existing methanol-to-propylene projects[471]

Project	Location	Capacity in tonnes/year	Status
Datang international power generation	Inner Mongolia	460,000 (1.68 million t/a integrated methanol supply)	Operating
Shenhua Ningxia coal industry group	Ningxia	500,000 (integrated 1.67 million t/a methanol unit)	Operating
Total		960,000	

Table 6.18 China: Upcoming approved methanol-to-propylene projects (planning projects excluded)[471]

Project	Location	Capacity in tonnes/year	Start date
Ningbo Heyuan (Skyford)	Zhejiang	600,000	November 2012
Ningxia coal industry	Ningxia	500,000	2014
Total		1,100,000	

Due to the short time since commissioning, reliable figures for the economic efficiency of MTO/MTP processes in China are not yet available. Earlier studies, such as Nexant in 2003 [472], are based on data that are rather uncertain or have in the meantime been substantially modified. Additionally, a generalisation of the

economic performance of the present Chinese production of lower olefins via methanol is rather uncertain [472]. The cost of coal and other utilities, the installation cost and the operating cost are at the present time either not reported in actual studies or recorded only with relatively large uncertainty margins. The limitations of a generalisation are due to the fact that the presently installed capacity is based on coal-based methanol as feedstock, whereas in other areas natural gas or flared gas as raw materials may be the favourable feedstock for methanol.

As shown in Fig. 6.77, a large variety of chemicals and fuels can be produced efficiently based on a combination of methanol/MTP technology, going downstream to many other high-value products. In the early 1970s, researchers at Mobil Central Research discovered that methanol can be converted into higher hydrocarbons over the zeolite H-ZSM-5 [473–475]. These hydrocarbons consisted of a mixture of aromatic compounds, olefins and paraffins and delivered a gasoline of high quality.

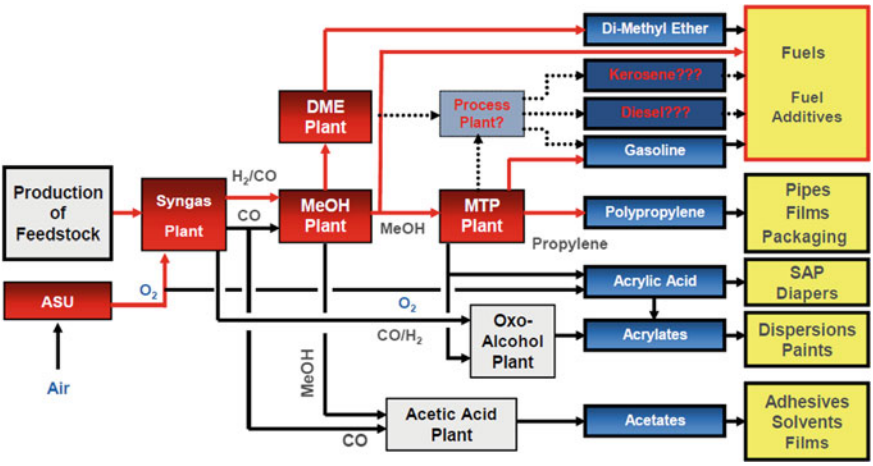

Fig. 6.77 Products based on methanol/methanol-to-propylene (MTP) technology. DME, dimethyl ether [476]

Olefins from a methanol-to-hydrocarbon (MTHC) route have an advantage compared to olefins from steam cracker: the olefins obtained via methanol are of polymer grade. The MTHC technology is reviewed in Sect. 6.4. The MTO technology chain provides the key to make almost everything from coal/biomass/natural gas that can be made out of crude oil [477].

In the view of an increasing demand for on-purpose propylene, Lurgi developed the MTP Process. The MTP technology—usually as part of a gas-/coal-to-propylene concept (GTP/CTP; see Fig. 6.78)—is characterised by its low operating cost and, hence, its reduced risk of exposure to fluctuations in propylene pricing. Furthermore, the feedstock price is decoupled from oil pricing; therefore, high oil prices provide an excellent environment for a successful GTP/CTP project (Fig. 6.78).

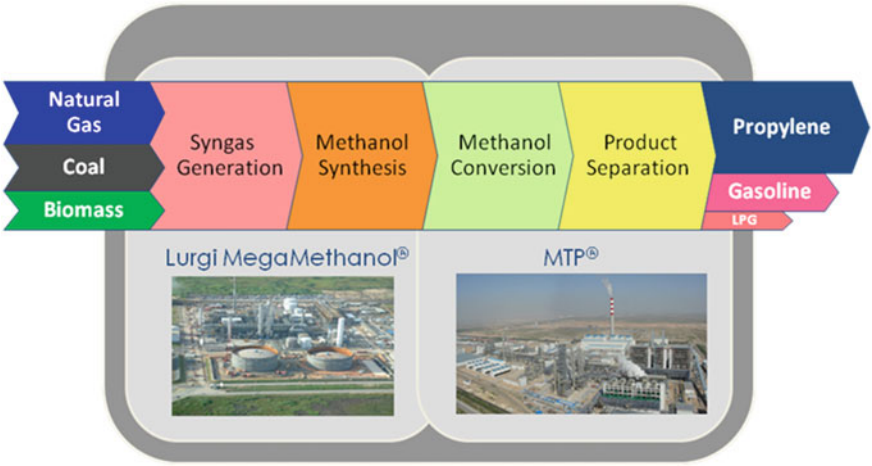

Fig. 6.78 Lurgi processes from alternative feedstock to propylene production (Air Liquide Global E&C Solutions). LPG, liquefied petroleum gas

Process Overview

Lurgi's MTP process is based on an efficient combination of the most suitable reactor system and a very selective and stable zeolite-based catalyst. Süd-Chemie AG (now part of the Clariant Group) manufactures the fixed-bed catalyst commercially. The catalyst provides maximum propylene selectivity and has a low coking tendency, a very low propane yield and also limited byproduct formation. In turn, this leads to a simplified purification scheme that requires only a reduced cold box system as compared to on-spec ethylene/propylene separation.

In Lurgi's MTP process, propylene is produced from methanol in two steps. First, methanol is converted into an almost equilibrium mixture of DME and methanol. This mixture is converted in a second step to dominantly propylene. This is the major common feature between the MTP and the MTO technology (see Sect. 6.4.2). The major differences between MTP and MTO technology lie in the process technology and in the catalyst used. Apart from the early MTO 100-BPD demonstration plant, which operated using an H-ZSM-5 catalyst with MFI topology, all other technical-scale MTO plants are based on catalysts with at least one zeotype component with chabazite (CHA) topology. The advantage of the CHA structure type in MTO reactions is that the carbon number of the product hydrocarbons peaks at lower values. However, the gain in C_2 and C_3 olefins compared to ZSM-5-based catalysts is obtained at the expense of a high C_1 formation, mainly coke. The coke formation requires frequent regeneration. This is the main reason for the necessity to apply fluid-bed technology in case of the state-of-the-art MTO processes. In contrast, Lurgi's MTP process is based on a catalyst with H-ZSM-5 as an active component that has a very low coking tendency. This in turn allows the application of a fixed-bed technology that is easy to scale-up with low capital expenditure.

A MTP plant with a feed of 5,000 t/d methanol produces typically 1,410 t/d propylene, 540 t/d MTP gasoline and 109 t/d MTP-liquefied petroleum gas (LPG). In addition, with an extension of the plant, 60 t/d of ethylene can be recovered from the purge gas, which is otherwise used as fuel. Approximately 2,800 t/d of process water is generated from the methanol.

Both the propylene and the ethylene are of polymer grade. MTP gasoline and MTP-LPG are produced as co-products, contributing additional value to the economy of the technology. The MTP gasoline has excellent characteristics as a blending stock because it is free of sulphur, has low benzene content and has a high octane number. Technology solutions are also available to process the MTP gasoline to pump-grade gasoline. The process can be described along the simplified process flow diagram given in Fig. 6.79.

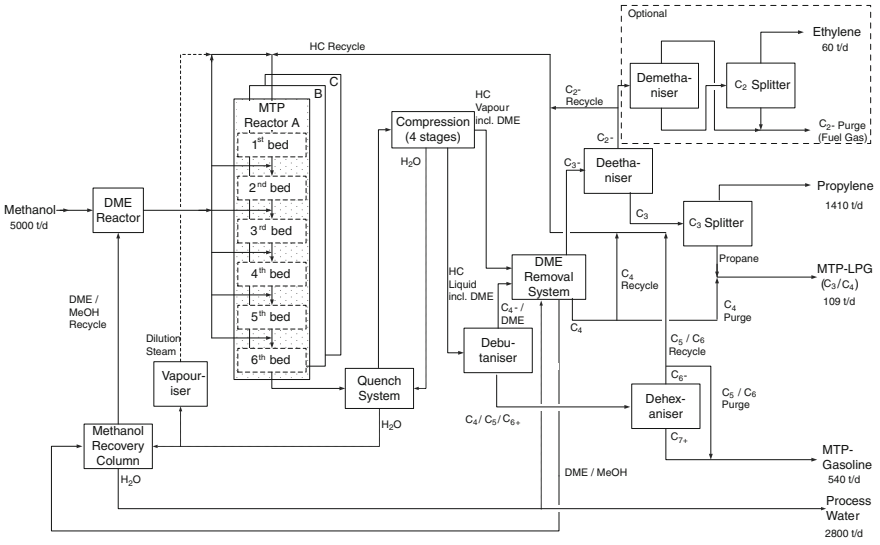

Fig. 6.79 Simplified block flow diagram: methanol-to-propylene (MTP) reaction section. DME, dimethyl ether; LPG, liquefied petroleum gas

The MTP Reactor Section

Methanol (MeOH) is used as feed to the MTP unit. The majority of the MeOH feed is vapourised, superheated and fed to the DME reactor (see also Sect. 6.4.4). A smaller part of the feed MeOH is used as solvent for oxygenate removal in the fractionation section of the MTP unit. The DME reactor is a single-stage adiabatic reactor where most of the MeOH vapour is converted to DME on an aluminium oxide catalyst according to the following equation:

$$2CH_3OH(MeOH) \rightleftharpoons CH_3OCH_3(DME) + H_2O$$

The catalyst features high activity and high selectivity, achieving an almost thermodynamic equilibrium. The reaction is exothermic and the reaction

equilibrium is nearly independent of the operating pressure. Unconverted MeOH is separated from the aqueous stream in the methanol recovery column and sent back as additional feed to the DME reactor.

The MTP synthesis features a 2 + 1 reactor concept (two reactors in operation and one reactor in regeneration mode or standby), which ensures regeneration as well as exchange of the catalyst at continued production. Each reactor represents 50 % of the plant capacity and comprises six adiabatic reactor stages for a better approach to isothermal conditions in order to achieve maximum propylene yield.

In the MTP reactor, the DME/MeOH mixture is converted to olefins on a ZSM-5 catalyst. The conversion of MeOH via a zeolite-based catalyst has been extensively investigated and discussed in past decades by various scientists. The reaction mechanism is elaborately described in Sect. 6.4. The selectivity of the MTP reaction is a result of the relative reactive rates of the reactive pool in combination with the shape selectivity of the zeolite catalyst, which through its pore structure influences the atomic structure of the produced molecules. The MTP catalyst is tailored for maximum propylene yield and maximum total olefin yield. Furthermore, coke formation of the MTP zeolite catalyst is less than 0.5 mol% (carbon conversion) depending on the lifetime of the catalyst. This low coking tendency results in excellent carbon efficiency of the MTP synthesis.

Almost 85 % of the carbon of the fresh feed (DME or MeOH) reacts in the MTP reactors to olefins in the range of C_2 to C_8 with the peak at propylene. Side products from the reactions in the MTP reactors are naphthenes, paraffins, aromatic components and light ends. The oxygen that is chemically bound in the methanol results in process water.

The product of the DME reactor is sent to the MTP reactor section and split to feed the reactor stages of each MTP reactor in operation. Before entering the first catalyst bed, the DME feed is mixed with a hydrocarbon recycle stream and dilution steam from the process steam vapouriser. The hydrocarbon conversion over the MTP catalyst bed is dominated by exothermic reactions, which results in an adiabatic temperature rise over each bed. The MTP process is designed in a way to control the temperature rise over each reactor bed while a high average operating temperature over the six reactor stages is maintained.

The intermediate reaction product from each catalyst bed is cooled and mixed with additional fresh DME/MeOH feed before entering the next catalyst bed. The quantity of fresh DME/MeOH feed to each catalyst bed is adjusted to guarantee similar reaction conditions and maximum overall propylene yield.

One result of the hydrocarbon conversion over the zeolite catalyst are also small amounts of heavy hydrocarbons, which partly block the pore structure and the active sites, which reduce the overall conversion over the catalyst. To minimise coke formation, process steam is added to the process. Steam serves as an inhibitor for coke formation and has also a role as a heat sink for the exothermic reaction, supporting temperature control over the catalyst bed.

The hydrocarbon recycle to the first MTP reaction stage increases the propylene yield by conversion of olefins other than propylene to the same product range as the DME feed. In addition, like the process steam, the hydrocarbons serve as a heat

sink for the exothermic reaction, supporting additional temperature control over the catalyst bed.

Nevertheless, the coke formation cannot be fully prevented and the catalyst has to be regenerated when the overall conversion falls below the economical limit. Typical operating cycles of one MTP reactor are approximately 600 h. The regeneration of the MTP reactor is performed in situ by controlled combustion of coke with an air/nitrogen mixture. The catalyst is regenerated at temperatures close to the normal operating temperature, thus keeping the possible thermal stress to a minimum.

Water Hydrocarbon Separation Section

The MTP reactor effluent is cooled in a heat recovery system and finally in the quench system, where the hydrocarbon product is separated from the bulk of the water. The hydrocarbons leave the quench system as overhead vapour, whereas the water is condensed and sent to the methanol recovery column. There, MeOH and DME are recovered and subsequently fed as unconverted fresh feed to the DME reactor. The stripped water containing traces of methanol is finally routed as process water to battery limits. This process water can be used as supplemental raw water for utilisation in the petrochemical complex or for irrigation after appropriate and inexpensive treatment.

Hydrocarbon Compression Section

The hydrocarbon vapour product from the quench system is compressed to approximately 2.5 MPa by a multistage centrifugal compressor. Between the compression stages, the product is cooled and partially condensed. Water and hydrocarbon liquid are separated from the vapour phase. The vapour phase is further compressed. The condensed water is recycled to the quench system, whereas hydrocarbon liquid and hydrocarbon vapour are sent to the purification section.

The hydrocarbon streams are dried by molecular sieves before the hydrocarbon liquid is fed to the debutaniser column and the hydrocarbon vapour is processed in the DME removal system.

Hydrocarbon Purification Section

The debutaniser column separates light boiling components C_{4-} and DME from C_{4+} hydrocarbons. The C_{4+} bottom product is fed to a dehexaniser distillation column, where aromatics and C_{7+} are separated from the C_{6-} stream. The major portion of this C_{6-} fraction is sent back to the MTP reaction. The remainder, along with the C_{7+} dehexaniser bottom product, form the MTP gasoline product. The compressed hydrocarbon vapours, including light olefins and DME, and the overhead C_{4+}/DME product from the debutaniser are fed to the DME removal system. Here, C_{3-} hydrocarbons are separated from C_{4+} hydrocarbons and oxygenates.

The methanol and DME-containing streams are routed to the methanol recovery column so that methanol and DME can be recycled to the DME reactor. The C_4 hydrocarbon fraction is recycled to the MTP reaction system for further propylene production. A smaller portion is purged out of the reaction loop, forming the C_4 component in the MTP-LPG product.

The C_{3-} product (including all C fractions below C_3), which is free from DME and any other oxygenates, is fed to the deethaniser. From the deethaniser, a C_{2-} stream (defined as above) is recovered as the top product. One part of the C_{2-} stream is recycled to the MTP reactor, whereas the rest is sent to the ethylene purification unit. The C_3 bottom product, containing propylene (~97 wt%) and propane (~3 wt%), but no unsaturated components such as methyl acetylene or propadiene, flow through a safeguard bed of activated alumina to the C_3 splitter. The C_3 splitter column separates propane from the polymer-grade propylene product. The propane forms the C_3 component in the MTP-LPG product.

Ethylene Purification Section

The ethylene purification is achieved in a two-column system, the demethaniser and the C_2 splitter column. The overhead vapours from the demethaniser contain C_1, hydrogen and inert material, whereas the bottom product C_2 (paraffinic and olefinic) is heated up and sent to the C_2 splitter. The C_2 stream is split and rectified to polymer-grade ethylene in the overhead system of the C_2 splitter. The ethane stream, which is drawn off from the bottom section of the splitter column, is mixed with the overhead stream of the demethaniser and is used internally as fuel gas for heater firing. If no polymer-grade ethylene is to be produced, the ethylene purification section is not needed; accordingly, the C_2 feed stream is used as internal fuel gas and minimises the fuel requirements of the MTP process plant.

Product Description Data

The products listed in Table 6.19 are based on a feed rate of 5,000 t/d methanol.

Wastes and Emissions

The catalyst of the DME reactor is an aluminium oxide catalyst with an expected lifetime of 10 years, whereas the catalyst of the MTP reactor is a ZSM-5 catalyst with an expected lifetime of more than 1 year. Both catalysts can be safely disposed in a landfill after use. The only emissions of note are the typical flue gases from gas-fired heaters/boilers and the catalyst regeneration gas, which basically consists of nitrogen-diluted air with a somewhat elevated CO_2 content.

From Laboratory Scale to Commercial Reference

Lurgi launched the MTP process development in 1999. During this time, the first tests of the MTP reaction with the Süd-Chemie catalyst (today Clariant) were performed at the Lurgi Research and Development centre. A catalyst test unit was used for tests under idealised conditions (polytropic and once-through operation) to allow optimisation studies of the reaction temperature, pressure and space velocity. The first tests showed very positive and promising results, which justified the construction of a larger-scale pilot plant to enable adiabatic test conditions and artificial recycle streams.

By means of the two test units, the basic process design data for the MTP process were derived from more than 9,000 operating hours. Parallel to the various tests, Lurgi decided to build a larger-scale demonstration unit to test the new

Table 6.19 Product description data

Product	Property
1,410 t/d propylene (polymer grade)	
Purity	>99.60 wt%
60 t/d ethylene (polymer grade)	
540 t/d gasoline	
Density at 15 °C	740–790 kg/m^3
Equivalent dry vapour pressure	35–70 kPa
Research Octane Number	90–95
Composition	
Paraffins	15–35 wt%
Olefins (increasing over run time of catalyst)	30–60 wt%
Aromatics (decreasing over run time of catalyst)	50–15 wt%
Benzene	< 1 wt%
Total sulphur components	< 0.1 wt/ppm
109 t/d liquefied petroleum gas	
Composition	
C_2 hydrocarbons	< 0.2 vol%
C_3 hydrocarbons	> 10 vol%
C_4 hydrocarbons	< 90 vol%
C_5 hydrocarbons	< 1.5 vol%
Total sulphur components, maximum	< 0.1 wt/ppm
2,800 t/d process water (either for use as raw water supplement, such as cooling water makeup, or for irrigation purposes after biological treatment)	

process in the site stream of a world-scale methanol plant, with continuous (24 h/day, 7 days/week) operation using real methanol feedstock. During the design of the pilot plant and demonstration unit, care was taken to optimise them for a possible scale-up of the MTP reactors. For example, the bed heights in the smaller units were chosen to be identical to their projected commercial-size counterparts. In this respect, the beds in the laboratory and demonstration plant can be seen as a cutout of the commercial MTP reactor. The laboratory plant was then also optimised to have an ideal adiabatic multistage operation like in the commercial plant so as to get a good prediction of the temperature profiles and the resulting propylene yields and byproducts (Fig. 6.80).

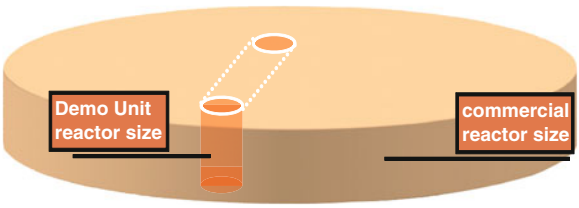

Fig. 6.80 Scale-up visualisation

After a cooperation agreement with Statoil ASA was signed in January 2001, the demonstration unit was assembled in Germany and transported to the Statoil methanol plant at Tjeldbergodden (Norway) in November 2001. Borealis joined the co-operation in 2002. The demonstration unit started continuous operation in January 2002.

In September 2003, the demonstration unit completed the scheduled 8,000 h lifecycle test. The 8,000 h test was an important milestone because the main purpose of the demonstration unit was achieved: to demonstrate that the catalyst lifetime meets the commercial target of 8,000 h on stream. Cycle lengths between regenerations were longer than expected. Deactivation rates of the methanol conversion reaction decreased with operation time. Propylene selectivity and yields were in the expected range for this unit, with only a partial recycle. Another important milestone was the successful polymerisation of the propylene from the MTP process into polypropylene in collaboration with Borealis, Norway (see Fig. 6.81). The polymerisation tests demonstrated that MTP propylene exhibits the same quality as regular, crude-oil based propylene and does not contain any new or harmful poisons for the very demanding polymerisation catalysts.

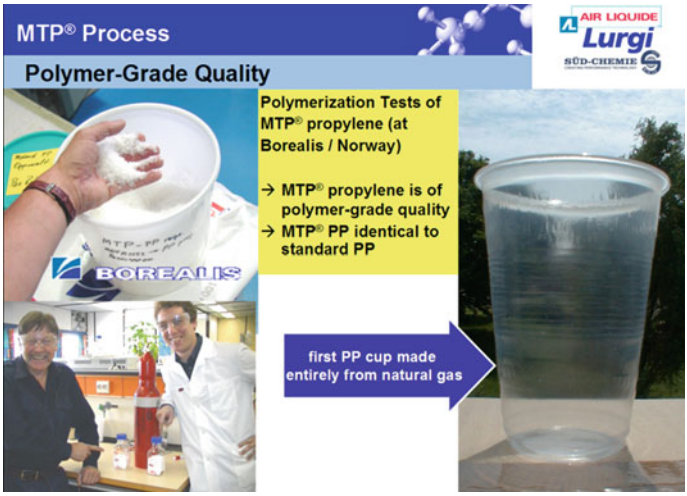

Fig. 6.81 The first polypropylene (PP) cup made from the Lurgi methanol-to-propylene (MTP) process

The demonstration tests also proved the high quality of the byproduct gasoline. After the 8,000 h test, the demonstration unit was operated for another 3,000 h with a second batch of catalyst to obtain verification and new results from variation of operating conditions. Thus, after successfully logging 11,000 h in an industrial environment, the demonstration unit was brought home to Lurgi's Research and Development centre. There, for further investigations and fine-tuning, a new process demonstration unit (PDU) was erected, which is a representation of a

commercial unit in all relevant process and recycle streams. Currently this PDU delivers continuously additional data for further developments of the process as well as support purposes for engineering. Today, the catalyst development has been completed and the supplier Clariant commercially manufactures the catalyst. Nevertheless, because there is always room for improvement, new studies have been initiated to possibly raise propylene yield and/or lifetime.

In September 2010, the Shenhua Ningxia Coal Industry (Shenhua Ningmei) Group started up its commercial coal-to-propylene complex. The gasification was licensed by Siemens GSP, producing 520,000 Nm^3/h raw syngas (see Sect. 4.4.6). The air separation unit was supplied by Air Liquide, producing 190,000 Nm^3/h of oxygen. The polypropylene technology was licensed by ABB (gaseous phase process). 6x460 t/h steam boilers and a 150 MW power plant complete the project. Only one month later, the MTP plant, as part of the coal-to-propylene complex, produced first-time on-spec propylene with a purity of 99.69 %. The commercial scale-up of the MTP process was realised based on research and development data only. A scale-up factor of more than 6,900 compared to the demonstration unit in Norway (based on feed rate) has been realised (Fig. 6.82).

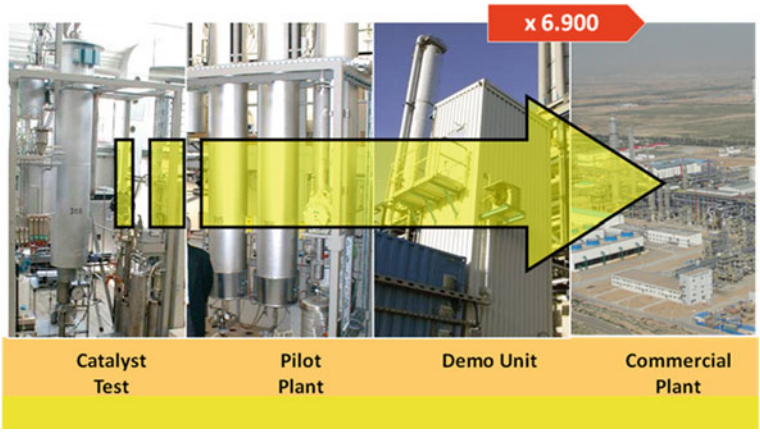

Fig. 6.82 Scale-up from pilot plant to commercial plant

The smooth commercial commissioning and operation of the first coal-to-propylene complex has been an outstanding success for the MTP development history. The comparison of performance data from the commercial MTP plant with the performance data of the process demonstration unit in the Research and Development (R&D) centre are in very good agreement. This comparison underpins the R&D capabilities for prediction of yields and even product properties of commercial MTP plants. Fig. 6.83 presents the good agreement of product slate of the commercial plant with results of the process demonstration unit operated in the R&D laboratories.

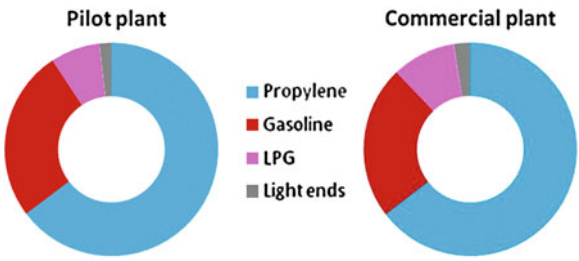

Fig. 6.83 Comparison between product slates in pilot plant versus commercial plant. LPG, liquefied petroleum gas

Operating Experience

The Shenhua Ningxia Coal Industry Group MTP plant started construction in April 2008. After mechanical completion in August 2010, commissioning started on September 6, 2010. The first on-spec propylene production was achieved on October 4, 2010, achieving a propylene purity of more than 99.69 wt%. Since then, the plant has been in smooth, stable operation. The production of propylene has been maximised through increased selectivity via reaction temperature optimisation. Ethylene is produced only in very small quantities, but enough to be able to produce valuable high-impact co-polymers based on propylene. No catalyst attrition has been observed. Regeneration of the catalyst is done in situ via an air/nitrogen mixture at about the same temperatures as the reaction, thus avoiding temperature imbalances during cycle changes. The carbon loss during coking is very low (<0.5 %). The cycle time is between 600 and 800 h. In comparison to the extensive laboratory tests (in total >60,000 h using essentially three pilot and one demonstration unit), the large-scale operation shows the same or even better results. The fixed-bed reactors are simple and easy to operate.

Commercial References

Today, Lurgi offers the MTP process on fully commercial terms. In 2005 and 2006, contracts were signed for two full-size MTP plants of 1,410 t/d propylene capacity in China. Both complexes are coal based and use third-party coal-gasification technology (Siemens GSP EF technology; see Fig. 6.84), Lurgi's licensed Rectisol syngas cleaning, Lurgi's MegaMethanol technology and Lurgi's MTP technology. In both plants, the produced propylene is converted into polypropylene by a third-party technology.

The Shenhua Ningxia Coal Industry (Shenhua Ningmei) Group started construction of their coal to propylene complex in April 2008. Mechanical completion was achieved in August 2010 and commissioning started in September 2010. The first propylene was produced in October 2010, which was the first propylene production at a world-scale MTP plant in commercial operation at that time. From the beginning of commercial operation, the operating experience was extremely satisfying because it was the first commercial MTP plant based on an upscaling factor of more than 6,900.

Fig. 6.84 Methanol-to-propylene plant at Shenhua Ningxia Coal Industry Site

No crucial issues appeared during start-up, which would have resulted in a substantial change of the plant concept. The six-stage MTP fixed-bed reactor design showed a stable and very reliable operating behaviour from the beginning. Ramp-up and fine-tuning of the MTP plant required some time, as expected for a first-of-its-kind plant. This was also influenced by the fact that upstream of the MTP plant a whole process chain, starting with coal gasification, went into commercial operation. Today, the plant is in smooth operation and produces on-spec propylene that is polymerised into polypropylene. The performance test run of the MTP plant was successfully executed in May 2012. All performance indicators have been achieved without any issues. All product description data, as listed in Table 6.19, were met or exceeded. As a result of this success story, Shenhua Ningxia Coal Industry Group has ordered a second MTP unit from Lurgi (Fig. 6.85).

In parallel to the coal-to-propylene complex for the Shenhua Ningxia Coal Industry Group, a second coal-to-propylene complex was built by Datang International Power Generation. The complex, which also uses third-party coal-gasification technology (Shell EF Gasification) and Lurgi's licensed Rectisol syngas cleaning, Lurgi's MegaMethanol technology and Lurgi's MTP technology, is producing propylene for the production of polypropylene. It represents the second MTP reference in commercial operation.

As of early 2013, five licenses have been sold worldwide. Currently, Lurgi (as an affiliate of Air Liquide global E&C Solutions) is involved in several further MTP projects with a total capacity of approximately 3,000,000 t/y. The projects, which are either in the study or project development phase, are based on gas, coal, and direct methanol feed.

Fig. 6.85 Shenhua Ningxia Coal Industry Group's coal-to-polypropylene complex (Ningdong, Province of Ningxia, China). See also Sect. 4.4.6. DME, dimethyl ether; MTP, methanol-to-propylene

Economy

With the implementation of Lurgi's MegaMethanol technology at the beginning of the twenty first century for single-train production of 5,000 t/d of methanol and more, methanol production costs have decreased significantly. The capability of low production price, the constant trend of increasing crude oil prices and increasing demand for high-value commodities such as propylene are some reasons why developments of methanol-based downstream technologies stepped into the focus of the petrochemical industry. Attention was also paid to the monetisation of stranded gas. Actual gas prices during the early twenty first century reached levels that forbade investments in gas conversion, which was incidentally one of the reasons why the first MTP plants are coal based.

Today, on a worldwide basis, the exploitation of large conventional and unconventional (shale gas in North America and Australia) natural gas reserves, coupled with the differential value between such reserves and benchmark crude oil, reflects the consideration of this feedstock for conversion to high-value petrochemical commodities. Using the specific example of the US Gulf Coast region, the increasing differential between natural gas and crude oil prices in the early twenty first century is illustrated in Fig. 6.86. This high differential is causing a variety of gas-based processes, including MTG and others, to be investigated for gasoline and chemical production in the USA.

Lurgi's MTP (or in a broader sense, gas-to-propylene [GTP]) process presents a simple, cost-effective and highly selective on-purpose propylene production technology. Both routes allow for the production of petrochemicals that then would be gas-based. In this section, the economics of a GTP complex are presented on the basis of an internal rate of return calculation. The GTP complex considers a syngas production section, a methanol synthesis for 5,000 t/d methanol production, MTP synthesis and relative off sites and utilities.

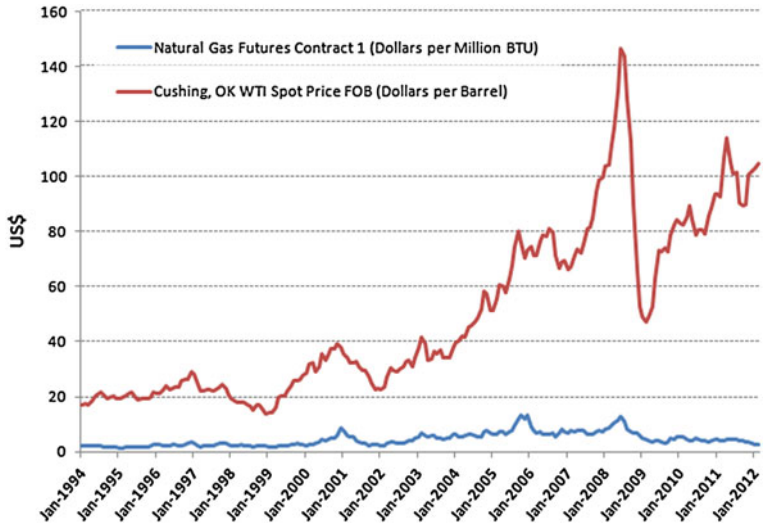

Fig. 6.86 Difference between natural gas and crude oil prices (US Gulf Coast Region)

The increasing attractiveness of the GTP technology stands in direct correlation with the increasing crude oil prices because MTP products are classic crude-based products, and product pricing is linked to crude oil economy. On the other hand, the attractiveness benefits from the feedstock costs. For GTP, the feedstock is natural gas, which remains at low and stable price levels.

Figure 6.87 presents the IRR of the GTP route as function of gas and crude oil pricing. It shows that the MTP technology stands for a stable feasibility already at

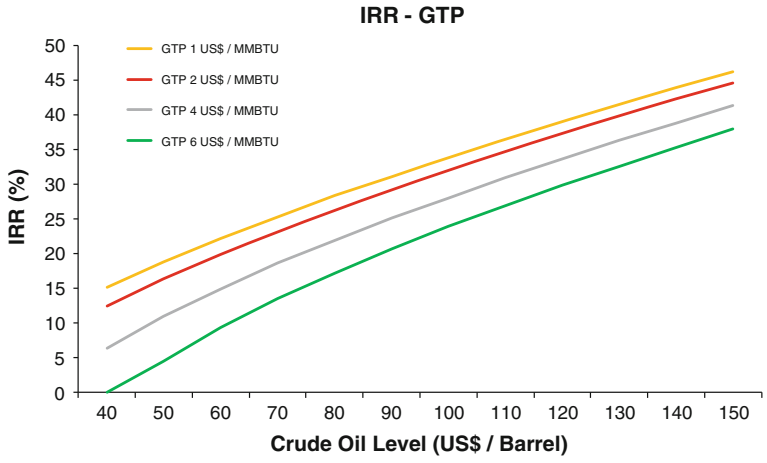

Fig. 6.87 IRR of a gas-to-propylene complex

low crude oil prices, taking up speed with increasing crude oil prices. As the spread between natural gas and crude oil prices increases, it contributes directly to the profit if the GTP route. Traditional propylene production technologies (Cracker, PDH) will not benefit from the spread because their feedstock cost and product prices rise with crude oil cost.

Another advantage of the GTP route is the robustness of the technology against fluctuations in feedstock cost. A doubling of natural gas price from 2 to 4 US$/MMBTU results in a IRR reduction in the range of approximately 3 % points, which is still very attractive, especially in today's crude oil price scenarios.

6.4.4 Other Methanol Derivatives

Friedrich Schmidt[1] and Ludolf Plass[2]

[1]*Angerbachstrasse 28, 83024 Rosenheim, Germany*
[2]*Parkstraße 11, 61476 Kronberg, Germany*

6.4.4.1 Introduction

The reactions of oxygenates (primarily alcohols and more specifically methanol) to hydrocarbons have enormous societal significance because these reactions involve two of the most important areas of modern industrial society—namely, to secure and broaden the resource base (1) for mobility and (2) for the production of polymers (aromatics, polyethylene and polypropylene for the production of consumer goods). In the early 1970s, researchers at Mobil Central Research discovered that methanol can be converted into higher hydrocarbons over the zeolite H-ZSM-5 [478–480]. These hydrocarbons consisted of a mixture of aromatic compounds, olefins and paraffins and delivered a gasoline of high quality.

Some reviews covered the MTHC topic from an academic viewpoint [481–483] and from a semi-technical viewpoint [480, 484]. A review by Stöcker covered the details of catalyst and reaction mechanisms of the MTHC processes, especially the methanol-to-gasoline (MTG), methanol-to-olefins (MTO) and Mobil's olefin-to-gasoline and distillate (MOGD) processes [485]. Keil presented a paper focusing on the technology of the MTG, MTO and MOGD processes but did not discuss those processes, which are presently operating commercially [484].

6.4.4.2 Dimethyl Ether

The Catalyst Group Resources [486] summarises the commercial situation for DME as follows:

In general, all companies that offer MegaMethanol technologies can modify their processes to produce DME instead. They will use the same reactor technology as they use for methanol production. All the current commercial plants use conventional methanol technology and then add a dehydration reaction to make DME. The only other plant design change is to modify the distillation sequence to recover DME instead of methanol.

JFE (formerly NKK) offers a direct DME process that uses a slurry phase reactor. The reactor technology was proven over a five year period in a 5 tpd pilot plant, starting in 1999, in Hokkaido, Japan. It was then proven in a 100 tpd plant, starting in 2002, at the same site. Toyo Engineering built the 110,000 tonnes per year (tpy) DME plant in Luzhou, China that started DME in the fuels market, and the 1,000,000 tpy plant in Inner Mongolia.

They used their own proprietary reactor technology for methanol dehydration. Air Products offers a process analogous to the liquid phase methanol synthesis process, LPMEOH, to make DME directly, and call it the Liquid Phase Dimethyl Ether Process (LPDME). Haldor-Topsøe provided the design basis for a 800,000 tpy DME plant in Assuluyah, Iran for Zagros Petrochemical Company—the first mega-scale DME project in the world. Startup has been delayed somewhat, originally projected for 2008. More recently, Haldor-Topsøe has been selected to supply DME technology for two plants in China [486].

DME has excellent diesel properties (cetane number 55–60, sulphur and aromatic content of zero) and thus represents a future alternative to conventional diesel fuel for mobile applications. DME is also regarded as an environmentally friendly alternative to diesel for power generation (MtPower [487]) because DME burns completely sootless. DME as fuel component reduces NO_x up to 90 %. The DME is completely free of sulphur. Due to the similarity of its physical properties with those of LPG, DME can easily add or replace LPG (especially for storage and transportation). For the concept of electricity with methanol and/or DME, methanol is produced using low-cost natural gas. The electricity is then carried out in places that have no gas supply pipelines or liquefied natural gas.

The synthesis of ethers with the aid of activated alumina as a catalyst has been known since 1928 through the work of Adkins and Perkins [488]. The promoting effect of using high-surface area γ-alumina for methanol dehydration has been widely studied and reported by many authors [489–494]. It is now well established that the activity of methanol dehydration is largely promoted by the number of free acidic sites. These sites are directly proportional to the specific surface area of the γ-alumina catalyst. The dehydration of methanol is a strongly exothermic reaction [495].

DME is one of the most promising diesel and LPG substitutes and has gained huge interest in research and industry [496]. In comparison to common fuels, the combustion of DME is soot-free and hardly emits any harmful particles [497]. DME can be produced by either dehydrating methanol over an acid catalyst (MT-DME) or in a single-step process from synthesis gas (syngas-to-dimethyl ether—STD) [498].

Currently, there are several licensors that offer technology for the production of DME based on a two-step process, including Haldor Topsøe, Lurgi, Mitsubishi Gas Chemical, Toyo Engineering Corporation and Uhde [499]. The existing DME plants in the world are based on the conventional methanol route; in most cases, their capacity is only of the order of 10–20 kt per year capacity. (Topsøe has supplied DME catalysts and technology for a number of plants in China, with capacities up to 400,000 tonnes per year.)

The conventional DME plants are producing DME for chemical use, such as solvents and spray propellant for cosmetics. Due to the limited size of these markets, the price of DME could stay at a very high level. However, if the objective is to produce DME for fuel market, the price of DME must be competitive in the existing fuels market. For this market, the size of a single DME plant should be at least 1–2 million tonnes/year capacity, which requires scale-up to a larger plant that is more than 100 times the size of existing conventional plants [500].

Direct DME Synthesis Reactions

Methanol synthesis is an equilibrium-restricted reaction. When the dehydration reaction takes place simultaneously, the syngas conversion rises dramatically. Figure 6.88 shows stoichiometric equilibrium syngas conversion of DME synthesis (a) and (b) at 5 MPa, and methanol synthesis (c) at 5 and 9 MPa. DME synthesis reaction (a) gives much higher syngas conversion in all temperature conditions than reaction (b).

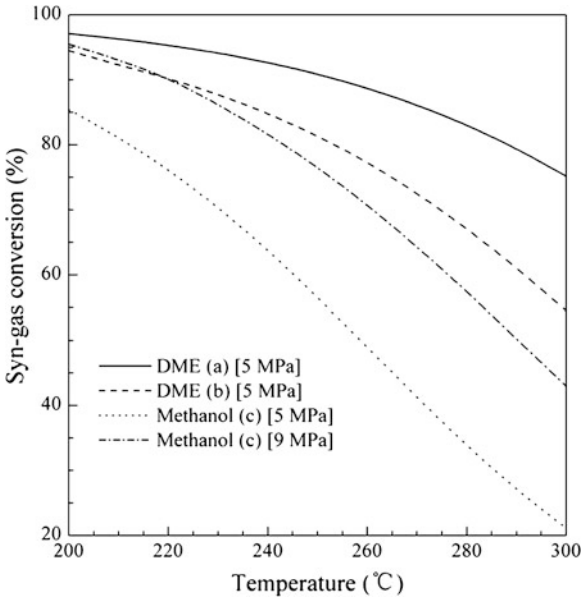

Fig. 6.88 Stoichiometric equilibrium conversion of dimethyl ether (DME) and methanol synthesis [501]

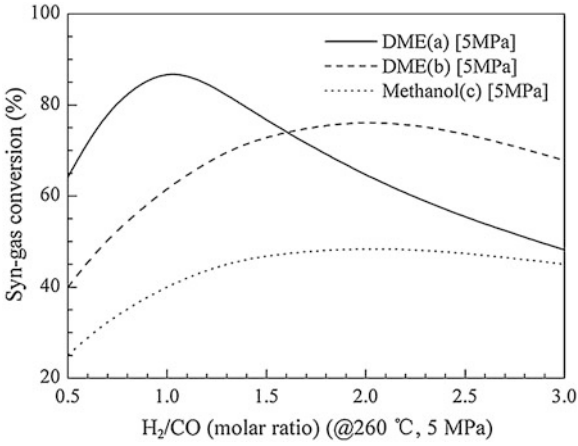

Fig. 6.89 Equilibrium conversion of synthesis gas versus H_2/CO ratio [501]. DME, dimethyl ether

Figure 6.89 shows syngas conversions of the two overall DME syntheses, (a) and (b), and the methanol synthesis (c), as a function of H_2/CO ratio of syngas. In each reaction, the equilibrium conversion reaches its maximum point when the H_2/CO ratio is equal to its stoichiometric number, which is 1.0 for (a) and 2.0 for both (b) and (c). The maximum equilibrium conversion of (a) is higher than (b) by more than 10 %.

MT-DME Two-Step Technology

The Production Process

To achieve an economic price, the production of DME needs to be on megascale. Traditionally, DME was a byproduct of high-pressure methanol synthesis. Since the development of the low-pressure methanol synthesis process, DME is produced from methanol by dehydration in the presence of a suitable catalyst. This process is carried out in fixed-bed reactors. The product is cooled and distilled to pure DME (Fig. 6.90).

A modification of the conventional methanol synthesis process would enable the production of DME in the methanol synthesis loop as a byproduct in higher yields (two-step process, below). This pathway, however, has two major drawbacks. During the dehydration of methanol, the water vapour content increases and thus reinforces the water–gas shift reaction. Through the conversion of CO to CO_2, the quality of the synthesis gas declines. The rate of the reaction of CO_2 and H_2 is slower than the rate of the reaction of CO and H_2. In order to compensate for this drawback, the volume of the synthesis catalyst and the circulating volume need to be increased. A further drawback is the low boiling point of DME, which requires a cryogenic separation of DME [502].

In the case of a combination of a DME unit with a MegaMethanol system, the methanol three-column distillation unit can be reduced to a single column, with corresponding savings. In the Lurgi DME process (MT-DME, methanol-to-DME,

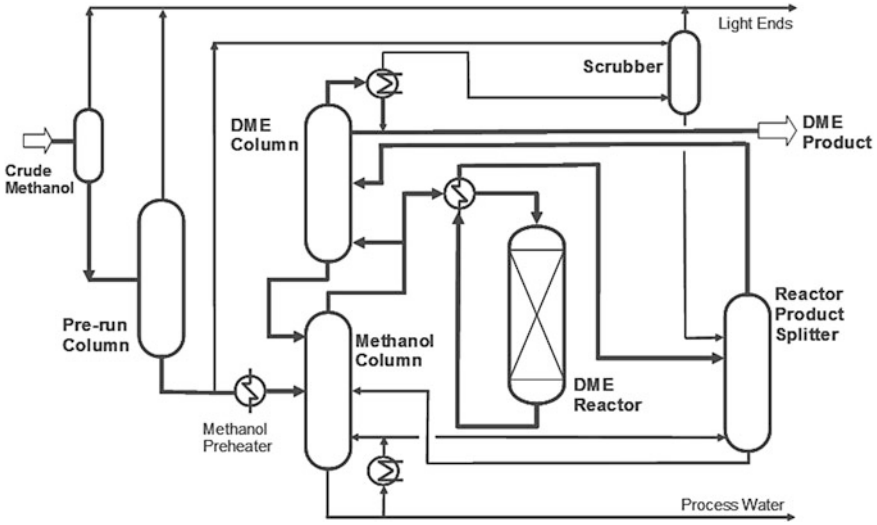

Fig. 6.90 Dehydrating methanol over an acid catalyst (MT-DME). DME, dimethyl ether

MTD, or MegaDME), all types and qualities of DME can be produced. The different requirements for fuels or to generate electricity (MtPower) or for DME as chemical can be achieved by varying the size and the design of the DME distillation columns.

Economic Evaluation

The economics of the Lurgi DME process are summarised in Table 6.20 [503].

The following assumptions were made:

- Natural gas consumption and product value are normalised to an equivalent of methanol (capacity: 7,500 t/d methanol).
- The DME product quality meets the specifications.
- The natural gas consumption figures include the energy required for an air separation plant and a power generation unit.

Table 6.20 Economy of dehydrating methanol over an acid catalyst (MT-DME)

Characteristics and costs	MegaMethanol and dehydration
DME capacity (t/d)	5,000
Specific MMBtu/$t_{Methanol}$	28.5
Consumption of natural gas (MMBtu/t_{DME})	40.2
Total fixed costs for EPC (US$)	415 million
DME production cost (US$/$t_{DME}$)	93

DME, dimethyl ether; EPC, engineering, procurement and construction

- The total fixed costs include an air separation unit, a power generation unit and the other components.
- The price of natural gas was assumed to be 0.50 US$/MMBtu.
- The depreciation of 10 % of the total fixed cost was recognised.
- The return on investment of 20 % of total fixed cost was fixed.
- Operating costs for operating personnel, plant overhead, upkeep/maintenance, and materials are included.

The budgeted costs are given with an accuracy of ±20 %. Specific location factors are not included in these figures.

When it is produced in large quantities, DME (as traditional methanol derivative) is therefore a promising complement to existing diesel fuel, LPG, electricity generation and also olefin production. The production of DME by dehydration of methanol is an economic way [495].

DME Direct from Syngas Competing with the Methanol Route

STD Direct Synthesis Route (Typical)

The production of DME from synthesis gas (STD) [504] is reported to be favourable if a biomass-derived synthesis gas is applied that is carbon monoxide-rich with typical H_2/CO-ratios of approximately 1 or lower. The STD process requires catalyst systems that comprise highly active sites for methanol synthesis and acid sites for methanol dehydration. The water–gas shift reaction is the third simultaneously proceeding reaction in the STD process. All three reactions are described in Table 6.21.

Table 6.21 Direct syngas-to-dimethyl ether (STD) reactions

	Reaction			Reaction heat in kJ/mol
MeOH	$CO + 2H_2$	$\rightleftharpoons$	CH_3OH	90.3
MeOH dehydration	$2CH_3OH$	$\rightleftharpoons$	$CH_3OCH_3 + H_2O$	23.4
Shift	$CO + H_2O$	$\rightleftharpoons$	$CO_2 + H_2$	40.9
Overall	$3CO + 3H_2$	$\rightleftharpoons$	$CH_3OCH_3 + CO_2$	245.7

Catalyst systems for the direct synthesis of DME are usually mechanically mixed systems containing a copper-based methanol catalyst ($CuO/ZnO/Al_2O_3$, CZA) and a solid acid, such as zeolites or γ-Al_2O_3. Recently, the preparation of bifunctional catalysts that combine both types of active sites in one compound have been prepared and investigated [505].

Ahmad et al. reported the synthesis of alumina- and zeolite-based bifunctional catalysts with various copper and zinc oxide loadings using different preparation methods, such as co-precipitation, impregnation, sol–gel, or hydrothermal processes. These catalyst systems yielded the same conversion and selectivity as an admixed reference system containing a commercially available CZA catalyst and γ-Al_2O_3 [506].

Toyo Jumbo DME

For the Toyo JFE Pilot Plant in Japan (100 t/d), no commercial performance experience has been reported [504].

Topsøe DME from Synthesis Gas

Haldor Topsøe developed a one-step process technology for large-scale production of DME via direct synthesis from natural gas, without having to first produce and purify methanol. An illustration is given in Fig. 6.91.

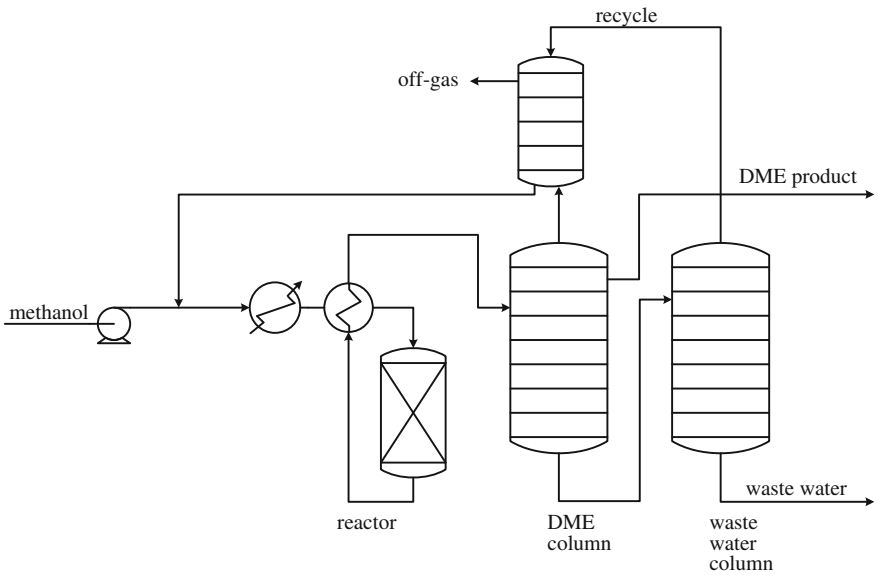

Fig. 6.91 Topsøe dimethyl ether (DME) Plant

6.4.4.3 Methanol-to-Aromatics

Methanol can be also used as synthesis feedstock for aromatics: "methanol-to-aromatics" or "Conversion of Methanol to Aromatics". The conversion of methanol to aromatics over H-ZSM-5 or H-gallosilicate (H-GaMFI) zeolite, with different Si/Ga ratios and degrees of H^+ exchange, which is calcined at different temperatures (600–1,100 °C), and pretreated hydrothermally at different temperatures and partial pressures of steam at 400 °C.

Clariant (formerly Süd-Chemie AG) offers the commercially proven catalysts for this process. The aromatisation activity and product distribution in the methanol-to-aromatics conversion are found to be influenced strongly by the above zeolite factors and calcination/pretreatment parameters. The aromatisation activity

of the zeolite shows a close relationship with its strong acidity (measured in terms of pyridine chemisorbed at 400 °C). H-GaMFI and H-ZSM-5 zeolites (having almost the same Si/(Ga + Al) ratio and degree of H^+ exchange and pretreated under similar conditions) and H-GaMFI show much higher aromatisation activity.

Applying advantageous conditions, high selectivity toward the desired aromatic product can be obtained. An example for this is the synthesis of *p*-xylene. It can be produced in great excess of the thermodynamic equilibrium distribution by using large H-ZSM-5 crystals and reaction parameters that reduce the degree of reactions taking place at the outer zeolite surface [507]. Under certain laboratory conditions, metal-doped ZSM-5 zeolites with Ag, Ni and Cu also show a higher selectivity to aromatics compared to unmodified ZSM-5 [508, 509]. Clariant (formerly Süd-Chemie AG) offers the commercial proven catalysts for this purpose.

Competition is represented by a process developed by BP, now licensed by UOP. Light alkane aromatisation over zeolite-based catalysts is well known [510–512]. The BP Cyclar process converts LPG directly into a liquid, aromatic product in a single processing step. The Cyclar process provides a route to upgrade low-value propane and butane, recovered from gas fields or petroleum refining operations, into a high-value, liquid aromatic concentrate that is ideal as feedstock in an aromatics complex.

The activity of Ga/ZSM-5 is consistently high (>95 % conversion) over the temperature range of 300–460 °C. The Ga-modified zeolite produced predominantly benzene, toluene and the xylenes and other heavier aromatics [513]. This difference in product distribution is consistent with the short-chain alkanes formed within the internal pore structure of the zeolite being intermediates in a Cyclar-type aromatisation mechanism. UOP also offers the commercially proven catalysts for this process. For converting paraffins to aromatics (CPA), Clariant (formerly Süd-Chemie AG) offers the commercial proven CPA-1 catalyst, which is a Ga-free H-ZSM-5.

6.4.4.4 Methanol-Derived Poly(oxymethylene) Dialkyl Ethers

Poly(oxymethylene) dialkyl ethers (also named polyethyleneglycol dialkyl ethers), particularly poly(oxymethylene) dimethyl ethers (POMDMEs), may serve as components of tailored diesel fuel [514].

The fuel blend comprises (1) fuel oil and (2) polyoxymethylene dialkyl ethers of the general formula R-O-$(CH_2O)_n$-R′, with the following meanings for R, R′ and n:

- R: methyl, ethyl, propyl, butyl, preferably methyl, ethyl, more preferably methyl,
- R′: methyl, ethyl, propyl, butyl, preferably methyl, ethyl, particularly preferably methyl,
- n: 2, 3, 4, 5, 6, 7, 8.

The oligomer POMDMEs of the general structure CH_3-O-$(CH_2$-$O)_n$-CH_3 open a new route for tailoring diesel fuels. POMDMEs belong to the group of oxygenates that reduce soot formation in the combustion when added to diesel fuels. POMDMEs can be produced on a large scale based on methanol.

POMDME produced from synthesis gas-based methanol results in an increase in the cetane number when added to diesel fuel, as well as in a clean burning of the diesel fuel, causing a reduced soot formation. The gas can come from geological sources, preferably those that are designated as "flared gas" or "stranded gas" or from those sources that are obtained as a byproduct of oil production. The methanol can also be equally of biological origin derived from biomass.

Hagen et al. reported on the preparation of POMDMEs by catalytic conversion of methanol-based DME with formaldehyde formed by oxidation of methanol [515]. In general, after the feedstream is passed over the catalyst, it will contain a mixture of organic oxygenates—at least one of which is of higher molecular weight than the starting DME. Effluent mixtures can be water, methanol, formaldehyde, DME, methylal and other POMDMEs having a structure represented by $CH_3O(CH_2O)_nCH_3$, in which n is a number ranging between 2 to approximately 7. Conditions of reaction include temperatures in a range from approximately 150–250 °C.

The stoichiometry of this condensation may be expressed by the following equations:

$$CH_3OCH_3 + n\ CH_2O \rightarrow CH_3O(CH_2O)_nCH_3 \tag{6.13}$$

$$2CH_3OH + m\ CH_2O \rightarrow CH_3O(CH_2O)_mCH_3 + H_2O \tag{6.14}$$

which may be combined as in the following equation when n is equal to m;

$$CH_3OCH_3 + 2CH_3OH + 2n\ CH_2O \rightarrow 2CH_3O(CH_2O)_nCH_3 + H_2O \tag{6.15}$$

As shown, the synthesis of methylal and higher POMDMEs from DME, methanol and formaldehyde is a reversible reaction that yields water as a co-product. Under certain conditions, at least a portion of the water may be consumed in a dehydrogenation reaction expressed by the following equations:

$$CH_3OCH_3 + CH_3OH + H_2O \rightarrow 3CH_2O + 3H_2 \tag{6.16}$$

and

$$CH_3OCH_3 + H_2O \rightarrow 2CH_3OH \tag{6.17}$$

Suitable DME sources may contain other oxygen-containing compounds, such as alkanol and/or water—preferably not more than approximately 15 % methanol and/or water by weight.

The ratio of formaldehyde to DME is between approximately 2:1 and 1:2 mol. Preferred temperatures are approximately 115–125 °C. Preferred pressures are approximately 15–25 bar. The reaction mixture feed gas flow rate, expressed as gas hourly space velocity, can be approximately 100–2,000 h^{-1}. Unconverted DME can be recovered from the mixture by well-known methods, including the use of distillation of the condensed product. The catalyst system is preferably a

crystalline borosilicate molecular sieve [515]. This type of process replaced the older, less benign and more expensive productions of polyethylene glycol dialkyl ethers, which are summarised by Arpe [516].

It has been known that POMDMEs can be prepared starting from methanol and paraformaldehyde at high temperatures. In the Dupont patent US 2,449,469, the polyformals are prepared starting from paraformaldehyde and dialkyl with sulphuric acid as the catalyst (acid concentrations of about 0.1–2 % by weight) [517–519].

> "A mixture of alkoxy-terminated poly-oxymethylenes, having a varied mixture of molecular weights, is blended with diesel fuel to form an improved fuel for autoignition engines. The base diesel fuel, when blended with the mixed alkoxy-terminated poly-oxymethylenes in a volume ratio of from about 2 to about 5 parts diesel fuel to 1 part mixed alkoxy-terminated poly-oxymethylenes, provides a higher quality fuel having significantly improved lubricity and reduced smoke formation, without degradation of the cetane number or smoke formation characteristics when compared with the base diesel fuel." From [520]

Such fuel blends on diesel base are described in US patient 5,746,785, WO 86/10351 and EP-A 1070755 [521]. Advantages of these blends are (1) a reduction of soot formation just for "heavy" diesel engines, which generally cannot be provided without loss of performance with particulate filters; (2) the preferred blends, due to their composition and their benefits, reduced freezing in storage, handling use and transport at low temperatures; and (3) an optimisation of the flash point.

Particularly preferred are polyoxymethylene with three or four oxymethylene units and mixtures thereof, especially tetra-oxymethylendimethylether ($n = 4$). The blending component contains a weight fraction of $H_3C–O–(CH_2O) \geq 4\text{-}CH_3$.

The BASF process for preparing POMDMEs, in particular of polyoxymethylene with $n = 3$ and 4 (trimer, tetramer) uses methylal ($n = 1$) or DME and trioxane. These components are preferably fed into a reactor and reacted in the presence of an acid catalyst, whereby the volume of water introduced into the reaction mixture of methylal/trioxane is less than 1 wt% of the reaction mixture. During the conversion of methylal with trioxane to polyoxymethylene, no water is formed as a byproduct. The reaction is generally conducted at a temperature of 90–150 °C and a pressure of 2–10 bar. The molar ratio of methylal to trioxane is generally from 0.5 to 5.

According to the BASF patent, the addition of 5 vol% tetraethylene to a diesel fuel reduced particulate emissions of a single-cylinder diesel engine up to 70 % at constant NO_x emission (according to EN 590), depending on the operating point. The reduction of the heating value of the fuel by the addition of tetraethylene is as low as 1.6 %. The oxygen content of the mixture is about 1.8 %. Polyethylene glycol dialkyl has good solvent properties. Therefore, necessary materials such as elastomers and plastics, as well as coatings that come into contact with polyethylene glycol dialkyl ethers, should be selected carefully [522].

The corresponding flash point of the mixture was measured according to DIN EN ISO 13 [736], and was 61 °C. The corresponding mixture had filterability (EN 116) of less than 54 °C. The cloud point (according to EN 23015) was −53 °C. The cetane number of the mixture was not determined in a MWM test engine. From the measurement of mixtures with 30/50/70 % kerosene, however, a borderline cetane number of 98.6 could be determined. The blends were prepared on a

static mixing system. A blend of glycol DME mixture (10 %) with diesel fuel (90 %) was prepared and tested in a DaimlerChrysler OM646 DE 22La engine in a dynamometer test. The result was a reduction of the soot emission compared to the operation of pure diesel fuel of up to 60 %.

MAN reported similar results [523]. A single-cylinder research engine had a capacity of 1.75 L, an engine power of 55 kW, a common rail injection system (rail pressure: 1,800 bar), a compression ratio of 20.5, and a start of injection before top of −8 °C a crank angle and an exhaust gas recirculation rate of 20 %. In this engine, a fuel mixture was tested consisting of 95 vol% diesel fuel according to EN 590 and 5 vol% oxymethylen-(dimethylglycol)ether (also known as bis(2-methoxyethoxy)methane; $C_7H_{16}O_4$; boiling point 197/205 °C; Alfa Aesar, Karlsruhe, Germany). For comparison, a diesel fuel without additive additions according to EN 590 was tested.

Diesel Fuel News reported on Snamprogetti's research results, referencing "cheap diesel fuel 'poly-oxy-methylenes'" that could cost less than ordinary diesel fuel, because it is basically a reaction of methanol with formaldehyde. Both of these products are considered to be relatively inexpensive feedstocks, especially if they are produced from low-cost remote gas [524]. According to Snamprogetti's preliminary process cost analysis on the basis of the year 2001, the oxy-diesel product could be produced at about US$130/tonne with gas feed at 50 cents/million BTU, or US$150/tonne with gas at US$1/MmBTU—cheaper than ordinary diesel fuel, even when crude trades around US$23/barrel. Snamprogetti's proposed process would use a cationic resin catalyst operating at 90–100 °C, with greater than 98 % product selectivity and greater than 95 % formaldehyde conversion. Catalyst life tests have not shown deactivation problems. Furthermore, the blend would not cause any product quality or environmental/health problems.

Snamprogretti's oxy-diesel was described as a "proprietary tailored mixture produced via proprietary process" with "3-6 [CH_2]-O units, no C–C bonds, high oxygen percentage and high cetane number." Although the product has fewer BTUs per gallon than diesel fuel, fuel consumption is "almost unchanged" at blend volume levels of 5–10 %. At the 10 % level, fuel oxygenate content is 4.5 wt%.

After synthesis of hundreds of litres for product testing, tests of the fuel properties showed a cetane number of 80–100. Blended diesel flash point was not affected and good cold-flow properties were realised. In vehicle tests on a modern Alfa-Romeo 156 1.9 TDI with common-rail injection, a 10 % blend of the oxy-diesel with 90 % baseline diesel (30 ppm sulphur) cut particulate matter emission by 15–20 %, carbon monoxide/hydrocarbon by 5–10 % and left nitrogen oxides almost unchanged. Only the best Euro diesel fuels (such as Swedish Class 1) were found to match the performance of the oxy/diesel blend, as reported by the company [525].

The oxy component biodegradability is similar to diesel fuel and 10 times more degradable than MTBE. A preliminary investigation on toxicology did not indicate any negative information. In addition, the product does not have any foul odour, which is a major advantage over many other fuel oxygenates. Still, social

acceptance research is not complete, as "toxicology, biodegradability, and all other health/safety/environmental impacts are to be severely checked" prior to any commercialisation effort.

The Snamprogetti polyoxymethylene product does not seem to have the market-killing volatility problems of DME and DMM, the huge cost (and taxpayer subsidy problems) of biodiesel, the flashpoint problems of ethanol–diesel and the water-pollution/odour problems that are typical of ether oxygenates.

6.5 Other Methanol Utilisation Technologies

6.5.1 Methanol Splitting and Reforming for Hydrogen-Rich Gases

Jürgen Roes[1], Michael Steffen[2] and Hans Jürgen Wernicke[3]

[1]*Institute of Energy and Environmental Process Engineering, University of Duisburg-Essen, Lotharstraße 1, 47048 Duisburg, Germany*

[2]*The fuel cell research centre ZBT GmbH, Carl-Benz Straße 201, 47057 Duisburg, Germany*

[3]*Kardinal–Wendel-Straße 75 a, 82515 Wolfratshausen, Germany*

Introduction

Methanol has many advantages as an energy carrier for mobile, portable and off-grid applications [526]. Compared to hydrogen stored as gas, liquid, or hydride, methanol requires a far lower volume for the same energy content. Methanol can easily be transported and stored on site; hence, compared to natural gas or LPG, it is an attractive hydrogen and energy carrier for decentralised supply.

in comparison to other alcohols and hydrocarbons, generating hydrogen or synthesis gas methanol is attractive, not only because of its low reforming temperature but because of the low steam-to-carbon (S/C) ratio that is required, its good solubility in water, and the usually very low sulphur content. Methanol is the only alcohol or hydrocarbon that can be reformed at temperatures as low as 180–300 °C to convert it into a hydrogen-rich gas mixture. The basic physical data of methanol are summarised in Sect. 5.1. Its toxicity and procedures for safe handling and transport are discussed in Sects. 5.2 and 5.3.

Methanol Production

Methanol is produced on an industrial scale from synthesis gas containing hydrogen, carbon monoxide and carbon dioxide and is based on fossil and regenerative raw materials (see Chap. 4). Methanol is used as feedstock for numerous synthesis reactions, such as to produce acetic acid, formaldehyde, or ethanol (see Sect. 6.2) or as a component in fuels (see Sects. 6.3 and 6.4). Conversely, methanol can be

decomposed into its starting products hydrogen, CO, and CO_2 by means of "dry" splitting or "wet" reforming in the presence of steam. This process is being used for specific purposes of hydrogen generation on a smaller scale or for generation of special gas mixtures, mainly for materials treatment.

Thermodynamics of Methanol Splitting and Reforming

When methanol is used to produce a synthesis gas containing carbon monoxide and hydrogen, the simplest process is the splitting of methanol (Eq. 6.18):

$$CH_3OH \rightarrow 2H_2 + CO \quad \Delta_R H^{\emptyset} = 128\ \text{kJ/mol} \tag{6.18}$$

Other possibilities are the partial exothermic oxidation into hydrogen and CO_2 (Eq. 6.19):

$$CH_3OH + 0,5O_2 \rightarrow 2\,H_2 + CO_2 \quad \Delta_R H^{\emptyset} = -155\ \text{kJ/mol} \tag{6.19}$$

In the presence of steam, methanol reforming, which is less endothermic than methanol splitting (as shown in Eq. 6.18) leads to maximum hydrogen output (Eq. 6.20):

$$CH_3OH + H_2O \rightarrow CO_2 + 3H_2 \quad \Delta_R H^{\emptyset} = 49\ \text{kJ/mol} \tag{6.20}$$

The combination of partial oxidation and steam reforming allows maximising hydrogen yield under autothermal conditions (Eq. 6.21):

$$2CH_3OH + H_2O + 0,5O_2 \rightarrow 5H_2 + 2CO_2 \quad \Delta_R H^{\emptyset} = \pm 0\ \text{kJ/mol} \tag{6.21}$$

The method that is most often applied in practice to produce a hydrogen-rich synthesis gas from methanol is the steam-reforming process (Eq. 6.20). Depending on process conditions and desired application of the product gas, it will lead to a mixture of hydrogen, carbon monoxide and carbon dioxide. The reaction usually takes place at 180–350 °C and is accelerated by catalysts typically based on copper/zinc or precious metals. The steam-reforming reactions are expressed as a series of reactions [527, 528]: first, the endothermic decomposition of methanol (Eq. 6.18) followed by the slightly exothermic water–gas shift reaction

$$CO + H_2O \rightleftharpoons CO_2 + H_2 \quad \Delta_R H^{\emptyset} = -41\ \text{kJ/mol} \tag{6.22}$$

To reach a high degree of conversion and high catalyst activities, high reaction temperatures are preferable. Figure 6.92 shows the composition of the product gas (on a dry basis) at thermodynamic equilibrium as a function of the temperature at a pressure of 0.5 MPa and an S/C ratio of 1.5 [529].

As temperatures increase, the equilibrium shifts towards higher carbon monoxide contents in the product gas (Fig. 6.93). The influence of temperature and S/C ratios on the equilibrium concentration of carbon monoxide is shown elsewhere.

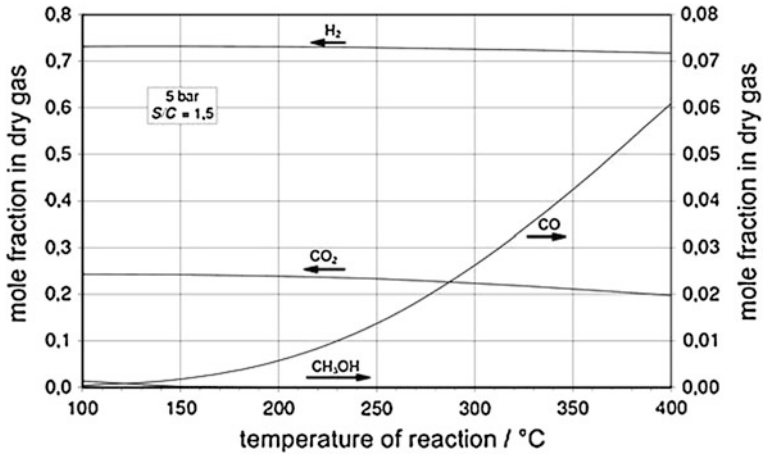

Fig. 6.92 Product gas composition in thermodynamic equilibrium for methanol steam reforming as a function of reaction temperature [529] S/C: steam-to-carbon ratio

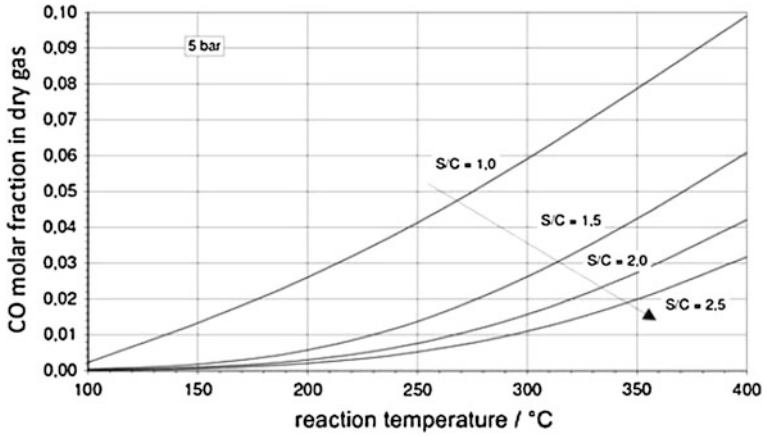

Fig. 6.93 Carbon monoxide fraction in the dry product gas in thermodynamic equilibrium for methanol steam reforming at 5 bar [529]

An increase of the S/C ratio increases the hydrogen yield and decreases the carbon monoxide yield in the product gas due to an increased CO conversion by the water–gas shift reaction. The correlation of the composition of the dry product gas as a function of the S/C ratio in the feed is shown in Fig. 6.94.

From the equilibrium calculations as shown in Figs. 6.92, 6.93, 6.94, optimal conditions for temperature and (costly) steam addition are in the range of 200–300 °C and S/C ratios are in the range of 1.1–1.5.

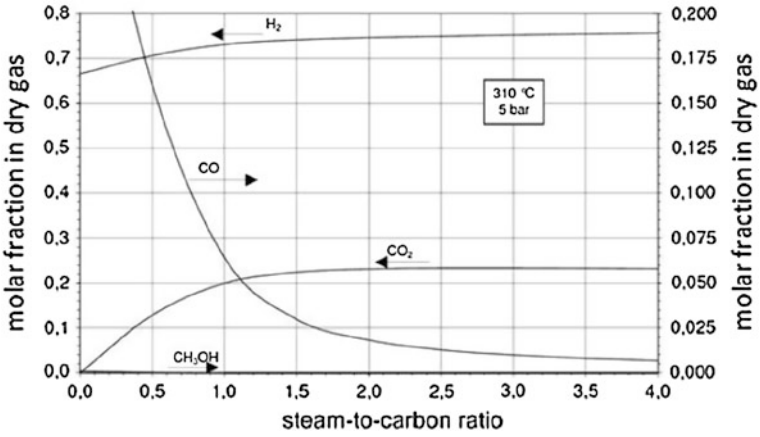

Fig. 6.94 Product gas composition in thermodynamic equilibrium for methanol steam reforming at 310 °C and 5 bar [529]

Reaction Mechanism of Methanol Steam Reforming

In addition to the desired reforming reaction of methanol, side reactions such as methanisation of products CO and CO_2 are possible (Eq. 6.23 and 6.24):

$$CO + 3H_2 \rightarrow CH_4 + H_2O \quad \Delta_R H^{\emptyset} = -206.1\,\text{kJ/mol} \tag{6.23}$$

$$CO_2 + 4H_2 \rightarrow CH_4 + 2H_2O \quad \Delta_R H^{\emptyset} = -164.94\,\text{kJ/mol} \tag{6.24}$$

Another side reaction is the formation of carbon by the Boudouard reaction (Eq. 6.25):

$$2CO \rightleftharpoons CO_2 + C \quad \Delta_R H^{\emptyset} = -172.45\,\text{kJ/mol} \tag{6.25}$$

Deposition of carbon on the catalyst results in a reduction of its activity as the carbon occupies the active sites of the catalyst and is blocking the catalyst pores [527, 530]. It will also contribute to an increased pressure drop of the reactor system. The formation of carbon by the Boudouard reaction is favoured by low reaction temperatures, high total pressures and low S/C ratios. Thermodynamic calculations were performed by Formanski [529] in order to determine the regime of potential carbon formation.

Two different models were considered, which differ in the consideration of methane as a product. Although model 1 (H_2, CO, CO_2, C(s)) disregards methane, model 2 (H_2, CO, CO_2, CH_4, C(s)) allows the formation of methane in the reaction mechanism. The equilibrium of the reactions for both models is iteratively calculated using mass balance and equilibrium approaches. For the calculation, pressures of 0.01, 0.1 and 1 MPa were assumed and the reaction temperature was varied between 300 and 800 K (27–527 °C).

Figure 6.95 illustrates the thermodynamic calculations under these conditions, which result in areas with and without potential carbon formation. For model 1 (methane formation disregarded), a temperature over 530 K (260 °C) would be necessary in order to prevent carbon deposition at S/C ratios above 1.3. For model 2 (methane formation included) and S/C ratios above 1.3, reaction temperatures above 450 K (177 °C) are sufficient to be outside the regime of potential carbon formation.

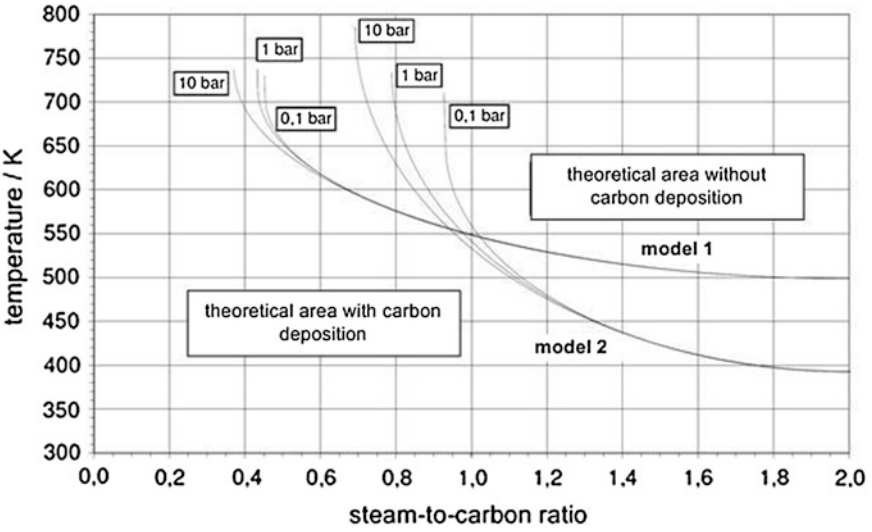

Fig. 6.95 Limiting conditions for the deposition of solid carbon for steam reforming of methanol [529]

Figure 6.96 shows the principal pathways of methanol steam reforming, including the formation of byproduct methane [527]. If the methane formation can be suppressed by a sufficiently selective catalyst, it results in a simplified reaction scheme, as shown in Fig. 6.97 [527]. Typical catalysts that minimise methanisation are copper/zinc catalysts, which are also applied for the water–gas shift conversion of carbon monoxide and for methanol synthesis. In this way, methanol reforming can simply be described as a combination of methanol decomposition (reverse synthesis) and water–gas shift reaction [527]. In addition to copper/zinc catalysts, chromium and iron-containing copper catalysts are more temperature stable. Mechanistic studies of the assumed combination of methanol decomposition followed by the water–gas shift reaction are contained in various sources [527, 528, 531].

If the reaction temperature is increased or the space velocity through the catalyst bed is increased, the concentration of carbon monoxide in the product gas is somewhat below the thermodynamic equilibrium, which can be seen in Fig. 6.98 [532].

The various effects of higher catalyst space velocities on the product yields, the approach to equilibria and the underlying potential reaction mechanisms are

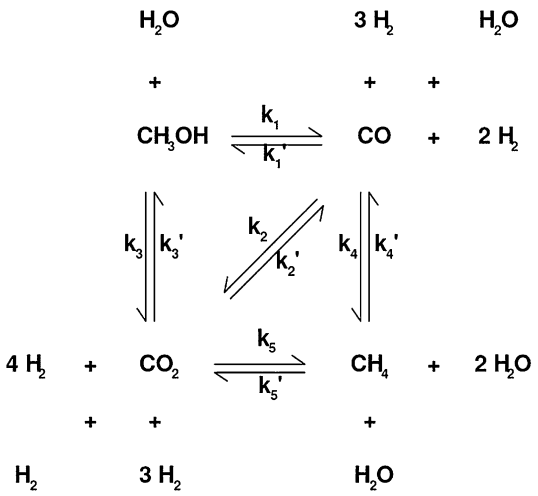

Fig. 6.96 General reaction scheme of methanol steam reforming [527]

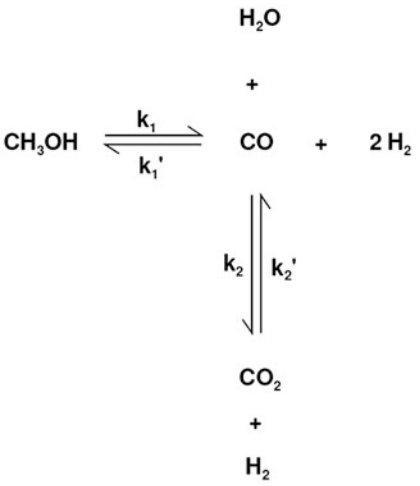

Fig. 6.97 Simplified reaction scheme of methanol steam reforming [527]

described in various sources [527, 533, 534]. Generally, nonnoble catalysts based on promoted CuO/ZnO are used for the steam reforming of methanol. The composition of these catalysts is very similar to catalysts used for the low-temperature water–gas shift reactions. CuO/ZnO catalysts are only used in a moderate temperature region because they tend to sinter on higher temperatures. They are pyrophorous in their active (reduced) form. They are also sensitive to entrained liquid water or condensing steam, as well as to poisons such as sulphur or chlorine compounds and nonsaturated hydrocarbons.

Noble metal-based catalysts that are used for methanol reforming (mostly promoted palladium or platinum on alumina carriers) are more robust by means of handling. Driven by mobile applications and small power generators based on

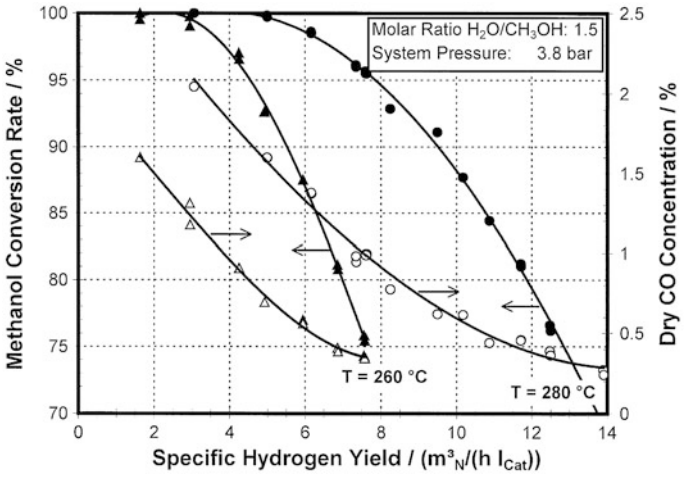

Fig. 6.98 Methanol conversion and carbon monoxide fraction as a function of catalyst load [532]

methanol fuel cells, more active noble metal catalysts have been developed, which are impregnated on wash-coated, low-pressure drop ceramic or metal substrates.

Methanol Decomposition in Absence of Steam

One option to produce hydrogen (and CO) is the endothermal splitting of methanol, carried out thermally or in presence of catalysts. The resulting reducing gas is used for protection of materials against oxidation or (with the presence of CO) for special heat treatments. Thermal decomposition is performed by injecting a mixture of nitrogen and methanol directly into the heat treatment furnace at temperatures over 750 °C. At these temperatures, methanol predominantly splits into carbon monoxide and hydrogen [538]. At temperatures below 640 °C, the methanol decomposition is thermodynamically favoured; exothermic side reactions lead to H_2O, CO_2 and CH_4.

The composition of the gas from methanol splitting (i.e., its carbon content) can be flexibly adjusted by varying the inlet feed methanol-to-nitrogen ratio as needed for the respective application. For the carburisation of materials, an inlet feed that has a high methanol-to-nitrogen ratio will be used. For the purpose of normalising, bright annealing, or sintering, a treatment gas richer in nitrogen is used. Sometimes, other gases are co-fed, such as propane or natural gas, to control carbon content or ammonia for nitriding. Companies offering such treatment systems are named in various sources [535–537].

To significantly reduce the operation temperature, the methanol splitting can be done with the use of catalysts, which are selective to generate CO and hydrogen and avoid undesired side reactions such as methanisation. Common catalysts for this “dry catalytic reforming” are based on promoted copper/zinc, which are also used for methanol synthesis or on precious metal, usually platinum or palladium

on a carrier [538]. In mobile applications, on-board methanol decomposition has been investigated to produce a CO/hydrogen fuel for internal-combustion engines or (with the addition of a water–gas shift reactor) to produce pure hydrogen for fuel cells [539, 540]. Methanol-based fuel cells are comprehensively described in Sect. 6.5.1.

Methanol Reforming with Steam

For hydrogen maximisation from methanol, reforming in the presence of steam is preferred. Although natural gas as a feedstock for hydrogen generation would be cheaper (also in smaller hydrogen plants), methanol steam reformers benefit from significantly lower investment costs due to the considerably lower reforming temperatures and a simpler process flow sheet. Using methanol avoids feed conditioning (sulphur removal) and high or low temperature shift conversion, which overall saves 20–30 % investment costs. Typical capacities for methanol steam reformer plants range from 50 to 3,000 Nm^3/h hydrogen.

The main feed streams for the process are methanol and demineralised water, which are premixed in a mixing tank. For the production of 1 Nm3 H_2 (compared to a thermal hydrogen output of 3 kW), approximately 0.65 kg methanol (compared to 20.3 mol CH_3OH or a thermal methanol output of 3.6 kW based on a lower heating value of 637.7 kJ/mol) is required. This leads to a very high thermal efficiency of approximately 83 % due to an internal heat recovery by preheating the feed against cooling the flue gas [542].

Figure 6.99 shows a simplified process flow sheet for methanol steam reforming. This process typically takes place at operating pressures of

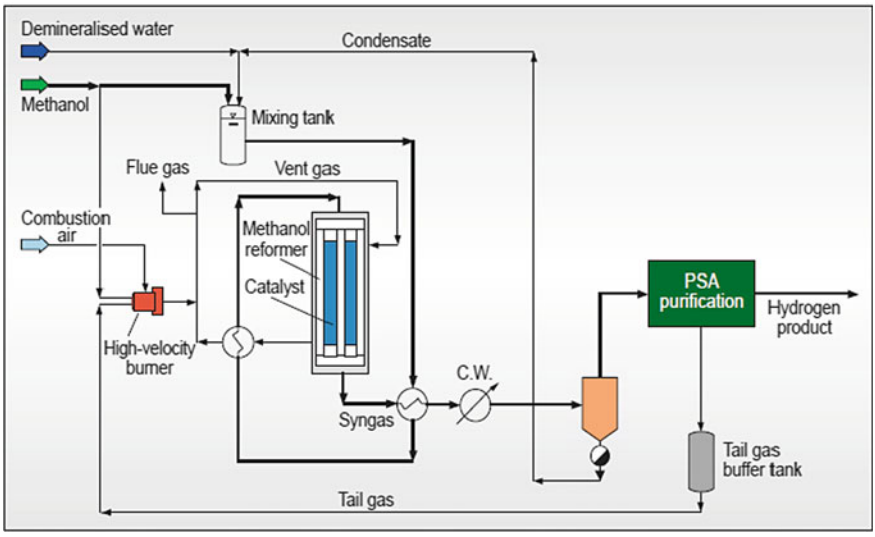

Fig. 6.99 Process scheme of a methanol steam reformer system (Caloric Anlagenbau, Gräfelfing, Germany) [541–543]. PSA, pressure swing adsorption

approximately 2–3 MPa and reforming temperatures between 250 and 300 °C given by the thermodynamic equilibrium (see Fig. 6.92) and the operating temperature range of the Cu/Zn catalyst, which is applied here.

All components of heat management are combined in a so-called hot box, including preheating of the feed, evaporation of the methanol water mixture, the steam-reforming reactor and the product gas cooling. A burner is heating the hot box with circulating flue gas by convective heat transmission. The large volume of circulating flue gas leads to an even heat distribution. The flue gas adjusts the reactor temperature to about 300 °C and is controlled to the optimum operation temperature of the catalyst for maximum yields and catalyst life. Figures 6.100 and 6.101 show a typical arrangement and a photograph of a complete methanol-to-hydrogen plant with reformer, gas purification (by pressure swing adsorption, PSA) and buffer tank setup by Caloric Anlagenbau. The hydrogen output of the shown plant is 750 Nm^3/h.

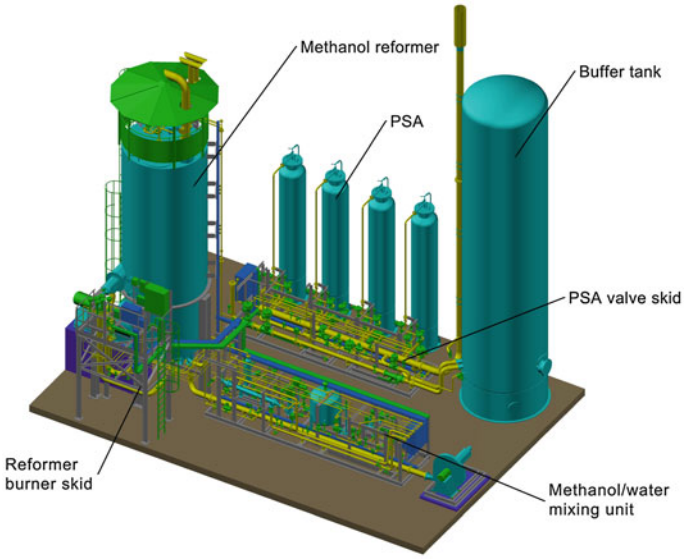

Fig. 6.100 Configuration of a 1,500 Nm^3/h methanol-to-hydrogen plant with reformer and pressure swing adsorption (PSA). (Caloric HM process) [541]

Another industrial example is the Hydroform-M plant by Mahler AGS [544], which has a hydrogen capacity from 100 to 3,000 Nm^3/h and a purity up to 99.999 %. A typical design pressure delivers hydrogen at 1.3 MPa at the exit of the PSA unit (alternatively at 2.6 MPa). The unit uses a thermo-oil cycle for heat management. As shown in Fig. 6.102, demineralised water and methanol from the battery limit are fed into the feed storage vessel (D 10). The feed mixture is pumped and heated up in the process gas heat exchanger (E 10) against the

Fig. 6.101 Caloric HM methanol steam reforming plant with a hydrogen capacity of 750 Nm^3/h [541]

reformed process gas coming from the methanol reformer reactor (R 10). Thereby, part of the feed is already vapourised. Complete vapourisation and a temperature of approximately 260 °C is achieved in a thermo-oil heat exchanger (E 20) before entering the reformer reactor (R 10).

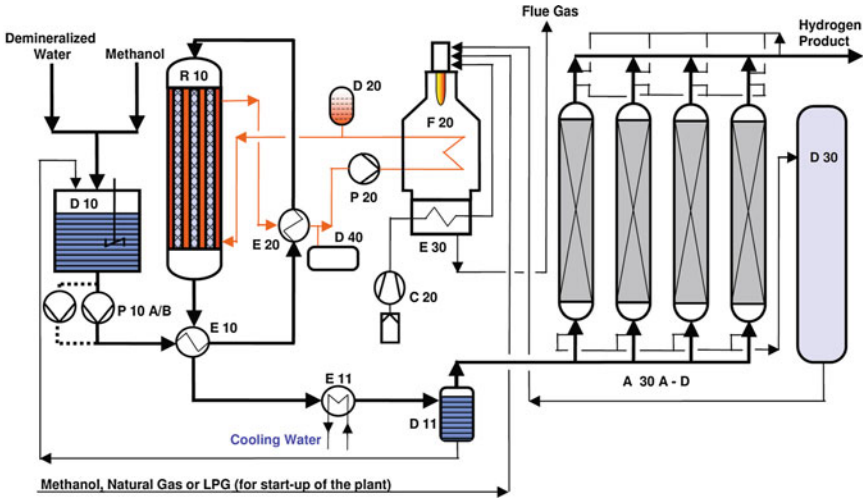

Fig. 6.102 Flow diagram of the Mahler Hydroform-M process [544]. A 30 = A-D pressure swing adsorption unit, C 20 = combustion air blower, D 10 = feed storage vessel, D 11 = knockout drum, D 20 = thermal oil expansion vessel, D 30 = pure gas puffer, D 40 = thermal oil drain tank, E 10 = feed preheater, E 11 = water cooler, E 20 = feed superheater, E 30 = combustion air preheater, F 20 = thermal oil heater, P 10 = feed pump, P 20 = thermal oil pump, R 10 = reactor

Reaction conditions are maintained by circulation of thermo-oil (pump P 20) through the reformer reactor, the thermo-oil heat exchanger (E 20), and the heater (F 20). The final cooling of the process gas to approximately 38 °C takes place against cooling water in a water cooler (E 11). Excess water vapour of the syngas is condensed and separated in a so-called knockout drum (D 11) and then sent back into the feed storage vessel (D 10).

The purification of the process gas is performed in a four-bed PSA unit. The hydrogen product downstream the PSA can achieve a purity of more than 99.999 vol%. Typically, the purge gas from the PSA is collected in buffer (D 30) and sent to the burner in the heater (F 20) and used as burner fuel. During normal operation, a small amount of additional methanol fuel is required; during start-up of the plant only, additional heat is generated by burning of methanol. The combustion air provided by the air blower (C 20) is preheated in the flue gas system of the thermal oil unit (E 30) in order to save fuel [544]. The thermal oil as the heat transfer medium helps to avoid temperature peaks and thereby protects the catalyst for the complete lifetime, as well as reduces the needed instrumentation for the process. A photograph of a Mahler Hydroform-M plant is shown in Fig. 6.103 [544].

Fig. 6.103 Mahler Hydroform-M plant [544]

The product gas from the methanol steam reformer usually has a maximum hydrogen content of 70–80 vol% (on dry basis) at elevated pressures and is usually treated in a PSA to further concentrate the hydrogen to more than 99.9 vol% (up to 99.999 vol%). The PSA process is a gas purification system using different adsorption capacities of solid adsorbent materials and pressure differences between adsorption and desorption steps. Typical adsorbents are activated carbon, zeolithic molecular sieves, silica gel and carbon molecular sieves. Such a PSA unit consists of at least two but mostly four adsorber towers, with several layers of different adsorbent materials in order to produce an almost continuous pure hydrogen flow from the alternating adsorption, desorption (depressurising), regeneration and re-pressurising steps. The principal arrangement of a unit with four single adsorbers is shown in Fig. 6.104 (Hydroswing, Mahler AGS) [545].

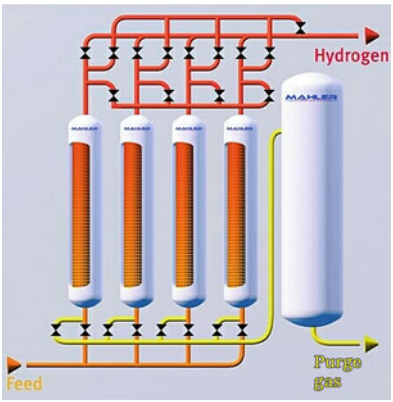

Fig. 6.104 Principal arrangement of a pressure swing adsorption unit for pure hydrogen production

For lower purity requirements, an enrichment of hydrogen from the product gas in a continuous process can be achieved by polymer membranes. Examples are the PRISM separator from Air Products [546] or the PolySep separator from UOP [547]. Very pure hydrogen (>99.9999 vol%) can be generated by application of selective membranes consisting of Pd–Ag or Pd/Cu alloys.

Major Applications of Methanol Reforming

In mobile applications, on-board reforming of methanol for hydrogen/CO driven ignition motors (see review [539]) has not yet found broader applications. However, the use of hydrogen in fuel cell systems may have some future applications (see Sect. 6.5.1). More important are stationary plants to generate hydrogen in locations where the demands falls in between a supply in cylinders or cylinder bundles and the larger hydrogen capacity of natural gas steam reformers. Limited, decentralised hydrogen demand can be found in specialty chemicals and pharmaceutical applications, in edible oil processing (fat hardening) and recycling, hydrofinishing of lubes and waxes and in the production of float glass.

The broadest application is the supply of protective gas against oxidation of materials during heat treatment. Various gas mixtures of methanol with other components are used for special treatment of materials, mostly of metal alloys to modify their physical and mechanical properties. An example for a variety of metallurgical treatments is the Tempron process by Westfalen AG [537]. An overview of such applications is given in Table 6.22.

Table 6.22 Heat treatment of metal alloys with various mixtures of inert gases with methanol, ammonia, hydrocarbons and oxygen [537]

Application	Steel (< 0, 3 % C)	High Carbon Steel (> 0, 3 % C)	Cr- and Mn- steel	Corrosion-, Acid- and Heat-resistant Steels	Casted Iron and Steel	Non-ferrous metals Silver, Nickel, Copper. Brass	aluminium and aluminium Alloys
Carburising	NM, NME, NMP, NMO	NME, NMP	NM, NMP				
Bright Annexing	NH, NM	NH, NM, NMP	NM, NH, NMP	NH, Ar	N	0NH, NM, H	NH. NM, N
Nitriding	NA	NA	NA				
Nitrocarburising	NMA, NCA	NMA, NCA, NWEA	NMA				
Dry-cyaniding	NMA, NPA	NMA, NMPA, NMEA, NPA	NMA, NMPA. NMEA, NPA				
Decarburising, Blueing	NO, NH + H20	NO, NH + H20	NO, N + H20	NH, H, AfH + H20	Air + H20		
Normalising	N, NM, NP	NM, NP, NMP	N, NM, NP, NMP	Af	NM NPO, NMP		
Sintering	NH, NM, NP	NH, NM, NP, NME, NMP	NH, ArH, H	NH. A(H, H		NH, NM	NH, NM
Oven soldering, Brazing	NH, MM	NH, NM, NP	NH, ArH	H, NftAfH		NH, NM	NH

Abbreviations: Ar = argon, N = nitrogen, H = hydrogen, ArH = argon + hydrogen, NH = nitrogen + hydrogen, NP = nitrogen + propane, NM = nitrogen + methanol, NME = nitrogen + methanol + ethanol, NMP = nitrogen + methanol + propane, NMO = nitrogen + methanol + oxygen, NMEA = nitrogen + methanol + ethanol + ammonia, NMPA = nitrogen + methanol + propane + ammonia, NMA = nitrogen + methanol + ammonia, NPA = nitrogen + propane + ammonia, NCA = nitrogen + CO_2 + ammonia, NA = nitrogen + ammonia, NO = nitrogen + oxygen

Summary

Methanol is widely available from fossil and regenerative sources, and as a liquid it can be easily transported and stored. In specific cases of decentralised supply with hydrogen or other gas mixtures, a stationary methanol splitting or reforming unit can be advantageous as a technically proven and economical alternative. Typical capacities of those units range from 50 to 3,000 Nm^3/hour. The broadest application of methanol and its decomposition products is the heat treatment of metals, either as a protective atmosphere or a functional treatment to change the metallurgical properties. Mobile applications by means of on-board methanol reforming to fuel ignition engines are still in experimental status, whereas on-board hydrogen generation for fuel cells may find broad applications in the future (see Sect. 6.5.2).

6.5.2 Methanol Fuel Cells

Gerd Sandstede[1] and Angelika Heinzel[2]

[1]*Esperantostraße 5, 50598 Frankfurt/M, Germany*

[2]*Institute of Energy and Environmental Process Engineering, University of Duisburg-Essen, Lotharstraße 1, 47048 Duisburg, Germany*

6.5.2.1 Introduction

Methanol is an energy carrier with several advantages compared to other fuels [548]. The properties of methanol are the subject of several other chapters of this book. In this chapter, the use of methanol as fuel for fuel cells is discussed. This includes the direct methanol fuel cell (DMFC), which is properly designed for methanol as fuel, as well as fuel cells connected to a methanol reformer, which generate electricity from hydrogen being contained in the reformate. In this introduction, the different types of fuel cells are described in some detail before special developments for the use of methanol as fuel are given. This includes basic thermodynamic information, material properties and electrochemical aspects. Finally, state-of-the-art developed systems and their properties are presented. Advantages and disadvantages are discussed, leading to the conclusion and vision for the future use and application of methanol as fuel for fuel cells.

6.5.2.2 Introduction of Fuel Cells

Reasons for the Application of Fuel Cells

The modern development of fuel cells started in the United States in the 1960s for application as an electricity generator during space missions. This initiated widespread research and development (R&D) efforts in the United States, as well as in Europe and Japan, leading to different types of fuel cells for various terrestrial applications, such as stationary combined heat and power supply and power supply for electric drives and portable devices as a battery replacement or range extender.

The increasing awareness of the environmental challenges connected to the use of fossil energy carriers and the need for cleaner and more efficient energy conversion processes gave a good reason to foster the development of fuel cell technology. One of the driving factors was the demand for reduction of traffic-related emissions in regional conurbations by introducing zero-emission vehicles. This request was at first formulated in the Californian Clean Air Act [549] and has led to significant efforts in realising electric vehicles. The various types of batteries—even the recently introduced high-energy–density lithium-ion battery—enable typical passenger cars for a limited driving range and require quite long charging (fueling) times; therefore, fuel cells have been considered to be an attractive option.

Some reasons for the use of fuel cells are

- High conversion efficiency, at least of hydrogen as fuel into electricity
- Low or even no emissions, except water from the electrochemical conversion process
- Good scalability due to the modular design of the fuel cell
- Independent choice of power (size of fuel cell) and energy (size of fuel tank)
- Suitability for combined heat and power supply
- Availability of different technologies for different operation temperatures and thus for different fields of application
- Electrochemical energy conversion that does not require moving parts and does not emit noise

In a fuel cell, chemical energy is directly converted in an electrochemical conversion process into electricity and heat. The theoretical maximum efficiency is determined by the ratio between the free Gibbs energy (free enthalpy) and the enthalpy of the reaction under consideration and is not limited by the Carnot factor, as it is the case for conventional thermal energy conversion processes as used in engines or in power plants. Depending on the fuel, a fuel cell might require a preceding fuel processing step, which generates a hydrogen-rich gas from the fuel (e.g. natural gas, methanol). The enthalpy and free enthalpy values of various combustion reactions under constant pressure are well known and can be taken from classical thermodynamic tables [550] in order to calculate the maximum of electrical energy and the theoretical limit for the efficiency that can be delivered by a certain fuel cell.

Some Thermodynamic Aspects

To understand the operation principle of fuel cells, energy conversion processes have to be considered. In contrast to conventional combustion reactions that are based on direct chemical reaction of a fuel with oxygen (in general, taken from the ambient air), fuel cells divide this reaction into two parts: the electrochemical oxidation of the fuel and the reduction of oxygen. For this purpose, separate fuel and oxygen (air) compartments or half cells are realised, being equipped with an electrocatalyst that is especially designed to catalyse the electrochemical reaction, even at relatively low reaction temperatures. Hydrogen is a fuel that is highly reactive, even at low temperatures (in the presence of a platinum catalyst). Equation 6.26 shows the exothermal chemical reaction.

$$2H_2 + O_2 \rightarrow 2H_2O \qquad \Delta_R H^0 = -285.8\,\text{kJ/mol} \tag{6.26}$$

The heat of reaction at normal conditions (0.101325 MPa, 273.15 K) and constant pressure $\Delta_r H^0$ is negative, meaning that heat is released from the system.

For methanol, the reaction with oxygen gives carbon dioxide and water.

$$2CH_3OH + 3O_2 \rightarrow 4H_2O + 2CO_2 \quad \Delta_R H^0 = -726\,\text{kJ/mol} \tag{6.27}$$

Both reactions are valid for the combustion process and the electrochemical process as well. For energy conversion devices, the efficiency of conversion is one of the most important criteria.

Characteristics of Fuel Cells

Electrochemical energy conversion devices differ significantly from those for chemical conversion. The latter usually scale with the volume, but electrochemical conversion is related to an area. The reason is easy to understand because the fuel and the oxygen have separately to be brought into contact with an electrode comprising the electrocatalyst and a current collector. On one side of the electrode, the chemical substances (educts and products) are circulating in the electrode compartment; electrons (electrical energy) are transported in the electrode itself and the adjacent current collectors. In the case of a fuel cell, continuous feeding of fuel and oxidant results in continuous energy release. The operation principle of a fuel cell is depicted in Fig. 6.105. Here, the simplest reaction is chosen, the conversion of hydrogen.

The electrodes and electrocatalysts are highly porous and therefore have a high specific surface area; the gas diffusion layers (GDLs) are also porous, but much less so because they serve as current collectors and for the distribution for the reactant gases. The electrolyte is gas tight but water can diffuse through it. Reviews in the literature about fuel cells give much more details [551–564].

Electrochemical Reactions

Electrochemical reactions are characterised by the local separation of the reduction reaction—here, for example, the reduction of oxygen molecules to oxygen ions

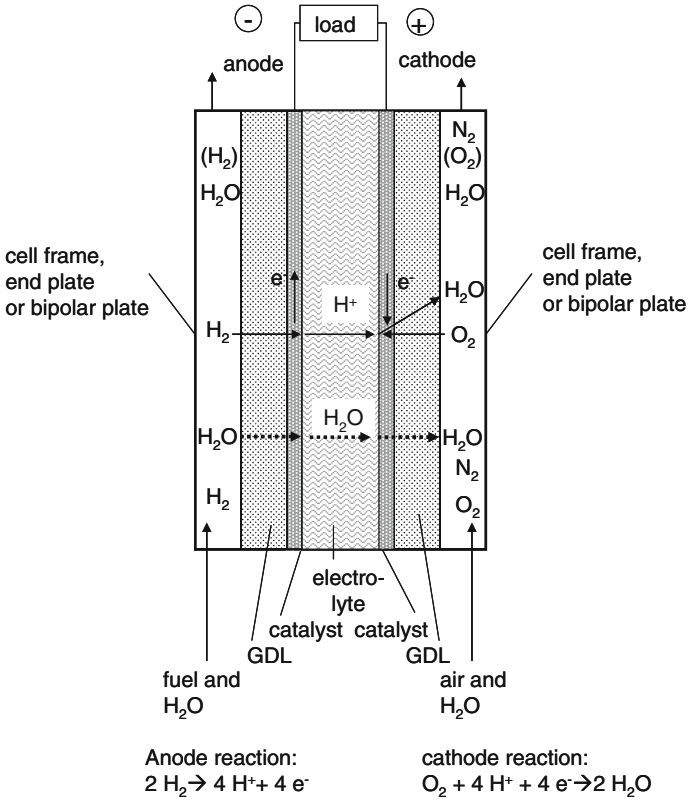

Fig. 6.105 Hydrogen fuel cell with proton conducting electrolyte. GDL, gas diffusion layer

and the oxidation reaction of hydrogen to protons (Eq. 6.28 and 6.29). Reduction reactions take place at the cathode; the anode serves for oxidation. The separate reactions occur at the electrodes, leading to a certain electrode potential. Due to this potential, the reaction stops as electrons cannot longer be transferred to or from the charged electrodes. A continuous reaction requires a closed electrical cycle. For this purpose, the cathode and the anode have to be connected to an electric load, allowing electrons to flow from the anode to the cathode. A second prerequisite is that hydrogen ions must reach the cathode compartment and must react with oxygen in order to form water as a product. This can be realised by an electrolyte that is proton conductive.

$$2H_2 \rightarrow 4H^+ + 4e^- \tag{6.28}$$

$$O_2 + 4H^+ + 4e^- \rightarrow 2H_2O \tag{6.29}$$

The ideal theoretical difference between the electrode potentials, the cell voltage, can be calculated from thermodynamic values. The basic equation is the

Gibbs equation, giving the relationship between the Gibbs free enthalpy at normal conditions $\Delta_r G^0$ and the enthalpy $\Delta_r H^0$ of a reaction (Eq. 6.30).

$$\Delta_R G^0 = \Delta_R H^0 - T\Delta_R S^0 \quad \Delta_R G^0 = -237.1\,\text{kJ/mol} \tag{6.30}$$

Although the free enthalpy of the reaction can be converted into electrical energy, the remaining part, $T\ \Delta_R S^0$, represents a heat. Conversion of 1 mol of hydrogen allows the calculation of U_{rev}, the reversible cell voltage:

$$U_{rev} zF = \Delta_R G^0 \quad \text{or} \quad U_{rev} = \Delta_R G^0 / zF = 1.229\,\text{V} \tag{6.31}$$

with

z Number of transferred electrons per mole of substance (2 for hydrogen) and
F Faraday constant = 96,485 C for 1 mol of electrons being transferred.

If the value of $\Delta_R H^0$ would be used to calculate the voltage, a value of U ($\Delta_R H^0$) = 1.48 V would result. This value cannot be achieved due to thermodynamic reasons.

Efficiency of the Fuel Cell

For the derivation of an equation for the theoretical efficiency of a fuel cell, again the Gibbs equation (Eq. 6.30) is used. The maximum thermodynamic efficiency of a fuel cell is defined by Eq. 6.32.

$$\eta_{theor} = \Delta_R G^0 / \Delta_R H^0 = U_{rev} / U\left(\Delta_R H^0\right) = 83\,\% \tag{6.32}$$

Here it should be mentioned that all values are related to the generation of liquid water; thus, the higher heating value is used as basis, leading to lower efficiency values. In a fuel cell, the operation temperature determines how much water in liquid and in gaseous form is generated.

So far, ideal thermodynamic considerations have been used to explain fuel cell behaviour. However, these ideal conditions typically cannot be achieved in technical devices. The open circuit voltage (no load connected to the fuel cell) is lower than the calculated, theoretical voltage U_{rev} and if a current is drawn from the cell, additional losses are observed. A typical current voltage dependence measured with a real fuel cell is depicted in Fig. 6.106.

At open circuit conditions, a voltage of 1 V or even a bit lower is measured. These losses of approximately 20 % are mainly caused by the oxygen reduction reaction. Because the oxygen molecule has to be split into atoms and four electrons have to be transferred, this reaction is complicated and side reactions are possible. The formation of hydrogen peroxide is a well-known side reaction, leading to the formation of a mixed potential, which is described in Sect. 6.5.2.5. Another factor is the permeability of the electrolyte for fuel and oxygen. Hydrogen at the cathode side (or vice versa, oxygen at the anode side) will lead to direct chemical reactions at the catalyst, not contributing to the electrical energy generation.

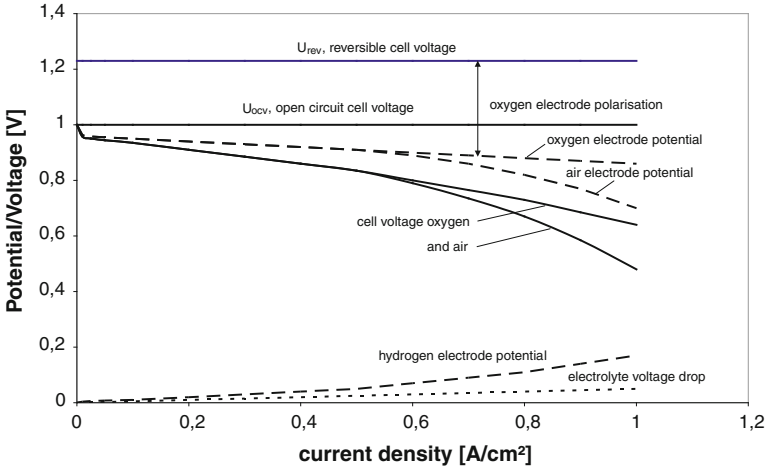

Fig. 6.106 Performance of a fuel cell; current–voltage/potential curves

The current–voltage characteristic of a fuel cell is of utmost technical interest, in addition to its technical construction principles. Both main properties determine the ratio of cost related to power. To better compare different types of cells, the current density is given as current divided by the active electrode area. For detailed electrochemical investigations, it might additionally be of interest to analyse the behaviour of one electrode of the cell separately without the influence of the second electrode. In that case, a third electrode—a reference electrode with constant potential—has to be introduced. The electrode potential versus current density curves gives detailed insight about occurring losses, namely overpotentials due to different temperatures, pressures, concentrations of the educts, side reactions, impurities and interactions between electrode and electrolyte and catalytic properties of the electrocatalyst, ohmic losses, as well as incomplete fuel usage (Coulomb or Faradaic efficiency η_{coul}). In systems, the consumption of electrical system components can significantly contribute to a reduction of efficiency. For example, a cell that is operated at 0.2 A/cm^2, according to Fig. 6.106, gives a cell voltage of 0.72 V. With these values, a voltage efficiency η_V of 49 % can be calculated.

6.5.2.3 Types of Fuel Cells with Respect to the use of Methanol

Operation of Different Fuel Cells with Methanol

In this chapter, the different types of fuel cells are shortly described because in principle they are suitable for operation with methanol. The different materials for electrodes and electrolytes being used for the construction of the cells determine

the operation temperature. The required operation temperature is dominated by the ionic conductivity of the electrolytes, and thus the type of electrolyte is chosen for the classification of the fuel cell. In Table 6.23, the types of fuel cells and some of their important properties are summarised.

For all types of fuel cells, it is valid that numerous single cells have to be connected electrically in series to reach a technically interesting operation voltage. In most cases, this is achieved by flat cell design for cell frames, which are manufactured from conducting materials. Thereby, it is possible to connect the anode of the first cell with the cathode of the second and so forth, leading to a bipolar design of the plate type cell frames, the bipolar plates. This design is shown in Fig. 6.107. Especially for the solid oxide fuel cell (SOFC), tubular designs have also been realised.

Another important question is the kind of fuel being used. Most fuel cells operate best with pure hydrogen. But here, the availability of the fuel is a major problem to be solved. The generation, storage and transport of hydrogen are complicated and are the subjects of different textbooks [553, 562, 563, 565]. However, almost any energy carrier can be converted to a reformate gas containing hydrogen, carbon dioxide and carbon monoxide with oxygen or steam as reaction partner [566]. The possible reaction equations are given for gaseous methanol:

$$CH_3OH + H_2O \rightleftharpoons CO_2 + 3H_2 \qquad \Delta_R H^0 = 49.3\,\text{kJ/mol} \tag{6.33}$$

$$CO_2 + H_2 \rightleftharpoons CO + H_2O \qquad \Delta_R H^0 = 41.0\,\text{kJ/mol} \tag{6.34}$$

The conversion of methanol is a fast reaction at Cu/Zn catalysts and is theoretically complete at temperatures of above 200 °C. Because the water–gas shift reaction (Eq. 6.34) is endothermic, the higher the temperature, the more CO is formed. The equilibrium concentration of CO at a temperature of 200 °C is about 0.5 vol%. All other fuels (e.g. natural gas, LPG, gasoline, diesel) require reforming temperatures exceeding 700 °C. Therefore, depending on CO tolerance of the fuel cell, catalytic CO removal is necessary. For this purpose, this reaction is used in reverse direction, which can be realised by cooling the reformat in the presence of a suitable catalyst. For the low-temperature fuel cells, where the electrocatalyst is especially sensitive to CO poisoning due to the adsorption and slow oxidation kinetics of CO, a fine purification is required. This final catalytic step is realised as selective oxidation in most cases. A small amount of air is mixed into the reformate stream. At a highly selective catalyst, more or less only the CO is oxidised to CO_2; the hydrogen should not react to a significant amount. These types of fuel processors have been developed for a variety of fuel cell applications.

Alkaline Fuel Cells

Due to the alkaline electrolyte, the electrode potentials of an alkaline fuel cell (AFC) are shifted to more negative values of approximately −400 mV for the hydrogen electrode and +830 mV for the oxygen electrode. This makes the use of

Table 6.23 Types of fuel cells, including the operation with methanol and reformate (e.g. from methanol)

Fuel cell	Abbreviation	Electrolyte	Operation temperature	Operation with methanol	Operation with reformate
Alkaline fuel cell	AFC	30 % KOH in H_2O	-20 to 90 °C	Yes (DMFC), but K_2CO_3 precipitation, consumes electrolyte	Yes, K_2CO_3 precipitation
Polymer electrolyte membrane fuel cell	PEMFC	Perflourinated, sulfonated polymer membrane	-20 to 90 °C	Yes, called DMFC	Yes, but CO removal is required
	HT-PEMFC	Polybenzimidazole/H_3PO_4	120–180 °C	Yes, called HT-DMFC	Yes
Phosphoric acid fuel cell	PAFC	Phosphoric acid	200 °C	Yes, called HT-DMFC	Yes
Molten carbonate fuel cell	MCFC	Eutectic mixture of Li_2CO_3 and K_2CO_3	650 °C	No	Yes
Solid oxide fuel cell	SOFC	Y dot. ZrO_2	900–1,000 °C	No	Yes

DMFC, direct methanol fuel cell; HT, high temperature

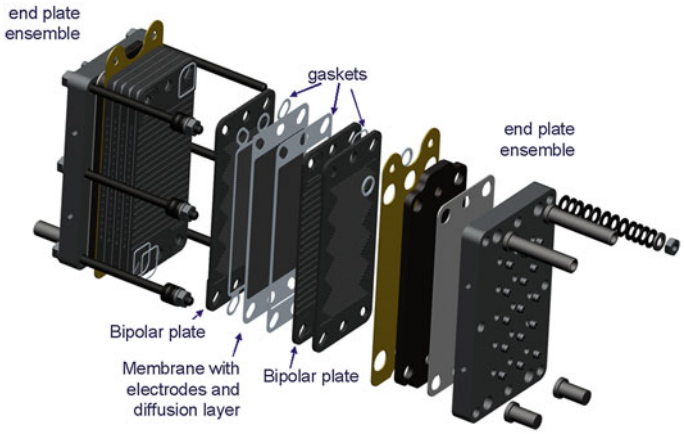

Fig. 6.107 Fuel cell stack with bipolar design

relatively cheap materials and electrocatalysts possible, such as Raney nickel or silver. The electrolyte is soaked in a porous separator, which forms a barrier between the reaction gases. Pressure differences between the fuel and oxygen sides should be avoided.

The main disadvantage of the AFC is the reaction of the electrolyte with CO_2, leading to the precipitation of solid K_2CO_3. Therefore, the operation with reformate gas is not feasible. Even if air is used as oxidant, CO_2 removal or frequent electrolyte regeneration is required. The development and use of AFCs were therefore more or less restricted to space applications. AFCs were used in Apollo and space shuttle missions and operated with pure hydrogen and oxygen.

Proton Electrolyte Membrane Fuel Cells

As already mentioned above, the polymer electrolyte has two functions: it is proton conducting and it safely separates the reaction gases. This approach to realise a safe fuel cell was first reported by Grubb and Niedrach 1958 [556], who proposed to sulphonated a polymer backbone in order to realise the proton conducting polymer electrolyte. The breakthrough was reached when Grot [567] used a perfluorinated polymer material for this purpose. At present, different chemical companies offer such membranes, even as assemblies with optimised electrode coatings for commercial products (called membrane electrode assemblies). Membrane thickness can vary between 20 and 120 μm. A good protonic conductivity is only achieved if liquid water is present. Therefore, the water management of a proton electrolyte membrane fuel cell (PEMFC) is crucial.

Because water is mainly transported from the anode to the cathode and the reaction water as well is formed at the cathode, strong humidity gradients can lead to significant differences in ionic conductivity from fuel and air inlet to outlet. Dry

conditions as well as very wet conditions lead to a reduction in power; therefore, drying out of the membrane as well as flooding of the electrocatalyst have to be avoided. To cope with these difficult requirements, gas diffusion media have been developed, with a gradient in pore structure and hydrophobic properties. A scanning electron microscopy picture of a cross-section of a GDL with a micro porous layer and catalyst layer on top of a membrane is shown in Fig. 6.108.

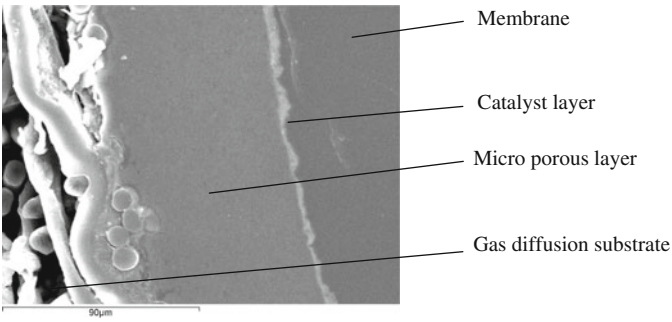

Fig. 6.108 Scanning electron microscopy image of a membrane electrode assembly with a gas diffusion layer from Freudenberg. (Courtesy of University of Duisburg-Essen)

Due to the acid electrolyte, air and CO_2-containing reformate gases can be used as fuels; even methanol can be supplied to the anode. At low operation temperatures, CO leads to severe poisoning of the catalyst. As mentioned above, a fine purification for CO removal has to be included in the fuel processor if the PEMFC will be operated with reformate gas. Additionally, special alloy catalysts have been developed, mainly on the basis of platinum and ruthenium for accelerated CO oxidation [568–570]. Similar problems occur during the direct electrochemical oxidation of methanol.

Phosphoric Acid Fuel Cells

As the name indicates, concentrated phosphoric acid is used as an electrolyte in phosphoric acid fuel cells (PAFCs). The acid is soaked in a porous SiC matrix, which is covered on both sides by a porous carbon electrode with platinum as an active catalyst in a fine dispersion at the interface. The concentrated H_3PO_4 allows operation temperatures up to 200 °C. The higher temperatures lead to a significant increase in tolerance of the catalyst with respect to CO poisoning. The tolerable CO content is approximately 1 vol%. These cells are typically operated with reformate gas being generated by a preceding fuel processing step using natural gas as fuel. The typical application is combined heat and power supply at industrial sites.

High-Temperature Polymer Electrolyte Membrane Fuel Cells

A fuel cell combining the properties of a PEMFC and a PAFC is the high-temperature polymer electrolyte membrane fuel cell (HT-PEMFC) [570, 571]. Here, a polymer with good temperature stability is used, such as polybenzimidazole (PBI). The porous polymer matrix with alkaline imid-groups (R_2N) are able to bind phosphoric acid quite tightly and maintain a good proton conductivity. The operation temperature of this type of fuel cell lies between 130 and 180 °C. The advantage of the more secure separation of fuel and oxidant in the cell compared to PAFC and the robustness towards CO poisoning comes with a longer startup phase compared to PEMFC and problems of electrolyte loss upon condensation, mainly occurring during start and stop procedures. The HT-PEMFC can be operated with 1 vol% CO in hydrogen without any loss in performance, as CO desorption is significantly accelerated at 160 °C compared to the 80 °C of the low-temperature PEMFC. An important drawback of the high temperature is the accelerated corrosion of carbon carrier materials, catalysts and construction materials.

Liquid-Fuel Fuel Cells

The DMFC is described in detail in Sect. 6.5.2.5. Various other liquid fuels have been investigated as possible option for direct electrochemical conversion. Ethanol is the most interesting one due to its environmental friendliness and biological source. However, because C–C bonds generally are difficult to split in electrochemical processes, only incomplete conversion is observed [572]. The higher alcohols, diols such as ethylene glycol and formic acid were the low-molecular C-, H- and O-containing species being investigated in R&D. Other options for compounds releasing hydrogen are hydrazine and alkali boron hydrides, but commercial use was not realised. Hydrazine is the most active compound, but unfortunately it is poisonous (carcinogenic). Some electrochemical data are summarised in Table 6.24.

Molten Carbonate Fuel Cells

The molten carbonate fuel cell (MCFC) was an earlier development, using a mixture of molten alkali carbonates as electrolyte. The eutectic mixture of Li_2CO_3 and K_2CO_3 performed best, with respect to corrosion and wettability of the electrodes. The operation temperature is well above the melting point at about 650 °C. The molten salts are sucked in a porous matrix consisting of $LiAlO_2$. The pores have to be finer than those of the adjacent electrodes in order to stabilise the electrolyte film for gas separation. In an MCFC, oxygen is reduced to oxygen ions, but the conduction path requires an additional molecule of CO_2. The formed carbonate ions are transported through the electrolyte to the anode compartment, where CO_2 is released again. Thus, the MCFC requires a CO_2 recycling path from

Table 6.24 Thermodynamic and electrochemical data of fuel reactions [550]

No.	Fuel	Reaction	z	$\Delta_R H^0$ (kJ/mol)	$\Delta_R G^0$ (kJ/mol)	U_{rev} (V)	η_{theor} (%)
1	Hydrogen	$H_2 + 0.5O_2 \rightarrow H_2O$	2	−286.0	−237.3	1.229	83.0
2	Carbon	$C + 0.5O_2 \rightarrow CO$	2	−110.6	−137.3	0.712	124.2
3	Carbon	$C + O_2 \rightarrow CO_2$	4	−393.7	−394.6	1.020	100.2
4	Carbon monoxide	$CO + 0.5O_2 \rightarrow CO_2$	2	−283.1	−257.2	1.066	90.9
5	Methane	$CH_4 + 2O_2 \rightarrow CO_2 + 2H_2O$	8	−890.8	−818.4	1.060	91.9
6	Methanol	$CH_3OH + 1.5O_2 \rightarrow CO_2 + 2H_2O$	6	−726.6	−702.5	1.214	96.7
7	Formaldehyde	$HCHO + O_2 \rightarrow CO_2 + H_2O$	4	−561.3	−522.0	1.350	93.0
8	Formic acid	$HCOOH + 0.5O_2 \rightarrow CO_2 + H_2O$	2	−270.3	−285.5	1.480	105.6
9	Ethanol	$C_2H_5OH + 3O_2 \rightarrow 2CO_2 + 3H_2O$	12	−1,367	−1,325	1.145	97
10	Dimethyl ether	$CH_3OCH_3 + 3O_2 \rightarrow 2CO_2 + 3H_2O$	12	−1,460[a]	−1,387[a]	1.20	95

[a] Calculated from U_{rev} and η_{theor}

the anode to the cathode. Therefore, the MCFC is the only fuel cell that cannot be operated with pure hydrogen.

The cathodic and anodic reaction are shown in Eqs. 6.35 and 6.36.

$$O_2 + 2CO_2 + 4e^- \rightarrow 2CO_3^{2-} \tag{6.35}$$

$$H_2 + CO_3^{2-} \rightarrow CO_2 + H_2O + 2e^- \tag{6.36}$$

Due to the high operation temperature, the electrochemical kinetics are fast. Noble metal catalysts are not required; typical electrode materials are nickel for the anode and nickel oxide for the cathode. Another advantage of the high temperature is the option for internal reforming.

One of the MTU MCFC systems was operated in Berlin at a BEWAG (the former electric utility of Berlin; today called Vattenfall) site with methanol as fuel. The adaptation from natural gas to methanol was easily done according to the communication of the owner and MTU.

Solid Oxide Fuel Cells

At even higher temperatures in the range of 800–1,000 °C, some ion-conducting ceramic electrolytes are known. The first modern investigations of laboratory cells were carried out by Weissbart and Ruka, Moebius, Sandstede et al., Tannenberger, and others in the early 1960s [556, 573]. The higher the temperature, the higher is the mobility of the ions in the lattice. Most interesting would be a solid proton conducting material, but R&D in the field did up to now not lead to suitable materials. However, oxygen conduction materials are well known, because Nernst used doped zirconium oxide as material for gas mantles. The mobility of oxygen ions originate from lattice defects, which are formed by doping the ZrO_2 with an

oxide with a three or two-valent material, such as yttrium oxide (Y_2O_3) or calcium oxide (CaO). For a long time, yttrium-doped ZrO_2 (YSZ) was used for SOFC, showing the maximum conductivity of 0.1 S cm^{-1} at a temperature of 1,000 °C at a composition of 8 mol % yttrium.

The operation principle can be explained using Fig. 6.105. However, because the electrolyte is oxygen ion-conducting, oxygen reduction at the cathode directly leads to the required conducting ions. Water vapour is formed at the anode by reaction, with the protons being formed by hydrogen oxidation at the anode.

As for the MCFC, the SOFC does not require highly active catalysts. More important are thermal expansion coefficients, as each startup procedure means also a heating process for the layers of the cell. At an operation temperature of 900 °C, the reversible cell voltage is 0.89 V at operation with hydrogen and oxygen. But typically, the SOFC is operated with natural gas and air. The reforming process can be carried out either external or internal of the fuel cell stack; the latter process gives the option of using the endothermic reforming reaction for cooling of the cell. There are detailed reviews about high-temperature fuel cells MCFC and SOFC [553, 562–564].

6.5.2.4 Gaseous and Liquid Fuels: Thermodynamic Data

Because fuel cells can be operated with synthesis gas, the combination of fuel cell systems with fuel processors in which the reforming of any fuel takes place are state of the art. In Sect. 6.5.2.6, the detailed description of methanol fuel processing for fuel cells is given. Possible fuels for fuel cell systems are briefly listed and their most important properties are summarised. Thus, methanol as a fuel can easily be ranked in comparison to other fuels.

The thermodynamic values of the electrochemical oxidation reactions determine the achievable cell voltage U_{rev} and can be calculated according to (6). From a theoretical point of view, the most interesting reaction would be the direct electrochemical conversion of coal. For the first partial combustion step leading to carbon monoxide, a theoretical reversible cell voltage U_{rev} of 0.71 V and a theoretical efficiency of 124 % can be calculated. This high-efficiency value of more than 100 % can be explained by the increase in entropy during the course of the reaction, which usually is the case for the generation of gaseous products from solid or liquid educts. The complete conversion to CO_2 would result in a reversible cell voltage of $U_{rev} = 1.02$ V as given in line 3 of Table 6.24. The third possibility is the electro-oxidation of CO to CO_2, leading to $U_{rev} = 1.066$ V.

The electro-oxidation of methanol (Table 6.24, line 6) leads to carbon dioxide if the oxidation reaction is complete. As intermediates, formaldehyde and formic acid can be formed. Both substances can be oxidised further; formic acid has even been used as fuel for a fuel cell in early experiments. DME can easily be synthesised from methanol and also be easily electro-oxidised according to the equation given in Table 6.24 (line 10).

6.5.2.5 Direct Methanol Fuel Cells

Basic Principle of a DMFC System

Usually, the DMFC is operated with liquid methanol as fuel. The construction principle (see Fig. 6.109) is the same as for a hydrogen consuming PEMFC. Some minor changes are required for liquid operation. Although the air side remains the same, the anodes need hydrophilic structures to facilitate access of liquid fuel to the electrode. During methanol oxidation, the generated CO_2 has to be removed from the cell (see Eq. 6.37). A second important difference is the significant diffusion of methanol through the polymer electrolyte. This can be understood because of the chemical similarity of the water molecule and the methanol molecule and the complete miscibility of the two substances. This permeation or crossover is highest under OCV conditions and diminishes upon increasing load, as methanol in the vicinity of the electrode is depleted. The permeated methanol is reacting at the cathode with oxygen, leading to a loss in cell voltage, a loss in fuel,

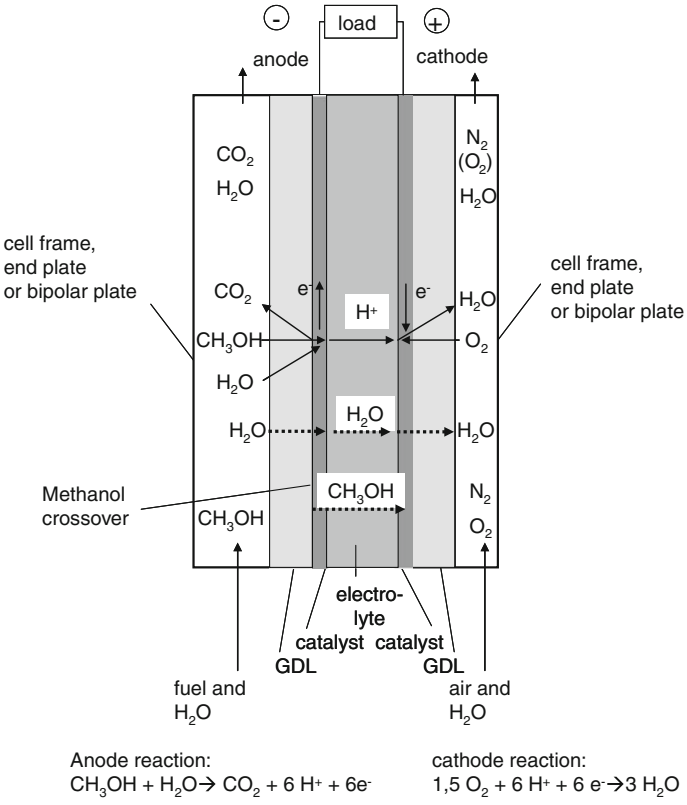

Fig. 6.109 Direct methanol fuel cell. GDL, gas diffusion layer

and thus resulting in a reduction of efficiency. Additionally, during the electro-oxidation of methanol, CO adsorbates are formed on the anode catalyst.

$$\text{Anodic reaction}: \quad CH_3OH + H_2O \rightarrow CO_2 + 6H^+ + 6e^- \tag{6.37}$$

$$\text{Cathodic reaction}: \quad 1.5O_2 + 6H^+ + 6e^- \rightarrow 3H_2O \tag{6.38}$$

The total cell reaction for methanol oxidation is as follows:

$$CH_3OH + 1.5O_2 \rightarrow CO_2 + 2H_2O \tag{6.39}$$

Thermodynamic and electrochemical values for the methanol fuel cell and further detailed information are given in Sect. 6.5.2.4.

Although methanol is one of the most reactive liquid fuels, it has some drawbacks compared to a hydrogen-fueled cell. The principle of electrochemical conversion of methanol is known since 1922. The cell was realised as alkaline fuel cell with a certain concentration of methanol in the liquid-fed anode chamber. These early cells were operating robustly but at low power density. The introduction of a technically mature product on the basis of this operation principle was never successful. However, new R&D efforts were undertaken, when proton-conducting membranes were available for PEMFC. In that architecture, a mixture of water and methanol could be used as fuel. For more historical details, see Sect. 6.5.2.3. Meanwhile, the first DMFC-based products became commercially available. Besides the advantage of methanol being a liquid fuel and therefore easily to carry, there is another favourable property—namely the fact that the specific energy content is quite high at 6.30 kWh/kg.

Besides the theoretical cell voltage of the methanol cell (1.214 V, Table 6.24), the reversible methanol electrode potential is of interest:

$$u_{revanode} = u_{revO2} - U_{revcell} = 1.229 - 1.214\,V = 0.015\,V \tag{6.40}$$

Theoretically, the difference between the methanol and the hydrogen electrode potential is small.

In principle, a DMFC system can be constructed quite simply, as depicted in Fig. 6.110. The fuel cell stack is connected to a methanol and water circuit, consisting of a tank and a pump. CO_2 is released in the tank. To supply air to the cathode, a fan can be used. But long-term stable operation requires some more controls; mainly, the water balance of the system has to be actively regulated. According to Eq. 6.37, water is consumed at the anode and released at the cathode. Additional water is transferred by the electro-osmotic drag and the total amount of water is released as liquid or as humidity with the excess of air. The ratio of liquid water and steam is strongly dependent on temperature and air flow.

A certain methanol/water mixture is used as fuel, but during operation the concentration relations change due to the reasons mentioned above. Therefore, a methanol sensor is frequently used for controlling the supply of fuel. If a methanol–water mixture has to be refuelled, the energy density of the fuel is significantly

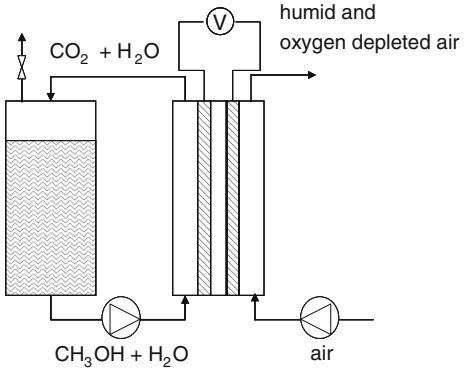

Fig. 6.110 Direct methanol fuel cell system

reduced compared to pure methanol. Therefore, much development effort was put into closing the water loop inside the system. The water being released at the cathode with the excess air has to be condensed and fed back to the anode side. The remaining task is the dosing of the correct amount of methanol to the fuel side of the cell.

Fundamentals of the Methanol Oxidation Reaction

It has been known that hydrogen oxidation can occur along two pathways. Because hydrogen also has to be oxidised during the process of methanol electro-oxidation, the basic principles are given. Immediately after adsorption of hydrogen molecules at the electrode surface, dissociation and electron transfer occurs.

$$2Pt + H_2 \rightarrow 2Pt - H \tag{6.41}$$

$$Pt - H \rightarrow Pt + H^+ + e- \tag{6.42}$$

The oxidation of methanol to CO_2 as product is the desired reaction, as six electrons are transferred and are available for power production. However, this total oxidation proceeds stepwise with numerous possible side products and intermediates. The reaction at the platinum surface can be formulated as follows:

$$2Pt + CH_3OH \rightarrow Pt - CH_2OH + Pt - H \tag{6.43}$$

$$2Pt + Pt - CH_2OH \rightarrow Pt_2 - CHOH + Pt - H \tag{6.44}$$

$$Pt + Pt_2 - CHOH \rightarrow Pt_2 - COH + Pt - H \tag{6.45}$$

Each Pt–H- site is reacting according to Eq. 6.42 to a proton and an electron. The COH adsorbate being formed according to Eq. 6.45 might even be triple bonded. Using (infrared) spectroscopy, adsorbed CO could finally be detected on the electrode surface.

$$(Pt) + Pt_2 - COH \rightarrow Pt - CO + Pt - H \tag{6.46}$$

For the further oxidation of this strongly adsorbed CO species, oxide species at the catalyst surface are required, such as Pt–OH. Adjacent CO and OH- species react according Eq. 6.48 and finally CO_2 is generated.

$$Pt + H_2O \rightarrow Pt - OH + H^+ + e^- \tag{6.47}$$

$$Pt - CO + Pt - OH \rightarrow Pt - COOH + Pt \tag{6.48}$$

$$Pt - COOH \rightarrow Pt - H + CO_2 \tag{6.49}$$

This mechanism was explained stepwise by many authors (including reviews) [555, 557, 568, 574–578]. If the electrode surface is brought into contact with a methanol-containing electrolyte, the adsorption takes place. In order to oxidise the adsorbate, the potential can be raised, for example, by means of a potentiostat by sweeping the potential and recording the current (see Fig. 6.111). From the charge being transferred during the oxidation current peak at 675 mV, it can be calculated that it amounts to 1.8 electrons per platinum atom. Consequently, the adsorbate consists to a large extent of Pt–CO. At higher potentials, oxidised platinum sites are abundantly available and the oxidation of methanol occurs.

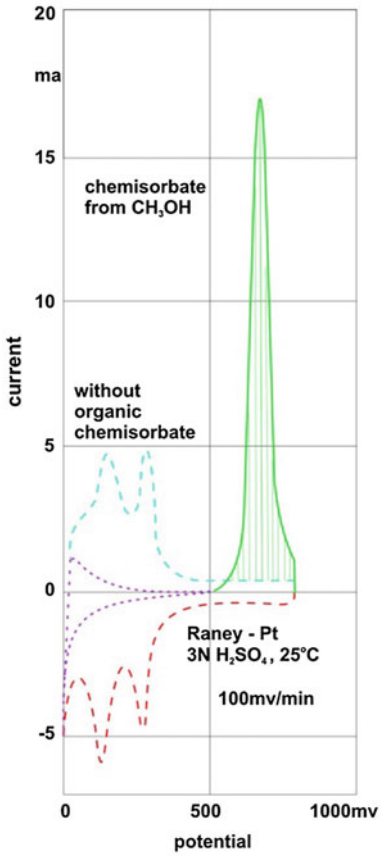

Fig. 6.111 Potentiodynamic current–voltage curve with Raney-Platin with methanol chemisorbate, which is removed by anodic oxidation

Because the potential loss in continuous fuel cell operation by these surface-blocking intermediates would be significant, much R&D effort was designated to this topic, in addition to the methods of surface analysis and the development of improved electrocatalysts compared to platinum. Formaldehyde and formic acid can also be formed under certain conditions, depending mainly on temperature and electrocatalysts.

Anode Electrocatalysts: Stability Against CO

As explained in Sect. 6.5.2.3, CO-like adsorbates block the anode electrocatalyst and prevent methanol oxidation at low potentials. For example, ruthenium is known to form Ru-oxide covered surfaces at much lower potential than platinum, so a Pt/Ru alloy or mixture was assumed to improve electrooxidation of methanol. The Ru–O surface species are able to transfer oxygen to the CO adsorbates on Pt, thus leading to a further oxidation at lower potentials of about 500 mV (see Fig. 6.112).

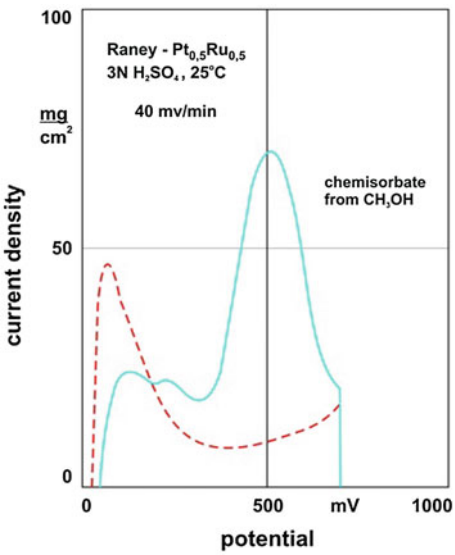

Fig. 6.112 Potentiodynamic current–voltage curve with Raney-Platin-Ruthenium with methanol chemisorbate, which is removed by anodic oxidation

The development of improved electrocatalysts proceeded approximately simultaneously with the research about the mechanism of the anodic oxidation of methanol. Besides ruthenium and other platinum metals, nonnoble metals also have been investigated. Thus, tin and molybdenum have been discovered as alloy components, which increase the activity of platinum. These results have been obtained by several research groups almost in parallel in the 1960s [555, 579–581]. Further groups are mentioned in later works [557, 562].

To demonstrate the activity increase of platinum, two figures from (8) are used. Galvanostatic anodic potential-current density curves of platinum black with molybdenum and other components are shown in Fig. 6.113. A significant improvement by using molybdenum/platinum instead of pure platinum black or addition of tungsten or lead is obvious from the measurements. Corresponding curves with Raney platinum alloyed with gold, iridium, osmium, palladium, rhodium and ruthenium are shown in Fig. 6.114; the activity increases in this order from platinum/gold alloy to platinum/ruthenium.

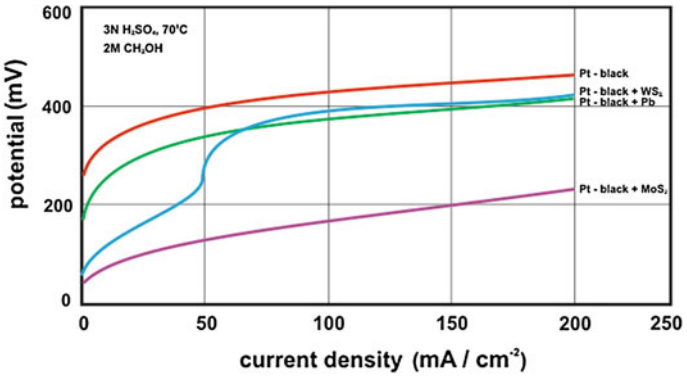

Fig. 6.113 Stationary current–voltage curves with platinum black and Mo, Pb, or W

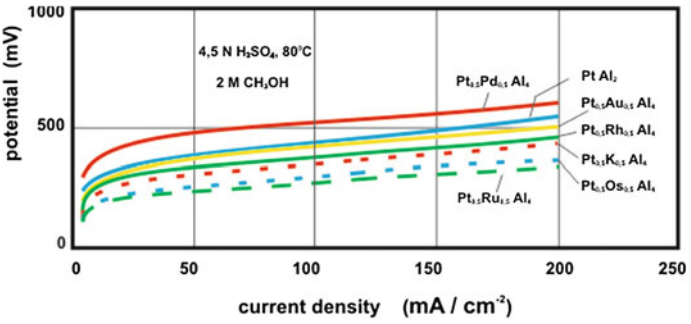

Fig. 6.114 Stationary current–voltage curves with Raney platinum alloys, especially $Pt_{0.5}Ru_{0.5}$

Furthermore, the activity increase depends on the percentage of the additional components in the platinum alloy. The dependence of the activity for the methanol oxidation (true current density) on the composition of the platinum-ruthenium alloy is displayed in Fig. 6.115. In this case, 30 % ruthenium gives the maximum effect.

Later on, even more active catalysts using ternary or even quaternary alloys with platinum as the basic catalyst alloyed with further noble and non-noble metals were investigated [562, 582–588]. Nevertheless, a quite high noble metal content of the electrode still is required in order to achieve stable operation at acceptable power density.

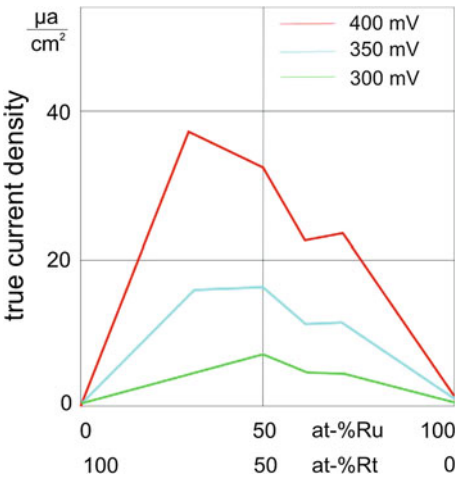

Fig. 6.115 True current density for methanol oxidation on Raney platinum-ruthenium at 70 °C, 3 N H_2SO_4 and 2 M CH_3OH

Cathode Electrocatalysts: Stability Against Methanol

Basically, the cathode side of the DMFC remains unchanged in comparison to a hydrogen-fueled cell. In the case of DMFCs, the anode is limiting the current density and even higher over voltages occur with methanol oxidation than with oxygen reduction, if the electrochemical reactions are carried out separately in so-called half-cell arrangements. Thus, the lessons learned by improving PEMFC with respect to cathode electrocatalyst were directly transferred to the DMFC.

A closer look analysing the surface of platinum as cathode catalyst shows that the surface is covered with oxide species at positive potentials. The mechanism of the oxygen reduction reaction representing a transfer of four electrons per oxygen molecule in order to form water directly has to be considered in detail. At first, two electrons are transferred to give hydrogen peroxide:

$$O_2 + 2H^+ + 2e^- \rightarrow H_2O_2 \tag{6.50}$$

The H_2O_2 will not electrochemically be reduced further to give water because the equilibrium potential according to Eq. 6.52 amounts to 1.77 V, which means that this reaction is very improbable. Therefore, the further reaction of H_2O_2 is the chemical disproportionation [552, 557].

$$H_2O_2 + 2H^+ + 2e^- \rightarrow 2H_2O \tag{6.51}$$

$$2H_2O_2 \rightarrow 2H_2O + O_2 \tag{6.52}$$

In acid electrolyte, the standard potential of the oxygen electrode is 1.23 V; the corresponding potential of the hydrogen peroxide formation is lower with 0.682 V. If both reactions can occur at the cathode during operation, the potential decreases to a value of a mixed potential (Fig. 6.106) and thus the efficiency of the cell also decreases. In addition, H_2O_2 accelerates corrosion processes.

The objective of the catalyst research is therefore to improve the surface properties in such a way that the adsorption of the oxygen molecule is stronger so that up to four electrons can be transferred and H_2O_2 formation be avoided. This can be achieved by alloying platinum with non-noble metals such as chromium and cobalt; ternary alloys are best. Such catalysts also have already been developed for the hydrogen/oxygen PEMFC.

As mentioned in Sect. 6.5.2.2 and shown in Fig. 6.106, methanol is being transferred through the membrane material, especially at low current density—a process that is called methanol cross over. Thus, methanol, air and catalyst are present in the cathode chamber. The electrocatalyst of the cathode, finely dispersed Pt on carbon, is active for direct chemical methanol oxidation, even at low temperatures. Thus, methanol is combusted and heat is released. If the combustion reaction is not fast enough, mixed potentials are formed, leading to a reduction in cell voltage. This effect could be avoided if the catalyst and thus the potential of the cathode were not influenced by the presence of methanol. Again, ruthenium was found to be an effective additional compound for improving the platinum catalyst. Thus, ruthenium is active for methanol oxidation at the anode; at the cathode, it is effective for the protection of the oxygen reduction against methanol. By now, there are more components and compositions known, such as sulphur compounds [589] and Chevrel phases [590–592]. Further information about this subject can be found in the literature [576, 585, 593–596].

In liquid alkaline electrolyte, the problem does not occur or is negligible. The best catalyst for the cathodic oxygen reduction is silver. However, also in alkaline electrolyte, the four-electron mechanism is not likely to occur. The reduction will also proceed via the peroxide step, namely forming of the peroxide ion (Eq. 6.53).

$$O_2 + H_2O + 2e^- \rightarrow HO_2^- + OH^- \tag{6.53}$$

Again, the further reaction of HO_2^- is a chemical disproportionation [552, 560]:

$$2HO_2^- \rightarrow 2OH^- + O_2 \tag{6.54}$$

Silver has a big advantage because it does not catalyse the methanol oxidation, which is of importance for the alkaline DMFC (see Sect. 6.5.2.5).

Cell Structures: Electrolytes

In principle, in addition to acid, alkaline electrolytes are also suitable for DMFC. The alkaline electrolyte is methanol in aqueous KOH solution; the acid electrolyte typically is a sulphonated polymer as proton exchange membrane. From the electrochemical reactions, it can be seen that the reaction mechanism is different. In alkaline solution (Eq. 6.55 and 6.56), hydroxyl ions are consumed at the anode and water

and CO_3^- is formed, with acid electrolyte gaseous CO_2 (see Eq. 6.37 and 6.39). For a liquid alkaline electrolyte, dilution occurs in the anode loop upon operation.

$$CH_3OH + 8OH^- \rightarrow CO_3^{2-} + 6H_2O + 6e^- \quad \text{anode reaction} \tag{6.55}$$

$$1.5O_2 + 3H_2O + 6e^- \rightarrow 6OH^- \quad \text{cathode reaction} \tag{6.56}$$

$$CH_3OH + 1.5O_2 + 2OH^- \rightarrow CO_3^{2-} + 3H_2O \quad \text{total reaction} \tag{6.57}$$

At the cathode, hydroxyl ions are formed (but less than are consumed at the anode), and water is consumed. Therefore, balancing measures are required: the removal of water from the (anode) electrolyte and the transfer of OH^--ions from cathode to anode and the removal of precipitated K_2CO_3. A porous separator is used in order to separate the reactant gases during operation, requiring accurate differential pressure control.

In acid mechanism, the protons are formed during methanol oxidation; they migrate to the cathode and there, product water is formed. CO_2 is released again in the anode chamber. In a DMFC with a solid membrane electrolyte, the water is partly evaporating and carried out of the cell with the cathode off-gas; water and methanol as well have to be fed to the anode of the acid DMFC. In acid DMFC, liquid is only present in the anode chamber; the cathode is a usual gas-consuming electrode.

If an acid DMFC with liquid electrolyte is used, a gas diffusion electrode is required for the cathode, separating the air from the liquid electrolyte but still enabling the electrochemical reaction. A hydrophobic electrode with fine pores has been developed for alkaline fuel cells, enabling transfer of oxygen and preventing the electrolyte from penetration. Sufficient current densities can only be achieved if a large surface area of the triple-phase boundary (electrode, electrolyte and gas) can be achieved. The possibility of using PTFE as binding material for the electrodes was discovered by many research groups in the 1960s, by Kordesch, Sandstede, Winsel and others [552, 560, 597, 598]. The latter developed a rolling process to fabricate suitable electrodes from PTFE mixed with silver catalyst powder. This process was the basis for air-breathing electrodes in the chlorine electrolysis.

Methanol Crossover

In DMFC with an acid electrolyte, protons with hydrate shells migrate from anode to cathode; in an alkaline cell, hydroxyl ions migrate from cathode to anode. This difference explains why methanol crossover is a more severe problem in acid electrolytes [599]. Because various power losses add up in a DMFC, R&D efforts were undertaken to determine the losses due to methanol crossover. Chemical analysis has been used to determine the transfer through the membrane during stand still, flushing the cathode with an inert gas. However, when a current is drawn from such a cell, the only possible electrochemical reaction at low cell

voltage is the oxidation of methanol. Thus, the methanol crossover could be determined in terms of a current density. A typical result [600] is depicted in Fig. 6.116. For many years, polymer scientists developed membrane materials with lower methanol crossover to diminish the losses [571, 591, 592, 601].

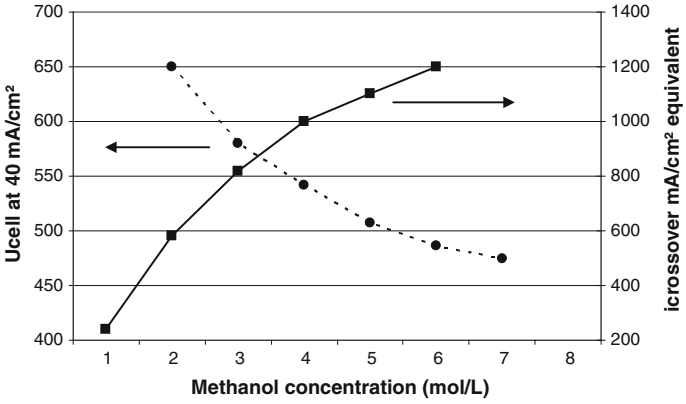

Fig. 6.116 Concentration dependence of cell voltage and methanol crossover at low current density of a liquid-fed direct methanol fuel cell. Nafion 105 temperature = 90 °C. Anode: Pt/Ru at 5.3 mg/cm^2, pa = 0.15 MPa, flow 4 mL/min. Cathode: Pt at 6.4 mg/cm^2 pc = 0.3 MPa, flow = 4 L/min

6.5.2.6 Types of DMFC

Dissolved Fuel Cells

As explained in Sect. 6.5.2.5, liquid methanol can be fed to the fuel cell in alkaline electrolyte or in a mixture with water (compare also Fig. 6.110). A high methanol concentration would be desirable to achieve a high current density and (for the purpose of fuel storage) a high energy density. The first goal proved not to be simply realizable because high methanol concentrations led to high methanol crossover and thus high fuel losses (see Fig. 6.116).

In the acid DMFC with proton exchange membrane, technical solutions were investigated. In principle, it should be possible to store pure methanol in the tank of the system, to close the water cycle in the cell by condensing humidity from the cathode gas stream, and to use a methanol sensor in order to keep the methanol concentration in the fuel in an optimal range. For several years, the development of methanol sensors was an important field for R&D and many different measuring principles have been patented: density, refractory index and infrared absorption, to name a few. This type of fuel cell was developed to first systems and marketable products (see Sect. 6.5.2.7).

Vapour-Fed DMFC

Instead of using a liquid methanol–water mixture as fuel, it is likewise possible to construct the fuel cell in such a way that the fuel mixture can be fed as vapour into the cell [602]. For this purpose, a vapourising device can be incorporated in the fuel cell system, by which a mixture of methanol and water vapour is produced. This fuel gas is introduced to the fuel compartment of the DMFC system (Fig. 6.110) and then distributed into the anode chambers of the stack. After the reaction of the methanol at the anodes to yield carbon dioxide, the remaining methanol water vapour mixture is condensed in a cooling unit to separate it from the carbon dioxide.

During the operation, the whole DMFC system has to be kept at a higher temperature (e.g. 150 °C). Of course, the materials (including the electrolyte membrane) have to be mechanically and chemically stable at this temperature. At a first glance, this concept poses a membrane material problem. Typical sulphonated membranes are known to swell as well in contact with methanol and water; the swelling becomes more pronounced at elevated temperatures. Thus, the gain in kinetics, resulting in higher current density at a given electrode potential, may be overcompensated by fuel losses by crossover through the swollen membrane. It should be stated that the methanol will not be reformed during the operation at the electrode catalyst. The higher performance would make the vapour-fed DMFC especially suitable for the drivetrain of a bus and truck. Therefore, research is continuing for the optimisation of this DMFC [562, 597]. The typical membrane materials being used in PEMFC and DMFC do not fulfil the stability requirements. Thus, vapour-fed DMFC has not yet been developed to marketable systems.

Alkaline Direct Methanol Fuel Cell

Typically, DMFC is called a fuel cell, which contains an acid electrolyte; this means that the gaseous carbon dioxide, being the oxidation product of methanol, will not be dissolved in the acid solution and thus is able to escape off the cell. Also, in a cell with a proton-conducting membrane, the membrane will reject the carbon dioxide. In contrast, carbon dioxide would not be formed because the complete oxidation of methanol would result in the formation of carbonate ions if an alkaline medium were present. The electrochemical reactions are given in Eqs. 6.50–6.52.

The alkaline methanol fuel cells were the first to have been developed because they had a big advantage. The electrocatalyst for the oxygen electrode was silver, which did not have any activity for the methanol oxidation. Thus, it was not necessary to separate anolyte and catholyte completely. Furthermore, the catalysts were cheaper than those for the acid electrolyte, which were derived from platinum.

Otherwise, a platinum metal catalyst would be necessary for the methanol oxidation in alkaline electrolyte, but here methanol is not so strongly bound to the catalyst surface as in acid electrolyte. Regarding the mechanism of the methanol oxidation in alkaline electrolyte, there are a lot of investigations [552, 554, 558, 560, 598, 603, 604]; some of these results are described in Sect. 6.5.2.9.

A few examples of the first alkaline DMFCs are cited here, which were developed in the early 1960s. Some of them were single cells with a performance of about 1 W [552, 603], whereas others consisted of stacks with a power of up to 100 W [552, 559]. The Battelle Institute in Frankfurt, Germany described an alkaline methanol cell in 1961; the electrodes had a size of 13 cm^2. A small stack of several cells with a total surface size of 60 cm^2 was subsequently presented in 1964 and a 30-watt methanol battery was exhibited in 1967. The single cell, shown in Fig. 6.117, served as a demonstration object for electrochemistry courses at DECHEMA (the German Society for Chemical Engineering and Biotechnology) for decades. The anodes of these cells were made from nickel together with a Raney-palladium catalyst, which was alloyed with further metals; the hydrophobic cathodes were produced from nickel, silver carbonate and polytetrafluoroethylene (PTFE) as well as some filler. The voltage-current density curves obtained with the Battelle methanol battery are shown in Fig. 6.118 [554, 605–607].

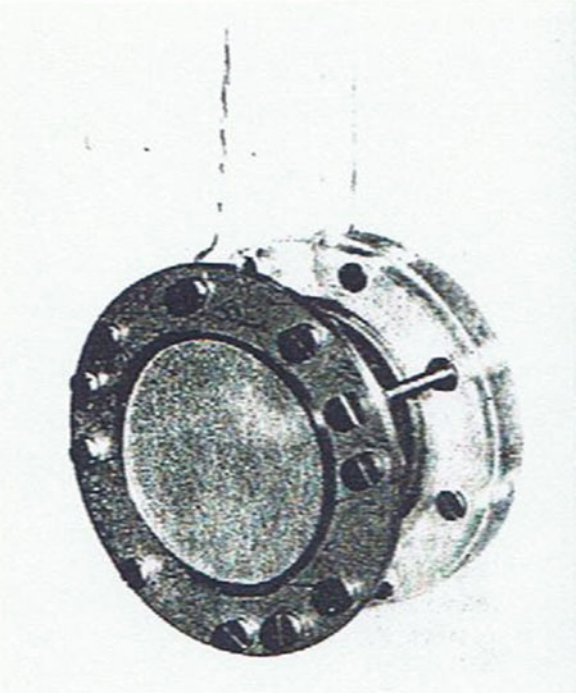

Fig. 6.117 Single alkaline DMFC with approximately 7-cm diameter (ACHEMA 1961)

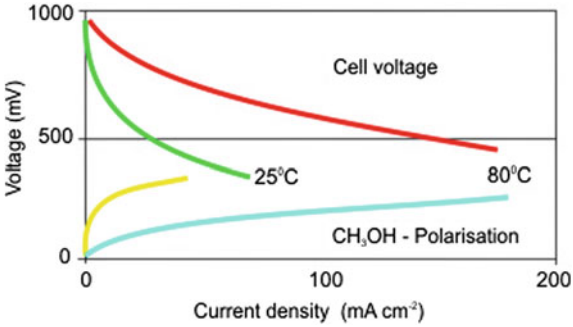

Fig. 6.118 Alkaline methanol cell voltage and polarisation versus current density

6.5.2.7 Indirect Methanol Fuel Cell Systems

Characteristics of the Indirect Systems

The importance of the indirect methanol fuel cell system (IMFC) is increasing because the technology practically is a PEMFC, which has meanwhile been developed to be a reliable and cost-effective product. On the other hand, the methanol reformer is also very advantageous, as has been described already. The IMFC is also called the reformed methanol fuel cell (RMFC) [608].

In Sect. 6.5.2.5, it was shown that methanol can be used as a fuel for practically all possible fuel cells; in Sect. 6.5.2.4, the properties of gaseous fuels are listed. Most fuels have to be converted before feeding them into the fuel cell. In this chapter, the technology of the methanol-reforming reactions are described. Because the limited power density of a DMFC could not be overcome yet, the combination of a methanol reformer with a PEMFC is an interesting concept. Of course, the additional weight and volume and efficiency loss of the reforming unit has to be compensated by the smaller, more efficient and cheaper fuel cell [561, 566, 609, 610].

Because there are several possibilities of conversion of methanol into a reformat that can be fed into a fuel cell, the basic reactions are described in this subchapter, before the different applications are explained in Sect. 6.5.2.8. The big advantage of methanol over other fuels, such as hydrocarbons, is the fact that its reforming takes place at relatively low temperatures; therefore, the technical apparatus can be extremely compact. The steps in the total fuel processing sequence are summarised in Fig. 6.119.

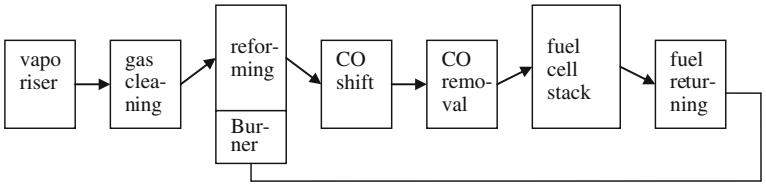

Fig. 6.119 Fuel processing of methanol and its conversion to heat and electricity (gas cleaning and CO shift are optional)

Because methanol is a synthetic product, it can be very clean. It does not contain any disturbing ingredients like products derived from crude oil, which often contain sulphur, which is a poison for the catalyst. However, if it stems from a reprocessing of used products, it may also contain sulphur. In that case, a gas cleaning apparatus, especially for sulphur removal, has to be introduced. After that, the conversion of methanol vapour to reformat can take place. It can be carried out in three different ways, which may comply with the application of the whole system. To discuss this situation, the three reaction equations are presented here and the thermodynamic enthalpies are given for all the substances in the gaseous state:

$$\text{Dissociation} \quad CH_3OH \rightarrow CO + 2H_2 \quad \Delta_R H = +90.9\,\text{kJ/mol} \tag{6.58}$$

$$\text{Reforming} \quad CH_3OH + H_2O \rightarrow CO_2 + 3H_2 \quad \Delta_R H = +49.3\,\text{kJ/mol} \tag{6.59}$$

$$\text{Partial oxidation} \quad CH_3OH + 0.5O_2 \rightarrow CO_2 + 2H_2 \quad \Delta_R H = -192.2\,\text{kJ/mol} \tag{6.60}$$

The dissociation is a kind of decomposition, which takes place at a relatively low temperature, namely 200–250 °C. Although it is a simple process, it is applied quite seldom because the carbon monoxide is harmful for the platinum catalyst of the fuel cell. The CO content of the reformate must be less than 10 ppm; this concentration is tolerated by the platinum electrocatalyst of the fuel cell. The higher the temperature in the reformer is, the more carbon monoxide can be formed according to reverse shift reaction (Eqs. 6.4.2-9). Also, nonhomogeneous concentration profiles may occur. Therefore, it is necessary to remove most of the rest of the CO in a further reactor (Fig. 6.119 and Sect. 6.5.2.6).

Furthermore, there is a method of influencing the CO concentration by the steam-to-methanol ratio, which can be seen in Fig. 6.120. That is why the process is typically run with an excess of steam. Although the stoichiometric ratio is 1, a ratio of 1.5 is often used for the feed.

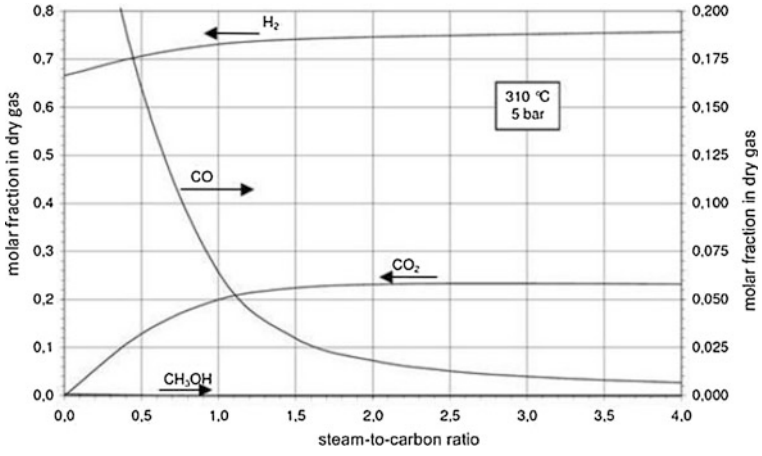

Fig. 6.120 Methanol reforming; gas composition versus steam-to-methanol ratio

The third way of generating hydrogen from methanol is not really a reforming reaction but a partial oxidation; however, for the sake of classification it is subsumed under reforming. This reaction is exothermic and does not need additional heating of the reformer, only initial heat for ignition (see Sect. 6.5.2.5). Depending on the conditions of reforming and the way the fuel consumption is controlled, there may be an anode off-gas, which can be returned and used in the burner of the reformer if necessary (see Fig. 6.119).

Historically, the development of reformers started in the 1960s. The Battelle Institute in Frankfurt developed a reformer that was used for the reforming as well as the splitting of methanol at approximately 250 °C with a Zn/Cu-catalyst from BASF. This reformer was connected to a fuel cell with an anode containing a tungsten carbide catalyst and a hydrophobic air cathode. The carbon monoxide being formed according to Eq. 6.58 was partly anodically oxidised and did not harm the catalyst. The electrodes of this laboratory assembly had a diameter of approximately 10 cm; it was demonstrated at the ACHEMA exhibition in Frankfurt/Germany in 1970 [611]. The device, shown in Fig. 6.121, was run for months without any loss in performance, which accounted for about 100 mA/cm^2 at room temperature.

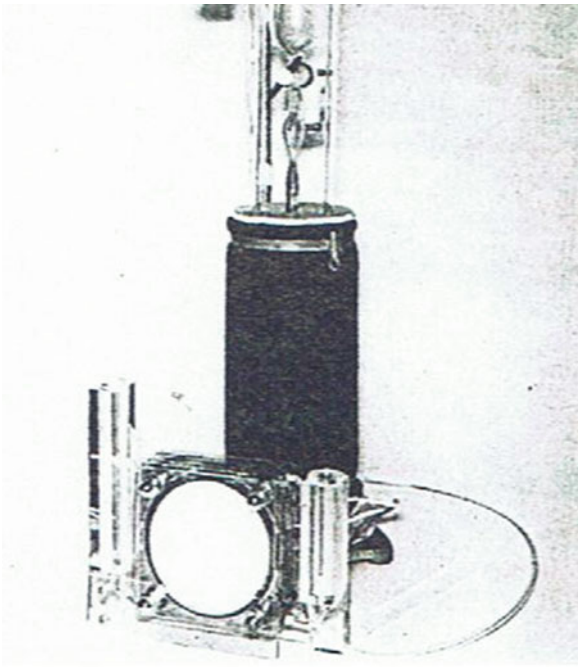

Fig. 6.121 Methanol reformer and reformat fuel cell (ACHEMA demonstration 1970)

Syngas Production from Methanol

According to thermodynamic data, methanol should be easy to reform and different reactions can be used to generate hydrogen from methanol. Besides steam reforming and partial oxidation, auto-thermal reforming has been developed as a combination of both of the processes. The first step of each reforming process is the vapourisation of the fuel and (if required) of the educt water. In any case, heat is required to operate a reforming reactor, which can be supplied by a burner or by using waste heat from any part of the process or a combination of both.

The steam reforming of methanol is kinetically inhibited; a significant reaction velocity even in presence of a suitable catalyst cannot be observed at temperatures below 150 °C. According to the thermodynamic equilibrium, methanol conversion should be complete at that temperature already and the highest possible yield of hydrogen will be achieved. As catalyst, Cu/ZnO on aluminium oxide has set the standard. In a temperature range between 250 and 300 °C, steam reforming leads to a gas with high hydrogen content. For the dry gas and complete conversion, 75 % would be the theoretical limit, with the remaining 25 % being CO_2. But at 300 °C, for example, when the reaction velocity is high, the shift reaction leads to a significant CO content in the product gas. The higher the temperature in the reforming reactor, the higher the CO concentration in the reformate will be, according to Eq. 6.4.2-9. The Cu/ZnO catalyst is active for this reaction as well.

The important thermodynamic data are

Steam reforming of liquid educts: $\Delta_R H^0 = +131.4\,\mathrm{kJ/mol}$

Steam reforming of gaseous educts: $\Delta_R H^0 = +49.3\,\mathrm{kJ/mol}$

Heat of evaporation for methanol: $\Delta_V H = +37.6\,\mathrm{kJ/mol}$

Heat of evaporation of water: $\Delta_V H = +44.0\,\mathrm{kJ/mol}$

It can be seen that a higher amount of heat is required to vapourise methanol and water than is required for the steam reforming of the gas mixture.

For partial oxidation, oxygen (air) is supplied to the reforming reactor and ignition is sufficient to start the exothermic reaction. Partial oxidation could even occur without any catalyst. Typically, however, a catalyst is used because the product water of the combustion reaction can be used for achieving higher hydrogen yields by CO conversion and methanol steam reforming. For partial oxidation of methanol, noble metal catalysts have mainly been investigated because they are active at low temperatures and much more stable than transition metal catalysts. If the stoichiometric ratio of educts is applied, the reaction of partial methanol oxidation releases $\Delta_R H^0 = -192.5$ kJ/mol.

The autothermal reaction is a combination of partial oxidation and steam reforming. The condition of net reaction enthalpy is reached with the following stoichiometry [612]:

$$CH_3OH + 0.1O_2(+0.4N_2) + 0.8H_2O \rightarrow CO_2 + 2.8H_2 + (0.4N_2) \qquad (6.61)$$

Without the dilution by nitrogen from air and with perfect selectivity of oxygen to react with the carbon atom, the hydrogen content could theoretically amount to nearly 74 %.

The product gas being generated by a methanol reformer can be fed directly to high- and medium-temperature fuel cells; even the HT-PEMFC is able to tolerate the typical CO levels of some vol% CO in the fuel. Only for PEMFC is a further CO removal required.

The possible CO removal processes being developed and applied in fuel cell systems in the past decades include the following:

- Shift reaction
- Selective oxidation
- Selective methanisation
- Membrane separation.

The shift reaction typically plays a minor role because the CO content of reformat from methanol already is quite low, and the best catalyst for low temperature shift reaction is Cu/ZnO.

The selective oxidation is carried out by feeding a small air stream into the reformate using a highly selective catalyst. Only special formulations of noble metals exhibit the required selectivity, avoiding significant hydrogen losses:

$$CO + 0.5O_2 \rightarrow CO_2 \quad \Delta_R H^0 = -284\,\text{kJ/mol} \tag{6.62}$$

The best selectivity of this exothermal reaction is typically only achieved in a narrow temperature window.

For methanisation, the reaction conditions also have carefully to be controlled because methanisation of CO and CO_2 can compete. Even if the selectivity of the catalyst is high, remarkable amounts of hydrogen are consumed.

$$CO + 3H_2 \rightarrow CH_4 + H_2O \quad \Delta_R H^0 = -206\,\text{kJ/mol} \tag{6.63}$$

Nevertheless, the methanisation might be interesting when the anode off-gas of the fuel cell is used in a burner. In addition, safety aspects are in favour of methanisation compared to selective oxidation because feeding air to a reformate gas stream implies some risks.

Palladium separation membranes for hydrogen purification are known from various applications. This technique also has been considered to be suitable for separation of hydrogen from reformate. To achieve good selectivity and sufficient hydrogen flux through the membrane, the membrane itself has to be adapted and a pressurised system concept has to be developed. Typically, a palladium-silver alloy for an operation temperature of about 300 °C is applied. Because this operation temperature of the membrane is quite close to that of a methanol steam reformer, the combination of these technologies has been successfully realised. The liquid educts water and methanol can be pressurised without much energy effort.

From a thermodynamic point of view, the efficiency of a methanol reformer can be calculated from the heating values of the product hydrogen (and CO) and of methanol:

$$\eta = \mathrm{LHV}(\mathrm{H_2})/\mathrm{LHV}\ (\mathrm{CH_3OH}) \tag{6.64}$$

For steam reforming, this simple calculation would lead to an efficiency value of 107 %, not taking into account the heat that is required to perform the process. If the heat of reaction has to be covered by combustion of methanol, the required amount of educt would increase and a maximum efficiency value of 75.8 % is the result.

6.5.2.8 Applications for DMFCs

Overview on Different Technologies for Applications

As described in section Sect. 6.5.2.5, DMFCs in general exhibit a quite low energy efficiency, require a higher amount of expensive noble metal loadings on the electrode catalysts, and also achieve limited current densities. Thus, for a required total system power, a DMFC is always much more expensive and also larger than a hydrogen-fueled fuel cell. Therefore, the DMFC so far has been developed for applications with limited power (about 100 W) and long run times [613–616]. Examples of such applications include the following:

- Remote sensors, such as fire detection in forests
- Military applications, such as power for soldiers
- Leisure applications, such as mobile homes
- Consumer electronics, such as grid-independent battery charging systems
- Light traction applications, such as scooters
- Forklift trucks or other material handling systems.

For all these applications, volume and weight are critical (except perhaps forklift trucks). Robust systems that are simple to operate are a basic requirement for commercialisation.

The first results of research and development towards higher power are described in here. An argument for using methanol as fuel instead of hydrogen is easy handling and refuelling by connecting a new methanol containing canister to the system. Various DMFC systems have been realised and tested. The first power generators are already commercially available, with some tens of thousands being already sold, mainly to the military sector but also to owners of mobile homes. The most important company to date is SFC Energy (Brunnthal, Germany).

Commercial DMFC System by SFC Energy

The SFC DMFC system is marketed under the brand name EFOY in a power range from 25 to 110 W. In the hybrid system, a battery is charged by the fuel cell.

The battery voltage is monitored and the fuel cell is automatically started if the voltage drops below a threshold value and also is automatically switched off as soon as the battery is fully charged. This results in reliable, continuous power, reduces the battery capacity needed and extends the lifetime as damaging deep discharge conditions can be avoided. In this hybrid system, the high power density of batteries is favourably combined with a high-energy density DMFC system. The DMFC is operated at constant power, as fluctuating demand is covered by the battery. Long-term autonomy is achieved for the application, as is long lifetime for the fuel cell (up to 5 years warranty is given).

In SFC's fuel cell systems, water recycling is realised, making the use of 100 % methanol as replacement fuel possible. Thus, including all efficiency losses, 31 kWh of electricity can be generated from a 22 kg fuel cartridge. Up to now, several thousand camping cars and mobile homes have been equipped with an EFOY fuel cell system, adapted to the 12 V onboard electricity systems. The industrial market is growing. Whenever small amounts of energy are needed in off-grid or rural areas such as along highways, coasts, or in the mountains, DMFC are a suitable power source. In many examples, a 1 km distance to the grid is worthwhile for a fuel cell installation because it will pay off within the first month. Examples for stationary applications are traffic management, environmental data acquisition, surveillance and security applications and even applications in the wind industry. SFC offers a portable fuel cell system JENNY 600S including a fuel cell and a Li-battery with a volume lower than 3.5 L and a weight less than 2 kg. This backpack system uses 350 ml methanol cartridges and can provide 25 W continuous for 16 h before a replacement cartridge is needed.

For military applications, SFC also provides a power managing device together with the portable fuel cell, which allows the user to set the output voltage for up to four different connected devices to the level needed. The SFC power manager also provides charging features for lithium batteries, and a solar cell or a vehicle power outlet can also be connected.

For on-board power supply in vehicles, DMFCs offer long autonomy and reduced weight. Because many specialised vehicles of authorities need a lot of electronic equipment to communicate, receive data and send data, cost and weight savings can be achieved by using such a fuel cell (Figs. 6.122, 6.123, 6.124).

Fig. 6.122 The EFOY Pro fuel cell on board a vehicle

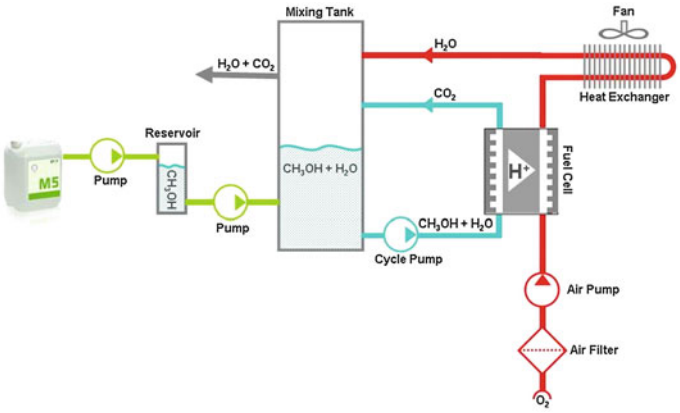

Fig. 6.123 Operation principle of the EFOY direct methanol fuel cell system

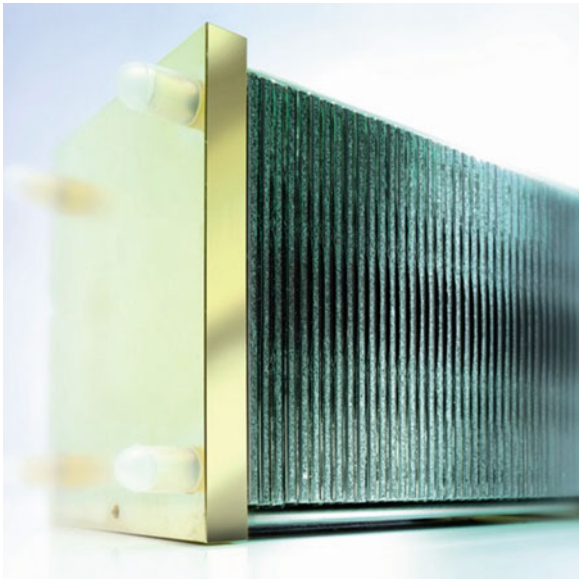

Fig. 6.124 Direct methanol fuel cell stack

Further Examples of Portable DMFC Devices

In the electronic sector, a charger for mobile phones was introduced in 2008 by Toshiba into the Japanese market. The first limited edition quickly sold out, but the improved capacity of Li-Ion accumulators seemed to hinder further commercialisation.

A number of chargers on the basis of a DMFC have been developed by research institutes [617, 618]. An effective technology was developed by Gottesfeld et al. of the Los Alamos Laboratory in 2000, and a 50 W system was applied by the Ball Aerospace Corporation. Another charging device with another technology was

developed by Jörissen of ZSW in Ulm and demonstrated in 2002, shown in Fig. 6.125. A dozen or so examples for portable DMFC devices can be found in literature [584]. There are a number of institutes in Germany (DLR, FZJ, HIAT, ICT, ISE, ZBT, ZSW) that continue research about methanol fuel cells. A further example is shown in Fig. 6.126, a micro-DMFC system of 100 W; it was developed in the frame of the Project Battext in cooperation with the DLR, University of Stuttgart ICVT and the companies Freudenberg FCCT, Staxon, and Kopf Solarschiff in 2010. This battery extender can be used in numerous portable, mobile and stationary applications. Meanwhile, a 1 kW system has been developed.

Fig. 6.125 Direct methanol fuel cell charging device by ZSW

Fig. 6.126 Micro-direct methanol fuel cell of 100 W, applied as support for the solar battery system, by DLR

Stringent miniaturisation might be a further chance for DMFC systems for future industrial application; robust power supplies to moving parts of robots and other systems in the factory automation might be another future chance. Passive air breathing stacks and systems have been demonstrated by various companies (e.g. Motorola, Toshiba, Sanyo, MTI micro fuel cells) and research institutions (Jet Propulsion Laboratory), but so far a breakthrough has not been achieved.

DMFC Applications for Light Traction

At the U.S. National Renewable Energy Laboratory, the development of DMFC for forklift trucks (pallet jacks) was pursued within a 2-year project (2011–2012). It is expected to achieve longer runtime and lower greenhouse gas emissions because methanol from renewable sources shall be used. For the battery in this designed hybrid energy system, a longer lifetime is expected as well. The project partner Oorja Protonics will have access to operational data from 75 pallet jacks being equipped with this DMFC system (OorjaPac). Within this project, methanol infrastructure is regarded as well. The outdoor storage and indoor dispenser for the methanol are not expected to be costly.

Pictures of the forklift trucks, including the methanol hybrid energy system, are shown in Figs. 6.127 and 6.128. The OorjaPac units act as an on-board battery charger, allowing grid independence. Battery change-out is eliminated by this construction. In addition, there is increased autonomy by quick refuelling with methanol and up to 14 h on single refuelling [619]. One big warehouse company said that they will initiate deployment of DMFC units at all sites.

The OorjaPac unit is a variant of a PEM fuel cell system that uses an anode catalyst to extract hydrogen from the methanol molecule; therefore, the anode catalyst for methanol is not much different from that for hydrogen. The specifications

Fig. 6.127 OorjaPac direct methanol fuel cell power pack

Fig. 6.128 OorjaPac direct methanol fuel cell power pack

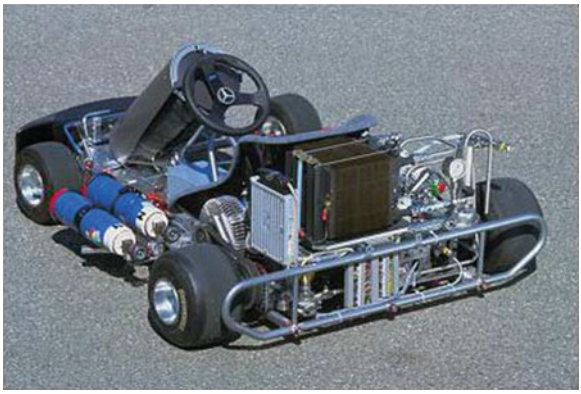

Fig. 6.129 Daimler-Go-Cart with direct methanol fuel cell technology

of the OorjaPac model 3 embrace a power output of 1.5 kW; an output voltage of 24, 36 and 48 V; a methanol tank volume of 12 L; and therefore an energy output of 20 kWh per tank.

In 2003, Daimler developed a drivetrain for a Go-Cart on the basis of DMFC technology [620], which is shown in Fig. 6.129. Net power of the DMFC system is approximately 2 kW [621]. Apparently, the amount of noble catalysts was too high for a commercial product. Daimler continued catalyst research, but so far no new results have become known.

FZJ researchers have been engaged for many years in the development of DMFC drive trains for light traction. The first DMFC system was put into operation in a conventional scooter in the year 2004 [622, 623]. Pictures of the scooter are shown in Figs. 6.130 and 6.131. The DMFC stack consists of 100 cells and has a nominal power of 1.3 kW and a peak power of 1.9 kW. As can be recognised from Fig. 6.131, the DMFC stack is a real drive train, which is exchanged for the battery inside the scooter for the operation of the electric motor. Thus, it is not a hybrid system.

A drive module for a forklift truck was also demonstrated by FZJ, which has been developed since 2007 [624]. This DMFC system, which is shown in Fig. 6.134, is a kind of hybrid system with a battery. The DMFC stack has a nominal power of 1.3 kW and the total system has a peak power of 7 kW, which

Fig. 6.130 Scooter with direct methanol fuel cell drive train, by FZJ

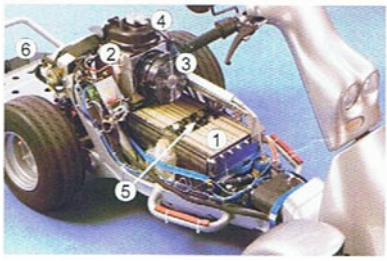

Fig. 6.131 Scooter with the FZJ direct methanol fuel cell (DFMC) drive train, showing a look inside

mainly stems from the battery. Because the nominal power is also the steady state power, the MEAs deliver a permanent power density of 75 mW/cm^2 at a voltage of 450 mV, which means a good success, but the noble metal loading is still a bit high (4.5 mg/cm^2) (Fig. 6.132).

Fig. 6.132 Direct methanol fuel cell battery hybrid system, by FZJ

6.5.2.9 Applications of the Indirect Methanol Fuel Cell Systems

Remarks About the Advantage of the IMFC Systems

The main differences between DMFC and PEMFC with a methanol reformer is the elevated temperature of the reformer (~300 °C). A laser welded compact ($90 \times 32 \times 100$ mm^3) integrated reformer and burner prototype has been developed by the Institut für Mikrotechnik, Mainz (Germany) for applications up to 100 W (see Fig. 6.133).

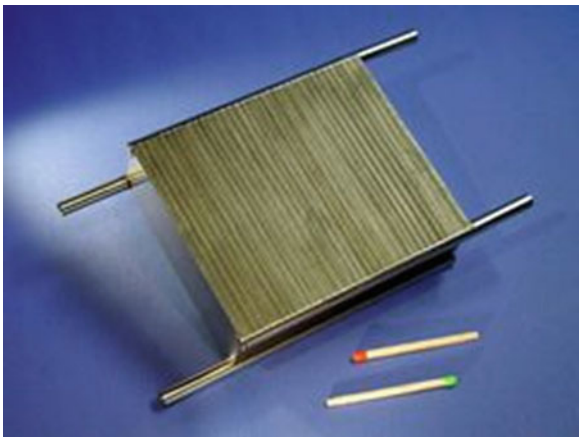

Fig. 6.133 Microstructured methanol reformer of Institut für Mikrotechnik Mainz

According to the data given in Sect. 6.5.2.3, the reformate gas contains about 1 vol% of CO. This reformat can be fed directly without further purification to every fuel cell except to low-temperature PEMFC. For PEMFC, a fine purification reactor for CO has to be included in the system. Although this two-staged fuel processor is more complicated, the first commercially available systems used this principle. At present, they directly compete with the DMFC as well, related to the target applications and also with respect to cost.

The company Ultracell (USA) is engaged in developing methanol reformer PEMFC systems. In 2007, the company announced that they participated in a contest being performed by the U.S. military. Additionally, the Danish company Serenergy is marketing a RMFC with a HT-PEMFC with a power output of 350 W, a volume of 27 L and a weight of 13.7 kg. As a new chance for an even simpler and more compact power generator for methanol as fuel, an integrated reformer/HT-PEMFC system (see Fig. 6.134) has been developed in several R&D projects. The waste heat of the HT-PEMFC being operated at temperatures up to 200 °C shall be used optimally for the vapourisation of the methanol–water mixture. Low-temperature reforming might be possible because the hydrogen being formed is consumed instantaneously upon formation, and thus a shift in equilibrium is possible.

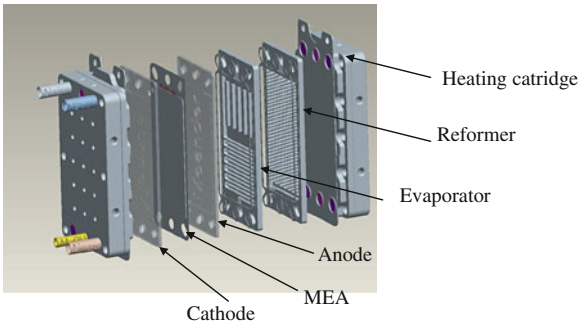

Fig. 6.134 Laboratory prototype of an integrated reformer/high-temperature proton electrolyte membrane fuel cell module (ZBT)

This approach combines a simple reformer with a hydrogen fuel cell with good power density. Due to good heat integration, the system might be the smallest in comparison with DMFC and reformer/low-temperature PEMFC. For startup, electrical heaters or (catalytic) methanol burners are required because neither the fuel cell nor the reformer can be started at room temperature. This leads to a somewhat extended startup period.

According to recent investigations, CO is not converted electrochemically at the HT-PEMFC anode. This means that the possible release of CO from the system has to be avoided by a postcombustion process, using the anode off-gas for delivering additional heat to the fuel processor (see Fig. 6.119).

At present, methanol as fuel is not state-of-the art for transportation or domestic use, so the possible applications will remain limited. The more renewable electrical power will be used, the more important is the generation of storable fuel. The first step will be the generation of hydrogen, but the second step could be the synthesis of methanol, thereby leading to more applications for methanol fuel cells.

Interim Development of Passenger Cars with IMFC Drive Train

The first research car with methanol reformer was developed by Daimler in 1997 (Figs. 6.135 and 6.136) [625], and 1 year later an Opel/GM-Zafira with methanol drive train was presented [626].

Around the year 2000, the car manufacturers did not yet know which fuel would be best for which fuel cell for driving a car. Therefore, they experimented with all possible fuels: gaseous hydrogen, liquid hydrogen, methanol, gasoline, diesel, sodium hydride, ethanol and others. LBST shows a complete compilation of all those experimental cars from the year 1807 until now in Wikipedia under the heading "Hydrogen and Fuel Cell Vehicles Worldwide". Cars with IMFC drivetrains have been listed from Daihatsu, Daimler, Ford, Georgetown University, Honda, Hyundai, Mazda, Mitsubishi, Nissan, Opel/GM, Subaru, Toyota and Volkswagen. All these automobile companies presented complete prototypes that could have been used for starting a model series.

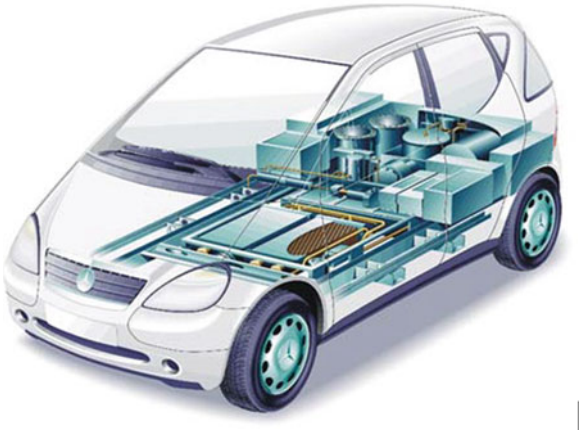

Fig. 6.135 NECAR III methanol reformer and fuel cell (1997)

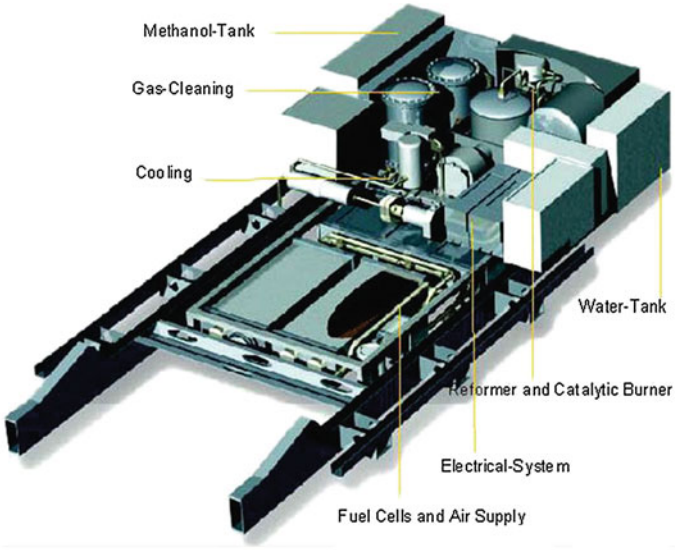

Fig. 6.136 NECAR III underfloor concept

The NECAR 3 by Daimler (NECAR = new electric car) got a successor, the NECAR 5, which was a comfortable car like other conventional cars. From Figs. 6.137 and 6.138, it can be seen that the volume for the complete reformer and fuel cell was limited to a sandwich floor of the car.

Not only the volume but also the weight was reduced drastically, altogether by more than 300 kg. The PEMFC from Ballard was improved to a great extent.

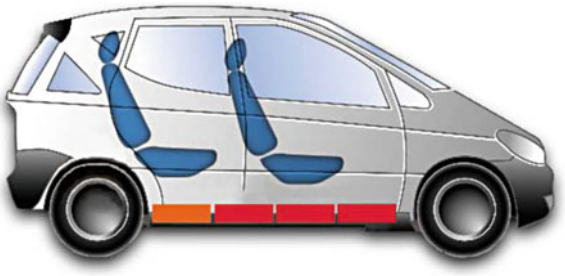

Fig. 6.137 NECAR 5 methanol tank (orange box), reformer and fuel cell (red boxes) in the sandwich floor (1998)

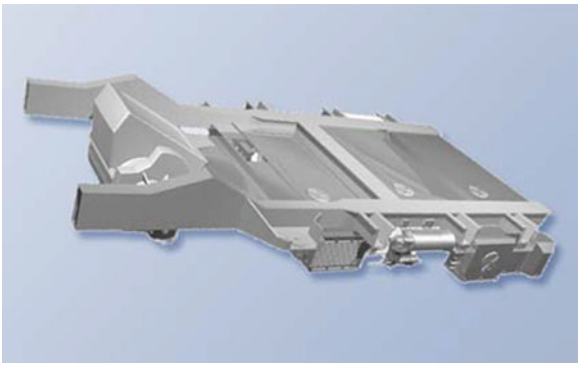

Fig. 6.138 NECAR 5 fuel cell system

Whereas NECAR 3 had two stacks with 150 single cells and a power of 50 kW in total, NECAR 5 was equipped with only one stack, whose nominal power amounted to 75 kW. The operational temperature was kept to 80 °C. The catalyst for the reforming was developed by BASF and was also improved. The tank volume amounted to 38 L, which covered a travelling distance of 300 km. The rated power of the electric motors amounted to 45 and 55 kW and the top speeds to 120 and 150 km/h for NECAR 3 and 5, respectively.

Although there was no cooperation between the two big automobile companies, their fuel cell cars had similar data. The first methanol car of Opel was presented a few months later. Its electric motor had a power of 50 kW, which was sufficient for a top speed of 120 km/h. The methanol tank capacity was approximately 54 L and the water tank was approximately 20 L.

Thus, the cruising range was somewhat higher. The curb mass was 1,850 kg. Figures 6.139 and 6.140 show the first prototype car by Opel, in which the methanol reformer system appears to be a small chemical plant on board the car.

Together, Daimler, Ballard, BASF, BP, Methanex and Statoil founded the Methanol Fuel Cell Alliance. They issued together a joint position document in 2002, in which they declared that their objective would be to go on the market very soon [621]. A few years later, most developments of methanol cars were stopped because the car manufacturers and oil companies changed their mind and decided

Fig. 6.139 Opel/GM-Zafira methanol concept car with reformer and fuel cell (1998)

Fig. 6.140 Opel/GM-Zafira methanol concept car with reformer and fuel cell in the rear

to continue on the basis of hydrogen. There is still some research going on, but it is unclear whether methanol will play a role in the general automobile market in the future. Despite this, special applications may still come out one day.

Special Applications of IMFCs

As was mentioned in Sect. 6.5.2.7 about the practical application of DMFC systems, there are likewise quite a number of examples for IMFC systems that could be described. In particular, two publications should be referred to when looking for demonstration of IMFCs, namely those by Garche, [612, 627] including the first book about IMFC, titled *Methanol Fuel Cell Systems: Advancing Towards Commercialization*. Among other companies, he mentioned IdaTech and Protonex Technology., which developed two IMFC systems called ElectraGen3 and ElectraGen5, rated with 3 and 5 kW respectively.

More recently, a new type of combination system was demonstrated. The company Wärtsilä started with the development of an ideal power source for special services, the power of which should be 10 or 50 kW or even more. They were the first to present an indirect fuel cell system using a SOFC. Early in 2011, they teamed up with Versa Power Systems (VPS), a developer of high-power SOFCs with headquarters in Littleton, Colorado, USA. Wärtsilä had developed reformers for an IMFC and an indirect hydrocarbon fuel cell, and they looked for a suitable fuel cell to combine with. Therefore, they presented the first IMFC system with a SOFC fuel cell. The target of the agreement with VPS was to develop commercial Wärtsilä fuel cell products that generate power and heat for various applications in the distributed energy, including marine markets. The demanding objective was to use the power source also on-board of a ship, which meant that it had to comply with outstanding environmental requirements. Figures 6.141, 6.142 and 6.143 show pictures of the transportation and installation of the WFC20 fuel cell unit on board the Swedish Wallenius Lines [628].

The WFC20 is a fuel cell system of a methanol reformer and a SOFC with a power of 20 kW. The development and installation has been carried out by the international METHAPU consortium, whose participants are Wärtsilä, Wallenius Marine, Lloyd's Register, Det Norske Veritas and the University of Genoa, who are active in the field of fuel cell system integration and environmental assessment in shipping.

Fig. 6.141 Wärtsilä's WFC20 fuel cell unit in operation

Fig. 6.142 Wärtsilä's fuel cell unit WFC20 started its journey in Finland

Fig. 6.143 Installation of the Wärtsilä WFC20 fuel cell unit on-board of the "Undine" of the Swedish Wallenius Lines

6.5.2.10 Conclusion

History of the Methanol Fuel Cell

A few steps were especially important for the development of the DMFC and the IMFC. The fuel cell effect was discovered with gaseous reactants as early as 1838 by Schönbein in Basel, who published it in the January 1839 edition of the (*British*) *Philosophical Magazine*. At the same time William Grove, who lived in London and who was a friend of Schönbein, carried out similar experiments (namely electrolysis of dilute sulphuric acid) and measured a voltage afterwards, while hydrogen and oxygen gases were present at the electrodes. He published it in the February 1839 edition of the same magazine. Whereas Schönbein investigated the effect further and discovered ozone, Grove recognised that he had invented a gaseous battery, as he called it; therefore, he knew that he had discovered an electricity generating device. The reason for his quick recognition was that he had invented several battery elements before [629, 630].

Therefore, the continuation of the research about the fuel cell effect lead to the investigation of a solid fuel, namely coal, which did not find success, even now. After all, one has to take into account that the designation "fuel cell" was used in 1889 (by Mond and Langer for the first time) and that the mode of operation of a fuel cell was recognised in 1894 by Wilhelm Ostwald, who got the Nobel Prize for his work on catalysis a few years later. Thus, the basis was laid for a target-oriented and purposeful research about fuel cells for technical applications. Despite these facts:

– it took a lot of time until the first investigation of a fuel cell with methanol as a dissolved fuel was carried out by Taitelbaum in 1910 [552].

– There were only few investigations about the electrochemical oxidation of methanol every now and then in the course of time. The next researcher was Müller 1922, and then Kordesch and Marko dealt with dissolved fuel cells and proposed the DMFC with alkaline electrolyte in 1951. It took a further 10 years or so for real DMFCs to be developed. All of a sudden, a number of groups presented cells or stacks during the 1960s—some with alkaline electrolyte and some with acid electrolyte or both. Among the first were Justi in Braunschweig and Vielstich in Bonn, along with their students, as well as the Battelle Institute in Frankfurt and the companies Allis Chalmers, Bosch (Fig. 6.144), Esso, Shell, Siemens and Varta (Fig. 6.145) [631].

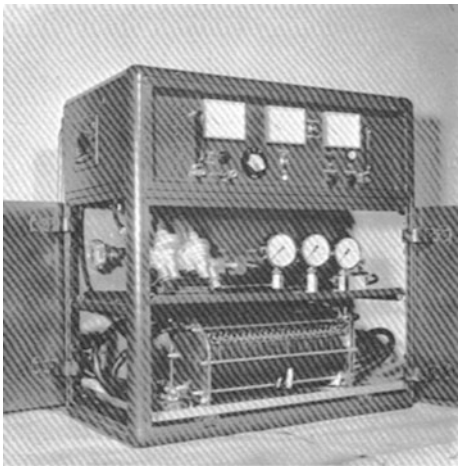

Fig. 6.144 Alkaline direct methanol fuel cell with a power of 100 W, developed in the 1960s by the Bosch company

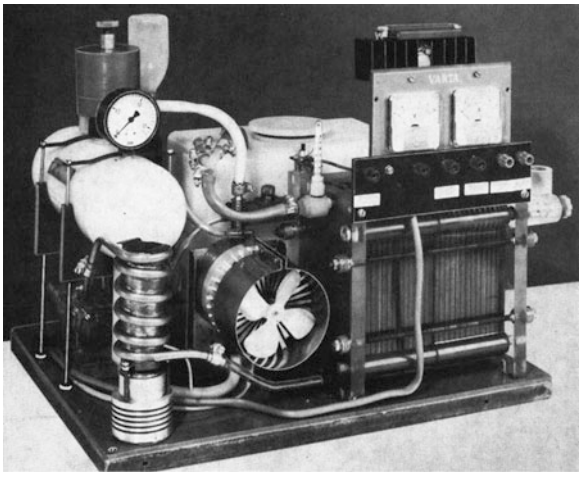

Fig. 6.145 Alkaline direct methanol fuel cell with a power of 140 W at 60 °C, developed in the 1960s by the Varta company

Fig. 6.146 Direct methanol fuel cell module of a power of 300 W with acid liquid electrolyte, developed in the 1960s by Shell Research

Shell and Esso tried to develop real prototypes of DMFC with acid electrolyte, but were not satisfied with the durability of the stacks. One example is shown in Fig. 6.146.

From the mid-1960s until the end of the 1990s, the progress was slow. However, many companies, especially small companies, tried to develop small portable DMFC units, as has been reported in Sects. 6.5.2.5 and 6.5.2.7. The DMFC was based on the same components as the PEMFC in the 1980s; after this, the hydrogen fuel cell type won great success in the 1990s. Two examples may be mentioned—the equipment of submarines with H_2/O_2-PEMFCs by Siemens and the development of the electrotraction of passenger cars and buses with compressed hydrogen/air-PEMFCs by many automobile companies all over the world, as a preparation of electromobility of the traffic for environmental reasons [630].

Also, Siemens developed a small DMFC of the PEMFC type, whose design data and performance results were already quite interesting. It was a three-cell stack for the purpose of demonstration; the operational area of the electrodes amounted to approximately 550 cm^2 and the working temperature was about 90 °C. The electrocatalyst of the anode consisted of supported platinum-ruthenium of an amount of 2.6 mg/cm^2 and the one of the cathode contained platinum, approximately 4 mg/cm^2; the methanol concentration (methanol/water mixture) amounted to 0.5 M. A current density of 0.1 A/cm^2 and a voltage of 0.5 V were measured. Thus, the little methanol battery delivered a power of 83 W at an efficiency of 42 % and of 113 W at maximum [632].

DMFC batteries in the kW range were also successful; they have been described in Sect. 6.5.2.7. They were useful for special applications; however, for a broad applications concerning passenger cars, the units are still too expensive, which mainly originates from the noble metal loading of the electrodes. Therefore, the automobile industry changed to the other type of methanol cells, the IMFC. The cars with drivetrains with IMFCs have been developed around the year 2000; they have been described in Sect. 6.5.2.9. The development of the IMFC drive

train systems was not yet completely finished when a decision about the future transportation fuel had to be made, which is known to have become hydrogen. As was described in Sect. 6.5.2.9, special applications of the IMFC are just in the process of entering the market.

Prospects of Methanol Fuel Cells

Reflecting about the prospects of methanol fuel cells, one has to investigate (in our opinion) the objectives of the existing developments of the various types of methanol cells. Furthermore, one has to find out whether these objectives can be extrapolated into the future, if this is desirable at all, and whether there are possibilities to change them (either to expand or to narrow them for whatever reason). In addition, the discussion has to deal with the technological goals as well as the commercial targets. To detect these indicated objectives, it is helpful to look into the history of the different methanol fuel cells so far developed (see Sect. 6.5.2.9 and elsewhere in this publication).

In addition, the description of the broad technological field of the fuel cells, which can use methanol as fuel, in the preceding chapters can be completely divided into two areas. All the very different modes and designs—be they of a microscale or a size up to megawatts-can be allotted to the DMFC type or to the indirect methanol fuel cell type (IMFC). If one considers the situation from the technological side and has observed the huge spectrum of possible kinds of methanol fuel cells, then there is certainly no loss of hope for a suitable new type of DMFC or IMFC in the future.

What has to be considered as a main goal for each new device is the target of an acceptable and appropriate cost and price situation. This situation depends either on the task you will substitute for or on the new task the fuel cell will attack to solve. There are two main functions for which the methanol fuel cell can be applied. First, it can be a powering device for any situation, to make electricity available at remote spots, and even to provide a backup facility. This may be a substitute for a battery, which has been used for this purpose up to now and which does not fulfil the requirement of being as reliable and durable as the new fuel cell. On the other hand, methanol fuel cells can be used as a charging device for a battery. Commercial examples have been described in Sect. 6.5.2.7. They are called “on-board battery charger” or “fuel cell battery hybrid system” and are in general powering devices.

The second group of methanol fuel cells are the IMFCs, which are practically a combination of a PEMFC and a reformer for methanol, which changes the methanol into hydrogen. Now, the importance of the indirect methanol fuel cell, which is also called reformed methanol fuel cell, is increasing because the hydrogen fuel cell has meanwhile been developed to a reliable and cost-effective product and the methanol reformer has also made good progress and can be developed to any size. Therefore, the IMFC is an ideal system and can also be applied as a drivetrain for all kinds of vehicles. Although the big automobile

manufacturers have decided to use the pure hydrogen system as fuel cell drive for passenger cars, there are enough future mobile applications for the methanol system.

The DMFC needs a bit longer for the introduction into the consumer market. However, this market is not satisfied with the accumulator technology for the time being and is expecting a portable power source of small sizes quite soon. At present, from the efficiency point of view, the DMFC may be a niche system for small power applications. After all, various DMFC systems have been realised and the first power generators are already commercially available, with some tens of thousands being already sold (mainly to the military sector but also to owners of mobile homes). Up to now, about 30 companies are involved in relevant fuel cell development. In addition, the state of the art of fundamental research shows that there is a big amount of basic knowledge still missing, which means that university and high school research is necessary and can support the education and training of very many students, who carry the progress of science and technology. It may be possible that fuel cells will change the telecommuting world by powering all kinds of digital handheld devices in the not-too-distant future. In addition, all other applications of methanol fuel cells will profit from the situation mentioned.

Methanol is a commercial fuel suitable for stationary, vehicle and military applications, but as at present, it is not the state of the art for transportation or domestic use. The more renewable electrical power will be used, the more important is the generation of storable fuel. The first step will be the generation of hydrogen, but the second step could be the synthesis of methanol, thereby giving more applications for methanol fuel cells a chance. In addition, we must not forget that approximately 50 % of the energy generated is not electricity but heat; thus, the heating of a mobile home or any other room or piece would save a large amount of energy.

The advantage of methanol fuel cells is that they are able to cope with a lot of demands and requirements, be they of legal or societal nature. Thus, DMFC devices can be used in airplanes, including the cartridges for the fuel, either as pure methanol or methanol–water mixtures. However, the demands for the methanol fuel cells are much broader and eclectic. They are to supply electrical energy in form of very clean energy so that the process of powering is not a burden for the environment and that everything operates sustainably. Raw material has to be preserved and the fuel efficiency must be as high as possible. Furthermore, two problems of mankind can be solved by methanol: Biomass can be easily changed into methanol and thus is available as energy source; and garbage can also be easily changed into methanol and thus removed from the surface, presenting clean energy in the process.

6.5.3 Methanol in Biotechnology

Sebastian Hippmann[1], Martin Bertau[1], Dirk Holtmann[2], Frank Sonntag[2], Thomas Veith[2] and Jens Schrader[2]

[1]*Institute of Chemical Technology, Freiberg University of Mining and Technology, Leipziger Straße 29, 09599 Freiberg, Germany*

[2]*DECHEMA Research Institute, Theodor-Heuss-Allee 25, 60486 Frankfurt/M., Germany*

Introduction

Methylotrophs play a key role in the global cycling of C_1 compounds and offer biotechnological opportunities for the production of commodity chemicals from methanol [633]. The major proportion of the annual plant-released methanol does not enter the atmosphere. The methanol is converted by methanol-oxidising prokaryotes. These methylotrophic bacteria belong to different classes including Proteobacteria, Verrucomicrobia, Firmicutes and Actinobacteria. The wide variety of bacteria (and also yeasts) are able to grow in inexpensive synthetic media with methanol as the sole or major source of carbon and energy. This is due to the presence of a few unique enzymes that enable these organisms to generate metabolic energy and synthesise cell constituents from this one-carbon substrate. As a feedstock for industrial fermentations, methanol is also attractive because of its low cost, ease of handling and abundant availability [634]. Furthermore, methanol is often used as a carbon source in biological wastewater treatment plants and as fuel in biofuel cells; it also can be produced by biological components.

6.5.3.1 Metabolism and Physiology

Metabolism of Methylotrophic Bacteria

Methylotrophy can be defined as the ability of (micro-)organisms "to grow at the expense of reduced carbon compounds containing one or more carbon atoms but containing no carbon–carbon bonds" [635]. Thus, besides methane and methanol, methanesulphonate and other methylated sulphur species, methylated amines, the halogenated hydrocarbons chloromethane, bromomethane and dichloromethane also can serve as sole carbon and energy source—either exclusively or in addition to methanol. Methylotrophy research dates back to 1906 with the discovery by Soehngen of a bacterium growing on methane or methanol, *Bacillus methanicus,* which was later renamed as *Methylomonas methanica*. Nowadays, numerous bacterial methylotrophs are known and several genomes have been published, including the smallest known genome of a (nonparasitic) free living cell to date: the marine methylotroph *Methylophilales bacterium* HTCC2181 [636]. Phylogenetically, bacterial methylotrophs mainly belong to the alpha, beta and gamma subclasses of Proteobacteria or the group of Gram-positive bacteria [637].

In a dissimilatory process, methylotrophic bacteria oxidise the reduced one carbon (C_1) source stepwise to CO_2. Thereby, adenosine triphosphate is generated due to the involvement of electron-transport-coupled phosphorylation. In this process, formaldehyde represents the key intermediate. It is the first intermediate after the oxidation of methanol. Besides its function in the dissimilatory pathway leading to CO_2, it also serves as input for C_1 assimilation pathways in methylotrophs (see below). The oxidation of methane to methanol is performed by a subgroup of methylotrophic bacteria, the methanotrophs. Two versions of the respective enzyme, methane monooxygenase (MMO), have been described: a soluble (s) cytoplasmic MMO and a particulate (p) membrane-bound MMO. Both enzymes are regulated due to the availability of copper. sMMO (a non-heme iron-containing enzyme) is expressed under low copper conditions, whereas pMMO (with a di-copper centre in the active site) is expressed under high copper conditions [638–640]. This biological methane oxidation is remarkable because the chemical methanol synthesis is a three-stage catalyst-requiring process, whereas the MMO reaction is carried out directly with di-oxygen [641]. Most attention has been focused on the iron-containing sMMO, especially from the species *Methylosinus trichosporium* and *Methylococcus capsulatus.* The ability of MMO to activate methane at room temperature and ambient pressure makes it an attractive target for research toward a potential enzymatic large-scale production of methanol [642].

After the uptake of methanol or its generation from methane in the case of methanotrophs, methanol is further converted by methanol dehydrogenase to formaldehyde. So far, periplasmic pyrroloquinolin quinone (PQQ)-dependent methanol dehydrogenases have been described for Gram-negative bacteria as well as nicotinamide adenine dinucleotide phosphate (NADP)-dependent enzymes in Gram-positive bacteria [643, 644]. The following conversion of toxic formaldehyde to CO_2 by methylotrophs can be achieved by several (linear or cyclic) pathways, of which some can occur in parallel within one organism [645]. Exemplarily, co-factor dependent linear pathways such as the tetrahydromethanopterine (H_4MPT) pathway, discovered in the alphaproteobacterium *Methylobacterium extorquens*, and glutathione (*Paracoccus denitrificans*) and mycothiol (Gram-positive methylotrophs) pathways, should be mentioned as well as the cyclic ribulose monophosphate (RuMP) pathway of Gram-negative Proteobacteria (e.g. *Methylobacillus flagellates*) [635, 646–648]. The latter is nearly identical to the assimilatory RuMP pathway mentioned afterwards (see Fig. 6.147) [635].

The assimilatory incorporation of C_1 compounds of bacterial methylotrophs can be roughly divided into two pathways, with both requiring the aforementioned formaldehyde as precursor (reviewed in Ref. [635]). Assimilation via the RuMP pathway uses all carbon needed from formaldehyde by catalysing the reaction from ribulose-5-phosphate to hexulose-6-phosphate by hexulose phosphate synthase (see Fig. 6.147). In contrast, the serine cycle for carbon assimilation of Alphaproteobacteria (e.g. *M. extorquens*) incorporates CO_2 additionally by carboxylation reactions besides formaldehyde assimilation via serine. This remarkable combination of pathways leads to accumulation of approximately 50 % biomass carbon

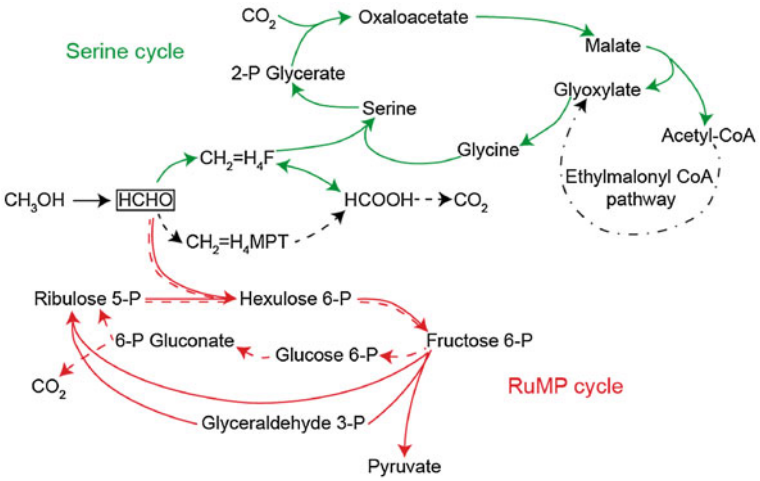

Fig. 6.147 Generalised scheme of methanol assimilation via the serine (green) and ribulose monophosphate (RuMP; red) cycles of methylotrophic bacteria. Note that formaldehyde plays a central role as branch point for all shown pathways (box). Dissimilatory processes are indicated by dashed arrows. The multistep conversion of acetyl-CoA to glyoxylate via the ethylmalonyl-CoA pathway is indicated by a dashed-dotted arrow

from CO_2 and thus to a refixation of CO_2 produced during the dissimilatory process described above [649, 650]. The fixation of CO_2 occurring within central pathways can be calculated from the difference between CO_2-utilising and CO_2-releasing fluxes [651]. Approximately 20 % of the formed CO_2 is recovered, which correlates to 16 % of the consumed methanol.

Although the general understanding of metabolism of methylotrophic bacteria is not as advanced as for model organisms such as *Escherichia coli* or baker's yeast, research on methylotrophy is advancing, especially considering *M. extorquens* is the probably best understood organism within methylotrophic bacteria. With the genome published [652] and a variety of genetic tools at hand, ubiquitous efforts have been made to study its (one carbon and multicarbon) metabolism, including proteome and transcriptome analyses as well as metabolite profiling (reviewed in Ref. [634]). Recently, the activities of all (postulated) enzymes required for methanol assimilation and their regulation in comparison to acetate and succinate grown cells, as well as metabolic adaptation processes occurring during the shift to C_1 carbon metabolism, were published [653, 654].

Physiology and Metabolism of Methylotrophic Yeasts

Contrary to prokaryotic cells, eukaryotic cells are substantially larger and possess membrane-surrounded compartments in which the reaction conditions for metabolic processes are ideally adjusted: short diffusion ways, the enrichment of the intermediates in sufficient concentrations, necessary enzymes and pH value. Thus, different reactions can take place at the same time in the cell without interacting [655].

The only known eukaryotes that can use methanol as carbon and energy source for growth belong to the yeasts (i.e., single-cell fungi). Yeasts are widely spread in nature and occur particularly in the ground and on plants. They have been in use by man for thousands of years in order to manufacture alcoholic beverages and bread. It was not until the nineteenth century that they were cultivated in larger quantities. Yeast cells are 5–10 μm large and they mostly belong to the group of the ascomycota. Their cell shape is predominantly round oval to cylindrical. Reproduction takes place either asexually via budding or sexually via formation of ascospores [656].

Yeasts using methanol for growth are called facultative methylotrophs; these were first mentioned in 1969 by Ogata [657]. "Facultative" means that they are not able to metabolise methane. However, they can use higher oxidised C_1-substrates, such as methanol, or substrates with C–C-bonds, such as glucose as a carbon and energy source [658]. Some important representatives of this group are shown in Table 6.25.

Table 6.25 Name of some methylotrophic yeast (year of renaming) [659]

Common Name	Scientific Name	Other Synonyms
Pichia angusta	*Ogataea angusta* (2010)	*Pichia angusta* (1984)
		Hansenula polymorpha (1959)
		Hansenula angusta (1961)
		Ogataea polymorpha (1994)
Pichia pastoris	*Komagataella pastoris* (1995)	*Pichia pastoris* (1956)
		Saccharomyces pastoris (1952)
		Zygowillia pastoris (1954)
		Zymopichia pastoris (1961)
Pichia guilliermondii	*Meyerozyma guilliermondii* (2010)	*Pichia guilliermondii* (1966)
		Yamadazyma guilliermondii (1989)
		Candida carpophila (2005)
Candida boidinii	*Candida boidinii* (1953)	*Candida methanolica* (1972)
		Candida methylica (1974)
		Candida queretana (1978)
		Hansenula alcolica (1975)
		Kloeckera boidinii (1975)

In nature, these yeasts can be found in spoiled fruits and vegetable products as well as in exudates and the bark of trees [660]. The existence of these eukaryotes in those habitats can be attributed to the fact that methanol becomes available by the degradation of the methoxy-moieties of lignin. Equally, most of the tested methylotrophic yeasts are able to grow on a medium with pectin-a polymer that is rich in methoxy-groups and is ubiquitous in fruit [661]. Unlike bacteria, yeasts are not equipped with methanol dehydrogenase to form formaldehyde. Instead, they possess specialised cell compartments, peroxisomes, in which methanol oxidation occurs. Peroxisomes are round organelles, approximately 0.5 μm large, surrounded by a membrane; they are located in the cytoplasm of eukaryotes. These vesicles proliferate if the cells are exposed to nutrients that require metabolism where peroxisomal

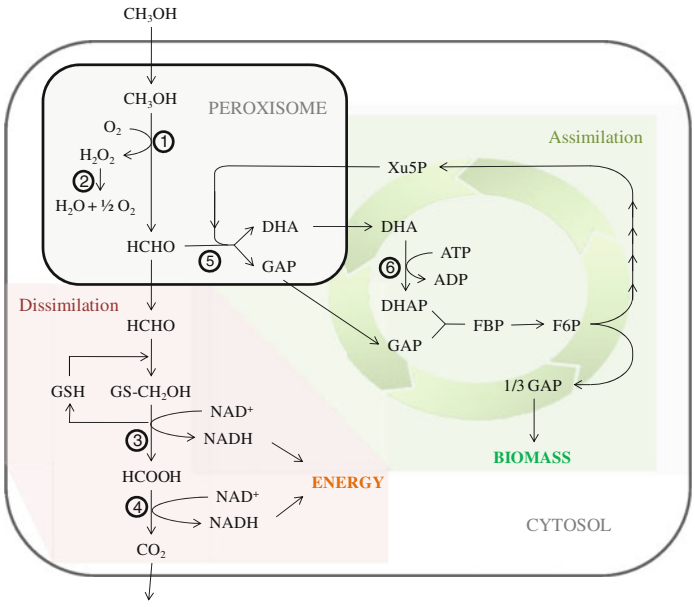

Fig. 6.148 Methanol metabolism pathway in methylotrophic yeasts[663] 1 – alcohol oxidase, 2 – catalase, 3 – formate dehydrogenase, 4 – formaldehyde dehydrogenase, 5 – dihydroxyacetone synthase, 6 – dihydroxyacetone kinase. GSH, glutathione; Xu5P, xylulose-5-phosphate; DHA, dihydroxyacetone; DHAP, dihydroxyacetone phosphate; GAP, glyceraldehyde-3-phosphate; FBP, fructose-1,6-bisphosphate; F6P, fructose-6-phosphate

functions and enzymes are involved. Therefore, in the presence of methanol, they account for up to 80 % of the total cell volume [662]. An overview of methanol metabolic pathways in methylotrophic yeasts is summarised in Fig. 6.148 [663].

Methanol metabolism is initiated by an alcohol oxidase mediated oxidation to formaldehyde, the key intermediate of methylotrophs, which takes place under oxygen consumption. This reaction goes along with hydrogen peroxide formation, upon which H_2O_2 degradation by catalase sets in. Therefore, compartmentalisation of this reaction is an elementary strategy to prevent cell damage caused by formaldehyde and hydrogen peroxide [664]. Subsequently, formaldehyde can be successively dissimilated to CO_2 and reduced nucleotides (energy). In detail, this process encompasses formaldehyde oxidation through the action of NAD^+ and glutathione-dependent formaldehyde dehydrogenase to form *S*-formyl-glutathione. This latter compound can now either be oxidised to CO_2 by formate dehydrogenase (NAD^+ dependent) or it can be hydrolysed by formylglutathione-hydrolase to formate, which is then oxidised to CO_2 by formate dehydrogenase. The assimilation of formaldehyde is accomplished through the xylulose monophosphate cycle. In this pathway, the C_1-entity formaldehyde reacts with C_5-building block xylulose-5-phosphate (Xu5P) to form two C_3-compounds: glyceraldehyde-3-phosphate (GAP) and dihydroxyacetone (DHA); the reaction is catalysed by

dihydroxyacetone synthase. Dihydroxyacetone kinase, the next enzyme involved, phosphorylates DHA to dihydroxyacetone phosphate, which in a next step reacts with glyceraldehyde-3-phosphate to form fructose-1,6-bisphosphate, a C_6-compound. Dephosphorylation leads to fructose-6-phosphate, which is further converted to GAP and Xu5P, thus rendering the pathway ready for the next cycle (Figs. 6.148 and 6.149). To produce one molecule of the C_3-body GAP, which is then funnelled into central metabolism to form biomass, the Xu5P-cycle has to be run three times.

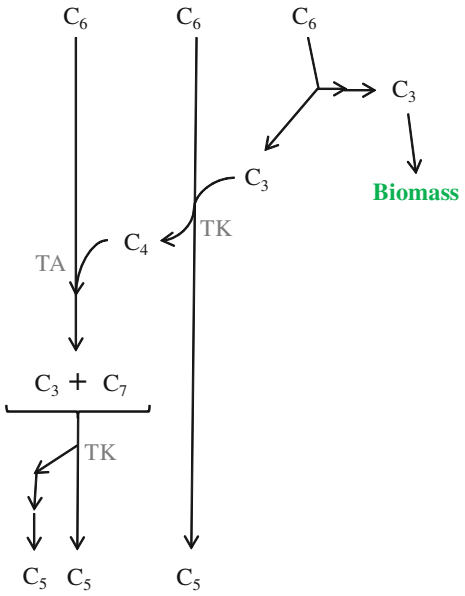

Fig. 6.149 Rearrangement reactions to convert three molecules fructose-6-phosphat (C_6) to three xylulose-5-phosphate (C_5) to keep Xu5P-cycle running [665]. C_3, glyceraldehyde-3-phosphate; C_4, erythrose-4-phosphate; C_7, sedoheptulose-7-phosphate; TK, transketolase; TA, transaldolase

Most yeasts, including the methylotrophic ones, possess "generally recognised as safe" status, for which reason they are used for a huge number of fermentations, as food additives, as a source of vitamins and also as "biofactories" for the production of various antibiotics, steroid hormones, homologous and heterologous proteins, as well as models for studying genetic regulation in eukaryotic cells [666].

6.5.3.2 Growth and Product Formation

Methylotrophic Bacteria

The key issues in the use of methylotrophic bacteria are productivity, carbon conversion efficiency and achievable product concentration. Various authors developed stoichiometric equations for biomass formation on methanol via the RuMP pathway the average values of which are shown in Eq. 6.65 [667–669].

$$1.63CH_3OH + 1.39O_2 + 0.23NH_3 + \text{nutrients} \rightarrow CH_{1.69}O_{0.38}N_{0.24}(\text{biomass}) + 0.63CO_2 + 2.76\ H_2O \quad \Delta H = -449.7\ \text{kJ/mol}_{MeOH} \tag{6.65}$$

The carbon balance shows that approximately 38 % of the methanol is dissimilated and 62 % is used for the formation of cellular mass. An amount of 0.85 g oxygen is required for the oxidation of 1 g of methanol and 0.52 g of carbon dioxide is produced. In Table 6.26, published data for biomass productivities and concentrations as well as yields are summarised. The table shows that high biomass productivities over 25 g biomass per litre an hour can be achieved. Surprisingly, the highest reported biomass concentration was 250 g/l [670]. This value has not been reproduced in the last 15 years. Optimum growth rates for biomass accumulation can be obtained by maintaining low and stable methanol concentrations. High methanol concentrations and sudden concentration shifts cause toxic effects on the bacteria due to the accumulation of formaldehyde [671, 672].

Table 6.26 Examples of growth parameters of microorganisms on methanol

Microorganisms	Pathway	Biomass productivity (g_{CDM} g/l)	Cell dry mass (g/l)	Cell yield (g_{CDM}/g_{MeOH})	Comment	Literature
Methylomonas methanolica	RuMP	25 (potential)	50	0.5	Industrial SCP process	[667]
Methylomonas sp.	RuMP	28.4	114	0.49	Continuous process ($\mu = 0.25\ h^{-1}$)	[673]
Methylobacterium organophilum	Serine	3.6	250	0.34	PHA process	[670]
Methylobacterium sp.	Serine	2	172		PHA process	[674]
Methylobacterium extorquens	Serine	1.2	56.1	0.28	GFP production, recombinant	[675]
Mixed culture		4.55	10.6	0.44	Continuous process	[676]

PHA, polyhydroxyalkanoates; RuMP, ribulose monophosphate; SCP, single-cell protein

Typical products of methylotrophic prokaryotes are polyhydroxyalkanoates (PHA) and amino acids. On the basis of known metabolic pathways, Leak compared predicted carbon conversion efficiencies for diverse products in different microorganisms either growing on methanol or glucose [677]. For extracellular polysaccharides, polyhydroxyalkanoates and glutamate, the predicted conversion efficiencies are similar. This indicates that, for high yielding organisms, methanol-based bioprocesses could be economically competitive. The higher oxygen demand of methylotrophs could be considered as a disadvantage. In the case of glutamate, the oxygen-based yield Y_{P/O_2} is predicted to be two- to threefold lower for the growth on methanol than for the growth on glucose. A comparison of the stoichiometric conversion of methanol to glutamate via either the RuMP or the

serine pathway indicates predicted yields of 0.76 and 0.92 g/g [677], respectively, whereas the theoretical yield for glutamate production of organisms growing on glucose is 0.82 g/g.

Comparison of lysine production by *Bacillus methanolicus* that starts from methanol with lysine production in *Corynebacterium glutamicum*, which employs glucose, shows that the yields were comparable [678]. The theoretical yields for both conversions of methanol to lysine with *B. methanolicus* were $Y_{P/S} = 0.82$ $g_{Lysin\text{-}HCl}/g_{methanol}$ and 0.71 $g_{Lysin\text{-}HCl}/g_{methanol}$, respectively. The highest productivity of PHA was described by Kim et al. [670]. The biomass and PHA formation rate reached 3.57 and 1.86 g h/l, respectively. The highest product yield was 0.2 g PHA per gramme of methanol. A recombinant *M. extorquens* strain produces PHA derivates. By cofeeding methanol and 5-hexenoic acid, functionalised PHA containing C–C double bonds were produced [679, 680].

A genetically modified strain of *Methylobacterium rhodesianum* was used for the production of the chiral compound *(R)*-3-hydroxybutyrate [681]. The product is formed during intracellular degradation of a PHA. In fed-batch cultivation, 2.8 g/l of *(R)*-3-hydroxybutyrate were produced. Wild-type strains of *B. methanolicus* can secrete more than 58 g/l of L-glutamate in fed-batch cultures [682] and mutants of *B. methanolicus* secreted 69 g/l of L-glutamate [683]. A further mutant of *B. methanolicus* produced L-Lysine up to 65 g/l [683]. Further products from the metabolism of methylotrophic microorganisms are polysaccharides [684, 685], indole-3-acetic acid[686], trans-zeatin [687, 688] as well as different proteins such as GFP [675, 689, 690], enterocin P [691], acylamide amidohydrolase [692], haloalkane dehalogenase [693] and an esterase [689, 694, 695]. Belanger et al. [675] carried out fermentation to produce the green fluorescent protein as a model protein to study the recombinant protein production. The maximum specific GFP production was 80 mg/g, representing approximately 16 % of the total cell protein.

Methylotrophic Yeasts

After discovering methylotrophic yeasts' ability to metabolise inexpensive substrates such as methanol, attempts were undertaken to use them for production of single-cell protein (SCP) and metabolites. Yeasts possess the advantages of a fast cell growth, the possibility of simple genetic engineering and simple process preparation due to their size [696].

Among the various yeast cultures studied, *Pichia pastoris* showed particularly high cell yield from methanol, high protein content and stable fermentation characteristics. Without optimisation, *P. pastoris* was slowly growing (doubling time: 5.5–6.0 h) [697]. The reason is that yeasts consume more metabolic energy for synthesis of one C_3-molecule compared to methylotrophic bacteria using the ribulose monophosphate cycle (RuMP cycle) for formaldehyde fixation. A stoichiometric equation with the average values for biomass formation on methanol via the Xu5P-cycle for the methylotrophic yeast *Kloeckera* sp. 2201 is shown in Eq. 6.66 [698].

$$2.06CH_3OH + 2.02O_2 + 0.15NH_3 + \text{nutrients} \rightarrow CH_{1.75}O_{0.5}N_{0.15}(\text{biomass}) + 1.06CO_2 + 3.47H_2O \quad \Delta H = -268.4\ \text{kJ/mol}_{MeOH} \tag{6.66}$$

The ratio of methanol and the formed biomass shows that approximately 49 % of the methanol is used to produce cellular mass and 51 % is dissimilated to gain energy. This is reflected in lower growth yields of yeasts (yeasts: 0.37–0.45 g/$g_{methanol}$; bacteria: 0.55 g/$g_{methanol}$) [699]. Additionally, yeasts have higher oxygen consumption when using methanol as carbon source. For example, for the oxidation of 1 g of methanol to 0.71 g of carbon dioxide by *Kloeckera* sp. 2201, an amount of 0.98 g of oxygen is required. This means this yeast needs 15 % more oxygen than bacteria (0.85 g O_2 per g methanol). Therefore, in order to use these microorganisms in biotechnological applications with methanol as sole carbon and energy source, a specific reactor design is needed (see Sect. 6.5.3.3).

The singular enzymes of methanol metabolism of methylotrophic yeasts offer special applications, which are discussed here. Formate dehydrogenase (FDH; EC 1.2.1.2), which can be obtained from the methylotrophic yeast *Candida boidinii,* catalyses the last step of methanol oxidation in methylotrophs and is located in the cytosol (Fig. 6.148). It consists of two identical subunits of approximately 36 kDa. FDH is moderately thermostable (30–60 °C), is insensitive against oxygen and is active along a broad pH range (pH 5–10) [700]. An important application of this enzyme is, in combination with formate, the in situ regeneration of NADPH or NADH in catalytic systems; the gaseous, volatile product CO_2 allows for easy shifting of the reaction equilibrium to the right (Fig. 6.150) [701, 702].

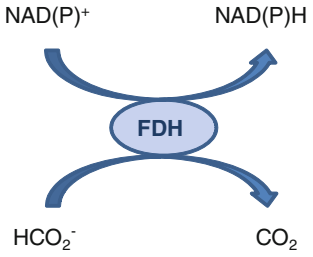

Fig. 6.150 In situ regeneration of NAD(P)H by formate dehydrogenase (FDH)

Because the concept proved successful and fields of applications are so broad, FDH is commercially available and used on an industrial scale in a large set of applications, such as production of tert-L-leucine [701–703]. Also, it was discovered that FDH selectively cleaves formic acid esters to the respective alcohol and carbon dioxide. FDH differentiates between formic acid esters and nonformic acid esters, contrary to hydrolases, which renders this enzyme particularly suitable for protective group chemistry. It was shown that even rather disubstituted esters, such as 1-acetoxy-4-formoxy butane, are a substrate for FDH, which catalysed the cleavage of the formate group while the acetate group remained unaffected [704].

Another enzyme belonging to the metabolism of methylotrophic yeasts is methanol oxidase or alcohol oxidase (AOX, EC 1.1.3.13), catalysing oxidation of

methanol in the peroxisomes to formaldehyde and hydrogen peroxide using oxygen as electron acceptor (Fig. 6.148). AOX consists of eight identical subunits (74 kDa [666]), and each one is noncovalently bound to one FAD as prosthetic group. The AOX has a large temperature and pH range, such as that of *P. pastoris* (temperature: 18–45 °C, pH: 6.5–8.3), under which conditions the enzyme displays at least 50 % of its original activity [705]. AOX oxidises most of the primary short chain alcohols to the corresponding aldehydes, for which reason it is used in combination with oxygen and hydrogen peroxide sensors for the determination of lower alcohols [666]. Additionally, it could be used as a potential catalyst for organic synthesis. It was found that AOX is able to oxidise 2-chloroethanol, 2-cyanoethanol and 2-methoxyethanol to their aldehydes, which are important intermediates in heterocycle synthesis [706]. Furthermore, AOX applications are the production of formaldehyde and hydrogen peroxide. Both were examined on a laboratory scale, obtaining 0.95 M formaldehyde by a mutant of *Candida boidinii* [707] and 10 mM H_2O_2 by chemically treated *Pichia pastoris* cells. The latter could be used for in situ bleaching, oxidising toxic organic compounds and disinfection [708].

Heterologous Gene Expression in Methylotrophic Yeasts

In methylotrophic yeasts, enzymes of the methanol metabolism can be produced in high quantities only by growing on methanol. This circumstance renders them very interesting targets for genetic engineering. A promoter that tightly regulates the AOX gene is responsible for the high expression of these proteins [709].

Methylotrophic yeasts, in particular *Pichia pastoris* and *Pichia angusta*, are used preferentially as expression systems for the production of heterologous proteins because of the easy handling, the inexpensive substrate and the strong methanol-induced promoter, which is missing in the model organism baker yeast (*Saccharomyces cerevisiae*). In addition, high protein yield, the possibility for high cell density approaches and the option for posttranslational modification of proteins render these methylotrophic yeasts attractive in industrial biotechnology. Thus far, more than 500 foreign proteins, including eukaryotic proteins, were successfully expressed, which were accessible in *E. coli* only as inactive inclusion bodies. Foreign proteins can be secreted into the medium, if behind the AOX promoter a secretion-signal sequence is cloned. In Table 6.27, some heterologous proteins are listed, which are produced by methylotrophic yeasts [710, 711].

6.5.3.3 Specific Bioprocess Characteristics

Compared to other microbiological cultivation techniques for the production of bulk chemicals, two important differences have to be considered. First of all, inexpensive, defined mineral media can be used because there is no need to supply the carbon source in a complex matrix, which is usually done to reduce costs in sugar-based fermentations. In addition, ammonia can be added as an inexpensive nitrogen source and costly vitamins or other organic molecules are not required.

Table 6.27 Selection of heterologous proteins expressed in *Pichia pastoris* (Pp), *Pichia angusta* (Pa), *Candida boidinii* (Cb) and *Pichia methanolica* (Pm) successfully

Protein	Mode	Host	Yield	Reference
Bacteria				
Pertussis pertactin protein (*Bordetella*)	C	Pp	3 g/l	[712]
Subtilisin inhibitor (*Streptomyces*)	S	Pp	0.5 g/l	[713]
Tetanus toxin C fragment (*Clostridium*)	C	Pp	12 g/l	[714]
Fungi				
1,2-Mannosyltransferase (*Saccharomyces*)	S	Pp	0.4 g/l	[715]
Adenylate kinase (*Saccharomyces*)	C	Cb	2 g/l	[716]
Alt a 1 allergen (*Alternaria*)	S	Pp		[717]
Catalase T (*Saccharomyces*)	C	Pa		[718]
Dipeptidyl-peptidase V (*Aspergillus*)	S	Pp		[719]
Glucoamylase (*Schwanniomyces*)	S	Pa	1.4 g/l	[720]
Glucose oxidase (*Aspergillus*)	S	Pa	0.9 g/l	[721]
Invertase (*Saccharomyces*)	S	Pa	1 g/l	[722]
Phytase (*Aspergillus*)	S	Pa	13.5 g/l	[723]
Plants				
Cyn d 1 allergen (Bermuda grass)	S	Pp		[724]
Glycolate oxidase (spinach)	C	Pp; Pa		[718, 725]
Malate dehydrogenase (water melon)	C	Pa		[726]
Phytochrome (oat)	C	Pa		[727]
Phytochromes A and B (potato)	C	Pp		[728]
Seed storage protein	C	Pa		[729]
Animal				
Aprotinin (bovine)	S	Pa	0.35 g/l	[730]
Bm86 antigen (tick)	C	Pp		[731]
Green fluorescent protein (jellyfish)	C	Pp		[732]
Hirudin	S	Pp; Pa	1.5 g/l	[733, 734]
Human				
μ-Opioid receptor	S	Pp		[735]
Haemoglobin	C	Pa		[737, 738]
Hepatitis B surface antigen	C	Pp; Pa	0.4 g/l	[738]
Human endostatin	S	Pp	0.02 g/l	[739]
Human glutamate decarboxylase	C	Pm	0.5 g/l	[740]
Human Lewis fucosyltransferase (Fuc-TIII)	S	Pp	0.03 g/l	[741]

Mode: C, cytosolic; S, secreted
Yield: g (protein)/l (medium)

This also significantly reduces downstream processing costs of products that are secreted to the medium. Furthermore, process instabilities caused by compositional variations in complex raw materials can be avoided.

The second important difference in sugar-based processes is the toxicity of the carbon source [671, 674, 742]. On the one hand, this tremendously reduces the risk of contaminations. On the other hand, toxicity has to be considered during the development of appropriate feeding strategies to maximise growth and product formation rates. Methanol has a higher reduction state than sugars; thus methanol

fermentations are characterised by higher oxygen demands. As heat evolution increases with oxygen consumption, the cooling requirements also rise for fermentations using methanol instead of sugar.

Bourque et al. [743]. developed high cell-density processes with *M. extorquens* for the production of PHA. Control algorithms were used to maintain both the methanol and the dissolved oxygen concentration at the desired setpoint value. Suzuki et al. [744]. also described a process for PHA production. Concentration of methanol was maintained automatically at 0.5 ± 0.2 g/l. Dissolved oxygen in the culture broth was controlled in the range of 2–3 mg/l. Kim et al. [670] carried out fed-batch cultures to avoid the inhibitory effect of methanol for cell growth in a 2.5 l fermenter equipped with standard control units and instrumentations. Schendel et al. [745]. carried out fed-batch cultivation of *Bacillus methanolicus* at 50 °C to produce the amino acid L-lysine. The higher fermentation temperature reduces the costs for cooling the reaction system.

The production of single-cell protein with methanol as substrate reached the industrial scale. The ICI process [669, 746–748] used a pressure airlift reactor with inner loop. The working volume was 1,500 m^3, capable of producing up to 50,000 tonnes per year. Under continuous fermentation conditions, runs in excess of 100 days without contaminations have been reported. To optimise the oxygen transfer, the reactor was driven with an overpressure of 0.3 MPa in the head of the reactor [749]. To avoid high, potentially toxic, local concentrations of methanol (>0.2 g/l), the carbon substrate was sparged via 3,000 outlets in the reactor [750].

The ICI process used the methylotrophic bacterium *Methylophilus methylotrophus.* At a maximum specific growth rate of approximately 0.55 h^{-1}, the continuous process was carried out at dilution rates of 0.16–0.19 h^{-1} [677]. Biomass concentration during fermentations reached 30 g/l and maximum cell yield was up to 0.5 g/g. The organism *Methylomonas clara* was used by Hoechst/Uhde, who employed 20 m^3 reactors to reach an annual production capacity up to 1,000 tonnes. The substrate concentration was controlled to a value of 0.005 %. The maximum growth rate was 0.5 h^{-1} and dilution rates of 0.3–0.5 h^{-1} were applied. Under these conditions, biomass production rates of 5 g h/l and a methanol-based biomass yield of 50 % were achieved.

In order to be able to run an industrial process economically, high biomass yields are required. Therefore, it is necessary to optimise medium component concentrations. It was observed that methanol concentration should be less than 6 vol%, to avoid toxic effects [751]. *P. pastoris* is able to grow at high cell density with a continuous mineral nutrient supply. Yeasts usually prefer temperatures of 25–35 °C and have a high oxygen demand when growing on methanol [752]. Consequently, the result of scale-up experiments showed that heat removal and oxygen transfer are the limiting factors on the large scale.

To minimise these limitations, reactors were modified or developed further, eventually leading to the Phillips/Provesta continuous high-cell density, direct-dry process [697]. Cell densities of 125–150 g/l dry cell weight were achieved at a pH of 3.5 and a temperature between 30 and 40 °C [753]. The reactor design allowed for an effective heat exchange and oxygen transfer up to 1 mol O_2/l h. The main

benefit of this particular process was the replacement of cell concentration steps by a direct drying of the culture broth through heat treatment. A 100 % recovery of yeast-soluble products was achieved, in combination with lower operating costs and easier processing [697]. Although SCP from methylotrophic yeasts are rich in essential amino acids and have a high protein content, all SCP production systems based on methylotrophic yeast were not produced any further because it was feared that the cells contain toxic residuals [754]. Additionally, the methanol price is not low enough in order to allow for fermentations being run economically compared to other commercial processes [755]. Yet, the advantages of the Phillips process led to the fermenter design being used for other yeast and bacteria, such as *Torula* yeast grown on sucrose to produce yeast products for human and animal food sector [756]. Today, SCP from nonmethylotrophic yeast is used in the form of yeast extract in small quantities as a flavour-enhancing component in food products or as meat substitutes [755].

6.5.3.4 Further Application of Methanol in Biotechnological Processes

Methanol as Carbon Source in Biological Wastewater Treatment

Denitrification is the biological reduction of nitrate to nitrogen gas by facultatively heterotrophic bacteria. Denitrification occurs when oxygen levels are depleted and nitrate becomes the primary oxygen source. The process is performed under anoxic conditions, when the dissolved oxygen concentration is less than 0.5 mg/l. For the denitrification process, the bacteria need a readily degradable carbon source such as methanol. The denitrification process can be described by Eq. 6.67.

$$6NO_3^- + 5CH_3OH \rightarrow 3N_2 + 5CO_2 + 7H_2O + 6OH^- \quad (6.67)$$

Methanol as a carbon source in denitrification has different advantages; it contains no solids and no additional nutrients, has a neutral pH, is inexpensive and contains 100 % readily degradable substrate [757]. The denitrification with methanol as carbon source is an established technique in municipal wastewater treatment plants [758–761]. Nevertheless, there are still some parameters to be optimised. A precise feeding of methanol is necessary. Low dosage rates can lead to an excess of NO_3^- in the effluent. If methanol is overfed, it may result in elevated effluent biochemical oxygen demand concentrations. The addition of methanol can also improve biological phosphorus removal by creating anaerobic conditions and increasing the availability of organic carbon in wastewater for polyphosphate accumulating organisms [759]. Unlike acetate, long-term application of methanol has no negative impact on the settling properties of the sludge.

Methanol Biofuel Cell

Biofuel cells are fuel cells that employ biocatalysts to convert chemical energy into electrical energy. The main types of biofuel cells are defined by the type of biocatalyst. Microbial biofuel cells employ living cells to catalyse the oxidation of

the fuel, whereas enzymatic biofuel cells use enzymes for this purpose [762]. There is growing interest in enzyme-based biofuel cells as a source of renewable and sustainable power [763]. They are attractive for special applications, such as implantable devices, sensors, drug delivery, microchips and portable power supplies. Several drawbacks, such as short lifetimes and low power density, limited enzyme-based biofuel cells from being used for practical applications.

Methanol oxidation sequentially follows the methylotrophic pathway to give formaldehyde, formate and carbon dioxide [764]. Each oxidation step releases two electrons, yielding six electrons per molecule of methanol. The cofactor nicotinamide adenine dinucleotide (NAD^+) is reduced in the enzyme-catalysed reactions and can be used as mediator to transport the electrons to an electrode. The formal redox potential of NAD^+/NADH is -0.56 V versus a standard calomel electrode [765]. However, the oxidation of NADH by electrodes has poor kinetics and requires large overpotentials. Mediators can be used to reduce the overpotentials and improve the electron transfer rates (Table 6.28). The first methanol biofuel cell used a diaphorase/benzyl viologen system as NADH oxidation catalyst [766]. Electropolymerised mediators such as methylene green, toluidine blue and neutral red can be used as stable catalysts with enhanced activity toward NADH oxidation [765, 767–770]. Often, the stability of the mediator restricts the performance of the biofuel cell [771]. By the addition of aluminium dioxide into the electrode paste, the mediator tetramethyl phenylenediamine can be stabilised.

Table 6.28 Characterisation of methanol biofuel cells

Catalyst	Mediator	Fuel cell characteristic	Literature
Alcohol dehydrogenase, aldehyde dehydrogenase and formate dehydrogenase	Benzyl viologen	Open-circuit voltage of the cell: 0.8 V, power output: 0.67 mW/cm^2 at 0.49 V	[766]
Methanol dehydrogenase from *Methylobacterium extorquens*	Tetra methyl phenylene diamine	Open-circuit voltage: 1.4 V, power density: 0.2 mW/cm^2, current density: 0.38 mA/cm^2 at 0.67 V	[771]
Alcohol dehydrogenase, aldehyde dehydrogenase and formate dehydrogenase	Poly(methylene green)	Power density: 0.26 mW/cm^2, current density: 0.85 mA/cm^{-2}	[769]

Miscellaneous

Enzymatic Reduction of CO_2 and Formaldehyde to Methanol

The NADH-mediated reduction of CO_2 for the production of methanol can be described as a multistep reaction process. The reaction consists of three reversible enzymatic steps: reduction of CO_2 to formate catalysed by formate dehydrogenase FDH reduction of formate to formaldehyde by formaldehyde dehydrogenase (Fald-DH) and reduction of formaldehyde to methanol by alcohol dehydrogenase (ADH) [772, 773]. Reduced nicotinamide adenine dinucleotide (NADH) acts as an electron donor for each dehydrogenase-catalysed reduction.

Thermodynamic studies have shown that the enzymatic conversion of carbon dioxide is highly sensitive to the pH value and ionic strength of the reaction solution [774]. It is possible to shift the metabolic reaction equilibrium constants by a factor of several orders of magnitude to favour the synthesis of methanol. Electrolysis of carbon dioxide-saturated buffer solution in the presence of the enzymes formate dehydrogenase and methanol dehydrogenase together with methylviologen or pyrroloquinoline quinone as an electron relay yielded formaldehyde and methanol as the reduction products [775, 776]. The combined photochemical and enzymatic synthesis of methanol from formaldehyde is possible by using alcohol dehydrogenase (ADH) from *Saccharomyces cerevisiae* and photoreduction of NAD^+ by zinc tetraphenylporphyrin tetrasulphonate (ZnTPPS) in the presence of methylviologen, diaphorase and triethanolamine [777]. In a similar approach, the synthesis of methanol from HCO_3^- using formate dehydrogenase, aldehyde dehydrogenase and alcohol dehydrogenase was shown [778].

Biotechnological Conversion of Methane to Methanol by P450 s

Besides methane mono-oxygenases, enzymes of the cytochrome P-450 family, with a less complicated structure than MMO, have been found to catalyse methane oxidation to methanol [779]. Cytochrome P450 enzymes are heme-dependent mono-oxygenases that catalyse the oxidation of formally nonactivated C–H bonds. The addition of chemically inert perfluoro carboxylic acids to P450 BM3 causes an activation of the enzyme for short-chain aliphatic substrates as a result of the conversion of the Fe/heme from a low-spin to a high-spin state, and the reduction of the binding-pocket size. Together, these effects allow otherwise inert substrates such as propane and even methane to be oxidised [779].

6.5.3.5 Conclusion and Outlook

The disadvantages associated with the conversion of food substrates into biofuels and bulk chemicals have stimulated the search for alternative raw materials. Methanol is an already important carbon feedstock in the chemical industries. As a feedstock for industrial fermentations, methanol is also attractive because of its similar costs compared with other raw materials and its abundant availability. Recent advances in understanding the physiology and biochemistry of methylotrophs made it possible to evaluate their potential in biotechnological processes.

Compared with chemical syntheses starting from methanol, biotechnological processes are particularly promising in cases where high selectivities are needed or complex products are desired, such as branched C_3 to C_6 metabolites. Furthermore, many metabolites of methylotrophic bacteria are not found in the metabolism of established microorganisms, such as *E. coli*. The special metabolites can be suitable building blocks for chemicals, such as for novel fuels and polymers [634, 679, 681, 780].

References

1. K.S. Deffeyes, *Hubbert's Peak: The Impending World Oil Shortage* (Princeton University Press, Princeton, 2011)
2. M.K. Hubbert, Drill. Prod. Prac. 7–25 (1956)
3. R.W. Bentley, Energ. Policy **30**, 189–205 (2002)
4. S. Sorrell, J. Speirs, R. Bentley, A. Brandt, R. Miller, Energ. Policy **38**, 5290–5295 (2010)
5. D. Zhu, S. Tao, R. Wang, H. Shen, Y. Huang, G. Shen, B. Wang, W. Li, Y. Zhang, H. Chen, Y. Chen, J. Liu, B. Li, X. Wang, W. Liu, Appl. Energ. **106**, 17–24 (2013)
6. New York Times, 13.11.2012
7. R. Bacon, S. Tordo, *Crude Oil Price Differentials and Differences in Oil Qualities: A Statistical Analysis* (Energy and Water Department, Washington, D.C., 2005). Can be found under http://www.esmap.org/sites/esmap.org/files/08105.TechnicalPaper_CrudeOilPriceDifferentialsandDifferencesinOilQualitiesAStatisticalAnalysis.pdf
8. B. Höhlein, P. Biedermann, T. Grube, *Methanol as an Energy Carrier*, Schriften des Forschungszentrums Jülich- Reihe Energietechnik/Energy Technology (2006)
9. G.A. Olah, A. Goeppert, G.K.S. Prakash, *Beyond Oil and Gas: The Methanol Economy* (Wiley-VCH, Weinheim, 2006)
10. A. Kuhlmann, H. May, F.G. Pischinger, *Methanol und Wasserstoff*: *Automobil-Kraftstoffe der Zukunft* (Verlag TÜV, Rheinland, 1976)
11. A. Kowalewicz, M. Wojtyniak, *Proc. Inst. Mech. Eng., Part D: J. Automobile Eng.***219**, 103–125 (2005)
12. Methanol Institute, *Methanol Gasoline Blends*: *Alternative Fuel For Today's Automobiles and Cleaner 'Burning Octane For Today's Oil Refinery*. Can be found under http://www.methanol.org/Energy/Transportation-Fuel/Fuel-Blending-Guidelines/Blenders-Product-Bulletin-(Final).aspx (2011)
13. L. Bromberg, W.K. Cheng, *Methanol as an Alternative Transportation Fuel in the US: Options for Sustainable and/or Energy-Secure Transportation* (2010), can be found under http://www.afdc.energy.gov/pdfs/mit_methanol_white_paper.pdf
14. Methanol Institute, *Methanol Transportation Fuel* (2011), can be found unter http://www.methanol.org/Energy/Transportation-Fuel.aspx
15. C. Duwig, P. Gabrielson, H. Nielsen, Haldor Topsøe A/S presentation at Marine Days, Gothenburg (2011)
16. P.L. Spath, D.C. Dayton, *Preliminary Screening*: *Technical and Economic Assessment of Synthesis Gas to Fuels and Chemicals with Emphasis on the Potential for Biomass-Derived Syngas* (2003), can be found under http://www.nrel.gov/docs/fy04osti/34929.pdf
17. A.B. Chemrec, Press release from 09.09.2010 (2010)
18. DIN EN 590, *Kraftstoffe für Kraftfahrzeuge—Dieselkraftstoff—Anforderungen und Prüfverfahren* (Beuth, 2011)
19. Statista GmbH, *Global biofuel production from 2000 to 2011* (2013), can be found under http://www.statista.com/statistics/198866/global-biofuel-production–production-in-oil-equivalent-since-2000/

References to Section 6.2

20. F. Asinger, *Methanol—Chemie- und Energierohstoff. Die Mobilisation der Kohle*, 1. Aufl. (Springer, Heidelberg, 1986)
21. H.J. Arpe, *Industrielle Organische Chemie: Bedeutende Vor- und Zwischenprodukte*, 6. Aufl. (Wiley-VCH, Weinheim, 2007)
22. D. Steinborn, *Grundlagen der metallorganischen Komplexkatalyse*, 2. Aufl. (Vieweg + Teubner, Wiesbaden, 2009)

23. N. Rizkalla (Halcon International), DE 2610036, 1976
24. R.V. Porcelli, V.S. Bhise (Halcon International), DE 3024353, 1981
25. G. Luft, G. Ritter, M. Schrod, Chem. Ing. Tech. **54**, 750–760 (1982)
26. C. Hewlett (Halcon International), DE 2441502, 1975
27. C. Elschenbroich, Organometallchemie, 6. Aufl. (Vieweg + Teubner, Wiesbaden, 2008)
28. D.L. King, J.A. Cusumano, R.L. Garten, Cat. Rev. Sci. Eng. **23**, 233–263 (1981)
29. S. Rebsdat, D. Mayer, Ethylene glycol. In: *Ullmann'sEncyclopedia of Industrial Chemistry*, 7th edn. (Wiley-VCH, Weinheim, 2012), pp. 531–546
30. T. Ikarashi, Chem. Econ. Eng. Rev. **12**, 31–34 (1980)
31. H.F. Willkie (US Industrial Alcohol Co.), US 1400195, 1921
32. Companie de Béthune, F.P. 673.051, 1929
33. Mitsubishi Gas Chemical Co., Japan. Pat. **15**, 3068–766 (1978)
34. Mitsubishi Gas Chemical Co., Japan. Pat. **15**, 3108–916 (1978)
35. Mitsubishi Gas Chemical Co., Japan. Pat. 46.821 (1978)
36. Mitsubishi Gas Chemical Co., GB 1546004, 1979
37. A. Aguilo, T. Horlenko, Hydrocarbon Process **142**, 120–130 (1980)
38. M. Ioneoka (Mitsubishi Gas Chemical Co.), DE 2716842, 1977
39. S. Jali, H.B. Friedrich, G.R. Julius, J. Mol. Catal. A: Chem. **348**, 63–69 (2011)
40. J.S. Lee, J.C. Kim, Y.G. Kim, Appl. Catal. **57**, 1–30 (1990)
41. F. Mathé, Y. Castenet, A. Mortreux, F. Petit, Tetrahedron Lett. **32**, 3989–3992 (1991)
42. Mitsubishi Gas Chemical Co., Japan. Pat. 30.253 (1973)
43. M. Fontaine, Y. Castanet, A. Mortreux, F. Petit, J. Catal. **167**, 324–336 (1997)
44. G. Jenner, Appl. Catal. A: Gen. **121**, 25–44 (1995)
45. K. Kondo, N. Sonoda, H. Sakurai, Tetrahedron Lett. **15**, 803–804 (1974)
46. P. Pennequin, M. Fontaine, Y. Castanet, A. Mortreux, F. Petit, Appl. Catal. A: Gen. **135**, 329–339 (1996)
47. S. Otsuka, A. Nakaruma, T. Yoshida, M. Namto, K. Atato, J. Am. Chem. Soc. **95**, 3180–3188 (1973)
48. G. Jemier, E.M. Nahmed, S. Libs-Konrath, J. Mol. Catal. **64**, 337–347 (1991)
49. http://en.wikipedia.org/wiki/Formic_acid
50. V.V. Gercev, J.J. Markov-Zemljanski, *J. Angew. Chem.* (*UdSSR*) **43**, 1633–1635 (1970)
51. Anonymous, Chem. Eng. News **48**(28), 24 (1970)
52. A.H. Hanson (A.B. Perstorp), SE 331990, 1971
53. L.J. Kaplan, *Chem. Eng*. 71–73 (1982)
54. J. Menzel (Uhde GmbH), EP 2010056154, 2010
55. G. Wietzel, K. Eder, A. Scheuermann (BASF AG), DRP 867.849, 1953
56. M. Jahrsdorfer, G. Schwerte (BASF AG), DE 7414, 1941
57. K. Pieroh (BASF AG), DRP Anm. J. 69072 (1941)
58. M. Müller, U. Hübsch, Dimethyl ether, in *Ullmann'sEncyclopedia of Industrial Chemistry*, vol. 11, 7th edn. (Wiley-VCH, Weinheim, 2011), pp. 305–308
59. G. Reuss, W. Disteldorf, A. O. Gamer, A. Hilt, Formaldehyde. In: *Ullmann'sEncyclopedia of Industrial Chemistry*, 7th edn., **2012**, Wiley-VCH, Weinheim, p. 735–768
60. http://www.icis.com/v2/chemicals/9076013/formaldehyde/uses.html, 2010
61. E. Jones, G.G. Fowlie, J. Appl. Chem. **3**, 206–213 (1953)
62. V.N. Gavrilin, B.I. Popov, *Kinet. Catal.* (*Engl. Transl.*) **6**, 799-803 (1965)
63. H. Schubert, U. Tegtmeyer, R. Schlögl, Catal. Lett. **28**, 383–395 (1994)
64. H. Schubert, U. Tegtmeyer, D. Herein, X. Bao, Muhler M, R. Schlögl, Catal. Lett. **33**, 305–319 (1995)
65. G.J. Millar, J.B. Metson, G.A. Bowmaker, R.P. Cooney, J. Chem. Soc., Faraday Trans. **91**, 4149–4159 (1995)
66. H. Sperber, Titel. Chem. Ing. Tech. **41**, 962–966 (1969)
67. H.B. Uhl, I.H. Cooper, *Heyden Chem. Corp.*, US 2465498, 1949
68. G. Halbritter et al. (BASF AG), DE 2442231, 1978

69. A. Aicher, G. Lehmann, N. Petri, W. Pitteroff, G. Reuss, H. Schreiber, R. Sebastian (BASF AG), EP 0150436 (1985)
70. A. Aicher, H. Haas, H. Sperber, H. Diem, G. Matthias, G. Lehmann (BASF AG), DE 2322757 (1974)
71. A. Aicher, H. Haas, H. Diem, C. Dudeck, F. Brunnmüller, G. Lehmann (BASF AG), DE 2655321 (1978)
72. H. Diem, A. Aicher, H. Haas, C. Dudeck, F. Finkbeiner (BASF AG), DE 2444586 (1976)
73. Anonymous, Chem. Week, **105**, 79 (1969)
74. D.G. Sleemann, *Chem. Eng. N.Y.*, **75**, 42–44 (1968)
75. M. Weimann, *Chem. Eng. N.Y.*, **77**, 102–104 (1970)
76. A. Chauvel, P. Courty, R. Maux, C. Petitpas, Hydrocarbon Process **135**, 179–184 (1973)
77. J.H. Marten, M.T. Butler, Oil Gas J. **72**, 71–72 (1974)
78. FR000001487093A (2013), download from: https://depatisnet.dpma.de/DepatisNet/depatisnet?action=pdf&docid=
79. W.A. Payne (Du Pont), US 2519788, 1950
80. E.S. Northeimer (Du Pont), US 3959383, 1976
81. G.L. Kiser, B.G. Hendricks (Du Pont), US 4 076 754, 1978
82. W.B. Meath (Allied Chemical and Dye Corp.), US 2462413, 1949
83. G.C. Bailey, A.E. Craver (Barrett Comp.), US 1383059, 1921
84. V.E. Meharg, H. Adkins (Bakelite Corp.), US 1913405, 1933
85. F. Traina (Montecatini), US 3198753, 1965
86. S.A. Bergstrand(Perstorp AB), GB 1 080 508, 1967
87. G.D. Kolovertnov, G.K. Boreskov, V.A. Dzisko, B.I. Popov,. D.V. Tarasova, G.C. Belugina, *Kinet. Catal./Engl.* (*Transl.*), **6**, 950–954 (1965)
88. G.D. Kolovertnov, G.K. Boreskov, L.M. Kefeli, L.M. Plyasova, L.G. Karakchiev, V.N. Mastikin, V.I. Popov, V.A. Dzisko, V.D. Tarasova, *Kinet. Catal./Engl.* (*Transl.*), **7**, 125–130 (1966)
89. T.S. Hodgins, F.J. Shelton (Reichhold Chemicals), US 2 973 326, 1961
90. J.J. Hukki, E.J. Honkanen (Laeaeketehdas Orion Oy), CH 392484, 1961
91. P. Jiru, B. Wichter1ova, J. Tichy, in *Proceedings of 3rd International Congress Catalysis*, Amsterdam, vol. 1, 1965, pp. 199–213
92. M. Dente, R. Poppi, I. Pasquon, *Chim. Ind.* (*Milan*) **46**, 1326–1336 (1964)
93. M. Dente, I. Pasquon, *Chim. Ind.* (*Milan*) **47**, 359–367 (1965)
94. M. Dente, A. Collina, *Chim. Ind.* (*Milan*) **47**, 821–829 (1965)
95. W.F. Brondyke, J.A. Monier (Du Pont), US 2 436 287, 1948
96. W.F. Brondyke, J.A. Monier (Du Pont) GB 589 292, 1947
97. Anonymus, *Chem. Eng. N.Y.***61**, 109-110 (1954)
98. Anonymus, *Chem. Process Eng.* (*London*) **51**, 100–111 (1970)
99. C.M. Sze (Lummus Comp.), US 3 277 179, 1966
100. A.W. Gessner (Lummus Comp.), US 3408309, 1968
101. G. Greco, U. Soldano, Chem. Ing. Tech. **31**, 761–765 (1959)
102. W. Exner, *Chem. Anlagen + Verfahren*, pp. 87–92 (1973)
103. G. Sextro, Polyoxymethylenes, in *Ullmann'sEncyclopedia of Industrial Chemistry*, vol. 29, 7th edn. (Wiley-VCH, Weinheim, 2011), pp. 367–379
104. M. Heym, Angew. Makromol. Chem. **244**, 67–92 (1997)
105. H. Staudinger, M. Lüthy, Helv. Chim. Acta **8**, 41–64 (1925)
106. H. Staudinger, H. Johner, R. Signer, G. Mie, J. Hengstenberg, Z. Phys. Chem. **126**, 425–448 (1927)
107. H. Staudinger, R. Signer, H. Johner, M. Lüthy, W. Kern, D. Rusidis, O. Schweitzer, Liebigs Ann. Chem. **474**, 145–275 (1929)
108. H. Staudinger, R. Sieger, Z. Kristallogr, Mineralog. Petrogr. A **70**, 193 (1929)
109. (Du Pont), FP 1082519, 1954
110. M.F. Bechtold, K. Square, R.N. Macdonald (Du Pont), BE 558693, 1957
111. R.N. Macdonald (Du Pont), DE 1037705, 1958

112. D.L. Funck, (Du Pont), DE 1057086, 1959
113. D.L. Funck, (Du Pont), DE 1090191, 1960
114. R.N. Macdonald, (DuPont), DE 1037705, 1958
115. W. Kern, H. Cherdron, V. Jaacks, Angew. Chem. **73**, 177–186 (1961)
116. S. Nogare, J.O. Punderson, S.H.J. Jun, F.C. Starr, W. Jun, G.S. Stamatoff, (Du Pont), DE 1223551, 1966
117. H. Amann, E. Baeder, (Degussa), DE 2003270, 1971
118. J. Hagimory, E. Kitajima, (Tsukamoto Sogyo Co. Ltd.), DE 1964527, 1970
119. W. Thomson, F. Brown, B.K. William, J. Polly, W. George, (Celanese Corp.), DE 1420283, 1969
120. W. Kern, V. Jaacks, (Degussa), DE 1194145, 1965
121. V. Jaaks, W. Kern, Makromol. Chem. **83**, 71–79 (1965)
122. M.A. Pacheco, C.L. Marshall, Energ. Fuels **11**, 2–29 (1997)
123. D. Delledonne, F. Rivetti, U. Romano, Appl. Catal. A: Gen. **221**, 241–251 (2001)
124. F. Rivetti, C.R. Acad. Sci. Paris, SerieIIc, Chem. **3**, 497–503 (2000)
125. N. Keller, G. Rebmann, V. Keller, J. Mol. Catal. A: Chem. **317**, 1–18 (2010)
126. H. Babab, A.G. Zeiler, Chem. Rev. **73**, 75–91 (1973)
127. M. Matzner, R.P. Kurkjy, R.J. Cotter, Chem. Rev. **64**, 645–656 (1964)
128. A. Shaikh, S. Sivaran, Chem. Rev. **96**, 951–976 (1996)
129. J. Knifton, (Texaco Inc.), US 4661609, 1987
130. L. Cassar, Chim. Ind. Milan **72**, 18–22 (1990)
131. U. Romano, R. Tesel, G. Cipriani, L. Micucci, (Anic S.p.a), US 4218391, 1980
132. U. Romano, F. Rivetti, (EnichemSintesi), EP 365083, 1988
133. H.-J. Buysch, Carbonic esters, in *Ullmann'sEncyclopedia of Industrial Chemistry*, vol. 7, 7th edn. (Wiley-VCH, Weinheim, 2011), pp. 45–71
134. F. Matsuda, K. Narita, H. Oikawa, Y. Okuda, T. Saito, Y. Takahashi, K. Ueno, K. Watanabe (Nippon Steel Corp.), EP 685453, 1995
135. M. Bertau, C. Pätzold, U. Singliar (TU Bergakademie Freiberg), DE 102007051072, 2007
136. K. Nagai, T. Ui, Sumitomo Kagaku (2), 1–12 (2004) (English translation)
137. Evonik Industries AG, Press release from 23.10.2009 (2009)
138. J. Burkhardt, in Symposium am 28 on Silicone Chemie und Technologie, April 1989 (Vulkan, Essen, 1989), pp. 23–27
139. H.-H. Moretto, M. Schulze, G. Wagner, Silicones, in *Ullmann's Encyclopedia of Industrial Chemistry*, vol. 32, 7th edn. (Wiley-VCH, Weinheim, 2011), pp. 675–679
140. W. Kalchauer, B. Pachaly, Müller-Rochow synthesis: the direct process to methylchlorosilanes, in *Ullmann'sEncyclopedia of Industrial Chemistry*, vol. 32, 7th edn. (Wiley-VCH, Weinheim, 2011), pp. 2635–2641
141. H. Brauer, *Handbuch des Umweltschutzes und der Umwelttechnik,* vol. 2*, Produktions- und produktintegrierter Umweltschutz*, 1. Aufl. (Springer, Heidelberg, 1996), pp. 467–468
142. H. Gysin, E. Knuesli, (Geigy AG), CH 337019, 1959
143. W. Draber, K. Dichore, Naturwissenschaften **55**, 446 (1968)
144. K. Westphal, W. Meiser, L. Fue, H. Hack, (Bayer AG), US 3671523, 1972
145. R. Schmidt, L. Eue, C. Metzger, K. Dickore, (Bayer AG), DE-OS 2407144, 1975
146. Degussa AG, Press release from 12.03.2003 (2003)
147. R. Dittmeyer, W. Keim, G. Kreysa, A. Oberholz (eds.) *Winnacker-Küchler: Chemische Technik*, vol. 5, 5th edn. (Wiley-VCH, Weinheim, 2006), p. 250
148. M. Fielding (Du Pont), US 3255075, 1966
149. K.-M. Roy, Thiols and organic sulfides, in *Ullmann'sEncyclopedia of Industrial Chemistry*, vol. 36, 7th edn. (Wiley-VCH, Weinheim, 2011), pp. 629–655
150. H.O. Folkins, E.L. Miller, Ind. Eng. Chem. Proc. Des. Dev. **1**, 271–276 (1962)
151. B.J. Aungst, N.J. Rogers, Int. J. Pharm. **53**, 227–235 (1989)
152. W. Qia, D. Dinga, R.J. Salvi, Hearing Res. **236**, 52–60 (2008)
153. G. Da Violante, N. Zerrouk, I. Richard, G. Provot, J.C. Chaumeil, P. Arnaud, Biol. Pharm. Bull. **25**, 1600–1603 (2002)

154. S.L. Moskowitz, Methanol, in Kirk-Othmer Concise Encyclopedia of Chemical Technology, vol. 2, 5th edn. (Wiley, New York, 2007), pp. 1006–1009
155. M. Liauw, T. Prinz, H.-M. Weber, A. Reitzmann, Aromatische Zwischenprodukte, in *Winnacker-Küchler, Chemische Technik*, eds. by R. Dittmeyer, W. Keim, G. Kreysa, A. Oberholz, vol. 5, 5th edn. (Wiley-VCH, Weinheim, 2005), pp. 374–375
156. T. Ren, M.K. Patel, K. Blok, Energy **33**, 817–833 (2008)
157. Directive 2003/30/EG of the European Parliament and Council from 8 May 2003 for the promotion of biofuels or other renewable fuels in traffic (2003)
158. P. Fairly, Taking pulp to the pump, download from: http://www.technologyreview.com/news/411363/taking-pulp-to-the-pump/?a=f, 2008
159. F. Pontzen, W. Liebner, V. Gronemann, M. Rothaemel, B. Ahlers, Catal. Today **171**, 242–250 (2011)
160. B. Ahlers, G. Birke, H. Kömpel, H. Bach, M. Rothaemel, W. Liebner, W. Boll, V. Gronemann, (Lurgi AG) WO2010/060566 A1, 2010
161. G. Pagani, (SnamProgetti), DE 2362944, 1974
162. GESTIS Data Base, Natriummethanolat
163. F.A. Carey, R.J. Sundberg, Organic Chemistry, 1. Aufl. (Wiley-VCH, Weinheim, 1995)
164. N. Wiberg, E. Wiberg, Lehrbuch der Anorganischen Chemie, 102. Aufl. (de Gruyter, Berlin, 2007)
165. P. Lamers, Market study biodiesel, Fuels of the Future, Berlin, 23.-24.01.2012 (2012)
166. S.W. Tse, US 1697 H 19971104
167. W. Shunkwok, US H001697, 1997
168. C.H. Hamann, P. Schmittinger, (Huels Chemische Werke AG), EP 0810193, 1997
169. H.-J. Sterzel, D. Schläfer, J. Guth, H. Friedrich, P. Zehner, (BASF AG), EP 1195369, 2002
170. A. Qwczarek (Inst. Tech. Elektronowej), PL 211292, 1979
171. R. Auschner, P. Schmittinger, S. Rudolf, (Dynamit Nobel AG), EP 0177768, 1986
172. J. Ruwwe, K.-M. Krüger, U. Knippenberg, V. Brehme, M. Neumann, (Evonik Degussa GmbH), EP 1997794, 2008

References to Section 6.3

173. K. Weidmann, *Alternative Kraftstoffe für Dieselmotoren*, Essen, 1985
174. H. Menrad, Wenpo Lee, W. Bernhardt, SAE-770790, 1977
175. B. Nierhauve, G. Seidel, H. Menrad, *BMFT-Study Voraussetzung für die Einführung von Alkoholkraftstoffen* (TÜV Rheinland, Köln, 1983)
176. H. Menrad, B. Nierhauve, SAE-831686, 1983
177. K. Weidmann, H.Menrad, SAE-841331, 1984
178. K. Weidmann, H. Menrad, MTZ **46**, 373 (1985)
179. G. Decker, Personal communication (2012)
180. P. Kuirun, Z. Hua, Y. Yun et al., in IX International symposium on alcohol fuels, Firenze, 1991, p. 768
181. U. Hilger, G. Jain, F. Pischinger et al., in IX International symposium on alcohol fuels, Firenze, 1991, p. 479
182. K. Hikino, T. Suzuki, S. Uematsu, in IX International symposium on alcohol fuels, Firenze, 1991, p. 485
183. G. Decker, H. Heinrich, U. Kammann, in IX International symposium on alcohol fuels, Firenze, 1991, p. 501
184. F. Pischinger, E. Scheid, U. Hilger, G. Schmitz (FEV Motorentechnik GmbH & Co. KG), DE 3843243 C2, 1988
185. L. Brabetz, M. Siedentop, G. Schmitz, in IX International symposium on alcohol fuels, Firenze, 1991, p. 552
186. Siemens Automotive Company, *Flexible Fuel Sensing Technology* (2006)

187. J. van der Weide, H.J. Dekker, A. de Voogd, in IX International symposium on alcohol fuels, Firenze, 1991, p. 509
188. K. Kollmann, J. Abthoff, D. Hüttebräucker, IX International symposium on alcohol fuels, Firenze, p. 518
189. Y-G. Shin, S.–S. Hwang, H-S. Lee, in IX International symposium on alcohol fuels, Firenze, 1991, p. 526
190. T. Suga, S. Kitajima, Y. Hamazaki, in IX International symposium on alcohol fuels, Firenze, 1991, p. 532
191. H. Nohira, S. Kudo, Y Tsukasaki et al., in IX International symposium on alcohol fuels, Firenze, 1991, p. 538
192. M. Namba, T. Yokohama, K. Iida et al., in IX International symposium on alcohol fuels, Firenze, 1991, p. 546
193. Research and Markets, Impact of Alternative Fuels: Fuel Lines, Seals and Injectors, Dublin (2011)
194. H. Menrad, M. Haselhorst, W. Erwig SAE-821210, 1982
195. P. Dedl, P.Hofmann, B. Geringer et al., 13th Symposium on the working process of the internal combustion engine, Graz, 2011
196. F. Pischinger, P. Burghardt, Cornelis Havenith, SAE-830552, 1983
197. F. Pischinger, U. Hilger, G. Jain et al. Wiener, Konzept eines 1,9 l DI-Methanolmotors für den Einsatz im Pkw, 11. Int. Wiener Motorensympos., Düsseldorf, 1990
198. U. Hilger, G. Jain, E. Scheid, SAE-901521, 1990
199. H. Nakamura, M. Oshima, M. Kido, in IX international symposium on alcohol fuels, Firenze 1991, p. 623
200. L.-J. Wang, R.-Z. Song, H.-B. Zhou et al., in *Proceedings of the Institution of Mechanical Engineering* Part D 222, 2008, p. 619
201. D.H. Qi, S.Q. Liu, J.C. Liu, C.H. Zhang, in *Proceedings of the Institution of Mechanical Engineering* Part D 219, 2005, p. 405
202. Fluid, **40**, p. 36 (2007)
203. F. Zhang, S. Shuai, J. Wang, Z. Wang, SAE-2009-01-1182, 2009

References to Section 6.3.1

204. K. D. Miller, 23rd Annual Dewitt Petrochemical Review, Houston (1998)
205. U. Peters et al., in B. Elvers (ed.) Handbook of Fuels (Wiley-VCH, 2008)
206. M. Winterberg, in Ullmann's Encyclopedia (Wiley-VCH, 2010)
207. CMAI, *World Butylenes Analysis* (2010)
208. CMAI, *World Methanol Analysis* (2012)
209. Chem. Systems, *Tertiary Amyl Methyl Ether* (1994)
210. CEH, *Gasoline Octane Improvers/Oxygenates* (2009)

References to Section 6.4

211. IZA Structure Commission, Database of Zeolite Structures, can be found under http://www.iza-structure.org/databases/
212. C. Baerlocher, D.H. Olson, L.B. McCusker, *Atlas of Zeolite Framework Types* (Elsevier, Amsterdam, 2007)
213. A. Dyer, *An introduction to zeolite molecular sieves* (Wiley, Chichester, New York, 1988)
214. E. Wiberg, N. Wiberg, *Lehrbuch der anorganischen Chemie* (Walter de Gruyter, Berlin, 1995)
215. C.D. Chang, Catal. Revs **25**, 1–118 (1983)

216. D.H. Everett, Pure Appl. Chem. **31**, 577–638 (1972)
217. R. Lago, W. Haag, R. Mikovsky, D. Olson, S. Hellring, K. Schmitt, G. Kerr in *Murakami (Hg.) 1986—New developments in zeolite science*
218. T. Mole in *Studies in Surface Science and Catalysis*, eds. by D.M. Bibby, C.D. Chang, R.F. Howe, S. Yurchak, vol 36 (Elsevier, Amsterdam, 1988)
219. K. Segawa, M. Sakaguchi, Y. Kurusu in *Studies in Surface Science and Catalysis,* eds. by D.M. Bibby, C.D. Chang, R.F. Howe, S. Yurchak, vol 36 (Elsevier, Amsterdam, 1988)
220. M. Stöcker, Microporous and mesoporous materials, **82** (2005)
221. T. Mokrani, M. Scurrell, Catal. Rev. Sci. Eng. **51**, 1–145 (2009)
222. S.R. Blaszkowski, R.A. van Santen, J. Am. Chem. Soc. **119**, 5020–5027 (1997)
223. G.F. Froment, W.J.H. Dehertog, A.J. Marchi in *Catalysis. A Review of Recent Literature*, ed. by J.J. Spivey. The Royal Society of Chemistry (Cambridge, England, 1992)
224. W. Loewenstein, *American Mineralogist*, pp. 92–96 (1954)
225. D.S. Coombs, A. Alberti, T. Armbruster, G. Artioli, C. Colella, E. Galli, J.D. Grice, F. Liebau, J.A. Mandarino, H. Minato et al., Can. Mineral. **35**, 1571–1606 (1997)
226. IZA Structure Commission
227. R.F. Howe in *Studies in Surface Science and Catalysis*, eds. by D.M. Bibby, C.D. Chang, R.F. Howe, S. Yurchak., vol 36 (Elsevier, Amsterdam, 1988)
228. J.A. Rabo, G.J. Gajda in Guidelines for mastering the properties of molecular sieves. Relationship between the physicochemical properties of zeolitic systems and their low dimensionality (Plenum Press, New York, 1990)
229. J.F. Haw, Phys. Chem. chem. Phys. pp. 5431–5441 (2002)
230. P.L. Benito, A.G. Gayubo, A.T. Aguayo, M. Olazar, J. Bilbao, J. Chem. Tech. Biotechnol. pp. 183–191 (1996)
231. C.D. Chang, Catal. Revs. **26**, 323–345 (1984)
232. M. Bjørgen, F. Joensen, M. Spangsberg Holm, U. Olsbye, K.-P. Lillerud, S. Svelle, Appl. Catal. A **345**, 43–50 (2008)
233. R.J. Argauer, G.R. Landolt, US 3702886, 1972
234. E.M. Flanigen, R.L. Patton, US 4073865, 1978
235. J.F. Haw, W. Song, D.M. Marcus, J.B. Nicholas, ChemInform **34** (2003)
236. Z.-M. Cui, Q. Liu, W.-G. Song, L.-J. Wan, Angew. Chem. Int. Ed **45**, 6512–6515 (2006)
237. C. Baerlocher, W.M. Meier, D. Olson, *Atlas of zeolite framework types* (Elsevier, Amsterdam, New York, 2001)
238. J.F. Haw, D.M. Marcus, Top. Catal. **34**, 41–48 (2005)
239. Honeywell International Inc., Honeywell UOP's Advanced Methanol-to-Olefins Technology Selected In China To Produce Chemical Products (2011), can be found under http://honeywell.com/News/Pages/Honeywell-UOP%E2%80%99s-Advanced-Methanol-To-Olefins-Technology-Selected-In-China-To-Produce-Chemical-Products.aspx
240. S. Bordiga, L. Regli, D. Cocina, C. Lamberti, M. Bjørgen, K.P. Lillerud, J. Phys. Chem. B **109**, 2779–2784 (2005)
241. J. Sefcik, E. Demiralp, T. Cagin, W.A. Goddard, III, Rational Design of Zeolites for catalysis and separation (1998)
242. G. Burgfels, S. Klingelhöfer, L. H. Ong, R. Olindo, J. Lercher, F. Schmidt, DE 102010005704, 2011
243. Y.-f. Chang, S.N. Vaughn, L.R.M. Martens, J.E. Baumgartner, S.L. Soled, K.R. Clem, US 2005/0137080, 2005
244. R. von Ballmoos, W.M. Meier, Nature **289**, 782–783 (1981)
245. A. Tissler, P. Polanek, U. Girrbach, U. Müller, K. Unger, pp. 399–408
246. V.S. Nayak, V.R. Choudhary, Appl. Catal. **10**, 137–145 (1984)
247. A. de Lucas, P. Canizares, A. Durán, A. Carrero, Appl. Catal. A **154**, 221–240 (1997)
248. G. H. Kühl in *Catalysis and zeolites. Fundamentals and applications*, eds. by J. Weitkamp, L. Puppe (Springer, New York, 1999)
249. V. Zholobenko, L. Kustov, V. Kazansky, E. Loeffler, U. Lohse, G. Oehlmann, Zeolites **11**, 132–134 (1991)

250. C.D. Chang, C.T.W. Chu, J.N. Miale, R.F. Bridger, R.B. Calvert, J. Am. Chem. Soc. **106**, 8143–8146 (1984)
251. D.S. Shibabi, W.E. Garwood, P. Chu, J.N. Miale, R.M. Lago, C.T.W. Chu, C.D. Chang, J. Catal. **93**, 471–474 (1985)
252. M. Kang, J. Mol. Catal. A: Chem. **160**, 437–444 (2000)
253. D.L. Obrzut, P.M. Adekkanattu, J. Thundimadathil, J. Liu, D.R. Dubois, J.A. Guin, React. Kinet. Catal. Lett. **80**, 113–121 (2003)
254. M. Salmasi, S. Fatemi, A. Taheri Najafabadi, J. Ind. Eng. Chem. **17**, 755–761 (2011)
255. T.L. Marker, C.D. Gosling, US 5817906, 1998
256. M.M. Mertens, M.J. Janssen, L.R.M. Martens, K.R. Clem, US 20060079397, 2006
257. T. Inui, M. Kang, Appl. Catal. A **164**, 211–223 (1997)
258. S. Yurchak in *Studies in Surface Science and Catalysis*, eds. by D.M. Bibby, C.D. Chang, R.F. Howe, S. Yurchak, vol 36 (Elsevier, Amsterdam, 1988)
259. P.L. Benito, A.G. Gayubo, A.T. Aguayo, M. Olazar, J. Bilbao, Ind. Eng. Chem. Res. 3991–3998 (1996)
260. H. Schulz, Catal. Today **154**, 183–194 (2010)
261. F.J. Keil, Microporous Mesoporous Mater. **29**, 49–66 (1999)
262. D.E. Krohn, M.G. Melconian in *Studies in Surface Science and Catalysis*, eds. by D.M. Bibby, C.D. Chang, R.F. Howe, S. Yurchak, vol 36 (Elsevier, Amsterdam, 1988)
263. T.V. Janssens, J. Catal. **264**, 130–137 (2009)
264. S. Teketel, U. Olsbye, K.-P. Lillerud, P. Beato, S. Svelle, Microporous Mesoporous Mater. **136**, 33–41 (2010)
265. U. Olsbye, M. Bjørgen, S. Svelle, K.-P. Lillerud, S. Kolboe, Catal. Today **106**, 108–111 (2005)
266. M. Guisnet, J. Mol. Catal. A: Chem. **182–183**, 367–382 (2002)
267. M. Guisnet, P. Magnoux, Appl. Catal. **54**, 1–27 (1989)
268. M. Guisnet, P. Magnoux, Appl. Catal. A **212**, 83–96 (2001)
269. S. Kolboe in *Studies in Surface Science and Catalysis*, eds. by D.M. Bibby, C.D. Chang, R.F. Howe, S. Yurchak, vol 36 (Elsevier, Amsterdam, 1988)
270. B.E. Langner, Appl. Catal. **2**, 289–302 (1982)
271. A.G. Gayubo, J.M. Ortega, A.T. Aguayo, J.M. Arandes, J. Bilbao, Chem. Eng. Sci. **55**, 3223–3235 (2000)
272. J. Li, Y. Tan, Q. Zhang, Y. Han, Fuel **89**, 3510–3516 (2010)
273. A.T. Aguayo, D. Mier, A.G. Gayubo, M. Gamero, J. Bilbao, Ind. Eng. Chem. Res. **49**, 12371–12378 (2010)
274. Topp-Jørgensen in *Studies in Surface Science and Catalysis*, eds. by D.M. Bibby, C.D. Chang, R.F. Howe, S. Yurchak, vol 36 (Elsevier, Amsterdam, 1988)
275. K.G. Allum, A.R. Williams in *Studies in Surface Science and Catalysis*, eds. by D.M. Bibby, C.D. Chang, R.F. Howe, S. Yurchak, vol 36 (Elsevier, Amsterdam, 1988)
276. I.I. Ivanova, Y.G. Kolyagin, Chem. Soc. Rev. 5018–5050 (2010)
277. C.D. Chang in *Studies in Surface Science and Catalysis*, eds. by D.M. Bibby, C.D. Chang, R.F. Howe, S. Yurchak, vol 36 (Elsevier, Amsterdam, 1988)
278. A.C. Gujar, V.K. Guda, M. Nolan, Q. Yan, H. Toghiani, M.G. White, Appl. Catal. A **363**, 115–121 (2009)
279. M. Stöcker, Microporous Mesoporous Mater. **29**, 3–48 (1999)
280. I.M. Dahl, S. Kolboe, Catal. Lett. 329–336 (1993)
281. I.M. Dahl, S. Kolboe, J. Catal. 458–464 (1994)
282. I.M. Dahl, S.Kolboe, J. Catal. 304–309 (1996)
283. T. Mole, G. Bett, D. Seddon, J. Catal. 435–445 (1983)
284. T. Mole, J.A. Whiteside, D. Seddon, J. Catal. 261–266 (1983)
285. W. Song, D.M. Marcus, H. Fu, J.O. Ehresmann, J.F. Haw, J. Am. Chem. Soc. **124**, 3844–3845 (2002)
286. M. Bjørgen, J. Catal. **221**, 1–10 (2004)
287. E.J. Munson, A.A. Kheir, N.D. Lazo, J.F. Haw, J. Phys. Chem. 7740–7746 (1996)

288. H. Adkins, P.D. Perkins, J. Phys. Chem. **32**, 221–224 (1928)
289. J.M. Parera, Ind. Eng. Chem. Prod. Res. Dev **15**, 234–241 (1976)
290. R. Abraham in DGMK Conference Future Feedstocks for Fuels and Chemicals, Berlin, Germany. Supplement to conference preprints, DGMK, Hamburg, Sept 29–Oct 1, 2008
291. G. Burgfels, K. Kochloefl, J. Ladebeck, F. Schmidt, M. Schneider, H.J. Wernicke, DE 3838710, 1990
292. Y. Wei, J. Li, S. Xu, S. Yuan, L. Xu, J. Chen, Y. Zhou, Y. Qi, Z. Liu, Complete prospect and carbon atom economy evaluation of methanol-to-olefins reaction. Abstract ICC 2012, can be found under http://events.dechema.de/events/en/Events/Materials+for+Energy+_+EnMat+II/Congress+Planer/Datei_Handler-tagung-564-file-7857-p-127866.htm
293. B.M. Lok, C.A. Messina, R.L. Patton, R.T. Gajek, T.R. Cannan, E.M. Flanigen, US 4440871, 1984
294. T.N. Kalnes, T.V. Voskoboynikov, US 7414167, 2008
295. E. Köhler, F. Schmidt, H.J. Wernicke, M. de Pontes, H.L. Roberts, Hydrocarbon technology international 37–40 (1995)
296. C. Knottenbelt, Catal. Today **71**, 437–445 (2002)
297. D.W. Leyshon, G.E. Cozzone, US 5043522, 1991
298. D.L. Johnson, K.E. Nariman, R.A. Ware, US 6222087, 2001

References to Section 6.4.1

299. R.J. Argauer, G.R. Landolt, US 3702886, 1972
300. C.D. Chang, A.J. Silvestri, J. Catal. 249–259 (1977)
301. C.D. Chang, A.J. Silvestri, ChemTech **17**, 624–631 (1987)
302. C.D. Chang, Catal. Revs. **25**, 1–118 (1983)
303. M. Stöcker, Microporous and Mesoporous Mater. 82 (2005)
304. C.J. Maiden in *Studies in Surface Science and Catalysis*, eds. by D.M. Bibby, C.D. Chang, R.F. Howe, S. Yurchak, vol 36 (Elsevier, Amsterdam, 1988)
305. K.G. Allum, A.R. Williams in *Studies in Surface Science and Catalysis*, eds. by D.M. Bibby, C.D. Chang, R.F. Howe, S. Yurchak, vol 36 (Elsevier, Amsterdam, 1988)
306. G.A. Mills, Fuel **73**, 1243–1279 (1994)
307. H.R. Grimmer, N. Thiagarajan, E. Nitschke in *Studies in Surface Science and Catalysis*, eds. by D.M. Bibby, C.D. Chang, R.F. Howe, S. Yurchak, vol 36 (Elsevier, Amsterdam, 1988)
308. T. Mokrani, M. Scurrell, Catal. Rev. Sci. Eng. **51**, 1–145 (2009)
309. Structure Commission of the International Zeolite Association (2008), can be found under http://izasc.ethz.ch/fmi/xsl/IZA-SC/ftc_fw.xsl?-db=Atlas_main&-lay=fw&-max=25&STC=MFI&-find
310. M. Stöcker, Microporous Mesoporous Mater. **29**, 3–48 (1999)
311. T. Mole in *Studies in Surface Science and Catalysis*, eds. by D.M. Bibby, C.D. Chang, R.F. Howe, S. Yurchak, vol 36 (Elsevier, Amsterdam, 1988)
312. G.F. Froment, W.J.H. Dehertog, A.J. Marchi in *Catalysis. A review of recent literature*, ed. by J.J. Spivey. The Royal Society of Chemistry (Cambridge, England, 1992)
313. J.F. Haw, W. Song, D.M. Marcus, J.B. Nicholas, ChemInform 34 (2003)
314. C.D. Chang in *Studies in Surface Science and Catalysis*, eds. by D.M. Bibby, C.D. Chang, R.F. Howe, S. Yurchak, vol 36 (Elsevier, Amsterdam, 1988)
315. F.J. Keil, Microporous Mesoporous Mater. **29**, 49–66 (1999)
316. I.I. Ivanova, Y.G. Kolyagin, Chem. Soc. Rev. 5018–5050 (2010)
317. S. Yurchak in *Studies in Surface Science and Catalysis*, eds. by D.M. Bibby, C.D. Chang, R.F. Howe, S. Yurchak, vol 36 (Elsevier, Amsterdam, 1988)
318. A.C. Gujar, V.K. Guda, M. Nolan, Q. Yan, H. Toghiani, M.G. White, Appl. Catal. A **363**, 115–121 (2009)
319. H. Schulz, Catal. Today **154**, 183–194 (2010)

320. M. Guisnet, J. Mol. Catal. A: Chem. **182–183**, 367–382 (2002)
321. M. Guisnet, P. Magnoux, Appl. Catal. **54**, 1–27 (1989)
322. M. Guisnet, P. Magnoux, Appl. Catal. A **212**, 83–96 (2001)
323. A.G. Gayubo, J.M. Ortega, A.T. Aguayo, J.M. Arandes, J. Bilbao, Chem. Eng. Sci. **55**, 3223–3235 (2000)
324. B.E. Langner, Appl. Catal. **2**, 289–302 (1982)
325. P.L. Benito, A.G. Gayubo, A.T. Aguayo, M. Olazar, J. Bilbao, Ind. Eng. Chem. Res. 3991–3998 (1996)
326. J. Li, Y. Tan, Q. Zhang, Y. Han, Fuel **89**, 3510–3516 (2010)
327. A.T. Aguayo, A.G. Gayubo, J. Ereña, R. Vivanco, J. Bilbao, Chem. Eng. J. **92**, 141–150 (2003)
328. T.V. Janssens, J. Catal. **264**, 130–137 (2009)
329. R.F. Howe in *Studies in Surface Science and Catalysis*, eds. by D.M. Bibby, C.D. Chang, R.F. Howe, S. Yurchak, vol 36 (Elsevier, Amsterdam, 1988)
330. A.T. Aguayo, D. Mier, A.G. Gayubo, M. Gamero, J. Bilbao, Ind. Eng. Chem. Res. **49**, 12371–12378 (2010)
331. Topp-Jørgensen in *Studies in Surface Science and Catalysis*, eds. by D.M. Bibby, C.D. Chang, R.F. Howe, S. Yurchak, vol 36 (Elsevier, Amsterdam, 1988)
332. S. Kolboe in *Studies in Surface Science and Catalysis*, eds. by D.M. Bibby, C.D. Chang, R.F. Howe, S. Yurchak, vol 36 (Elsevier, Amsterdam, 1988)
333. H.-H. Gierlich, W. Dolkemeyer, A. Avidan, N. Thiagarajan, *Umwandlung von Methanol zu Benzin nach dem Wirbelbett-Verfahren*, Innsbruck
334. K.H. Keim, J. Maziuk, A. Toennesmann, Erdöl and Kohle, Erdgas, Petrochemie **37**, 558–562 (1984)
335. K.H. Keim, F.J. Krambeck, J. Maziuk, A. Toennesmann, Erdöl, Erdgas, Kohle **103**, 82–85 (1987)
336. C.D. Chang, Catal. Revs. **26**, 323–345 (1984)
337. H.A. Zaidi, K.K. Pant, Ind. Eng. Chem. Res. **47**, 2970–2975 (2008)
338. I. Nexant, PERP Program: Developments in para-Xylene Technology, can be found under http://www.chemsystems.com/about/cs/news/items/PERP%200809S11_paraXylene.cfm
339. J. Scherzer, *Octane-enhancing, zeolitic FCC catalysts. Scientific and technical aspects* (M. Dekker, New York, 1990)
340. M.L. Occelli, P. O'Connor, *Fluid Cracking Catalysts* (M. Dekker, New York, 1998)
341. S. Tabak, ExxonMobil Methanol to Gasoline, can be found under http://www.uschinaogf.org/Forum7/7Topic23-SamuelTabak-ExxonMobil-English.pdf
342. J. Packer, The Production of Methanol and Gasoline, can be found under http://nzic.org.nz/ChemProcesses/energy/7D.pdf
343. J. Peckham, JAMG's Methanol-to-Gasoline Plant Starts-up, can be found under http://www.worldfuels.com/wfExtract/exports/Content/33fead92-fc2d-447d-bc2e-3e95a8ff6e12.html
344. M. Schneider, F. Schmidt, G. Burgfels, H. Buchold, F.-W. Möller, EP 0448000, 1991
345. ExxonMobil, ExxonMobil's Methanol to Gasoline (MTG) Techno logy Selected for DKRW Advanced Fuels' Coal to Liquids Project, can be found under http://www.dkrwaf.com/_filelib/FileCabinet/PDFs/Press_Releases/ExxonPressRelease.pdf?FileName=ExxonPressRelease.pdf
346. D.E. Krohn, M.G. Melconian in *Studies in Surface Science and Catalysis*, eds. by D.M. Bibby, C.D. Chang, R.F. Howe, S. Yurchak, vol 36 (Elsevier, Amsterdam, 1988)
347. M. Bjørgen, F. Joensen, M. Spangsberg Holm, U. Olsbye, K.-P. Lillerud, S. Svelle, Appl. Catal. A **345**, 43–50 (2008)
348. Methanex Corporation, Global Environmental Report 2005, can be found under http://www.methanex.com/environment/documents/2005_Environmental_Excellence_Report.pdf
349. S. Yurchak, US 4814536, 1989
350. J.H. Beech, Jr., F.P. Ragonese, US 5059738, 1991
351. W. Lee, S. Yurchak, N. Daviduk, J. Maziuk in Proceedings of the NPRA Annual Meeting, 1980

352. T. Sugiyama, Thesis, Massachusetts Institute of Technology, 1994
353. Green Car Congress, DKRW Selects ExxonMobil's Methanol-to-Gasoline (MTG) Technology for Coal-to-Liquids Project, can be found under http://www.greencarcongress.com/2007/12/dkrw-selects-ex.html
354. Lurgi GmbH, The R&D centre, can be found under http://www.gcg-es.com/PrincipalsProducts/18-Lurgi/Lurgi02-Researchcentre.pdf
355. M. Rothaemel, H.-D. Holtmann, Erdöl Erdgas Kohle 234–237 (2002)
356. G. Burgfels, K. Kochloefl, J. Ladebeck, F. Schmidt, M. Schneider, H.J. Wernicke, DE 3838710, 1990
357. H. Hartmann, Erdöl Erdgas Kohle **123**, 362–369 (2007)
358. W. Liebner, M. Wagner, Erdöl Erdgas Kohle 120 (2004)
359. PetroSA, COD Technology, can be found under http://www.petrosa.co.za/innovation_in_action/Pages/COD-Technology.aspx
360. S.A. Tabak, A.A. Avidan, F.J. Krambeck, Production of synthetic gasoline and diesel fuel from non-petroleum resources, can be found under http://web.anl.gov/PCS/acsfuel/preprint archive/Files/31_2_NEW YORK_04-86_0293.pdf
361. S. Lee, M. Gogate, C.J. Kulik, Fuel Sci. Technol. Int. **13**, 1039–1057 (1995)
362. M. Wang, GREET1.5a: Changes from GREET1.5 (2000), can be found under http://www.transportation.anl.gov/pdfs/TA/150.pdf

References to Section 6.4.2

363. Chemical Market Associates Inc. (CMAI), World Light Olefins Analysis (WLOA) (2009). http://www.ihs.com/products/chemical/index.aspx?pu=1&rd=cmai
364. D. Greer, M. Houdek, R. Pittmann, J. Woodcock, Erdöl Erdgas Kohle **118**(5), 242 (2002)
365. CMAI, World Light Olefins Analysis, Houston Texas 173–176 (2003)
366. R.J. Argauer, G.R. Landolt, US Patent 3,702,886
367. C.D. Chang, A.J. Silvestri, Catalysis **47**, 249–259 (1977)
368. C.D. Chang, A.J. Silvestri, ChemTech **10**, 624 (1987)
369. F.J. Keil, Microporous and Mesoporous Mater. **29,** 49–66 (1999) (Review Methanol-to-hydrocarbons: process technology)
370. Z.M. Liu, C.L. Sun, G.W. Wang, Q.X. Wang, G.Y. Cai, Fuel Process. Technol. **62**, 161–172 (2000)
371. J. Li, Y. Wei, G. Liu, Y. Qi, P. Tian, B. Li, Y. He, Z. Liu, Catal. Today **171,** 1 (2011)
372. T. Ren, M. Patel, K. Blok, Olefins from conventional and heavy feedstocks: Energy use in steam cracking and alternative processes. Energy **31**, 425–451 (2006)
373. T. Mokrani, M. Scurrell, Gas conversion to liquid fuels and chemicals: the methanol route-catalysis and processes development. Catal. Rev. **51**, 1–145 (2009)
374. C.D. Chang, in *Methanol to Hydrocarbons*, eds. by G. Ertl, H. Knözinger, Weitkamp. Handbook of Heterogeneous Catalysis, 1st edn, p. 1894
375. S. Kvisle, T. Fuglerud, S. Kolboe, U. Olsbye, K.P. Lillerud, B. Vora, in *Methanol-to-Hydrocarbons*. Handbook of Heterogeneous Catalysis, vol 2, p. 707
376. T.J. Gregor Remans, G. Jenzer, A. Hoek, *Gas-to-Liquids*. Handbook of Heterogeneous Catalysis, pp. 2994–3010 (2008)
377. Michael Stöcker, Methanol-to-hydrocarbons: catalytic materials and their behaviour. Microporous Mesoporous Mater. **29**(1–2), 3–48 (1999). doi:10.1016/S1387-1811(98)00319-9
378. J. Li, Y. Wei, G. Liu, Y. Qi, P. Tian, B. Li, Y. He, Z. Liu, Catal. Today **171**(1), 221–228 (2011)
379. C.D. Chang, Catal. Rev. Sci. Eng. **25**, 1(1983)
380. U.S. Pat. No. 3,931,349
381. U.S. Pat. No. 4,404,414

382. D. Chen, H.P. Rebo, K. Moljord, A. Holmen, Methanol Conversion to Light Olefins over SAPO-34. Sorption, Diffusion, and Catalytic Reaction. Ind. Eng. Chem. Res. **38**, 4241–4249 (1999)
383. A.G. Gayubo, A.T. Aguayo, M. Castilla, M. Olazar, J. Bilbao, Catalyst reactivation kinetics for methanol transformation into hydrocarbons. Expressions for designing reaction-regeneration cycles in isothermal and adiabatic fixed bed reactor. Chem. Eng. Sci. **56**, 5059–5071 (2001)
384. H. Hu, F. Cao, W. Ying, Q. Sun, D. Fang, Study of coke behaviour of catalyst during methanol-to-olefins process based on a special TGA reactor. Chem. Eng. J. **160**, 770–778 (2010)
385. A.J. Marchi, G.F. Froment, Catalytic conversion of methanol to light alkenes on SAPO molecular sieves.Appl. Catal. **71**, 139–152 (1991)
386. J. Luckner, Effect of process parameters on methanol-to-olefins reactions over SAPO catalysts. PhD Thesis, Auburn University, 2005
387. G. Qi, Z. Xie, W. Yang, S. Zhong, H. Liu, C. Zhang, Q. Chen, behaviours of coke deposition on SAPO-34 catalyst during methanol conversion to light olefins. Fuel Process
388. L. Travalloni, A.C.L. Gomes, A.B. Gaspar, M.A.P. da Silva, Methanol conversion over acid solid catalysts. Catal. Today 133–135, 406–412 (2008)
389. X. Wu, M.G. Abraha, R.G. Anthony, Methanol conversion on SAPO-34: reaction condition for fixed-bed reactor. Appl. Catal. A: Gen. **260**, 63–69 (2004)
390. A. T., Aguayo, D., Mier, A. G., Gayubo, M., Gamero, J. Bilbao, Kinetics of Methanol Transformation into Hydrocarbons on a HZSM-5 Zeolite Catalyst at High Temperature (400-550°C). Ind. Eng. Chem. Res.2010, 49, 12371–12378
391. S.M. Alwahabi, G.F. Froment, Single Event Kinetic Modeling of the Methanol-to-Olefins Process on SAPO-34. Ind. Eng. Chem. Res. **43**, 5098–5111 (2004)
392. D. Chen, H.P. Rebo, A. Grønvold, K. Moljord, A. Holmen, Methanol conversion to light olefins over SAPO-34: kinetic modeling of coke formation. Microporous Mesoporous Mater. 35–36, 121–135 (2000)
393. S.M. Al Wahabi, Conversion of methanol to light olefins on SAPO-34: Kinetic modeling and reactor design. PhD Thesis, Texas A&M University, 2003
394. N. Fatourehchi, M. Sohrabi, S.J. Royaee, S.M. Mirarefin, Application of a Fluidized bed reactor in the MTO (Methanol to Olefin) process: preparation of catalyst and presentation of a kinetic model. Petrol. Sci. Technol. **29**, 1578–1589 (2011)
395. A.G. Gayubo, A.T. Aguayo, A.E. Sánchez del Campo, A.M. Tarrío, J. Bilbao, Kinetic modeling of methanol transformation into olefins on a SAPO-34, Catalyst. Ind. Eng. Chem. Res. **39**, 292–300 (2000)
396. A.T. Najafabadi, S. Fatemi, M. Sohrabi, M. Salmasi, Kinetic modeling and optimization of the operating condition of MTO process on SAPO-34, Catalyst. J. Ind. Eng. Chem. **18**, 29–37 (2012)
397. S. Soundararajan, A.K. Dalai, F. Berruti, Modeling of methanol-to-olefins (MTO) process in a circulating fluidized bed reactor. Fuel **80**, 1187–1197 (2001)
398. A.T. Aguayo, A.G. Gayubo, R. Vivanco, A. Alonso, J. Bilbao, Initiation step and reactive intermediates in the transformation of methanol into olefinsover SAPO-18. Catal. Ind. Eng. Chem. Res. **44**, 7279–7286 (2005)
399. A.T. Aguayo, A.G. Gayubo, R. Vivanco, M. Olazar, J. Bilbao, Role of Acidity and microporous structure in alternative catalysts for the transformation of methanol into olefins. Appl. Catal. A: Gen. **283**, 197–207 (2005)
400. A.G. Gayubo, A.T. Aguayo, A. Alonso, J. Bilbao, Kinetic Modeling of the Methanol-to-Olefins Process on a Silicoaluminophosphate (SAPO-18) Catalyst by Considering Deactivation and the Formation of Individual Olefins. Ind. Eng. Chem. Res. **46**, 1981–1989 (2007)
401. A.G. Gayubo, A.T. Aguayo, A. Alonso, A. Atutxa, J. Bilbao, Reaction scheme and kinetic modeling for the MTO Process over a SAPO-18. Catal. Catal. Today **106**, 112–117 (2005)

402. Y. Kumita, J. Gascon, E. Stavitski, J.A. Moulijn, F. Kapteijn, Shape selective methanol-to-olefins over highly thermostable DDR catalysts. Appl. Catal. A: Gen. **391**, 234–243 (2011)
403. J. Li, Y. Wei, G. Liu, Y. Qi, P. Tian, B. Li, Y. He, Z. Liu, Comparative study of MTO conversion over SAPO-34, H-ZSM-5 and H-ZSM-22: Correlating catalytic performance and reaction mechanism to zeolite topology.Catal. Today **171**, 221–228 (2011)
404. D. Mores, J. Kornatowski, U. Olsbye, B.M. Weckhuysen, Coke Formation during the Methanol-to-Olefin Conversion: In Situ Microspectroscopy on Individual H-ZSM-5 Crystals with Different Brønsted Acidity. Chem. Eur. J. **17**, 2874–2884 (2011)
405. B. Valle, A. Alonso, A. Atutxa, A.G. Gayubo, J. Bilbao, Effect of nickel incorporation on the acidity and stability of HZSM-5 zeolite in the MTO process. Catal. Today **106**, 118–122 (2005)
406. E.M. Flanigen, B.M. Lok, R.L. Patton, S.T. Wilson1987 Aluminophosphate molecular sieves and the periodic table, in New Developments in Zeolite Science and Technology, in Proceedings of 7th international Zeolite Conference, Tokyo, eds. by Y. Murakami, A. Ijima, J.W. Ward (Elsevier, Amsterdam, 1986) pp. 103–112
407. S.W. Kaiser, US Patent 4 499 327, 1985
408. S.W. Kaiser, US Patent 4 524 234, 1985
409. S.W. Kaiser, Arab. J. Sci. Eng. **10**, 361 (1985)
410. G. Pop, G. Musca, D. Ivanescu, E. Pop, G. Maria, E. Chirila, O. Muntean, Chem. Ind. **46**, 443 (1992)
411. U.S. Pat. No. 4,440,871
412. J. Chen, P.A. Wright, S. Natarajan, J.M. Thomas in Studies in Surface Science and Catalysis **84**, 1731–1738 (1994)
413. U.S. Pat. No. 5,279,810
414. J. Chen, P.A. Wright, J.M. Thomas, S. Natarajan, L. Marchese, S.M. Bradley, G. Sankar, C.R.A. Catlow, P.L. Gai-Boyes **98**, 10216–10224 (1994)
415. J. Chen, J.M. Thomas, P.A. Wright, R.P. Townsend, Catal. Lett. **28**, 241–248 (1994)
416. A.M. Prakash, S. Unnikrishnan, J. Chem. Soc. Faraday Transactions, Royal Society of Chemistry, London, **90**, 2291 (1994)
417. Y. Xu et al. J. Chem. Soc., Faraday Transactions **86,** 2, 425–429 (1990)
418. E.M. Flanigen, B.M. Lok, R.L. Pattonand S.T.Wilson Aluminophosphatemolecular sieves and the periodictable, in New Developments in ZeoliteScience and Technology, in Proceedings 7th International Zeolite conference, Tokyo, 1986 eds. Y. Murakami, A. Ijima, J.W. Ward (Elsevier, Amsterdam,1987), pp. 103–112
419. Z.-M. Cui, Q. Liu, W.-G. Song, L.-J. Wan, Insights into the Mechanism of Methanol-to-Olefin Conversion at Zeolites with Systematically Selected Framework Structures. Angew. Chem. Int. Ed. **45**, 6512–6515 (2006)
420. C. Baerlocher, W.M. Meier, D.H. Olson, Atlas of Zeolite Framework Types, 5th edn. (2001)
421. J.F. Haw, W. Song, D.M. Marcus, J.B. Nicholas, The Mechanism of Methanol to Hydrocarbon Catalysis. Acc. Chem. Res. **36**, 317–326 (2003)
422. J.F. Haw, D.M. Marcus, Well-defined (supra)molecular structures in zeolite methanol-to-olefin catalysis. Topics Catal. **34**, 1–4, 41–48 (2005)
423. J.Q. Chen, A. Bozzano, B. Glover, T. Fuglerud, S. Kvisle, Recent advancements in ethylene and propylene production using the UOP/Hydro MTO process. Catal. Today **106**, 103–107 (2005)
424. PERP Program -Developments in para-Xylene Technology. http://www.chemsystems.com/about/cs/news/items/PERP%200809S11_paraXylene.cfm
425. J. Scherzer, Octane-enhancing, Zeolitic FCC Catalysts: Scientific and Technical Aspects (1990)
426. S. Tabak http://www.uschinaogf.org/Forum7/7Topic%2023-%20Samuel%20Tabak-%20Exxon Mobil-%20English.pdf, http://nzic.org.nz/ChemProcesses/energy/7D.pdf
427. http://www.worldfuels.com/wfExtract/exports/Content/33fead92-fc2d-447d-bc2e-3e95a8ff6e12.html

428. M. Schneider, F. Schmidt, G. Burgfels, H. Buchold, Friedrich-Wilhelm, Möller, Süd-Chemie AG, METALLGESELLSCHAFT AG, European Patent EP0448000
429. http://www.petrosa.co.za/cod_technology.php
430. Engineering and Construction: A New Lurgi-MTP® Unit for China 27/08/2011. http://www.cn.airliquide.com/en/news/local-news-and-events/engineering-construction-a-new-lurgi-mtp-unit-for-china.html
431. Coal Chemical Products (Methanol, PE, PP) http://www.shenhuagroup.com.cn/english/productsservices/product0introduction/coal0chemicals0products/index.shtml
432. M. Arné, H.W. Scheeline, PEP Report 146, Bulk Chemicals from Synthesis Gas, June 1982
433. S. Kvisle, T. Fuglerud, S. Kolboe, U. Olsbye, K.P. Lillerud, B.V. Vora, "Methanol-to-Hydrocarbons" in Handbook of Heterogeneous Catalysis, **2**, pp. 707
434. T. Xu, J.L. White, U. S. Patent 6,734,330, 2004, priority filingand PCT published Feb 2000
435. T. Xu, J.L. White, U. S. Patent 6,743,747, 2004, priority filingand PCT published Feb 2000
436. A. Dyer, *An Introduction to Zeolite Molecular Sieves* (Wiley, New York, 1988)
437. S.E. Volz, J.J. Wise, Development studies on conversion of methanol and related oxygenates to gasoline. Final Report ERDA Contract No. E(49-18)-1773 (1976)
438. A. Kam, W. Lee, Fluid-bed process studies of the conversion of methanol to high octane gasoline. Final Report Contract No. EX-76-C-01-2490 (1978)
439. K.-H. Keim, F.J. Krambeck, J. Maziuk, A. Tonnesmann, ERDÖL, ERDGAS, KOHLE, 103. Jahrgang, Heft 2, Feb 1987
440. C.D. Chang, C.T.-W. Chu, R.F. Socha, J. Catal. **86**, 289–296 (1984)
441. S.A. Tabak, F.J. Krambeck, Shaping Process makes Fuels. Hydrocarbon Process. **64**, 9, 72–74 (1985)
442. A.A. Avidan Gasoline and distillate fuels from methanol, in Methane conversion proceedings of a symposium on the production of fuels and chemicals from natural gas, ed. by D.M. Bibby, C.D. Chang, R.F. Howe, S. Yurchak, Studies in Surface Science and Catalysis, **36**, pp. 307–323 (1988)
443. N. Daviduk, J.H. Haddad; United States Patent4,431,856, Assignee: Mobil Oil Corporation (1984)
444. U.S. Pat. No. 6,023,005
445. http://www.syn.ac.cn/ennews/Technology/2009/6/09631633371761.html
446. Shenhua Ningxia Coal Industry Group Co is a joint venture between the Ningxia provincialgovernment and China's largest coal producer Shenhua Group Corp, with 49 and 51 % stake-holding, respectively
447. http://www.csclc.com.cn/ens/gsxx/gsjj/2010-12-15/238.shtml
448. http://publications.polymtl.ca/158/1/2009_MarineKeraron.pdf
449. E.N. Givens, C.J. Plank, Edward J.Rosinski; US Patent 3,960,978, 1976
450. D.Wei, T. Voskoboynikov*, M. Quick, UOP LLC, 50 East Algonquin Road, Des Plaines, IL 60017, USA, W. Vermeiren, ATOFINA Research, Zone Industrielle C, B-7181 Feluy, Belgium
451. DE000010233069C1 assigned to Lurgi AG, Frankfurt, DE, 19.07.2002
452. D.Wei, T.Voskoboynikov*, M.Quick, UOP LLC, 50 East Algonquin Road, Des Plaines, IL 60017, USA, W.Vermeiren, ATOFINA Research, Zone Industrielle C, B-7181 Feluy, Belgium
453. T. Ren, M.K. Patel, K. Blok, Energy **33**, 817–833 (2008)
454. Kvisle S, Nilsen HR, MTO: state of art and perspectives. In: DGMK conference: creating value from light olefins-production and conversion in Hamburg. Hamburg: German Society for Petroleum and Coal Science and Technology (2001)
455. US Patent Office. Methanol-to-olefin process with increased selectivity to ethylene and propylene (US Patent 6,534,692). UOP LLC, US Patent Office (2003)
456. J. Gregor Meeting the changing needs of the olefins market by UOP LLC. In: The 5th EMEA petrochemical technology conference in Paris. London: Euro Petroleum Consultancy Ltd. (2003)

457. J. Grootjans, V. Vanrysselberghe, W. Vermeiren, Integration of total petrochemicals: UOP olefins conversion process into a naphtha steam cracker facility. Catal. Today **106**(1–4), 57–61 (2005)
458. P. Keep, Comparison of remote gas conversion technologies (Synetix Inc., London, 1999). See also: www.synetix.com/methanol/pdfs/papers/imtof99-paper9(59w).pdfS
459. US Patent Office. Production of light olefins from oxygenate using framework gallium-containing medium pore molecular sieve (US Patent application 20030018231). ExxonMobil Inc., US Patent Office, 2003
460. W. Liebner, GTC-Gas to Chemicals Process Options for Venezuela by Lurgi Oel-Gas Chemie Engineering. In: PdVSA-EFO seminar. Caracas, Venezuela: Petro′leos de Venezuela S.A. (2002)
461. H. Koempel, W. Liebne, M. Wagner, MTP—an economic route to dedicated propylene. In: The 2nd ICIS-LOR world olefins conference (ICIS-LOR Inc., Amsterdam, 2003)
462. M. Rothaemel, H.D. Holtmann, MTP, Methanol-to-Propylene—Lurgi's way, in DGMK conference "creating value from light olefins—production and conversion" (German Society for Petroleum and Coal Science and Technology, Hamburg, 2001)
463. L. Yingxu Wei, J. Li, S. Xu, C. Yuan, L. Xu, J. Chen, Y. Zhou, Y. Qi, Z. Liu, 12th ICC, München 2012, Abstracts
464. http://www.icis.com/Articles/2007/11/05/9076035/methanol-uses-and-market-data.html, 12 Oct 2010
465. http://www.icis.com/Articles/2005/08/20/2009637/mtomtp-ready-to-takeoff.html
466. H. Hui, http://www.icis.com/Articles/2012/10/30/9604963/china-annual-methanol-demand-to-spike-on-mto-mtp-projects.html, 30 Oct 2012

References to Section 6.4.3

467. De Witt Bits 2011 Global Industry Overview, Methanol and Derivatives Service, 1st Feb 2012
468. R. Kempf, Advantages of Commercialization of the UOP Advanced MTO technology, 2011 Middle East Chemical Week Conference, 16–19 Oct 2011, Abu Dhabi National Exhibition centre
469. IHS INC, 2012
470. Propylene Feedstock Diversification Conference, Shanghai, 2012
471. H. Hui, 'China annual methanol demand to spike on MTO, MTP projects', ICIS news, Oct 2012, http://www.icis.com/Articles/2012/10/30/9604963/china-annual-methanol-demand-to-spike-on-mto-mtp-projects.html
472. ICIS 22nd Aug 2005 http://www.icis.com/Articles/2005/08/20/2009637/mtomtp-ready-to-takeoff.html (Source: ACN)
473. R.J Argauer, G.R., Landolt, US Patent 3,702,886
474. C.D. Chang, A.J. Silvestri, J. Catal., **47**, 249–259 (1977)
475. C.D. Chang, A.J. Silvestri, ChemTech **10**, 624 (1987)
476. P. Trabold, Sustainable Routes to Petrochemical Products, in 7th international petrochemical conference, Athene, 23th/24th June 2005
477. M. Stöcker, Microporous and Mesoporous Mater., 3–48 (1999)

References to Section 6.4.4

478. R.J. Argauer, G.R. Landolt, US Patent 3,702,886
479. C.D. Chang, A.J. Silvestri, J. Catal. **47**, 249–259 (1977)
480. C.D. Chang, A.J. Silvestri, ChemTech **10**, 624 (1987)

481. C.D. Chang, in *Methanol to Hydrocarbons*, Handbook of Heterogeneous Catalysis, Ertl, G., Knözinger, H. & Weitkamp, 1st edn., p. 1894
482. S. Kvisle, T. Fuglerud, S. Kolboe, U. Olsbye, K.P. Lillerud, B. Vora, in *Methanol-to-Hydrocarbons*. Handbook of Heterogeneous Catalysis, vol 2, p. 707
483. T.J. Gregor Remans, G. Jenzer, A. Hoek, Gas-to-Liquids. Handbook of heterogeneous catalysis, pp. 2994–3010 (2008)
484. F.J. Keil, Microporous Mesoporous Mater. **29**(1–2), 49–66 (1999)
485. M. Stöcker, Microporous and Mesoporous Mater. **29**(1–2), 3–48 (1999)
486. The Catalyst Group Resources, Inc., Volume 2: Syngas Conversion to Products Assessment, April 2007
487. Technologies of Lurgi Oel Gas Chemie, 302.e/02.03/40, Lurgi Oel Gas Chemie GmbH, 60295 Frankfurt/Main (2003)
488. Adkins, Perkins, J. Phys. Chem. **32**, 219 (1928)
489. H. Knözinger, Angew. Chem. Int. Ed. **7**, 791 (1968)
490. J.R. Jain, C.N. Pillai, J. Catal. **9**, 322 (1967)
491. H. Knozinger, R. Kohne, J. Catal. **5**, 264 (1966)
492. K.L. Ng, Ph.D. Thesis, Imperial College of Science, Medicine and Technology, London, **1999**
493. S.G. Hindin, S.W. Weller, J. Phys. Chem. **60**, 1501 (1956)
494. S.W. Weller, S.G. Hindin, J. Phys. Chem. **60**, 1506 (1956)
495. B. Höhlein, Th. Grube, P. Biedermann, H. Bielawa, G. Erdmann, L. Schlecht, G. Isenberg, R. Edinger, Methanol als Energieträger, Schriften des Forschungszentrums Jülich, Reihe Energietechnik/Energy Technology Band/Volume 28
496. T.H. Fleisch, A. Basu, M.J. Gradassi, J.G. Masin, Stud. Surf. Sci. Catal. **107**, 117–125 (1997)
497. T.A. Semelsberger, R.L. Borup, H.L. Greene, J. Power Sour. **156**, 497–511 (2006)
498. M. Stiefel, R. Ahmad, U. Arnold, M. Döring, Fuel Process. Technol. **92**, 1466–1474 (2011)
499. PERP Program: Dimethyl Ether Technology and Markets. http://www.chemsystems.com/about/cs/news/items/PERP%200708S3_DME.cfm, 6th June 2013
500. Hubert de Mestier du Bourg, 23rd World Gas Conference, Amsterdam 2006: http://www.igu.org/html/wgc2006/pdf/paper/add10696.pdf, 6th June 2013
501. T. Ogawa, N. Inoue, T. Shikada, Y. Ohno, J. Nat. Gas Chem. **12**, 219–227 (2003)
502. W. Balthasar, W. Hilsebein: Methanol as a Feedstock for Power, Fuel and Olefins, in 'Nitrogen & Methanol', p. 261, January/February, 2003
503. U. Wagner, W. Liebner, 'Gas To Chemicals: Advanced technologies for natural gas monetisation' in 12th International Oil, Gas and Petrochemical Congress, Iran 2007
504. http://www.syngasrefiner.com/dme/dmepres/HiroshiFukuyama_pres1.pdf, Toyo Engineering Corporation, 2005
505. G. Yang, N. Tsubaki, J. Shamoto, Y. Yoneyama, Y. Zhang, J. Am. Chem. Soc. **132**, 8129–8136 (2010)
506. R. Ahmad, U. Arnold, M. Döring, in Abstract 12th ICC 2012
507. E. Unneberg, S. Kolboe, Formation of p-Xylene from Methanol over H-ZSM-5, in *Methane Conversion*, ed. by D.M. Bibby, C.D. Chang, R.F. Howe, S. Yurchak (Elsevier Science Publishers B.V, Amsterdam, 1988)
508. M. Conte, J.A. Lopez-Sanchez, Q. He, D.J. Morgan, Y. Ryabenkova, J.K. Bartley, A.F. Carley, S.H. Taylor, C.J. Kiely, K. Khalid, G.J. Hutchings, Catal Sci. Technol. **2**, 105–112 (2012)
509. D. Zeng, J. Yang, J. Wang, J. Xu, Y. Yang, C. Ye, F. Deng, Microporous Mesoporous Mater. **98**, 214–219 (2007)
510. C.P. Nicolaides, N.P. Sincadu, M.S. Scurrell, Catal. Today **71**, 429 (2001)
511. J.A. Biscardi, E. Iglesia, J. Catal. **182**, 117 (1999)
512. C.D. Gosling, F.P. Wilcher, L. Sullivan, R.A. Mountford, Hydrocarb. Process. **69,** Dec 1991
513. S. Pradhan, R. Lloyd, J.K. Bartley, D. Bethell, S. Golunski, R.L. Jenkins, G.J. Hutchings, Chem. Sci. **3**, 2958–2964 (2012)

514. J. Burger, M. Siegert, E. Ströfer, M. Nilles, H. Hasse, AIChE Annual Meeting, 2011. http://www.aiche.org/cei/resources/chemeondemand/conference-presentations/polyoxymethylene-dimethyl-ethers-components-tailored-diesel-fuel-properties-synthesis-and, 6th June 2013
515. G.P. Hagen, M.J. Spangler, US Patent 6,166,266, 2000
516. H.-J Arpe, *Industrielle Organische Chemie*: *Bedeutende Vor- und Zwischenprodukte*, Wiley-VCH, Weinheim, 6. Vollständig überarbeitete Auflage, p. 176 (2007)
517. Helv. Chim. Acta 8, **64** (1925)
518. Ann. 474, 213, (1929)
519. Dupont patent US-2,449,469. Cited from EP1070755
520. D.S. Moulton, D.W. Naegeli, Southwest Research Institute, United States Patent, 5,746,785 May 5, 1998
521. R. Patrini, M. Marchionna, EP1070755, 2001
522. E. Stroefer, R. Sinnen, O. Schweers, J. Thiel, H. Hasse, WO/2008/074704
523. E. Jacob, WO/2011/012339
524. Diesel Fuel News, July 9, 2001 cited by Jack Peckham http://findarticles.com/p/articles/mi_m0CYH/is_14_5/ai_76908160/
525. D. Sanfilippo, R. Patrini, M. Marchionna, Patent US7,235,113

References to Section 6.5.1

526. G. Olah, A. Goeppert, S. Prakash, *Beyond Oil and Gas: The Methanol Economy* (Wiley-VCH, Weinheim, 2009)
527. J.C. Amphlett, M.J. Evans, R.A. Jones, R.F. Mann, R.D. Weir, Can. J. Chem. Eng. **63**, 605–611 (1985)
528. G. Colsmann, Dissertation, Berichte des Forschungszentrums Jülich, Jül-3127, Jülich 1995
529. V. Formanski, *dissertation, Fortschritt-Berichte VDI, Reihe 3 Verfahrenstechnik* (VDI Verlag GmbH, Düsseldorf, 2000)
530. J.C. Amphlett, M.J. Evans, R.A. Jones, R.F. Mann, R.D. Weir, Can. J. Chem. Eng. **59**(4), 720–727 (1981)
531. B. Ganser, Dissertation, Berichte des Forschungszentrums Jülich, Jül-2748, Jülich 1993
532. W. Wiese, B. Emonts, R. Peters, Int. J. Power Sour. **106**, 249–257 (1999)
533. M.S. Wainwright, C.J. Jiang, D.L. Trimm, N.W. Cant, Appl. Catal. **97**, 145–158 (1993)
534. M.S. Wainwright, C.J. Jiang, D.L. Trimm, N.W. Cant, Appl. Catal. **93**, 245–255 (1993)
535. Messer Group GmbH, *Variocarb-therm-process*, can be found under http://www.messergroup.com/de/Daten/Fachbroschueren/Metallurgie/Variocarb-therm.pdf, Krefeld, 2012
536. Air Liquide Deutschland GmbH, *Alnat C^{TM}-process*, can be found under http://www.airliquide.de/loesungen/business/metall/equipment/alnatc.html, Düsseldorf, 2013
537. Westfalen AG, *Tempron®-process*, can be found under http://www.westfalen-ag.de/fileadmin/user_uploads/Westfalen_AG/Technische_Gase/Allgemein/Prospekte_Technische_Gase/Perfekte_Atmos_Tempron.pdf, Münster, 2013
538. T. Weiss, Dissertation, Saarbrücken, 2008
539. L. Pettersson, K. Sjostrom, Combust. Sci. Technol. **80**, 265–303 (1991)
540. J.C. Brown, E. Gulari, Catal. Commu. **5**, 431–436 (2004)
541. Caloric Anlagenbau GmbH, *Caloric HM Plant for H_2Generation by Methanol Reforming*, can be found under http://www.caloric.com/en/produkte/h2-generation/methanol-reforming/methanol-reforming.html, Graefelfing, 2013
542. P. Neumann, F. von Linde, *inform*, *14*, 5, 313-315 (2003)
543. P. Neumann, F. von Linde, MPT. Metall. Plant Technol. Int. **2**, 72–75 (2003)
544. Mahler AGS GmbH, *Process description for Hydroform-M plant*, can be found under http://www.mahler-ags.com/hydrogen/hydroform-m.htm, Stuttgart, 2013

545. Mahler AGS GmbH, *Process description for Hydroform-M plant*, can be found under http://www.mahler-ags.com/hydrogen/hydroswing.htm, Stuttgart, 2013
546. Air Products and Chemicals, Inc., *Hydrogen Recovery and Purification*, http://www.airproducts.com/products/Gases/supply-options/prism-membrane-hydrogen-recovery-and-purification.aspx, Allentown, 2013
547. UOP LLC, *Hydrogen selection matrix*, www.uop.com/uop-hydrogen-selection-matrix, des Plaines, 2013

References to Section 6.5.2

548. F. Asinger, Methanol: Chemie- und Energierohstoff. Die Mobilisation der Kohle (Springer, Berlin, Germany 1986), p. 407
549. G.A. Olah, A. Goeppert, G.K.S. Prakash, *Beyond Oil and Gas: The Methanol Economy* (Wiley-VCH Verlag, Weinheim, Germany, 2006), p. 304
550. A.J. Appleby, F.R. Foulkes, *Fuel Cell Handbook* (Van Nostrand Reinhold Int. Co, New York, 1989), p. 763
551. E.W. Justi, A. Winsel, *Kalte Verbrennung, Fuel Cells* (Franz Steiner, Wiesbaden Germany, 1962), p. 414
552. W. Vielstich, Translated by Ives DJG. Fuel Cells (Wiley-VCH, Weinheim, Germany, 1965/70), p. 502
553. W. Vielstich, A. Lamm, H. Gasteiger (eds.), *Handbook of Fuel Cells* (Wiley, Chichester, UK, 2003), vol 1–4, p. 2606
554. G. Sandstede, Elektrochemische Brennstoffzellen, in Fortschritte der Chemischen Forschung (Springer, Berlin, Heidelberg, New York, 1967), pp. 171–221
555. G. Sandstede (ed.), *From Electrocatalysis to Fuel Cells* (University of Washington Press, Seattle and London, 1972), p. 415
556. H.A. Liebhafsky, E.J. Cairns, *Fuel Cells and Fuel Batteries* (Wiley, London, 1968), p. 692
557. J.O.M. Bockris, S. Srinivasan, *Fuel Cells: Their Electrochemistry* (McGraw-Hill Book Company, London, Sydney, Toronto, Mexico, 1969), p. 660
558. F. von Sturm, Elektrochemische Stromerzeugung (Verlag Chemie, Weinheim, Germany, 1969), p. 190
559. H.H. von Döhren, K.J. Euler, *Brennstoffelemente*, 6th edn., VARTA-Fachbuchreihe Bd 6, (VDI, Düsseldorf, Germany, 1971), p. 223
560. A.K. Kordesch, G. Simader, *Fuel Cells and their Applications* (VCH Verlagsgesellschaft Weinheim, Germany, 1996)
561. A. Heinzel, P. Beckhaus, Brennstoffzellen für portable Anwendungen: kleine Energiepakete (2006). GDCh-Wochenschau 32b: online: http://www.aktuelle-wochenschau.de/2006/woche32b/woche32b.html, p. 5
562. V.S. Bagotsky, Fuel cells: Problems and solutions (Wiley, New York, 2009), p. 322
563. J. Garche, Ch. Dyer, P. Moseley, Z. Ogumi, D. Rand, B. Scrosati (eds.), *Encyclopedia of Electrochemical Power Sources* (Elsevier, Amsterdam, 2009). (vol 1–5)
564. D. Stolten (ed.), *Hydrogen and Fuel Cells: Fundamentals, Technologies and Applications, Chapters* (Wiley-VCH Verlag, Weinheim, Germany, 2010), p. 878
565. D. Stolten (ed.), *Hydrogen Energy* (Wiley-VCH Weinheim, 2010)
566. G. Kolb, *Fuel processing for fuel cells* (Wiley-VCH, Weinheim Germany, 2008), p. 412
567. W. Grot, Perfluorinated cation exchange polymers, Chem. Ing. Tech. **47,** MS260/75, p. 617 (1975)
568. T. Iwasita, *Methanol and CO electrooxidation*, vol 2, eds. by W. Vielstich, A. Lamm, H. Gasteiger, Handbook of Fuel Cells (Wiley, Chichester, UK, 2003), pp. 603–624
569. A. Heinzel, Stand der Technik von Polymer-Elektrolyt-Membran-Brennstoffzellen—ein Überblick. CIT 81: 567–571 (Special Issue: Brennstoffzellen und Wasserstofftechnologie) (2009)

570. A. Heinzel, G. Bandlamudi, W. Lehnert, High Temperature PEMFCs, in *Encyclopedia of Electrochemical Power Sources*, ed. by J. Garche, Ch. Dyer, P. Moseley, Z. Ogumi, D. Rand, B. Scrosati (Elsevier, Amsterdam, 2009), pp. 951–957. (vol 2)
571. L. Gubler, D. Kramer, J. Belack, Ö. Ünsal, ThJ Schmidt, G.G. Scherer, A Polybenzimidazole-Based Membrane for the Direct Methanol Fuel Cell. J. Electrochem. Soc. **154**, B981–B987 (2007)
572. Q. Wang, G.Q. Sun, L.H. Jiang, Q. Xin, S.G. Sun, Y.X. Jiang, S.P. Chen, Z. Jusys, R.J. Behm, Adsorption and oxidation of ethanol on colloid-based Pt/C, PtRu/C and Pt3Sn/C catalysts: In situ FTIR spectroscopy and on-line DEMS Studies, Phys. Chem. Chem. Phys. **9**, pp. 2686–2696 (2007), www.rsc.org/pccp/altfuel
573. Tannenberger, in Sandstede G (ed) (1972) From Electrocatalysis to Fuel Cells, 415 pages, University of Washington Press, Seattle and London
574. A. Heinzel, R. Holze, C.H. Hamann, J.K. Blum, The electrooxidation of methanol and formaldehyde at a platinum electrode: A SEESR study of radical intermediates. Electrochim. Acta **34**, 657 (1989)
575. S. Wasmus, A. Küver, Methanol oxidation and direct methanol fuel cells_a selective review. J. Electroanal. Chem. **461**, 14–31 (1999)
576. V.S. Bagotsky, Y.S. Vassiliev, O.A. Khazova (1977) Generalized scheme of chemisorption, electrooxidation and electroreduction of simple organic compounds on platinum group metals, J. Electroanal. Chem. 81, 229
577. A. Hamnett (2003) Direct methanol fuel cells (DMFC). In: Vielstich W, Lamm A, Gasteiger H (eds) Handbook of Fuel Cells, Vol. 1: 305-322, Wiley, Chichester, UK
578. M. Neergat, D. Leveratto, U. Stimming, Catalysts for Direct Methanol Fuel Cells. Fuel Cells **2**(1), 25–30 (2002)
579. V.S. Bagotsky, Y.B Vassilyev (1964 and 67) Electrochimica Acta 9, 869 and 12, 1323
580. H. Binder, A. Köhling, G. Sandstede, The Anodic Oxidation of Methanol on Raney-Type Catalysts of Platinum Metals, in *Hydrocarbon Fuel Cell Technology*, ed. by B.S. Baker (Academic Press, New York and London, 1965), pp. 91–102
581. O.A. Petry, B.I. Podlovchenko, A.N. Frumkin, H. Lal, J. Electroanal. Chem. **10**, 253 (1965)
582. J.-F. Drillet, R. Dittmeyer, K. Jüttner, L. Li, K.-M. Mangold, New composite DMFC anode with PEDOT as a mixed conducter and catalyst support. Fuel Cells **6**(6), 432–438 (2006)
583. C. Cremers, M. Scholz, W. Seliger, A. Racz, W. Knechtel, J. Rittmayr, F. Grafwallner, H. Peller, U. Stimming, Developments for improved direct methanol fuel cell stacks for portable power. Fuel Cells **7**(1), 21–31 (2007)
584. A.S. Arico, V. Baglio, V. Antonucci (2009) Direct Methanol Fuel Cells: History, Status and Perspectives. In: Liu H, and Zhang J (eds) Electrocatalysis of Direct Methanol Fuel Cells:_From Fundamentals to Applications, Hardcover, Chapter 1: 1-78, Wiley, Chichester, UK, and Wiley Online Library, 582 pages: http://media.wiley.com/product_data/excerpt/75/35273237/3527323775.pdf
585. H. Liu, J. Zhang (2009) Electrocatalysis of Direct Methanol Fuel Cells: From Fundamentals to Applications, 606 pages, Wiley-VCH Verlag, Weinheim, Germany http://eu.wiley.com/WileyCDA/WileyTitle/productCd-3527323775.html
586. M. Watanabe, H. Uchida (2010) Catalysts for the electro-oxidation of small molecules, 18 pages, Wiley Online Library: http://onlinelibrary.wiley.com/doi/10.1002/9780470974001.f500007/full, http://onlinelibrary.wiley.com/doi/10.1002/9780470974001.f500007/pdf
587. J. Wu, F. Hu, P.K. Shen, C.M. Li, Z. Wei, One-step preparation of Pt on pretreated multiwalled carbon nanotubes for methanol electrooxidation. Fuel Cells **10**(1), 106–110 (2010)
588. C. Zhou, F. Peng, H. Wang, H. Yu, J. Yang, X. Fu, Facile preparation of an excellent Pt-RuO2-MnO2/CNTs nanocatalyst for anodes of direct methanol fuel cells. Fuel Cells **11**(2), 301–308 (2011)
589. H. Behret, H. Binder, G. Sandstede, Inorganic and Organic Non-Noble Metal Containing Electrocatalysts for Fuel Cells, in *Electrocatalysis*, ed. by M.W. Breiter (The Electrochemical Society Princeton, N.J, 1974), pp. 319–338

590. C. Fischer, A. Alonso-Vante, S. Fiechter, H. Tributsch, J. Appl. Chem. **25**, 1004 (1995)
591. T.S. Zhao, C. Xu, Direct Methanol Fuel Cell: Overview Performance and Operational Conditions, in *Encyclopedia of Electrochemical Power Sources, Vol 2: 381-389*, ed. by J. Garche, Ch. Dyer, P. Moseley, Z. Ogumi, D. Rand, B. Scrosati (Elsevier, Amsterdam, 2009)
592. T.S. Zhao, Z.X. Liang, J.B. Xu, Overview (Direct Alcohol Fuel Cells), in *Encyclopedia of Electrochemical Power Sources, Vol 2: 362–369*, ed. by J. Garche, Ch. Dyer, P. Moseley, Z. Ogumi, D. Rand, B. Scrosati (Elsevier, Amsterdam, 2009)
593. N.K. Beck, B. Steiger, G.G. Scherer, A. Wokaun, Methanol tolerant oxygen reduction catalysts derived from electrochemically pre-treated Bi2Pt2-yIryO7 pyrochlores. Fuel Cells **6**, 26–30 (2006)
594. A.M. Remona, K.L.N. Phani, Study of methanol-tolerant oxygen reduction reaction at Pt–Bi/C bimetallic nanostructured catalysts. Fuel Cells **11**(3), 385–393 (2011)
595. H. Wang, J. Liang, L. Zhu, F. Peng, H. Yu, J. Yang, High oxygen-reduction-activity and methanol-tolerance cathode catalyst Cu/PtFe/CNTs for direct methanol fuel cells. Fuel Cells **10**(1), 99–105 (2010)
596. J. Yang, C.H. Cheng, W. Zhou, J.Y. Lee, Z. Liu, Methanol-tolerant heterogeneous PdCo@PdPt/C electrocatalyst for the oxygen reduction reaction. Fuel Cells **10**(6), 907–913 (2010)
597. Ch. Hartnig, L. Jörissen, J. Kerres, W. Lehnert, J. Scholta, Polymer electrolyte membrane fuel cells, in *Materials for Fuel Cells*, ed. by M. Gasik (Woodhead Publisher Ltd, Cambridge, 2008), pp. 101–184
598. A. Winsel, Galvanische Elemente, Brennstoffzellen. In: Ullmanns Encyclopädie. Bd **12**, 113–136 (1974)
599. A. Heinzel, V.M. Barragán, A review of the state-of-the-art of methanol crossover in direct methanol fuel cells. J. Power Sources **84**, 70 (1999)
600. Jörissen L, and Gogel V (2009) Direct Methanol: Overview. In: Garche J, Dyer Ch, Moseley P, Ogumi Z, Rand D, and Scrosati B (eds) Encyclopedia of Electrochemical Power Sources, Vol 2: 370-380, Elsevier, Amsterdam
601. Ch. Hartnig, L. Jörissen, W. Lehnert, J. Scholta, Direct methanol fuel cells, in *Materials for Fuel Cells*, ed. by M. Gasik (Woodhead Publisher Ltd, Cambridge, 2008), pp. 185–208
602. N. Neergat, K.A. Friedrich, U. Stimming, New Materials for DMFC MEAs, in *Handbook of Fuel Cells, Vol 4: 856-877*, ed. by W. Vielstich, A. Lamm, H. Gasteiger (Wiley, Chichester, UK, 2003)
603. Justi, Winsel 1962
604. K. Scott, E. Yu (2009) Electrocatalysis in the Direct Methanol Alkaline Fuel Cell. In: Liu H, and Zhang J (eds) Electrocatalysis of Direct Methanol Fuel Cells:_From Fundamentals to Applications, Hardcover, Chapter 13: 487-525, Wiley, Chichester, UK, and Wiley Online Library, 582 pages: http://eu.wiley.com/WileyCDA/WileyTitle/productCd-3527323775.html
605. H. Binder, A. Köhling, W.H. Kuhn, W. Lindner, G. Sandstede, Hydrogen and methanol fuel cells with air electrodes in alkaline electrolyte, in *From Electrocatalysis to Fuel Cells*, ed. by G. Sandstede (University of Washington Press, Seattle and London, 1972), pp. 131–141
606. H. Binder, A. Köhling, G. Sandstede, Effect of alloying components on the catalytic activity of platinum in the case of carbonaceous fuels, in *From Electrocatalysis to Fuel Cells*, ed. by G. Sandstede (University of Washington Press, Seattle and London, 1972), pp. 43–58
607. H. Binder, A. Köhling, G. Sandstede, Platinum catalysts modified by adsorption or mixing with inorganic substances, in *From Electrocatalysis to Fuel Cells*, ed. by G. Sandstede (University of Washington Press, Seattle and London, 1972), pp. 59–80
608. Fuel Cell (2011) 31 pages, in: Wikipedia: http://en.wikipedia.org/wiki/Fuel_cell
609. J.B. Hansen (2003) Methanol reformer design considerations. In: Vielstich W, Lamm A, Gasteiger H (eds) Handbook of Fuel Cells, Vol. 3: 141-148, Wiley, Chichester, UK
610. C. Zhang, Z. Yuan, N. Liu, S. Wang, S. Wang, Study of Catalysts for Hydrogen Production by the High Temperature Steam Reforming of Methanol. Fuel Cells **6**(6), 466–471 (2006)

611. K. von Benda, H. Binder, A. Köhling, G. Sandstede, Electrochemical behaviour of tungsten carbide electrodes, in *From Electrocatalysis to Fuel Cells*, ed. by G. Sandstede (University of Washington Press, Seattle and London, 1972), pp. 87–100
612. D. Edlund, *Methanol Fuel Cell Systems: Advancing towards Commercialisation, 206 pages* (Pan Stanford Publishing Pte, Ltd, Singapure, 2011)
613. A. Heinzel (2001) Brennstoffzellen im kleinen Leistungsbereich – portable Anwendungen und Batterieersatz. In: Ledjeff-Hey K, Mahlendorf F, and Roes J (eds) Brennstoffzellen, Entwicklung Technologie Anwendung, 2. Ed.: 211-219, C.F.Müller Verlag, Heidelberg
614. A. Heinzel, C. Hebling, M. Müller, M. Zedda, C. Müller, Fuel cells for low power applications. J. Power Sources **105**, 250–255 (2002)
615. Heinzel A (2010) Brennstoffzellen - Mobil, stationär und portabel; Stand der Entwicklungen heute. GDCh-Wochenschau 33: 4 pages online: http://www.aktuelle-wochenschau.de/2010/w33/woche33.html
616. S.R. Narayanan, T.I. Valdez, Portable direct methanol fuel cell systems, in *Handbook of Fuel Cells, Vol 4: 1133-1141*, ed. by W. Vielstich, A. Lamm, H. Gasteiger (Wiley, Chichester, UK, 2003)
617. A. Heinzel, C. Hebling, Portable PEM Systems, in *Handbook of Fuel Cells, Vol 4: 1142-1151*, ed. by W. Vielstich, A. Lamm, H. Gasteiger (Wiley, Chichester, UK, 2003)
618. S.R. Narayanan, T.I. Valdez, N. Rohatgi (2003) DMFC system design for portable applications. In: Vielstich W, Lamm A, Gasteiger H (eds) Handbook of Fuel Cells, Vol. 4: 894-904, Wiley, Chichester, UK
619. T. Ramsden (2011) Direct methanol fuel cell material handling equipment demonstration, 21 pages, NREL National Renewable Energy Laboratory, US-DoE http://www.hydrogen.energy.gov/pdfs/review11/mt004_ramsden_2011_o.pdf
620. A. Lamm, J. Müller, System design for transport applications, in *Handbook of Fuel Cells, Vol 4: 878-893*, ed. by W. Vielstich, A. Lamm, H. Gasteiger (Wiley, Chichester, UK, 2003)
621. ballard, basf, bp, daimlerchrysler, methanex, statoil (2002) Methanol Fuel Cell Alliance, 236 pages: http://www.methanol.org/Energy/Resources/Fuel-Cells/MFCA-overall-document-from-09_06.aspx
622. H. Dohle, J. Mergel, D. Stolten, Heat and power management of a direct-methanol-fuel-cell (DMFC) system. J. of Power Sources **111**, 268–282 (2006)
623. J. Mergel, A. Glüsen, Ch. Wannek, Current Status of and Recent Developments in Direct Liquid Fuel Cells, in *Hydrogen and Fuel Cells: Fundamentals, Technologies and Applications, Chapter 3: 41–60*, ed. by D. Stolten (Wiley-VCH Verlag, Weinheim, Germany, 2010)
624. A. Glüsen, M. Müller, N. Kimiaie, I. Konradi, J. Mergel, D. Stolten (2010) Manufacturing Technologies for Direct Methanol Fuel Cells (DMFCs). In: 18th World Hydrogen Energy Conference - WHEC 2010 Proceedings, Parallel Sessions Book 1: 219-226, Stolten D, and Grube Th (Eds), Zentralbibliothek Forschungszentrum Jülich 2010, Schriften des Forschungszentrum Jülich, ISBN: 978-3-89336-658-4
625. H.-P. Schmid, J. Ebner, DaimlerChrysler fuel cell activities, in *Handbook of Fuel Cells, Vol 4: 1167-1171*, ed. by W. Vielstich, A. Lamm, H. Gasteiger (Wiley, Chichester, UK, 2003)
626. A. Rodrigues, M. Fronk, B. McCormick, General Motors/OPEL fuel cell activities – Driving towards a successful future, in *Handbook of Fuel Cells, Vol 4: 1172-1179*, ed. by W. Vielstich, A. Lamm, H. Gasteiger (Wiley, Chichester, UK, 2003)
627. Garche J (2010) Portable Applications and Light Traction. In: Stolten D (ed) Hydrogen and Fuel Cells: Fundamentals, Technologies and Applications, Chapter 35: 715-734, Wiley-VCH Verlag, Weinheim, Germany
628. Wärtsilä installs fuel cell unit on vessel (2010) http://www.wartsila.com/en/press-releases/newsrelease357
629. G. Sandstede, E.J. Cairns, V.S Bagotsky, K. Wiesener (2003) History of low temperature fuel cells. In: Vielstich W, Lamm A, Gasteiger H (eds) Handbook of Fuel Cells, Vol. 1: 145-218, Wiley, Chichester, UK

630. P. Kurzweil, History: Fuel Cells, in *Encyclopedia of Electrochemical Power Sources, Vol 3: 579–595*, ed. by J. Garche, Ch. Dyer, P. Moseley, Z. Ogumi, D. Rand, B. Scrosati (Elsevier, Amsterdam, 2009)
631. H. Hoogers (ed.), *Fuel Cell Technology Handbook, 360 pages* (CRC Press, Boca Raton, London, 2003)
632. A. Heinzel, F. Mahlendorf, J. Roes (eds.), *Brennstoffzellen Entwicklung-Technologie-Anwendung. 3rd. completly revised and extended Ed.* (C.F. Müller Verlag, Heidelberg, 2006)

References to Section 6.5.3

633. M. Madhaiyan, P. S. Chauhan, W. J. Yim, H. P. D. Boruah, T. M. Sa in *Bacteria in Agrobiology: Plant Growth Responses* (Ed.: D. K. Maheshwari), Springer Berlin Heidelberg, Berlin, Heidelberg, **2011**
634. J. Schrader, M. Schilling, D. Holtmann, D. Sell, M. Filho, A. Marx, J. Vorholt, Trends Biotechnol. **27**(2), 107–115 (2009)
635. C. Anthony, *The biochemistry of methylotrophs, Academic Press* (New York, London, 1982)
636. S.J. Giovannoni, D.H. Hayakawa, H.J. Tripp, U. Stingl, S.A. Givan, J.-C. Cho, H.-M. Oh, J.B. Kitner, K.L. Vergin, M.S. Rappé, Environ. Microbiol. **10**, 1771–1782 (2008)
637. M. E. Lidstrom in *The Prokaryotes* (Eds.: M. Dworkin, S. Falkow, E. Rosenberg, K.-H. Schleifer, E. Stackebrandt), Springer, New York, **2006**, 618
638. R. Balasubramanian, S.M. Smith, S. Rawat, L.A. Yatsunyk, T.L. Stemmler, A.C. Rosenzweig, Nature **465**, 115–119 (2010)
639. J.C. Murrell, B. Gilbert, I.R. McDonald, Arch. Microbiol. **173**, 325–332 (2000)
640. R.L. Lieberman, A.C. Rosenzweig, Crit. Rev. Biochem. Mol. Biol. **39**, 147–164 (2004)
641. H. Dalton, Philos. Trans. R. Soc. Lond. B Biol. Sci. **360**, 1207–1222 (2005)
642. G.A. Olah, A. Goeppert, G.K.S. Prakash, *Beyond oil and gas* (The methanol economy, Wiley-VCH, Weinheim, 2006)
643. C. Anthony, M. Ghosh, Prog. Biophys. Mol. Biol. **69**, 1–21 (1998)
644. P.W. van Ophem, J. van Beeumen, J.A. Duine, Eur. J. Biochem. **212**, 819–826 (1993)
645. L. Chistoserdova, L. Gomelsky, J. A. Vorholt, M. Gomelsky, Y. D. Tsygankov, M. E. Lidstrom, *Microbiology (Reading, Engl.)***2000**, *146 (Pt 1)*, 233-238
646. J.A. Vorholt, Arch. Microbiol. **178**, 239–249 (2002)
647. L. Chistoserdova, Science **281**, 99–102 (1998)
648. A.J. Beardsmore, P.N.G. Aperghis, J.R. Quayle, Microbiology **128**, 1423–1439 (1982)
649. P.J. Large, D. Peel, J.R. Quayle, Biochem. J. **81**, 470–480 (1961)
650. G.J. Crowther, G. Kosaly, M.E. Lidstrom, J. Bacteriol. **190**, 5057–5062 (2008)
651. R. Peyraud, K. Schneider, P. Kiefer, S. Massou, J.A. Vorholt, J.-C. Portais, BMC Syst. Biol. **5**, 189 (2011)
652. S. Vuilleumier, L. Chistoserdova, M.-C. Lee, F. Bringel, A. Lajus, Y. Zhou, B. Gourion, V. Barbe, J. Chang, S. Cruveiller et al., PLoS ONE **4**, e5584 (2009)
653. H. Šmejkalová, T.J. Erb, G. Fuchs, A. Herrera-Estrella, PLoS ONE **5**, e13001 (2010)
654. E. Skovran, G.J. Crowther, X. Guo, S. Yang, M.E. Lidstrom, R. Aramayo, PLoS ONE **5**, e14091 (2010)
655. K. Munk, *Biochemie - Zellbiologie* (Thieme Verlag, Stuttgart, 2008)
656. M. T. Madigan, J. M. Martinko, T. D. Brock, *Brock Mikrobiologie*, Pearson Studium, München [u.a.], **2006**
657. K. Ogata, H. Nishikawa, M. Ohsugi, Agric. Biol. Chem. **33**, 1519–1520 (1969)
658. A. Solà, P. Jouhten, H. Maaheimo, F. Sánchez-Ferrando, T. Szyperski, P. Ferrer, Microbiology **153**, 281–290 (2007)

659. F. Bisby, Y. Roskov, A. Culham, T. Orrell, D. Nicolson, L. Paglinawan, N. Bailly, W. Appeltans, P. Kirk, T. Bourgoin et al., "Species 2000 & ITIS Catalogue of Life, 3rd February 2012. *Saccharomycetes*", can be found under www.catalogueoflife.org/col/, **2012**
660. P. Kaszycki, M. Tyszka, P. Malec, H. Kołoczek, Biodegradation **12**, 169–177 (2001)
661. P. Blanco, C. Sieiro, T.G. Villa, FEMS Microbiol. Lett. **175**, 1–9 (1999)
662. M.A. Gleeson, P.E. Sudbery, Yeast **4**, 1–15 (1988)
663. G. Gellissen, G. Kunze, C. Gaillardin, J.M. Cregg, E. Berardi, M. Veenhuis, I. van der Klei, FEMS Yeast Res. **5**, 1079–1096 (2005)
664. H. Yurimoto, N. Kato, Y. Sakai, Chem. Record. **5**, 367–375 (2005)
665. R. Caspi, T. Altman, J.M. Dale, K. Dreher, C.A. Fulcher, F. Gilham, P. Kaipa, A.S. Karthikeyan, A. Kothari, M. Krummenacker et al., Nucleic Acids Res. **38**, D473–D479 (2009)
666. O. Negru, O. Csutak, I. Stoica, E. Rusu, T. Vassu, Rom. Biotechnol. Lett. **15**, 5369–5375 (2010)
667. H. Mogren, Process Biochem. **14**, 2–4 (1979)
668. U. Faust, P. Praeve, D.A. Sukatsch, J. Ferment. Technol. **55**(6), 609–614 (1977)
669. D. G. MacLennan, J. S. Gow, D. A. Stringer, *Proc. R. Aust. Chem. Inst.* **40**(3), (1973)
670. S. Kim, P. Kim, H. Lee, J. Kim, Biotechnol. Lett. **18**, 25–30 (1996)
671. J.H. Choi, J.H. Kim, M. Daniel, J.M. Lebeault, Kor. J. Appl. Microbiol. Biotechnol. **17**, 392–396 (1989)
672. S. B. Pluschkell, M. C. Flickinger, *Microbiology (Reading, Engl.)* **148**, 3223–3233 (2002)
673. L.K. Shay, H.R. Hunt, G.H. Wegner, J. Ind. Microbiol. **2**, 79–85 (1987)
674. P. Kim, J.-H. Kim, D.-K. Oh, World J. Microbiol. Biotechnol. **19**, 357–361 (2003)
675. L. Bélanger, M.M. Figueira, D. Bourque, L. Morel, M. Béland, L. Laramée, D. Groleau, C.B. Míguez, FEMS Microbiol. Lett. **231**, 197–204 (2004)
676. A. Crémieux, J. Chevalier, M. Combet, G. Dumenil, D. Parlouar, D. Ballerini, European. J. Appl. Microbiol. **4**, 1–9 (1977)
677. D. Leak in *Encyclopedia of Bioprocess Technology*, John Wiley & Sons, Inc, **2002**
678. T. Brautaset, Ø.M. Jakobsen, K.D. Josefsen, M.C. Flickinger, T.E. Ellingsen, Appl. Microbiol. Biotechnol. **74**, 22–34 (2007)
679. P. Höfer, Y.J. Choi, M.J. Osborne, C.B. Miguez, P. Vermette, D. Groleau, Microb. Cell Fact. **9**, 1–13 (2010)
680. P. Höfer, P. Vermette, D. Groleau, Biochem. Eng. J. **54**, 26–33 (2011)
681. T. Holscher, U. Breuer, L. Adrian, H. Harms, T. Maskow, Appl. Environ. Microbiol. **76**, 5585–5591 (2010)
682. F. J. Schendel, R. Dillingham, R. S. Hanson, K. Sano, K. Matsui, WO1999020785, **1997**
683. T. Brautaset, Ø.M. Jakobsen, K.F. Degnes, R. Netzer, I. Nærdal, A. Krog, R. Dillingham, M.C. Flickinger, T.E. Ellingsen, Appl. Microbiol. Biotechnol. **87**, 951–964 (2010)
684. D. I. Stirling (Celgene Corporation (Warren, NJ)),US 5071976, **1991**
685. D.K. Oh, J.H. Kim, T. Yoshida, Biotechnol. Bioeng. **54**, 115–121 (1997)
686. Z. Omer, R. Tombolini, A. Broberg, B. Gerhardson, Plant Growth Regul. **43**, 93–96 (2004)
687. M.E. Lidstrom, L. Chistoserdova, J. Bacteriol. **184**(7), 1818 (2002)
688. R.L. Koenig, R.O. Morris, J.C. Polacco, J. Bacteriol. **184**, 1832–1842 (2002)
689. C. B. Miguez, M. M. Figueira, L. Laramee, J. C. Murrell, WO2003046226, **2003**
690. M. M. Figueira, L. Laramee, J. C. Murrell, L. Belanger, D. Groleau, C. B. Miguez, US 20030104527, **2003**
691. J. Gutiérrez, D. Bourque, R. Criado, Y.J. Choi, L.M. Cintas, P.E. Hernández, C.B. Míguez, FEMS Microbiol. Lett. **248**, 125–131 (2005)
692. D. Byrom, M. Carver (Imperial chemical Industries PLC), US 5077212, **1991**
693. K.A. FitzGerald, M.E. Lidstrom, Biotechnol. Bioeng. **81**, 263–268 (2003)
694. Y.J. Choi, D. Bourque, L. Morel, D. Groleau, C.B. Míguez, Appl. Environ. Microbiol. **72**, 753–759 (2006)
695. Y.J. Choi, C.B. Miguez, B.H. Lee, Appl. Environ. Microbiol. **70**, 3213–3221 (2004)
696. C. Anthony, Adv. Microb. Physiol. **27**, 113–210 (1986)

697. G.H. Wegner, W. Harder, Antonie Van Leeuwenhoek **53**, 29–36 (1987)
698. T. Egli, N. Lindley, *J. Gen. Microbiol.* **130**, 3239–3249 (1984)
699. L. Dijkhuizen, T.A. Hansen, W. Harder, Trends Biotechnol. **3**, 262–267 (1985)
700. N. Kato, M. Kano, Y. Tani, K. Ogata, Agric. Biol. Chem. **38**, 111–116 (1974)
701. R. Wichmann, C. Wandrey, A.F. Bückmann, M.-R. Kula, Biotechnol. Bioeng. **23**, 2789–2802 (1981)
702. B. Bossow, C. Wandrey, Ann. N. Y. Acad. Sci. **506**, 325–336 (1987)
703. V.I. Tishkov, V.O. Popov, Biochemistry Mosc. **69**, 1252–1267 (2004)
704. P. Fröhlich, K. Albert, M. Bertau, Org. Biomol. Chem. **9**, 7941 (2011)
705. R. Couderc, J. Baratti, Agric. Biol. Chem. **44**, 2279–2289 (1980)
706. G. Dienys, S. Jarmalavičius, S. Budrien, D. Čitavičius, J. Sereikait, J. Mol. Catal. B Enzym. **21**, 47–49 (2003)
707. Y. Sakai, Y. TANI. Agric. Biol. Chem. **50**, 2615–2620 (1986)
708. M. Zhang, H.Y. Wang, Enzyme Microb. Technol. **16**, 10–17 (1994)
709. G. Gellissen, Appl. Microbiol. Biotechnol. **54**, 741–750 (2000)
710. G. Gellissen, C. P. Hollenberg in *Encyclopedia of Food Microbiology* (Ed.: Editor-in-Chief: Richard K. Robinson), Elsevier, Oxford, **1999**
711. K. Chitkala in *Encyclopedia of Food Microbiology* (Ed.: Editor-in-Chief: Richard K. Robinson), Elsevier, Oxford, **1999**
712. M.A. Romanos, J.J. Clare, K.M. Beesley, F.B. Rayment, S.P. Ballantine, A.J. Makoff, G. Dougan, N.F. Fairweather, I.G. Charles, Vaccine **9**, 901–906 (1991)
713. A. Markaryan, C.J. Beall, P.E. Kolattukudy, Biochem. Biophys. Res. Commun. **220**, 372–376 (1996)
714. J.J. Clare, F.B. Rayment, S.P. Ballantine, K. Sreekrishna, M.A. Romanos, Nat. Biotech. **9**, 455–460 (1991)
715. P.A. Romero, M. Lussier, A.M. Sdicu, H. Bussey, A. Herscovics, Biochem. J. **321**, 289–295 (1997)
716. Y. Sakai, T. Rogi, R. Takeuchi, N. Kato, Y. Tani, Appl. Microbiol. Biotechnol. **42**, 860–864 (1995)
717. M.W. de Vouge, A.J. Thaker, I.H. Curran, L. Zhang, G. Muradia, H. Rode, H.M. Vijay, Int. Arch. Allergy Immunol. **111**, 385–395 (1996)
718. G. Gellissen, M. Piontek, U. Dahlems, V. Jenzelewski, J.E. Gavagan, R. DiCosimo, D.L. Anton, Z.A. Janowicz, Appl. Microbiol. Biotechnol. **46**, 46–54 (1996)
719. A. Beauvais, M. Monod, J.-P. Debeaupuis, M. Diaquin, K. Hidemitsu, J.-P. Latgé, J. Biol. Chem. **272**, 6238–6244 (1997)
720. G. Gellissen, Z. A. Janowicz, A. Merckelbach, M. Piontek, P. Keup, U. Weydemann, C. P. Hollenberg, A. W. Strasser, *Biotechnology (N.Y.)* **9**, 291–295 (1991)
721. M. Hodgkins, P. Sudbery, D. Mead, D.J. Ballance, A. Goodey, Yeast **9**, 625–635 (1993)
722. R. Narciandi, L. Rodriguez, E. Rodriguez, R. Diaz, J. Delgado, L. Herrera, Biotechnol. Lett. **17**, 949–952 (1995)
723. A.F. Mayer, K. Hellmuth, H. Schlieker, R. Lopez-Ulibarri, S. Oertel, U. Dahlems, A.W.M. Strasser, A.P.G.M. van Loon, Biotechnol. Bioeng. **63**, 373–381 (1999)
724. P.M. Smith, C. Suphioglu, I.J. Griffith, K. Theriault, R.B. Knox, M.B. Singh, J. Allergy Clin, Immunol. **98**, 331–343 (1996)
725. M.S. Payne, K.L. Petrillo, J.E. Gavagan, L.W. Wagner, R. DiCosimo, D.L. Anton, Gene **167**, 215–219 (1995)
726. K. N. Faber, P. Haima, W. Harder, M. Veenhuis, G. AB, Curr. Genet. 1994, 25, 305-310
727. D. Mozley, A. Remberg, W. Gartner, Photochem. Photobiol. **66**, 710–715 (1997)
728. A. Ruddat, P. Schmidt, C. Gatz, S.E. Braslavsky, W. Gärtner, K. Schaffner, Biochemistry **36**, 103–111 (1997)
729. R.G. Buckholz, M.A.G. Gleeson, Nat. Biotech. **9**, 1067–1072 (1991)
730. C. Zurek, E. Kubis, P. Keup, D. Hörlein, J. Beunink, J. Thömmes, M.-R. Kula, C. P. Hollenberg, G. Gellissen, Process Biochem. 1996, 31, 679-689

731. M. Rodríguez, R. Rubiera, M. Penichet, R. Montesinos, J. Cremata, V. Falcón, G. Sánchez, R. Bringas, C. Cordovés, M. Valdés et al., J. Biotechnol. **33**, 135–146 (1994)
732. E.Z. Monosov, T.J. Wenzel, G.H. Lüers, J.A. Heyman, S. Subramani, J. Histochem. Cytochem. **44**, 581–589 (1996)
733. S.A. Rosenfeld, D. Nadeau, J. Tirado, G.F. Hollis, R.M. Knabb, S. Jia, Protein Expr. Purif. **8**, 476–482 (1996)
734. U. Weydemann, P. Keup, M. Piontek, A.W. Strasser, J. Schweden, G. Gellissen, Z.A. Janowicz, Appl. Microbiol. Biotechnol. **44**, 377–385 (1995)
735. F. Talmont, S. Sidobre, P. Demange, A. Milon, L.J. Emorine, FEBS Lett. **394**, 268–272 (1996)
736. S.C. Gilbert, H. van Urk, A.J. Greenfield, M.J. McAvoy, K.A. Denton, D. Coghlan, G.D. Jones, D.J. Mead, Yeast **10**, 1569–1580 (1994)
737. J.M. Cregg, J.F. Tschopp, C. Stillman, R. Siegel, M. Akong, W.S. Craig, R.G. Buckholz, K.R. Madden, P.A. Kellaris, G.R. Davis et al., Nat. Biotechnol. **5**, 479–485 (1987)
738. Z.A. Janowicz, K. Melber, A. Merckelbach, E. Jacobs, N. Harford, M. Comberbach, C.P. Hollenberg, Yeast **7**, 431–443 (1991)
739. T. Boehm, S. Pirie-Shepherd, L.-B. Trinh, J. Shiloach, J. Folkman, Yeast **15**, 563–572 (1999)
740. C.K. Raymond, T. Bukowski, S.D. Holderman, A.F.T. Ching, E. Vanaja, M.R. Stamm, Yeast **14**, 11–23 (1998)
741. P.F. Gallet, H. Vaujour, J.M. Petit, A. Maftah, A. Oulmouden, R. Oriol, C. Le Narvor, M. Guilloton, R. Julien, Glycobiology **8**, 919–925 (1998)
742. D. Bourque, B. Ouellette, G. André, D. Groleau, Appl. Microbiol. Biotechnol. **37**, 7–12 (1992)
743. D. Bourque, Y. Pomerleau, D. Groleau, Appl. Microbiol. Biotechnol. **44**, 367–376 (1995)
744. T. Suzuki, T. Yamane, S. Shimizu, Appl. Microbiol. Biotechnol. **23**, 322–329 (1986)
745. F.J. Schendel, C.E. Bremmon, M.C. Flickinger, M. Guettler, R.S. Hanson, Appl. Environ. Microbiol. **56**(4), 963–970 (1990)
746. R. Westlake, Chem. Ing. Technol. **58**, 934–937 (1986)
747. J.D. Windass, M.J. Worsey, E.M. Pioli, D. Pioli, P.T. Barth, K.T. Atherton, E.C. Dart, D. Byrom, K. Powell, P.J. Senior, Nature **287**, 396–401 (1980)
748. P.J. Senior, J. Windass, Biotechnol. Lett. **2**, 205–210 (1980)
749. K. Muttzall, *Einführung in die Fermentationstechnik* (Behr, Hamburg, 1993)
750. G.L. Solomons, CRC Crit. Rev. Biotechnol. **1**, 21–58 (1985)
751. E.W. Jwanny, M.M. Rashad, Acta Biotechnol. **7**, 31–38 (1987)
752. A.M. Henstra, J. Sipma, A. Rinzema, A.J.M. Stams, Curr. Opin. Biotechnol. **18**, 200–206 (2007)
753. E. H. Wegner, US 4414329, **1981**
754. R. Renneberg, *Biotechnologie für Einsteiger, Elsevier, Spektrum* (Akad. Verl, Heidelberg, 2006)
755. U. O. Ugalde, J. I. Castrillo in *Applied Mycology and Biotechnology : Agriculture and Food Production* (Ed.: George G. Khachatourians and Dilip K. Arora), Elsevier, **2002**
756. G.H. Wegner, FEMS Microbiol. Lett. **87**, 279–284 (1990)
757. A. Onnis-Hayden, A.Z. Gu, Proceedings of the Water Environment Federation **17**, 253–273 (2008)
758. I. Purtschert, H. Siegrist, W. Gujer, Water Sci. Technol. **33**(12), 117–126 (1996)
759. M. Ginige, J. Bowyer, L. Foley, J. Keller, Z. Yuan, Biodegradation **20**(2), 221–234 (2009)
760. H. Lee, J.A. Brereton, D.S. Mavinic, R.A. Fiorante, W.K. Oldham, J.K. Paisley, Environ. Technol. **22**(10), 1223–1235 (2001)
761. M. Komorowska-Kaufman, H. Majcherek, E. Klaczyński, Process Biochem. **41**(5), 1015–1021 (2006)
762. S.D. Minteer, B.Y. Liaw, M.J. Cooney, Curr. Opin. Biotechnol. **18**(3), 228–234 (2007)
763. J. Kim, H. Jia, P. Wang, Biotechnol. Adv. **24**(3), 296–308 (2006)
764. P.L. Yue, K. Lowther, Chem. Eng. J. **33**, B69–B77 (1986)

765. P. Kar, H. Wen, H. Li, S.D. Minteer, S.C. Barton, J. Electrochem. Soc. **158**(5), B580–B586 (2011)
766. G.T.R. Palmore, H. Bertschy, S.H. Bergens, G.M. Whitesides, J. Electroanal. Chem. **443**(1), 155–161 (1998)
767. A. A. Karyakin, in *Electropolymerization.* Wiley-VCH Verlag GmbH & Co. KGaA, **2010**, 93-110
768. A. A. Karyakin, E.E. Karyakina, W. Schuhmann, H.-L. Schmidt, S.D. Varfolomeyev, Electroanalysis **6**(10), 821–829 (1994)
769. P.K. Addo, R.L. Arechederra, S.D. Minteer, Electroanalysis **22**(7–8), 807–812 (2010)
770. R.A. Rincón, C. Lau, K.E. Garcia, P. Atanassov, Electrochim. Acta **56**(5), 2503–2509 (2011)
771. X.-C. Zhang, A. Ranta, A. Halme, Biosens. Bioelectron. **21**(11), 2052–2057 (2006)
772. R. Obert, B.C. Dave, J. Am. Chem. Soc. **121**, 12192–12193 (1999)
773. H. Wu, Z.Y. Jiang, S.W. Xu, S.F. Huang, Chin. Chem. Lett. **14**(4), 423–425 (2003)
774. F. Baskaya, X. Zhao, M. Flickinger, P. Wang, Appl. Biochem. Biotechnol. **162**(2), 391–398 (2010)
775. S. Kuwabata, R. Tsuda, K. Nishida, H. Yoneyama, Chem. Lett. **22**(9), 1631 (1993)
776. S. Kuwabata, R. Tsuda, H. Yoneyama, J. Am. Chem. Soc. **116**(12), 5437–5443 (1994)
777. Y. Amao, T. Watanabe, J. Mol. Catal. B Enzym. **44**(1), 27–31 (2007)
778. Y. Amao, T. Watanabe, *Appl. Catal., B* **86**(3-4), 109–113 (2009)
779. F. E. Zilly, J. P. Acevedo, W. Augustyniak, A. Deege, U. W. Häusig, M. T. Reetz, *Angew. Chem., Int. Ed.* **50**(12), 2720–2724 (2011)
780. B. Alber, Appl. Microbiol. Biotechnol. **89**(1), 17–25 (2011)